Acta Universitatis Agriculturae Sueciae

Doctoral Thesis No. 2026:23
Faculty of Natural Resources and Agricultural Sciences

Separation and destruction of PFAS from groundwater using an on-site treatment train

Oscar Liljeström

Separation and destruction of PFAS from groundwater using an on-site treatment train

Oscar Liljeström
Faculty of Natural Resources and Agricultural Sciences
Department of Aquatic Sciences and Assessment
Uppsala

SLU
SWEDISH UNIVERSITY OF AGRICULTURAL SCIENCES

DOCTORAL THESIS
Uppsala 2026

Acta Universitatis Agriculturae Sueciae
2026:23

Cover: Illustration of a “treatment train” generated using ChatGPT (OpenAI, GPT-5)

ISSN 1652-6880
ISBN (print version) 978-91-8124-240-9
ISBN (electronic version) 978-91-8124-270-6
https://doi.org/10.54612/a.6vofehpjfr

Swedish University of Agricultural Sciences, Department of Aquatic Sciences and Assessment, Uppsala, Sweden

Print: SLU Grafisk service, Uppsala 2026

Separation and destruction of PFAS from groundwater using an on-site treatment train

Abstract

Per- and polyfluoroalkyl substances (PFAS) are persistent and mobile contaminants that pose a considerable risk to groundwater resources. At contaminated sites, such as landfills, PFAS can migrate into groundwater, where their low sorption and high mobility facilitate plume formation and aquifer transport. Addressing this challenge requires an improved understanding of PFAS transport and effective treatment strategies. This thesis investigates PFAS behavior in groundwater systems and evaluated a field-scale integrated treatment train combining foam fractionation (FF), electrochemical oxidation (EO), and a constructed wetland (CW) for remediation of landfill leachate-impacted groundwater. The saturated paste extraction method (SPEM) was evaluated for determining PFAS solid–liquid partitioning coefficients (K_d). SPEM-derived values showed good agreement with field-based estimates and performed better than conventional batch leaching tests (L/S = 1) in low-sorption systems, confirming low K_d values and strong chain-length dependence in sandy, low organic-carbon aquifers. Full-scale FF achieved high separation of long-chain PFAS (>90%). The addition of co-foaming surfactants significantly increased short-chain separation, although separation of ≤C4 perfluoroalkyl carboxylic acids (PFCA) remained limited. The concentrated FF foamate was treated using EO, enabling substantial PFAS degradation, with high fluorine mass balance recovery indicating extensive mineralization. CW, evaluated both as a standalone and polishing step following FF, separated PFAS through substrate sorption and plant uptake, but showed limited effectiveness in reducing aqueous short-chain concentrations. Overall, the results demonstrate that combining FF and EO effectively separated and mineralized long-chain PFAS from groundwater. While co-foaming surfactants improved short-chain separation, additional polishing capable of treating ≤C4 PFCA should be considered. The limited ability of CW to reduce PFAS concentrations, however, limits its suitability for this purpose.

Keywords: PFAS, Groundwater, K_d, Foam fractionation, Electrochemical oxidation, Constructed wetland

Avskiljning och destruktion av PFAS i grundvatten genom en serie av reningssteg

Sammanfattning

Per- och polyfluorerade alkylsubstanser (PFAS) är persistenta, mobila föroreningar som utgör en risk för grundvattenresurser. Vid förorenade områden, såsom deponier, kan PFAS migrera till grundvattnet, där låg sorption och hög mobilitet bidrar till vidare spridning i akviferen. För att hantera detta krävs en förståelse för transport av PFAS i grundvattensystem samt effektiva reningslösningar. Denna avhandling undersöker PFAS-beteende i grundvattensystem och utvärderar en integrerad serie av reningssteg i fältskala för rening av grundvatten påverkat av deponilakvatten. Reningsstegen innefattade skumfraktionering (FF), elektrokemisk oxidation (EO) samt en anlagd våtmark (CW). Mättnadsextraktion (SPEM) utvärderades för bestämning av PFAS-fördelningskoefficienter mellan fast och flytande fas (K_d). Resultaten visade överensstämmelse med fältbaserade uppskattningar och bättre prestanda än konventionella skakförsök (L/S = 1) i system med låg sorption. Försöken bekräftade låga K_d-värden och ett tydligt samband mellan sorption och den perfluorerade alkylkedjans längd i sandiga akviferer med låga halter av organiskt kol. Fullskaleförsök med FF uppnådde hög avskiljning av långkedjade PFAS (>90 %). Tillsats av tensider ökade avskiljningen av kortkedjade PFAS, men avskiljningen av ≤C4 perfluorerade karboxylsyror (PFCA) var fortsatt begränsad. Det koncentrerade skummet från FF behandlades med EO, vilket möjliggjorde betydande nedbrytning av PFAS. En hög fluorbalans indikerade en omfattande mineralisering. Avskiljning av PFAS i CW utvärderades både som fristående reningssteg och som poleringssteg följande FF. PFAS avskiljdes både genom sorption till substrat och växtupptag. Metoden visade dock begränsad effekt för att reducera koncentrationen av kortkedjade PFAS i vattnet. Resultaten visar att kombinationen FF-EO kan utgöra en effektiv metod för att separera och mineralisera långkedjade PFAS från grundvatten. Även om tillsats av tensider förbättrade avskiljningen av kortkedjade PFAS, kvarstår behovet av ett poleringssteg för behandling av ≤C4 PFCA. Den begränsade förmågan hos CW att reducera PFAS-koncentration innebär dock att teknikens lämplighet för detta ändamål är begränsad.

Nyckelord: PFAS, Grundvatten, K_d, Skumfraktionering, Elektrokemisk oxidation, Anlagd våtmark

Dedication

To my amazing wife Vilma, the original Dr. Liljeström

Contents

List of publications 11

List of tables 15

List of figures 17

Abbreviations 19

AI declaration 23

1. Introduction 25

2. Aim and objectives 27

3. Background 29
   - 3.1 What are PFAS? 29
   - 3.2 PFAS classification 29
   - 3.3 Persistence 32
   - 3.4 Toxicity 33
   - 3.5 Regulations 35
   - 3.6 Sources 36
   - 3.7 Transport and biomagnification 37
   - 3.8 Treatment Methods 39
     - 3.8.1 Established separation techniques 40
     - 3.8.2 Emerging separation techniques 41
     - 3.8.3 Established destruction techniques 44
     - 3.8.4 Emerging destruction techniques 44
     - 3.8.5 Treatment trains 46

4. Materials and methods 49
   - 4.1 Site description 50
   - 4.2 Raw water acquisition 50
   - 4.3 Determining K_d values for aquifer materials (Paper **I**) 51
     - 4.3.1 Batch leaching tests 52
     - 4.3.2 Saturated paste extraction method 52

4.3.3 Field K_d 53
4.4 Treatment methods 53
4.4.1 Foam fractionation (Paper **II**) 53
4.4.2 Electrochemical oxidation (Paper **II**) 54
4.4.3 Constructed wetland treatment (Papers **III** and **IV**) 55
4.5 Chemical analysis 57
4.5.1 PFAS analysis in water 57
4.5.2 PFAS analysis in filter substrate and plant tissue 59
4.5.3 General chemistry 62
4.6 Data evaluation 62
4.7 Statistical methods 65

5. Results and discussion 67
5.1 Determining K_d values for aquifer materials (Paper **I**) 67
5.2 Foam fractionation for PFAS separation (Paper **II**) 69
5.3 Electrochemical oxidation for PFAS destruction (Paper **II**) 71
5.4 PFAS behavior in subsurface flow constructed wetlands (Papers **III** and **IV**) 74
5.5 The integrated treatment train for PFAS-contaminated water (Papers **II** and **IV**) 78

6. Conclusions 83

7. Outlook and future research needs 85

References 87

Popular science summary 111

114

Populärvetenskaplig sammanfattning 115

Acknowledgements 119

List of publications

This thesis is based on the work contained in the following papers, referred to by Roman numerals in the text:

I. Oscar Liljeström, Dan Berggren Kleja, Malin Ellbrant, Michael Pettersson, Anja Enell, Lutz Ahrens. Evaluating the saturated paste extraction method for determining PFAS solid–liquid partitioning coefficients (K_d) in low-organic-carbon sand aquifers. (Manuscript)

II. Oscar Liljeström, Robin Axelson, Sofia Bjälkefur Seroka, Helena Hinrichsen, Patrik Hollman, Wilma Högman, Phillip McCleaf, Say Svanström, Jose Jorge Espí Gallart, Mariana Eugenia Lombeida Lombeida, Dan Berggren Kleja, Anja Enell, Michael Pettersson, Lutz Ahrens. Integrated Foam Fractionation and Electrochemical Oxidation for Simultaneous Treatment of PFAS in Groundwater and Landfill Leachate. (Manuscript)

III. Oscar Liljeström, Dahn Rosenquist, Dan Berggren Kleja, Anja Enell, Lutz Ahrens (2025). Pilot scale treatment of PFAS-contaminated groundwater in a subsurface flow constructed wetland - evaluating multiple plant species. *Environmental Pollution,* 386, 127199. https://doi.org/10.1016/j.envpol.2025.127199

IV. Oscar Liljeström, Dahn Rosenquist, Dan Berggren Kleja, Anja Enell, Lutz Ahrens. Constructed wetland polishing after foam fractionation of PFAS-contaminated landfill leachate and groundwater. (Manuscript)

The published paper is published open access.

The contribution of Oscar Liljeström to the papers included in this thesis was as follows:

I. Conceptualization, methodology, validation, formal analysis, investigation, data curation, writing – original draft, visualization

II. Validation, formal analysis, investigation, data curation, writing – original draft, visualization

III. Conceptualization, validation, formal analysis, investigation, data curation, writing – original draft, visualization.

IV. Conceptualization, methodology, validation, formal analysis, investigation, data curation, writing – original draft, visualization.

List of tables

Table 1. List of PFCA and PFSA with perfluoroalkyl chain lengths of 1-14. 32

Table 2. Overview of PFAS analyzed in aqueous samples 58

Table 3. Overview of PFAS analyzed in solid samples 60

List of figures

Figure 1. PFAS classification.. 31

Figure 2. Overview of PFAS treatment methods. 40

Figure 3. Method overview. 50

Figure 4. Methods used for K_d determination. 52

Figure 5. Method schematic of FF and EO. 54

Figure 6. Schematic of the CW evaluated in Paper **III**. 56

Figure 7. Schematic of the CW evaluated in paper **IV**. 57

Figure 8. Average field and SPEM derived K_d values 68

Figure 9. Treatment efficiency of FF. 71

Figure 10. PFAS concentrations during EO treatment. 73

Figure 11. PFAS distribution in CW. 75

Figure 12. Bioconcentration factors of *Salix* Wilhelm. 77

Figure 13. Full treatment train including PFAS concentration and composition. 80

Figure 14. Full treatment train including PFAS mass. 81

Abbreviations

4:2 FTSA	4:2 fluorotelomere sulfonate
6:2 Cl-PFESA	9-chlorohexadecafluoro-3-oxanonane-1- sulfonic acid
6:2 FTAB	6:2 fluorotelomer sulfonamido betaine
6:2 FTSA	6:2 fluorotelomere sulfonate
8:2 Cl-PFESA	11-chloroeicosafluoro-3-oxaundecane-1- sulfonate acid
8:2 FTSA	8:2 fluorotelomere sulfonate
10:2 FTSA	10:2 fluorotelomere sulfonate
a_{aw}	Specific air-water interfacial area
AC	Activated carbon
AFFF	Aqueous film forming foams
AOF	Adsorbable organic fluorine
AIX	Anion exchange
BCF	Bioconcentration factor
BDD	Boron doped diamond
CTAB	Cetyltrimethylammonium bromide
CW	Constructed wetland
DMSO	Dimethyl sulfoxide
dw	Dry weight
EO	Electrochemical oxidation
EtFOSA	N-ethylperfluorooctane sulfonamide
EtFOSAA	N-ethylperfluorooctane sulfonamidoacetic acid
EtFOSE	N-ethylperfluorooctane sulfonamidoethanol
FBSA	Perfluorobutane sulfonamide
FF	Foam fractionation

FOSA	Perfluorooctane sulfonamide
FOSAA	Perfluorooctane sulfonamidoacetic acid
FPPP	Fluorinated plant protection product
GAC	Granular activated carbon
HALT	Hydrothermal alkaline treatment
HFPO-DA	Tetrafluoro-2-(heptafluoropropoxy)propanoic acid
HPFHpA	7H-perfluoroheptanoic acid
HRT	Hydraulic residence time
K_{aw}	Air-water interfacial adsorption coefficient
K_d	Solid-liquid partitioning coefficient
L/S	Liquid to solid ratio
LCA	Life cycle assessment
LCC	Life cycle costing
LD_{50}	Lethal dose
MeFOSA	N-methylperfluorooctane sulfonamide
MeFOSAA	N-methylperfluorooctane sulfonamidoacetic acid
MeFOSE	N-methylperfluorooctane sulfonamidoethanol
MOF	Metal organic framework
NaDONA	dodecafluoro-3H-4,8-dioxanonanoic acid
NF	Nano filtration
OC	Organic carbon
P37DMOA	Perfluoro-3,7-dimethyloctanoic acid
PFAA	Perfluoroalkyl acid
PFBA	Perfluorobutanoic acid
PFBS	Perfluorobutane sulfonic acid
PFCA	Perfluoroalkyl carboxylic acid

PFDA	Perfluorodecanoic acid
PFDoDA	Perfluorododecanoic acid
PFDoDS	Perfluorododecane sulfonic acid
PFDS	Perfluorodecane sulfonic acid
PFECHS	Perfluoro-4-ethylcyclohexanesulfonate
PFEtS	Perfluoroethane sulfonic acid
PFHpA	Perfluoroheptanoic acid
PFHpS	Perfluoroheptane sulfonic acid
PFHxA	Perfluorohexanoic acid
PFHxS	Perfluorohexane sulfonic acid
PFNA	Perfluorononanoic acid
PFNS	Perfluorononane sulfonic acid
PFOA	Perfluorooctanoic acid
PFOS	Perfluorooctane sulfonic acid
PFPeA	Perfluoropentanoic acid
PFPeDA	Pentadecafluorundecanoic acid
PFPeS	Perfluoropentane sulfonic acid
PFPrA	Perfluoro propionic acid
PFPrS	Perfluoropropane sulfonic acid
PFSA	perfluoroalkyl sulfonic acid
PFTeDA	Perfluorotetradecanoic acid
PFTeDS	Perfluorotetradecane sulfonic acid
PFTrDA	Perfluorotridecanoic acid
PFTrDS	Perfluorotridecane sulfonic acid
PFUnDA	Perfluoroundecanoic acid
PFUnDS	Perfluoroundecane sulfonic acid

PP	Poly propylene
RO	Reversed osmosis
SDS	Sodium dodecyl sulfate
SPE	Solid phase extraction
SPEM	Saturated paste extraction method
SS	Stainless steel
TFA	Trifluoroacetic acid
TFMS	Trifluoromethane sulfonic acid
TOP	Total oxidizable precursors
UPLC-MS/MS	Ultraperformance liquid chromatography coupled to tandem mass spectrometry
WWTP	Waste water treatment plant
θ_w	Volumetric water content
ρ_b	Porous medium bulk density

AI declaration

Generative AI tools were used in a limited and supportive capacity during the preparation of this thesis. ChatGPT (OpenAI, GPT-5) was used to assist in summarizing and restructuring text originally written by the author. It was also used to generate the cover figure and elements of Figure 4 illustrating the methods of Paper **I**.

In addition, ChatGPT (OpenAI, GPT-5) and Claude (Anthropic, Sonnet 4.6) were used as aids in developing R code for some of the visualizations presented in this thesis.

These tools were not used to generate original scientific content, perform analyses, or draw independent conclusions. All outputs were critically evaluated, edited, and verified by the author, who takes full responsibility for the final content of the thesis.

1. Introduction

Per- and polyfluoroalkyl substances (PFAS) represent one of the most challenging classes of environmental contaminants currently faced by society (Ritscher et al., 2018). Their exceptional chemical stability, driven primarily by the strength of the carbon-fluorine bond as well as the shielding by fluorine of the carbon backbone, underpins both their widespread industrial utility and their persistence in environmental systems (Evich et al., 2022; O'hagan, 2008). As a result of decades of extensive use and continuous emissions from both point and diffuse sources, PFAS have become ubiquitously distributed on a global scale, contaminating aquatic and terrestrial ecosystems, food webs, and drinking water resources (Giesy & Kannan, 2001; Yamashita et al., 2008). Groundwater contamination is of particular concern, as PFAS mobility facilitates the formation of large contaminant plumes that pose risks to drinking water supplies used by large populations (Sörengård et al., 2022).

While many PFAS exhibit relatively low acute toxicity, a growing body of epidemiological and experimental evidence has linked chronic exposure to adverse health outcomes, including metabolic, immunological, and carcinogenic effects (Mišľanová & Valachovičová, 2025). The heterogeneity of PFAS complicates risk assessment, yet the combination of persistence, bioaccumulation, and widespread exposure has motivated increasingly precautionary regulatory approaches (Brennan et al., 2021; European Union (EU), 2020; UNEP & Stockholm Convention, 2025).

Remediation of PFAS-contaminated groundwater remains technically complex and resource-intensive (Ross et al., 2018). No single treatment technology is universally effective across the full spectrum of PFAS, especially when addressing short-chain compounds. Consequently, treatment strategies increasingly rely on integrated treatment trains that combine separation and destruction techniques to balance efficiency, cost, and sustainability. While established methods such as granular activated carbon (GAC) and anion exchange (AIX) remain central, additional separation techniques such as foam fractionation (FF) are increasingly being applied. Emerging treatment technologies, such as phytoextraction and electrochemical oxidation (EO), also show considerable promise.

Despite growing awareness of PFAS contamination and the development of various treatment technologies, significant knowledge gaps remain

regarding their effectiveness under field-relevant conditions and their integration into scalable, on-site remediation strategies. In particular, there is a need to better understand PFAS behavior in subsurface environments, optimize separation processes for a broad range of compounds, and ensure effective destruction of concentrated waste streams. Addressing these challenges requires a systems-level approach that evaluates not only individual technologies but also their combined performance within treatment trains designed for real-world applications.

2. Aim and objectives

The overall aim of this thesis was to evaluate the use of an on-site treatment train for the remediation of PFAS-contaminated groundwater, combining foam fractionation for PFAS separation with subsequent concentrate destruction using electrochemical oxidation and post-treatment polishing in a constructed wetland system. The specific research objectives included:

- Determination of the aquifer solid-liquid partitioning coefficients (K_d) for PFAS present at contaminated sites, including the implementation of the novel method saturated paste extraction for K_d determination (Paper **I**).

- Evaluate the performance of a full-scale foam fractionation system for PFAS removal in landfill leachate-impacted groundwater, including the evaluation of the effect of co-foaming surfactant addition to increase short-chain PFAS removal (Paper **II**).

- Evaluate the performance of a full-scale boron-doped diamond electrode electrochemical oxidation system for the destruction of PFAS in the concentrated foamate generated by a foam fractionation system (Paper **II**).

- Evaluate, in pilot-scale, the use of planted subsurface flow constructed wetland systems for the separation of PFAS in landfill leachate-impacted groundwater, either directly or as a post-treatment polishing step following foam fractionation (Papers **III** and **IV**).

3. Background

3.1 What are PFAS?

PFAS are a family of fluorinated organic compounds and were defined by the OECD in 2021 as “fluorinated substances that contain at least one fully fluorinated methyl or methylene carbon atom (without any H/Cl/Br/I atom attached to it)” (OECD, 2021). Many compounds fall within this definition, and there are currently over 7 million PFAS registered in the PubChem database (Schymanski et al., 2023). The number of PFAS of economic, health, or environmental relevance is, however, lower. The Swedish chemical agency's public chemical database, as an example, only contains ~14 000 PFAS (Swedish Chemicals Agency, 2026). PFAS are anthropogenic, with one of their earliest known syntheses occurring in 1938 with the creation of tetrafluoroethylene, of which the polymer polytetrafluoroethylene (PTFE) is commonly known under the brand name Teflon® (Plunkett, 1941). Teflon® later found its use in the Manhattan Project during the development of early nuclear weapons (Goldwhite, 1986). PFAS have since then expanded both in chemical variety and applications (Dams & Ameduri, 2025), being used in, among many others, non-stick coatings, lubricants, and firefighting foams (Gaines, 2022).

3.2 PFAS classification

PFAS, being a diverse chemical family, can be categorized into numerous subdivisions (Figure 1). An important distinction is between the classes of polymeric and nonpolymeric PFAS. Polymeric PFAS are high molecular weight compounds in which fluorinated carbon chains are incorporated in a polymeric structure, such as Teflon® (Plunkett, 1941). Although annually produced in large quantities, estimated above 230 000 ton (Evich et al., 2022), they are generally characterized by lower mobility and bioavailability than their non-polymeric counterparts (Henry et al., 2018). It has, however, been shown that certain fluorinated polymers can degrade into more mobile and bioavailable compounds (Washington et al., 2015). Fluoropolymer production may also act as an emission source of other PFAS used or formed in the manufacturing process (Lohmann et al., 2020).

The non-polymeric PFAS constitute a very large and diverse molecular class, but are in many cases low molecular weight, highly mobile, and bioavailable (Adu et al., 2023; Brunn et al., 2023; Martin et al., 2003; Ragnarsdóttir et al., 2024; Rauert et al., 2018). This class can, in turn, be divided into the subclasses of polyfluorinated substances and perfluorinated substances, where every carbon atom of the alkyl moiety is fully fluorinated in a perfluorinated compound, as opposed to only some of the alkyl moiety carbon atoms in a polyfluorinated compound (Buck et al., 2011). The polyfluorinated compounds are, at present, produced in substantially higher quantities than the perfluorinated ones (Evich et al., 2022). They are also less stable than the perfluorinated compounds and are, in many cases, susceptible to environmental transformation (Butt et al., 2014), eventually resulting in a perfluoroalkyl end product (Evich et al., 2022). They are thus commonly referred to as PFAS precursors. The perfluoroalkyl moiety of a perfluorinated PFAS is, with the exception of the perfluoroalkanes, attached to a functional group based on which the compound can be further classified into groups. The group of most relevance within environmental science is the perfluoroalkyl acids (PFAA), and its subgroups of perfluoroalkyl carboxylic acids (PFCA) and the perfluoroalkyl sulfonic acids (PFSA) (Megson et al., 2025). The PFCA are characterized by a carboxylic acid functional group, such as perfluorooctanoic acid (PFOA), while the PFSA are characterized by a sulfonic acid functional group, such as perfluorooctane sulfonic acid (PFOS).

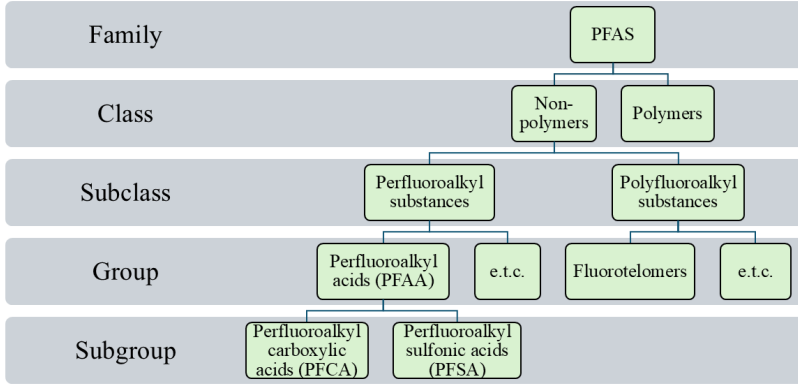

Figure 1. PFAS classification, using the hierarchical naming convention described by the Interstate Technology & Regulatory Council (ITRC) (Interstate Technology Regulatory Council (ITRC), 2026).

These subgroups of PFAS can then be further classified based on the length of the perfluoroalkyl chain (Table 1). The physicochemical properties of these compounds vary greatly with the length of this moiety, and perfluoroalkyl acids (PFAA) are thus often referred to as long- or short-chain based on their bioaccumulative behavior. Longer-chain PFAS have been shown to be more bioaccumulative (Conder et al., 2008). The most accepted definition is to classify PFSA with a perfluoroalkyl chain length $\geq$6 and PFCA with a perfluoroalkyl chain length $\geq$7 as long-chain PFAS, while shorter chained compounds are classified as short-chain PFAS (Buck et al., 2011; OECD, 2021). Additionally, the term ultra-short-chain PFAS was introduced in the environmental field in the late 2010s to describe PFAA with very short perfluoroalkyl chains ($\leq$2 for PFCA and $\leq$3 for PFSA), distinguishing them from conventional short-chain PFAS due to their high environmental mobility, associated analytical challenges, and difficulty of removal from water (Ateia et al., 2019; Björnsdotter et al., 2019, 2020).

Table 1. PFCA and PFSA with perfluoroalkyl chain lengths of 1-14. Ultra-short-chain PFAS are marked in blue, short-chain PFAS are marked in green, and long-chain PFAS are marked in yellow

Carboxylic acids	Sulfonic acids	Perfluoroalkyl chain length
Trifluoroacetic acid TFA	Trifluoromethane sulfonic acid TFMS	1
Perfluoro propionic acid PFPrA	Perfluoroethane sulfonic acid PFEtS	2
Perfluorobutanoic acid PFBA	Perfluoropropane sulfonic acid PFPrS	3
Perfluoropentanoic acid PFPeA	Perfluorobutane sulfonic acid PFBS	4
Perfluorohexanoic acid PFHxA	Perfluoropentane sulfonic acid PFPeS	5
Perfluoroheptanoic acid PFHpA	Perfluorohexane sulfonic acid PFHxS	6
Perfluorooctanoic acid PFOA	Perfluoroheptane sulfonic acid PFHpS	7
Perfluorononanoic acid PFNA	Perfluorooctane sulfonic acid PFOS	8
Perfluorodecanoic acid PFDA	Perfluorononane sulfonic acid PFNS	9
Perfluoroundecanoic acid PFUnDA	Perfluorodecane sulfonic acid PFDS	10
Perfluorododecanoic acid PFDoDA	Perfluoroundecane sulfonic acid PFUnDS	11
Perfluorotridecanoic acid PFTrDA	Perfluorododecane sulfonic acid PFDoDS	12
Perfluorotetradecanoic acid PFTeDA	Perfluorotridecane sulfonic acid PFTrDS	13
Pentadecafluorundecanoic acid PFPeDA	Perfluorotetradecane sulfonic acid PFTeDS	14

3.3 Persistence

The carbon-fluorine covalent bond is one of the strongest bonds known in organic chemistry, owing to fluorine being the most electronegative element in the periodic table, thus creating a highly polarized bond, with a strong

electrostatic attraction between the carbon and fluorine atoms (O'hagan, 2008). As a result, fluorinated carbon chains exhibit exceptional resistance to thermal, chemical, and biological degradation processes (Ochoa-Herrera et al., 2016; Toporek et al., 2021; Xiao et al., 2020). This stability is particularly pronounced in perfluoroalkyl substances, in which all hydrogen atoms on the carbon backbone are replaced by fluorine, effectively shielding the molecule from nucleophilic attack and oxidative or reductive transformation (Leung et al., 2023). These compounds consequently become highly persistent in environmental systems (Brunn et al., 2023; Rauert et al., 2018), earning the PFAS family its nickname "forever chemicals". Many polyfluoroalkyl substances, while initially more reactive, undergo stepwise degradation through abiotic or biotic pathways that ultimately yield highly stable perfluoroalkyl end products (Hamid et al., 2018; Lenka et al., 2021). There are increasing calls that the persistence of PFAS alone is sufficient to warrant regulation of the entire chemical family (Cousins et al., 2020).

3.4 Toxicity

Despite being a diverse chemical family, many PFAS exhibit relatively low acute toxicity (Ankley et al., 2021), with the lethal dose (LD_{50}) values of the most studied compounds, PFOA, and PFOS being measured in the hundreds of mg/kg body weight in rats, far exceeding environmentally relevant exposure levels (Peritore et al., 2023). Studies have, however, identified several potential chronic effects of PFAS exposure in humans, including, but not limited to, disrupted thyroid function (Lopez-Espinosa et al., 2011), liver cancer (Girardi & Merler, 2019), and increased cholesterol levels (Steenland et al., 2009).

A large epidemiological study carried out in the Ohio Valley, USA, encompassing 69 030 individuals exposed to PFOA in their drinking water from a fluorochemical plant, showed probable links between PFOA exposure and increased cholesterol levels, ulcerative colitis, thyroid disease, testicular cancer, kidney cancer, and pregnancy-induced hypertension (Steenland et al., 2020). Some of these findings have later been disputed by other researchers (Boston et al., 2025). Similar studies have been carried out in Ronneby, Sweden, where 16 150 individuals were exposed to PFAS in their drinking water, following contamination from a nearby firefighting training

area. These studies did not show evidence of an increased risk of thyroid disease or overall risk of cancer, although a modest increased risk of kidney cancer was observed (Andersson et al., 2019; H. Li et al., 2022), as well as a significant increase in cholesterol levels for the exposed cohort (Y. Li et al., 2020).

A study examining 101 German children under the age of 1, sampled during the 1990s, found significant correlations between the children's PFOA concentrations and their antibody response after receiving vaccines. This effect was seen at plasma concentrations of 12.2 µg/L for one of the vaccines, and the antibody expression between the lowest and highest exposure quintiles (Q1-Q5) was reduced for PFOA by between 53% and 86% (Abraham et al., 2020).

Work has been carried out to derive a set of relative potency factors for PFAS in order to be able to make a risk estimate of PFAS mixtures. Bil et al (Bil et al., 2021) have produced a widely cited set of these for PFAS based on liver toxicity. These relative potency factors have been expressed as PFOA equivalents, where C7-C12 PFAA were shown to be equally or more potent than PFOA while the opposite applies for <C7 and >C12 PFAA. The fluorotelomer alcohols and perfluoroalkyl ether carboxylic acids examined were found to be less potent than PFOA.

The heterogeneity of PFAS makes it difficult to draw generalized ecotoxicological conclusions for the family as a whole. While laboratory studies investigating the toxic effects of PFOS and PFOA are abundant (Mai et al., 2026; Sun et al., 2023; Y. Wang et al., 2024; D. Xu et al., 2013), there are relatively few ecotoxicological field studies on PFAS. Many of these, while identifying links between biomarkers and PFAS exposure, fail to draw any conclusions regarding actual adverse ecotoxicological effects (Ankley et al., 2021). Effects have, however, been identified, such as reduced reproductive success in great tit populations exposed to PFOS (Groffen et al., 2019) or enlarged livers in fish exposed to PFAS-containing aqueous film forming foams (AFFF) (Oakes et al., 2010). An example of the ecotoxicological heterogeneity of PFAS are the fluorinated plant protection products (FPPP), such as sulfluramid, that are, considerably more potent than PFSA or PFCA regarding invertebrate toxicity (Ankley et al., 2021), and intentionally so, as they are used as insecticides.

3.5 Regulations

As the health risks associated with PFAS became apparent, the PFAS chemical family came under increasing regulatory scrutiny. Consequently, PFOS was added to the list of restricted substances by the United Nations under the Stockholm Convention in 2009. PFOA and PFHxS, were subsequently added to the convention as substances to be eliminated in 2019 and 2022, respectively, followed by all long-chain PFCA in 2025 (UNEP & Stockholm Convention, 2025).

The approaches taken to PFAS regulation on the national level vary substantially (Brennan et al., 2021). The USA has, for example, at the federal level, introduced enforceable maximum contaminant levels in drinking water for six PFAS, including both single compound limits of 4-10 ng/L as well as levels of mixtures based on a hazard index (United States Environmental Protection Agency, 2025). Additionally, there is a patchwork of various state-based regulations (Brennan et al., 2021). Other countries, such as China, largely limit their policy responses in compliance with the Stockholm Convention, refraining from further regulations (Kookana et al., 2025), or like India, lack national PFAS regulations altogether (Norwegian Institute for Water Research (NIVA), 2025).

The European Union has taken a relatively stringent stance on PFAS, restricting several compounds under the REACH program (European chemicals agency, 2025). The recast European Drinking Water Directive, introduced in 2020 and enforceable across all EU Member States from 2026, limits the allowed PFAS concentrations in drinking water to 100 ng/L for a set of 20 PFAS and 500 ng/L for total PFAS, taking steps to regulate the entire chemical family (European Union (EU), 2020).

Certain EU member states, such as Sweden, have introduced even stricter regulations, including a 4 ng/L limit on drinking water for the sum of PFOA, PFNA, PFHxS, and PFOS (Livsmedelsverket, 2022). Sweden has also proposed preliminary accepted soil concentrations of PFOS (Petterson et al., 2015), and established legal threshold values for inland and coastal surface waters (Havs- och Vattenmyndigheten, 2019). The Swedish environmental quality criteria for groundwater are set to 4.4 ng/L PFOA equivalents for a set of 24 PFAS, utilizing the relative potency factor approach (Sveriges Geologiska Undersökning, 2023).

3.6 Sources

There are many potential emission sources for PFAS. Among point sources, one of the more obvious ones is the fluorochemical production plants, with the fluoropolymer production sites in Europe alone emitting more than 100 tons of PFAS to air and water in 2021 (Dalmijn et al., 2023). Numerous studies report risks to both ecological and human health in proximity to these production facilities (Groffen et al., 2019; Pan et al., 2017; Steenland et al., 2020; K. Xu et al., 2024), as well as the detrimental health effects on the industry's workers (Girardi & Merler, 2019). Industrial point sources of PFAS, however, are not limited to the factories where PFAS are produced, but also include industries where PFAS are used. These include the production of electronics, textiles, or electroplating, to name a few (Jia et al., 2025). Another major source of PFAS is AFFF use, as these are applied directly to the environment. PFAS source zones can be created after single application events, such as fire extinguishing (Aly et al., 2020), but more problematic are the firefighting training sites where AFFF has been applied to the same site on numerous occasions, creating a highly contaminated area with the risk of PFAS transport from the site, as an example, through migration into the groundwater (Pritchard et al., 2026). These sites are often located at airports or military installations (Salvatore et al., 2022).

Much of the PFAS from consumer products, such as PFAS leached from washed clothes or rinsing of PFAS-containing personal care products (Bălan et al., 2024; Schellenberger et al., 2022), combined with PFAS from consumed food and drink excreted by humans (Abraham et al., 2024), will eventually reach the wastewater system. These PFAS, combined with PFAS-containing stormwater from urban runoff (Kim & Kannan, 2007), will be collected in the wastewater treatment plants (WWTP). The WWTP, in turn, often lacks the capacity to treat PFAS, consequently making these facilities point sources for PFAS emission to aquatic ecosystems (Coggan et al., 2019). Many PFAS-containing consumer products will also eventually enter the solid waste system, where they, together with PFAS-containing industrial waste, might be landfilled. The landfill leachate plants are just like the WWTP, often unable to treat PFAS, resulting in environmental spread of PFAS from these facilities (J. Li et al., 2023).

A more diffuse source of PFAS is the agricultural sector. Here, PFAS is applied both intentionally in the form of FPPP (Joerss et al., 2024), as well as unintentionally through the fertilization of fields using sewage sludge or

other biosolids (Bolan et al., 2021; Johnson, 2022). Another diffuse source of PFAS are the so-called F-gases, including hydrofluorocarbons and hydrochlorofluorocarbons used as refrigerants. Many of these highly volatile compounds will, upon release, transform to the ultra-short PFCA trifluoroacetic acid (TFA) (Arp et al., 2024). Measurements of TFA in rainwater across different sites suggest that there is a well-mixed abundance of these precursor compounds in the atmosphere (Berg et al., 2000).

3.7 Transport and biomagnification

PFAS are highly mobile in the environment, exhibiting multiple modes of transport (Evich et al., 2022). Atmospheric transport has been shown not only for volatile PFAS, but also for ionizable PFAS sorbed to dust or dissolved in aerosols (Faust, 2022; H. Xu et al., 2025). While atmospheric transport distributes PFAS globally, these modes of transport are also important on a more local scale, such as coastal regions being affected by PFAS deposition from aerosols formed by sea spray (Casas et al., 2023). Most PFAS are also readily soluble in water and are thus transported through water systems and deposited through precipitation (Kurwadkar et al., 2022).

As a result of its persistence and mobility, PFAS have reached a ubiquitous status, being detected from deep oceans to polar snow (Xie & Kallenborn, 2023; X. Zhang et al., 2019), ultimately being deposited in the major long-term sink of the deep-sea sediments (Sackett et al., 2024).

There are several paths for PFAS to enter the food web. One of the main pathways in the terrestrial ecosystems is through plant uptake, as many PFAS are readily taken up and accumulated by plants through the transpiration process, and those that are not might still accumulate on or in root tissue (J. Xu et al., 2024). PFAS might also enter the food web directly, through the consumption of PFAS-containing water sources (Wilson et al., 2021). Other potential pathways include direct dermal or respiratory uptake (Hopkins et al., 2023; Ragnarsdóttir et al., 2024). PFAS might enter the aquatic food web through uptake by phytoplankton or macrophytes (Z. wei Chen et al., 2024; X. Zhang et al., 2019), and directly by aquatic animals such as fish (Xiong & Li, 2024). Many PFAS, particularly long-chain compounds, are bioaccumulative and biomagnification through the trophic levels has been shown in both aquatic and terrestrial ecosystems (Haukås et al., 2007; Huang

et al., 2022). Although trophic magnification appears comparable between aquatic and terrestrial food webs (Ricolfi et al., 2025), PFAS concentrations are generally higher in aquatic organisms. This likely reflects higher baseline exposure in aquatic environments, driven by the mobility and persistence of PFAS in water, combined with longer or more complex food webs that can amplify accumulation (Gkika et al., 2025).

Groundwater transport

One important transport pathway for PFAS is the infiltration into groundwater. This can occur directly from contaminated soil, such as from fire training facilities, from landfill leachate, or via contaminated precipitation (Guelfo & Higgins, 2013; Hepburn et al., 2019; Schroeder et al., 2021).

The transport of PFAS in groundwater systems can be described as advection (hydraulic flow) and dispersion (including diffusion) combined with a retardation factor unique to the PFAS and the characteristics of the groundwater system. A simplified equation for the PFAS retardation has been proposed by Brusseau et al (Brusseau & Guo, 2022), as shown in equation 1:

$$R_d = (1 + K_d \times \frac{\rho_b}{\theta_w} + K_{aw} \times \frac{a_{aw}}{\theta_w}) \quad \textbf{(1)}$$

Where K_d is the solid-liquid partitioning coefficient (cm3/g), K_{aw} is the air-water interfacial adsorption coefficient (cm3/cm2), a_{aw} is the specific air-water interfacial area (cm2/cm3), ρ_b is the porous-medium bulk density (g/cm3), and θ_w is volumetric water content (cm3/cm3).

This equation thus describes that PFAS retardation in the groundwater system is mainly influenced by sorption to the solid phase, governed by K_d, and the air-water interface, governed by K_{aw}. This tends to create a large PFAS reservoir in the vadose zone of contaminated areas, as this unsaturated zone contains an abundance of both types of interfaces (J. Zeng et al., 2021). PFAS in the vadose zone can then be mobilized by precipitation events, transporting them to the groundwater saturated zone (Das et al., 2024). The PFAS retardation in the groundwater saturated zone will, instead, largely be governed by the K_d, thus making this parameter highly important for predicting PFAS transport through a groundwater system.

The K_d of many PFAS is relatively low, especially in soils with low organic carbon (OC) content and coarser grain sizes (Hubert et al., 2023). Moreover, K_d values have been shown to be strongly correlated with perfluoroalkyl chain length as well as the functional group chemistry (Higgins & Luthy, 2006). This makes many PFAS highly mobile in the groundwater-saturated zone, resulting in large groundwater contaminant plumes from contaminated sites. There are numerous instances where these groundwater plumes have come to contaminate drinking water wells (Eschauzier et al., 2013; Hohweiler et al., 2024; Sörengård et al., 2022). As a substantial portion of the global drinking water supply originates from groundwater sources, it is crucial that efficient and sustainable solutions for treating PFAS-contaminated groundwater are developed.

3.8 Treatment Methods

Treatment methods for PFAS-contaminated groundwater can broadly be divided into *in situ* and *ex situ* solutions, where *in situ* treatment methods refer to methods that address contaminated groundwater directly within the aquifer. The most common *in situ* approach is to introduce soil amendments to the aquifer in order to increase the K_d of PFAS to such an extent that they are immobilized. This can be used to either stabilize a PFAS source zone or create a barrier across a contaminant plume (Divine et al., 2025; Niarchos et al., 2023). A range of different additives have been investigated, such as activated carbon (AC) (Niarchos et al., 2023), polymer resins (C. Liu et al., 2022), and biochar (Sørmo et al., 2024).

In contrast, *ex situ* remediation is based on the extraction of the contaminated water from the aquifer prior to treating it. A practice known as pump and treat. This can be done to reduce the contaminant mass of a hotspot, or to create a barrier across a contaminant plume by introducing a cone of depression, limiting groundwater flow (Newell et al., 2025).

The treatment methods applied to the extracted water can, in turn, be divided into methods for separating or destroying the PFAS. The following sections contain a non-exhaustive summary of established and emerging separation and destruction techniques that could be applied following groundwater extraction, as outlined in Figure 2, with an emphasis on the technologies covered by the experimental work of this thesis: FF, phytoextraction, and EO.

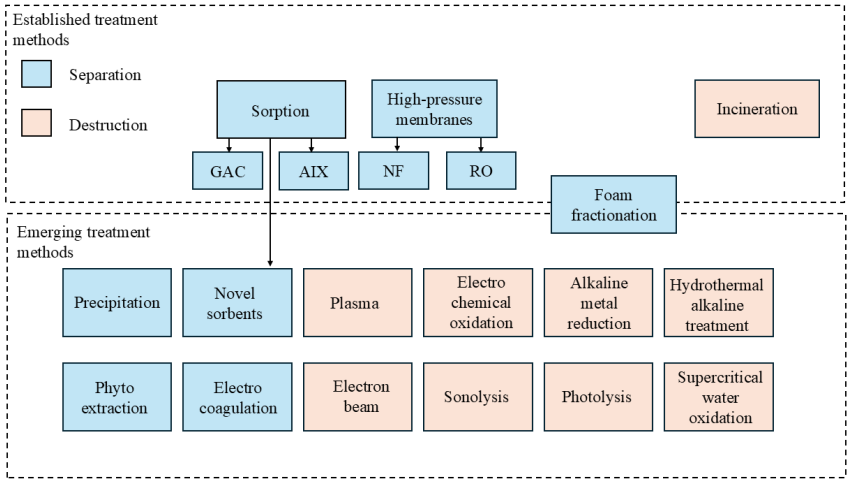

Figure 2. An overview of treatment methods applicable to PFAS-contaminated water streams. Note that this figure is not exhaustive for all methods currently being developed or tested for PFAS treatment. GAC = Granular activated carbon, AIX = Anion exchange, NF = Nanofiltration, RO = Reversed Osmosis.

3.8.1 Established separation techniques

Once contaminated water has been extracted, a technology is required to separate the PFAS from the water. Here, GAC has long been the industry standard (Elisabeth Hawley et al., 2012). Contaminated water is filtered through the carbon, which sorbs the PFAS, separating it from the water. This is especially efficient for long-chain PFAS, while short-chain PFAS achieves an earlier breakthrough (C. Zeng et al., 2020). A similar technique involves the use of resins, polymers with functional groups designed to capture PFAS. The treatment principle is similar to that of GAC; water is passed through the resins that sorb the PFAS. Particularly, AIX resins have been shown to be more efficient than GAC for PFAS capture, achieving higher treatment efficiencies and lasting longer before breakthrough (Rückbeil et al., 2025). The AIX sorbs PFAS through a combination of hydrophobic and electrostatic interactions, utilizing the negatively charged headgroup of many PFAS by containing positively charged functional groups (Mohammadi et al., 2025). Substantial developments are currently being made on the development of sustainable resin regeneration, removing the PFAS from the resins as a concentrated waste stream, enabling their re-use (Ellis et al., 2025; Ling et al., 2025).

Another option is membrane separation techniques, such as NF or RO. These processes rely on semi-permeable membranes but differ in their separation mechanisms. Nanofiltration membranes have pores and typically carry a surface charge, meaning separation occurs through a combination of size exclusion and electrostatic interactions. As a result, NF is generally more effective for long-chain PFAS, which are larger and more strongly repelled by the membrane, whereas short-chain PFAS can more easily pass through due to their smaller size and weaker interactions (Casella et al., 2026). In contrast, reverse osmosis membranes are effectively non-porous, and separation is governed by a solution-diffusion mechanism, where water dissolves into and diffuses across the dense membrane matrix while PFAS are rejected (Ma et al., 2024).

3.8.2 Emerging separation techniques

Beyond GAC and AIX, there is a range of novel sorbents being developed and tested for PFAS treatment (Burkhardt et al., 2025). Examples include metal organic frameworks (MOF), crystalline structures consisting of metal nodes interlinked by organic bridges, which PFAS diffuse into and sorb to (R. R. Liang et al., 2025). These materials have been shown to have very high PFAS sorption capacities, also for short-chain PFAS (Y. Zhang et al., 2024), be regenerable (R. R. Liang et al., 2024), and have additionally been shown to be able to act as catalysts for PFAS destruction (Y. Wang et al., 2021).

Another class of novel PFAS sorbents includes hydrogels, gel-like structures made of cross-linked polymers (Kumar et al., 2025). These polymers can then be given a range of functional groups to aid in PFAS capture, such as the ionic fluorogels combining charged and perfluoroalkyl groups to sorb PFAS through a mix of ion exchange and fluorophilic interactions (Kumarasamy et al., 2020). As with MOF, gels can also be given functional groups capable of acting as catalysts for PFAS destruction (Zhu et al., 2020).

While MOF and hydrogels are highly engineered advanced materials, with specific versions tailored for PFAS sorption, there is also growing interest in biochar as a low-cost and sustainable sorption material. Biochar is pyrolyzed biomass and comes in many forms depending on substrate and pyrolysis conditions used, with the aim of providing a more economical and sustainable alternative to fossil GAC (Akbarpour et al., 2026). With sorption

mechanisms similar to those of GAC, biochar has shown promise for the sorption of especially long-chain PFAS (Kearns et al., 2021).

Other emerging removal techniques include flocculation and precipitation, followed by sedimentation (Hubert et al., 2024) as well as electrocoagulation (Y. Liu et al., 2022).

Foam fractionation

A unit operation within chemical engineering that utilizes the surface-active properties of a compound to separate it from a liquid using air sparging is FF. A surface-active compound will partition to the air-water interface introduced as bubbles by the sparging and then rise to the surface of the liquid, from where it can be separated. FF has been used in industry since the 1960s, finding early uses in the separation of proteins from food process water (Buckley et al., 2022).

Many PFAS are surface-active, such as PFCA and PFSA, due to their hydrophilic head groups and hydrophobic tails, making them amenable to separation through FF. The company EPOC-Enviro has developed the foam fractionation technique into its surface-active foam fractionation unit (SAFF®). This unit deploys several foam fractionation steps in series to produce a highly concentrated foam and has been used to good effect for separating long-chain PFAS from contaminated waters. The separation effect is, however, less efficient for short-chain PFAS (Burns et al., 2021).

Studies using different FF systems confirm that long-chain PFAS are efficiently removed, and their short-chain counterparts less effectively so (Smith et al., 2022; Smith, Lewis, et al., 2023). One strategy to improve short-chain PFAS separation is the use of co-foaming additives, i.e. surfactants that increase foam formation, as well as improving foam properties and thus also increasing short-chain PFAS separation. The most effective additives are the cationic surfactants, as they both attract and reduce the repulsion between the negatively charged headgroups of many PFAA, with cetyltrimethylammonium bromide (CTAB) as an example (Buckley et al., 2023). Many classes of cationic surfactants are, however, toxic, due to their ability to interact with negatively charged biological membranes (Gilbert & Moore, 2005; C. Zhang et al., 2015). Therefore, a range of non-toxic co-foaming surfactants are being explored, such as a shea butter-derived surfactant (Klevan et al., 2025).

Another application of PFAS separation through FF is integrated FF, where foam created during conventional wastewater treatment methods is

collected in order to remove PFAS (Smith, Keane, et al., 2023; We et al., 2026).

Phytoextraction

Phytoremediation is the use of plants to remediate contaminated soil, water, or air. Plant uptake and accumulation of several PFAS have been shown in studies of agricultural crops, initially examining the issue from a food safety perspective (Felizeter et al., 2014; Krippner et al., 2014; H. Zhang et al., 2016). These studies have later been followed by specific phytoremediation studies, investigating plant uptake and translocation, also known as phytoextraction (Gobelius et al., 2017), as well as immobilization of PFAS in the root zone (T. Jiang et al., 2025; M. Liang et al., 2025). These phytoremediation trials show a clear correlation between PFAS translocation and chain length, with short-chain PFAS being translocated to above-ground plant parts, while long-chain PFAS are accumulated in root tissue. This is thought to be influenced by the casparian strip, a protective barrier within the plant root, which appears to be permeable by short-chain PFAS, but not by their long-chain counterparts (J. Xu et al., 2024).

While many studies have focused on phytoextraction from contaminated soil (Gobelius et al., 2017; Nassazzi et al., 2023; W. Zhang & Liang, 2025), there are also studies investigating the use of phytorextraction to separate PFAS from a water stream. This can be achieved by irrigating a field planted with vegetation selected for its potential to extract PFAS (Ramstedt, 2024); however, this approach carries the risk of contaminating large quantities of soil, as well as the potential migration of PFAS to the groundwater. As an alternative, the use of a constructed wetland (CW) could be a preferable option, as it allows better control over subsurface contamination. Several kinds of CW are being studied for PFAS remediation purposes, open water CW, where PFAS is separated through phytoextraction by plants growing on the bottom or banks of the system, as well as through sedimentation (P. Wang et al., 2019), and floating CW, where plants are placed on rafts on the water surface, enabling their roots to filter the water (Greger, 2021). There are also subsurface flow CW, where the water is passed through a filter medium perforated with the roots of the plants growing in the system. This solution allows for sorption of PFAS to the media itself or biofilm formed on the media, as well as separation through phytoextraction (Lott et al., 2023).

3.8.3 Established destruction techniques

After being separated from the water stream, the concentrated PFAS matrix (i.e. spent sorbent, foamate, biomass e.t.c.) needs to be handled safely with the goal of destroying the PFAS. The current standard for PFAS destruction, and the most widely established destruction technique for PFAS, is incineration (Longendyke et al., 2022). While highly thermally stable, PFAS will eventually degrade at sufficiently high temperatures. However, the exact temperatures necessary for complete thermal degradation are debated. Over 80% defluorination of PFAS has been achieved at 800 °C (J. Wang et al., 2022), but fluoroorganic byproducts have still been recovered at temperatures exceeding 1000 °C (Winchell et al., 2021). There is also evidence of incomplete PFAS degradation at commercial incineration facilities (Björklund et al., 2023; S. Liu et al., 2021). Various additives have been shown to reduce the defluorination temperature of PFAS (J. Chen et al., 2026), with one study finding calcium hydroxide to be highly efficient (F. Wang et al., 2015).

3.8.4 Emerging destruction techniques

There are several emerging destruction techniques for PFAS (Meegoda et al., 2022). One example is plasma treatment, which degrades PFAS through a combination of PFAS interaction with radicals formed in the media during treatment, such as hydroxyl radicals (•OH), and direct reduction by plasma electrons or hydrated electrons formed by the plasma (Nzeribe et al., 2019).

Another technique is photodegradation, where UV or vacuum-UV irradiation is applied to either weakly excite PFAS molecules, occasionally leading to direct photochemical transformation, or to activate photocatalysts such as TiO_2 that produce reactive charge carriers and radicals capable of indirectly degrading PFAS (F. Liu et al., 2022). This technology is suitable to combine with novel sorbent materials containing embedded catalysts such as MOF or hydrogels (Y. Wang et al., 2021; Zhu et al., 2020).

Sonolysis uses ultrasound to induce acoustic cavitation, leading to the formation and violent collapse of microbubbles that generate extreme localized temperatures and pressures capable of thermally decomposing PFAS (Tasca et al., 2026). The formation of highly reactive hydrated electrons has also been suggested as a potential pathway for PFAS degradation in ultrasound systems (James et al., 2020).

Electron beam technology, instead use magnetic fields to accelerate generated electrons into the target, resulting in reactive reductive and oxidative radicals, including highly reactive hydrated electrons (L. Jiang et al., 2022). A benefit of the electron beam technology is that it can be applied to both solutions and solid samples, with one study degrading 10 PFAS of varying chain length and functional groups to below detection limits in a contaminated soil (Lassalle et al., 2021). The technology has been shown to be highly pH dependent, showing higher treatment efficiencies at high alkaline conditions, likely due to the increased longevity of the hydrated electrons at higher pH (Feng et al., 2021).

Alkaline metal-mediated reduction of PFAS represents a recently emerging, laboratory-scale approach based on the reduction of PFAS by alkali metals. A recent study demonstrating 94% defluorination of PFOA through a lithium-mediated reduction reaction in dimethyl sulfoxide (DMSO) (Sarkar et al., 2026). While limited by the fact that the degradation takes place in an organic solvent, there might still be applications such as the treatment of sorbent regenerant solutions.

Hydrothermal treatment is another emergent technology for PFAS destruction, which can be conducted under subcritical or supercritical conditions (J. Li et al., 2022). Under supercritical conditions, known as supercritical water oxidation, PFAS is oxidized by radicals formed in the media such as •OH (Prasetya et al., 2025). This technology is in the early stages of commercializing for PFAS treatment with available commercial-scale systems shown to achieve >99% PFAS degradation when treating mixtures of short- and long-chain PFAS, by also adding hydrogen peroxide to the reactor, increasing radical formation (Scheitlin et al., 2023). Under subcritical conditions, increasing the pH shifts the dominant degradation pathway from hydrolysis to hydroxide nucleophilic attack, inducing C-F bond cleavage. This technique is called hydrothermal alkaline treatment (HALT), and has been proven to be highly efficient for PFAS degradation (Hao et al., 2021).

Electrochemical Oxidation

A destruction method that operates by inducing a current between two electrodes in the contaminated media is EO. PFAS degradation occurs through a combination of direct electron donation from the PFAS molecule to the anode and PFAS reaction with oxidizing agents, also formed at the anode surface, causing a consecutive stepwise chain shortening of the PFAS

molecule (Mirabediny et al., 2023). The choice of anode material is thus a crucial parameter. There are several different materials being tested, such as cerium-doped lead oxide (Niu et al., 2012), titanium (III,IV) oxide (S. Liang et al., 2022) or antimony-doped tin dioxide carbon aerogels (Zhao et al., 2013). One promising anode material is boron-doped diamond (BDD) (Tasca et al., 2025).

BDD exhibits a high oxygen evolution overpotential, which suppresses oxygen gas formation and allows operation at elevated anodic potentials. As a result, high concentrations of reactive, weakly adsorbed •OH can accumulate at the electrode surface, enabling strong direct oxidation of recalcitrant contaminants such as PFAS, making BDD particularly suitable for their degradation (Radjenovic & Sedlak, 2015). The production of BDD electrodes also requires a relatively low input of critical raw materials, as compared to other stable electrode materials, such as platinum-based electrodes (Pierpaoli et al., 2020). The cathode is usually made of titanium or stainless steel (Mirabediny et al., 2023), but it is possible to use BDD for both electrode types (Soriano et al., 2017). EO has been shown in some studies to efficiently degrade PFAS, with destruction rates >90 %, often coupled with high mineralization rates, calculated from mass balances (Niu et al., 2012; Soriano et al., 2017; Zhao et al., 2013).

While EO has demonstrated the ability to degrade PFAS, incomplete degradation and the formation of transformation products, including shorter-chain PFAS or other fluorinated by-products, remain a concern (Rehnstam et al., 2024), which is shared by all the destructive technologies discussed in this section.

3.8.5 Treatment trains

It has become apparent during the development of PFAS treatment techniques that there is currently no single perfect technology. As a result, several technologies are often combined in so-called treatment trains. One of the more common approaches is to combine a separation method with a destruction method, as the destruction methods are often too costly and energy-prohibitive to use on a dilute PFAS stream. Examples of this include separation of PFAS by NF followed by destruction with EO of PFAS in the concentrated reject water (Soriano et al., 2017). Destruction by EO has similarly been deployed for PFAS in concentrated foamate created by FF (Smith, Lauria, et al., 2023; Uwayezu et al., 2024) or the concentrated PFAS

waste stream created during the regeneration of AIX resins (S. Liang et al., 2022). Separation of PFAS from water using GAC has instead been coupled with thermal degradation of the PFAS sorbed to the carbon, which also regenerates the GAC (J. Wang et al., 2024; Xiao et al., 2020), while a hydrothermal approach has been tested to degrade PFAS in plant tissue, separated from a water stream through phytoextraction (W. Zhang et al., 2021).

There are also instances where multiple separation techniques are applied in series. This could be due to the original reject stream still being too dilute for cost-efficient destruction, such as applying FF, GAC, or IX to NF reject water (Franke et al., 2019; McCleaf et al., 2023). Alternatively, sequential treatment can also be used to prolong the life span of a sorbent, such as reducing the PFAS load on AIX resins by first applying FF, increasing the operational time until the resins need to be replaced (Burns et al., 2021).

Finally, there are also instances where several destructive techniques are combined to increase their potency. For example, combining EO and UV treatment has been proven to result in a higher treatment efficiency than either of the methods on their own. This is likely caused by UV turning oxidizing agents created by the EO into more reactive radicals in the bulk solution, thus not limiting PFAS degradation to the anode surface (Uwayezu et al., 2023).

4. Materials and methods

This thesis investigates PFAS behavior in the groundwater zone and evaluates PFAS treatment strategies for a landfill leachate-impacted aquifer (Figure 3).

- Paper **I** determined the K_d for PFAS found across three contaminated aquifers, including one impacted by landfill leachate. This included the evaluation of the saturated paste extraction method (SPEM) for the determination of PFAS K_d and the comparison of the method with conventional batch leaching tests and field-derived K_d.

- Paper **II** explored the implementation of a full-scale treatment train for the removal of PFAS from leachate and leachate-impacted groundwater, combining PFAS separation through FF with PFAS destruction using EO.

- Paper **III** investigated the use of a pilot-scale planted subsurface flow CW for the treatment of PFAS in leachate-impacted groundwater, including the evaluation of multiple plant species.

- Paper **IV** investigated the addition of a pilot-scale planted subsurface flow CW planted with *Salix* as a polishing step following the treatment train demonstrated in Paper **II**.

Detailed methods are given in each paper, and a general overview of the methodology is presented below.

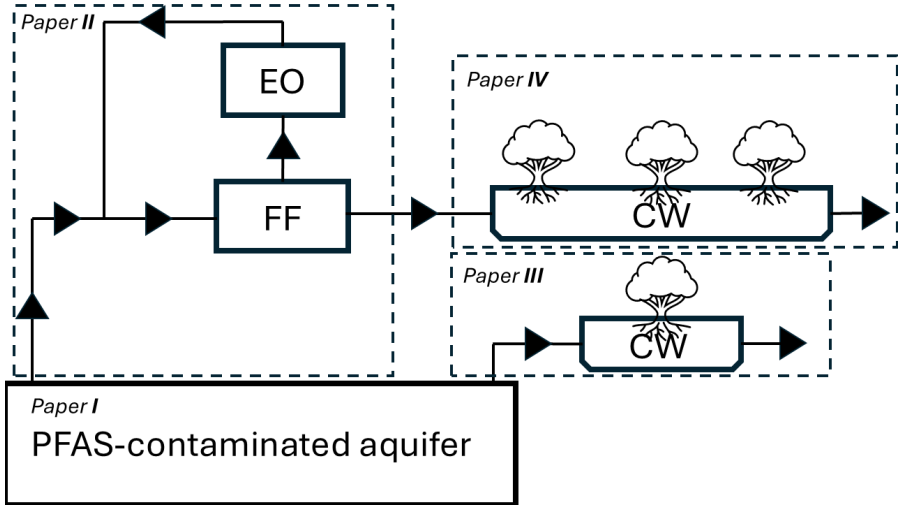

Figure 3. Method overview of the four papers included in the thesis.

4.1 Site description

All studies included in this thesis were partly or fully carried out at the same site. The site is an active municipal solid waste management facility, located in central Sweden. The site contains a discontinued landfill on which incineration ashes and other industrial waste were deposited from the 1970s to the late 2010s. The landfill was capped following discontinuation, with a maximum volume of 5 L m^{-2} $year^{-1}$, able to infiltrate through the capping.

Elevated PFAS concentrations in the groundwater have been detected by the site owner, with the highest concentrations found in monitoring wells positioned downstream in the groundwater flow direction from the capped landfill. A subterranean impermeable barrier has previously been installed to contain contaminants at the site. Additionally, there is a drainage system collecting landfill leachate as well as draining groundwater upstream of the impermeable barrier and transporting it to an on-site leachate treatment plant.

4.2 Raw water acquisition

For Paper **II**, raw water for treatment with FF was extracted from a previously established on-site groundwater well, as well as from the above mentioned drainage system. The daily amount of extracted water varied from 60 to 150 m^3 per day, with 36 m^3/d consistently extracted from the

groundwater well. This amounted to a total extracted volume of 27 900 m^3 during the 11-month treatment period.

For Paper **III**, raw water for treatment in the CW was extracted from the same groundwater well used for Paper **II**. 50 L each for the eight CW was extracted during the initial 21 days, which was increased to 100 L per CW for the remaining 66 days of the treatment period.

For Paper **IV**, water for treatment in the CW was mainly taken from the FF effluent stream generated in the Paper **II** study. When the FF experienced prolonged periods of maintenance-related downtime during the summer of 2024, water was instead collected from a treatment pond connected to the on-site leachate treatment plant. The water was collected using 2.2 m^3 steel tanks, transported to and applied to the wetlands using a wheel loader. A total of 57.5 m^3 of FF effluent and 15.4 m^3 of water from the treatment pond were applied during the 176-day treatment period.

4.3 Determining K_d values for aquifer materials (Paper **I**)

Drill cores were collected through sonic drilling from three aquifers with known PFAS contamination, including two AFFF training sites, and the solid waste management facility constituting the main study site of this thesis. Groundwater collection wells were established in the boreholes, enabling the collection of groundwater samples from the same depths as the corresponding solid aquifer samples. K_d was then determined using the three methods described below (Figure 4). Equations used for determining K_d can be found under section 4.6 Data evaluation.

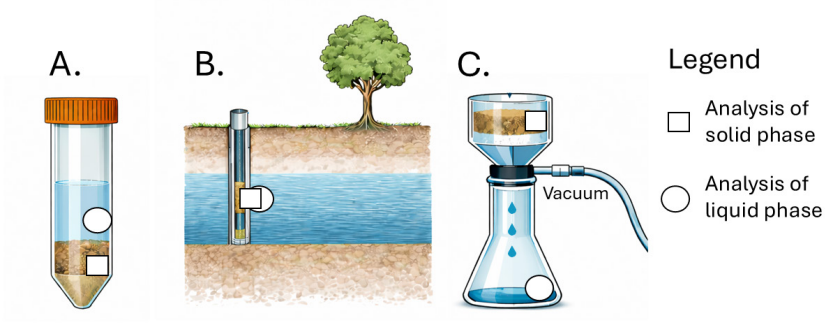

Figure 4. Overview of the different methods used for K_d determination in Paper **I**. A: batch leaching test. B: field-derived K_d. C: saturated paste extraction method (SPEM).

4.3.1 Batch leaching tests

Batch leaching experiments were performed at a liquid-to-solid ratio (L/S) of 1 using fresh soil samples. A total of 100 g dry weight (dw) equivalent soil was placed in 250 mL polypropylene (PP) centrifuge vessels, and ultrapure water was added to achieve L/S = 1, accounting for inherent soil moisture. The suspensions were agitated using an end-over-end shaker for 24 hours, followed by centrifugation to separate the solid and liquid phases.

Batch leaching tests are widely used to assess PFAS leaching, and there are multiple standard methods, usually employing an L/S of 0.5-20 and a test duration of 18-24 h (Navarro et al., 2024). Negative controls of centrifuge vessels with ultrapure water were used.

4.3.2 Saturated paste extraction method

SPEM is a leaching test conventionally used to assess soil salinity (Kargas et al., 2018), and has, to the best of the author's knowledge, not previously been used for PFAS K_d determination. The method was applied to soil samples by combining fresh material with ultrapure water until full saturation was reached, defined as the point just prior to the appearance of free-standing water. The saturated mixtures were covered and allowed to equilibrate at room temperature for 24 hours. Following equilibration, the

liquid phase was separated from the soil matrix using vacuum filtration through a PP Büchner funnel equipped with a glass fiber filter.

To evaluate the influence of extraction conditions, different vacuum filtration durations, ranging from 10 s to 1 h, were tested, including sequential collection of the liquid phase. Method performance was additionally assessed through negative controls consisting of ultrapure water and positive controls prepared from PFAS solutions of known concentration to evaluate potential contamination and the PFAS recovery of the method.

4.3.3 Field K_d

Field K_d was calculated based on the PFAS concentration of the solid aquifer material of the drill cores and corresponding groundwater samples collected at the same spatial location in the aquifer. Deriving field K_d values from drill cores and groundwater samples was recently done in a large survey of PFAS at U.S. military installations (Hunter Anderson et al., 2019).

4.4 Treatment methods

4.4.1 Foam fractionation (Paper **II**)

Full-scale FF was implemented using the 40-foot SAFF 20® containerized treatment system operated over 11 months (Figure 5). The system comprised two 2.6 m^3 primary FF vessels, in which air was introduced into the water column via venturi sparging to generate a PFAS-enriched foam, using a 20 min hydraulic residence time (HRT). The foamate was directed to a 1.6 m^3 secondary FF vessel to further concentrate PFAS and reduce the volume of the residual waste stream, using a 60 min HRT. The resulting concentrated foamate was extracted and collected for subsequent destructive treatment with EO, while the treated water phase from the secondary stage was recirculated within the system. Effluent from the primary stage was discharged for further treatment, with CW (Paper **IV**) or a conventional leachate treatment process. Water samples were collected from valves on the equipment (Figure 5) for a total of 16 FF batches.

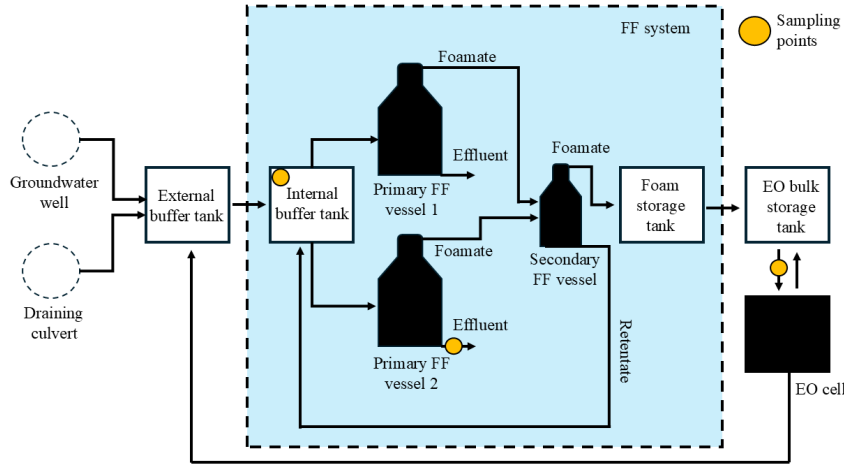

Figure 5. Method schematic of Paper **II**, depicting the FF and EO units.

In addition, the effect of co-foaming surfactants on PFAS separation was evaluated. The two non-ionic surfactants Polysorbate 20 and Polysorbate 80, as well as a cationic surfactant of which the composition is undisclosed due to patent protection, were dosed in separate experiments, into the primary fractionation stage at varying concentrations using the system's internal dosing equipment. These experiments were conducted with an extended HRT of 60 min to enhance the removal of short-chain PFAS and to assess the fate of the added surfactants within the treatment process. Water samples were collected for each test batch according to Figure 5.

4.4.2 Electrochemical oxidation (Paper **II**)

The collapsed concentrated foamate produced by the FF treatment was treated with EO, using a 1 L flow-through electrochemical cell with electrodes arrayed throughout the cell. Niobium coated with BDD was always used as the anode material, while the same material or stainless steel (SS) was used as the cathode. The total anode area was 10 dm^2. A voltage of 7 V and an electric current density of 10 mA/cm^2 were applied. The electrode polarity was reversed during the batches in order to limit electrode fouling. When BDD electrodes were used both as anode and cathode, this was done every hour. When SS cathodes were used, these only served as anodes for 10 min every 6^{th} hour, in order to not to deplete the cathode material. The collapsed foamate was continuously recirculated through the

electrochemical cell at a flow rate of 10 L/min from a 1000 L bulk storage tank, which was operated in batch mode with the entire volume replaced between batches. The collapsed foamate was returned to the external storage tank (Figure 5), following EO treatment, and thus returned to the FF. A total of nine batches were treated, where batch #1 exclusively used BDD electrodes, and batch nr #9 exclusively used the BDD-SS combination. The intermittent batches used both sets of electrodes as one set was in the cell while the other was in an acetic acid bath, with the two sets swapped several times per batch. This approach was taken in order to keep up continuous operation while also limiting electrode fouling. Samples were collected from a valve on the hose transferring foamate from the bulk storage tank to the flow cell (Figure 5). This was done prior to and at the end of each batch. Five and six samples were collected for batches #1 and #9, respectively, to assess the reaction kinetics.

4.4.3 Constructed wetland treatment (Papers **III** and **IV**)

The evaluation of treatment using CW was carried out at both pre-pilot (Paper **III**) and pilot (Paper **IV**) field scales for the treatment of PFAS-contaminated water. The systems were designed as lined planted basins filled with a filter substrate consisting of an 8:1:1 (v/v) mixture of lightweight expanded clay aggregates (LECA), peat, and biochar. The units were operated under saturated conditions, allowing horizontal subsurface flow through the basins.

At the pre-pilot scale (Paper **III**), eight parallel 1.2 m^2 CW were established to evaluate different plant species as well as unplanted controls (Figure 6). The selected wetland plants included tufted sedge (*Carex elata*), fiber hemp (*Cannabis sativa* - Futura 75), and two intercropped commercial hybrid willow cultivars (*Salix* Loden and *Salix* Wilhelm). Contaminated groundwater was supplied from a common buffer tank and distributed evenly across the systems. The CW were operated under controlled hydraulic loading conditions of 50 and later 100 L per day, with continuous inflow and internal recirculation. Effluent was discharged via overflow, and water samples were collected periodically for PFAS analysis. At the end of the 87-day experimental period (June – September 2022), plant tissues and substrate materials were collected to assess PFAS distribution within the system.

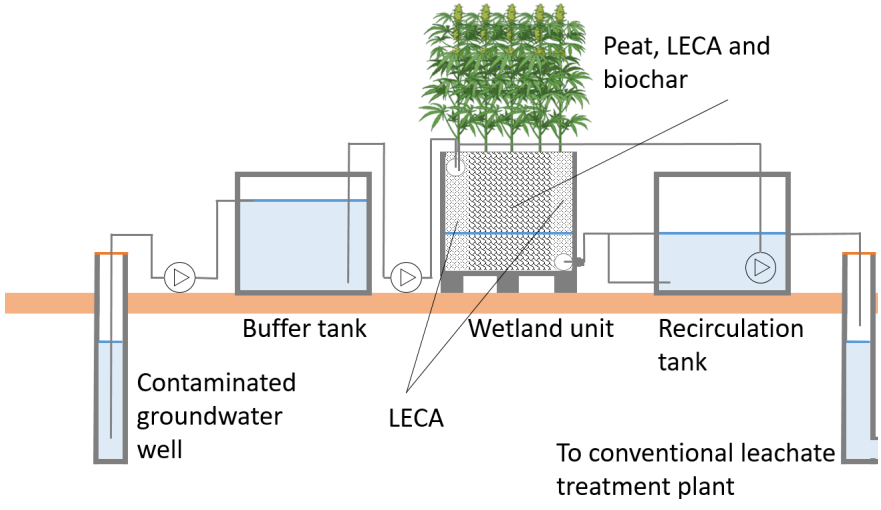

Figure 6. Schematic of the treatment setup used in Paper **III**. Republished with permission from Elsevier (Liljeström et al., 2025).

At pilot scale (Paper **IV**), a larger 147 m^2 CW was established as a sealed basin equipped with influent and effluent wells (Figure 7). The basin was filled with alternating sections of the same substrate mixture used in the study of Paper **III**, but also included LECA-only sections to improve flow through the system. The CW was planted with *S.* Wilhelm and allowed an initial establishment season prior to operation. During treatment, water was introduced at the influent well and allowed to be distributed throughout the CW, including through internal recirculation. Effluent discharge was controlled based on water levels, and effluent volume was monitored to regulate hydraulic loading, aiming for a 90% influent volume reduction. This reduction goal was, however, not met due to a combination of large volumes of water applied at once when water was taken from the treatment pond, overloading the system, and a faster than anticipated reduction in evapotranspiration rate in the fall, combined with rain events, achieving a total volume reduction of 48%. Influent and effluent streams were sampled monthly, and substrate and plant samples were collected at four time points, including one before the start and one after the end of the treatment period. The system was operated for 176 days (May - November 2024).

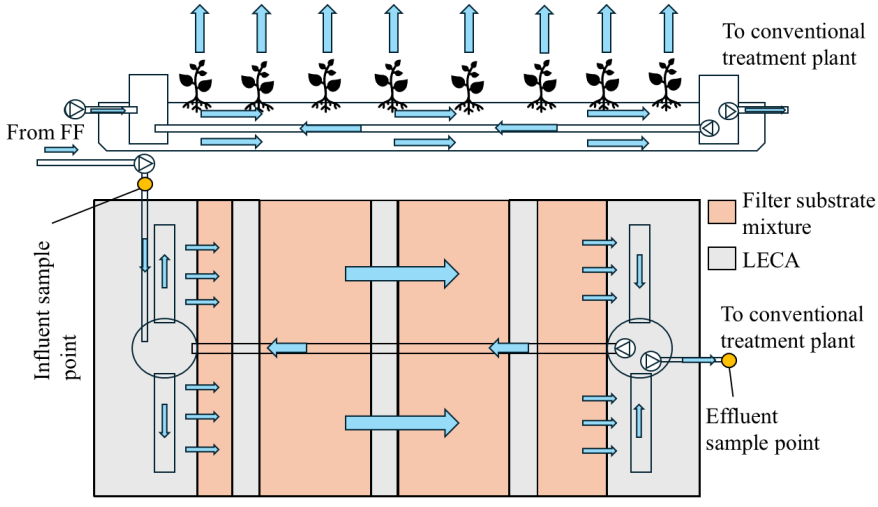

Figure 7. Schematic of the CW evaluated in paper **IV**.

4.5 Chemical analysis

4.5.1 PFAS analysis in water

For paper **III**, target PFAS analysis was performed in-house for 29 PFAS (Table 2) using a validated method previously described (Smith et al., 2022). Briefly, samples were filtered using 0.7 µm Whatman glass microfiber filters. Subsequently, samples were spiked with a mass-labelled standard mixture prior to solid phase extraction (SPE) with Oasis WAX cartridges (6 mL, 150 mg, 30 µm, Waters). Extracts were concentrated under a nitrogen stream before analysis on an ultraperformance liquid chromatography system coupled to tandem mass spectrometry (UPLC-MS/MS, Sciex Triple Quad 3500) using a Phenomenex Gemini® 3 µm C18 110 Å analytical column.

The water samples of Papers **I**, **II**, and **IV** were analyzed for 24-33 PFAS by Eurofins Sweden (Table 2).

A selection of FF influent samples was analyzed for total oxidizable precursors (TOP) by Eurofins Sweden, and all samples of one EO batch were analyzed for adsorbable organic fluorine (AOF) by Eurofins Sweden.

Table 2. Overview of PFAS analyzed in aqueous samples

PFAS	Paper I	Paper II FF	Paper II EO and co-surfactant tests	Paper III	Paper IV
PFBA	x	x	x	x	x
PFPeA	x	x	x	x	x
PFHxA	x	x	x	x	x
PFHpA	x	x	x	x	x
PFOA	x	x	x	x	x
PFNA	x	x	x	x	x
PFDA	x	x	x	x	x
PFUnDA	x	x	x	x	x
PFDoDA	x	x	x	x	x
PFTrDA	x	x	x	x	x
PFTeDA	x	x	x	x	x
PFBS	x	x	x	x	x
PFPeS	x	x	x	x	x
PFHxS	x	x	x	x	x
PFHpS	x	x	x	x	x
PFOS	x	x	x	x	x
PFNS	x	x	x	x	x
PFDS	x	x	x	x	x
PFDoDS	x	x	x		x
4:2 FTSA	x	x	x	x	x
6:2 FTSA	x	x	x	x	x
8:2 FTSA	x	x	x	x	x
6:2 FTAB	x				
HPFHpA	x	x	x		x
HFPO-DA				x	
PFECHS				x	
NaDONA				x	
FOSA	x	x	x	x	x
FOSAA	x		x		x
MeFOSA	x		x		x
MeFOSAA	x	x	x	x	x
MeFOSE	x		x		x

PFAS	Paper I	Paper II FF	Paper II EO and co-surfactant tests	Paper III	Paper IV
EtFOSA	x		x		x
EtFOSAA	x	x	x	x	x
EtFOSE	x		x		x
P37DMOA	x	x	x		x
6:2 Cl-PFESA				x	
8:2 Cl-PFESA				x	

4:2 FTSA = 4:2 fluorotelomere sulfonate, **6:2 FTSA** = 6:2 fluorotelomere sulfonate, **8:2 FTSA** = 8:2 fluorotelomere sulfonate, **6:2 FTAB** = 6:2 fluorotelomer sulfonamido betaine, **HPFHpA** = 7H-perfluoroheptanoic acid, **HFPO-DA** = tetrafluoro-2-(heptafluoropropoxy)propanoic acid, **PFECHS** = perfluoro-4-ethylcyclohexanesulfonate, **NaDONA** = dodecafluoro-3H-4,8-dioxanonanoic acid, **FOSA** = perfluorooctane sulfonamide, **FOSAA** = perfluorooctane sulfonamidoacetic acid, **MeFOSA** = N-methylperfluorooctane sulfonamide, **MeFOSAA** = N-methylperfluorooctane sulfonamidoacetic acid, **MeFOSE** = N-methylperfluorooctane sulfonamidoethanol, **EtFOSA** = N-ethylperfluorooctane sulfonamide, **EtFOSAA** = N-ethylperfluorooctane sulfonamidoacetic acid, **EtFOSE** = N-ethylperfluorooctane sulfonamidoethanol, **P37DMOA** = perfluoro-3,7-dimethyloctanoic acid, **6:2 Cl-PFESA** = 9-chlorohexadecafluoro-3-oxanonane-1- sulfonic acid , **8:2 Cl-PFESA** = 11-chloroeicosafluoro-3-oxaundecane-1- sulfonate acid, .

4.5.2 PFAS analysis in filter substrate and plant tissue

Plant and filter substrate sample preparation

Plant and filter substrate samples were prepared in-house for both Papers **III** and **IV**. For Paper **III**, the filter substrate was separated into LECA and organic fraction, whereas a combined substrate sample was used for Paper **IV**.

Plant material was divided into relevant tissue types depending on species and cleaned following a standardized protocol, as previously described (Nassazzi et al., 2022). Plant roots were carefully cleaned to remove adhering substrate, and all plant tissues were rinsed sequentially with ultrapure water and an ultrapure water/methanol solution to minimize external contamination. Plant tissue and substrate samples were subsequently freeze-dried and homogenized to ensure representative extraction.

Plant and filter substrate extraction and PFAS analysis

Extraction and target analysis of 29 PFAS (Table 3) for plant and filter substrate samples were performed in-house for Paper **III** using a previously validated method (Nassazzi et al., 2022). Briefly, the homogenized samples were spiked with mass-labelled standard mixture and subsequently extracted using repeated solvent extraction with methanol assisted by sonication. The extracts were separated from residual solids by centrifugation and subjected to clean-up using Supelco ENVY-carb cartridges (1 g, 12 cc, Supelco). Extracts were then concentrated under a nitrogen stream prior to instrumental analysis using UPLC-MS/MS as described in section 5.1.1.

Soil, plant, and filter substrate samples for Papers **I** and **IV** were analyzed for 22-33 PFAS (Table 3) by Eurofins Sweden.

Table 3. Overview of PFAS analyzed in solid samples

PFAS	Paper I	Paper III	Paper IV filter substrate	Paper IV plant tissue
PFBA	x	x	x	x
PFPeA	x	x	x	x
PFHxA	x	x	x	x
PFHpA	x	x	x	x
PFOA	x	x	x	x
PFNA	x	x	x	x
PFDA	x	x	x	x
PFUnDA	x	x	x	x
PFDoDA	x	x	x	x
PFTrDA	x	x	x	x
PFTeDA		x		
PFBS	x	x	x	x
PFPeS	x	x	x	x

PFAS	Paper I	Paper III	Paper IV filter substrate	Paper IV plant tissue
PFHxS	x	x	x	x
PFHpS	x	x	x	x
PFOS	x	x	x	x
PFNS	x	x	x	x
PFDS	x	x	x	x
PFDoDS	x		x	x
PFUnDS	x		x	x
PFTrDS	x		x	x
4:2 FTSA	x	x	x	
6:2 FTSA	x	x	x	x
8:2 FTSA	x	x	x	
10:2 FTSA	x		x	
6:2 FTAB	x			
HPFHpA				
HFPO-DA		x		
PFECHS		x		
NaDONA		x		
FOSA	x	x	x	x
FOSAA	x		x	
MeFOSA	x		x	
MeFOSAA	x	x	x	
MeFOSE	x		x	
EtFOSA	x		x	
EtFOSAA	x	x	x	
EtFOSE	x		x	
P37DMOA				
6:2 Cl-PFESA		x		
8:2 Cl-PFESA		x		

10:2 FTSA = 10:2 fluorotelomere sulfonate

4.5.3 General chemistry

General chemistry, including dissolved organic carbon (DOC), ions (including fluoride), metals, pH, and conductivity were analyzed in water samples by ALS Scandinavia for Paper **I** and Eurofins Sweden for Papers **II** and **IV**.

Nutrients for Papers **III** and **IV**, and general chemistry, including DOC, metals, and ions in Paper **III**, were analyzed by the accredited geochemistry laboratory at SLU.

Field measurements of pH and conductivity were carried out for Papers **II**-**IV**.

Additional fluoride measurements using a fluoride-selective electrode were performed for one EO batch in Paper **II**.

4.6 Data evaluation

K_d values were calculated as the ratio between PFAS concentrations in the solid and aqueous phases according to Equation 2:

$$K_d = \frac{C_s}{C_w} \quad \textbf{(2)}$$

Corrections were applied to account for residual porewater associated with solid samples, assuming equal concentrations of sampled liquid and solid porewater, which may introduce uncertainty, and a water density of 1 kg/L, according to Equation 3:

$$C_s = C_{tot:dw} - C_w \times \frac{(1 - TS)}{TS} \quad \textbf{(3)}$$

where $C_{tot:dw}$ is the analyzed solid phase concentration including PFAS in residual water, C_w is the concentration of PFAS in the water, and TS is the total solid fraction of the moist residual soil.

For field-based estimates, solid-phase concentrations were derived as weighted averages of soil layers corresponding to groundwater sampling intervals in cases where several soil samples overlapped one groundwater sample, according to Equation 4:

$$K_{d:field} = \frac{\left(C_{s:1} \times l_{overlap:1}\right) + \left(C_{s:2} \times l_{overlap:2}\right)}{l_{overlap:tot}} \Big/ C_w \quad \textbf{(4)}$$

where $C_{s:1}$ and $C_{s:2}$ are the PFAS concentrations of the two overlapping soil samples, $l_{overlap:1}$, $l_{overlap:2}$, and $l_{overlap:tot}$ are the respective overlap lengths with the groundwater collection filter screen, and C_w is the average PFAS concentration in groundwater (n = 3 to 7). Here, $C_{s:1}$ and $C_{s:2}$ are corrected for PFAS in the porewater (Equation 3).

Treatment performance in Papers **II** and **III** was evaluated using treatment efficiencies calculated from influent and effluent concentrations according to equation 5:

$$TE = 1 - \frac{C_{eff}}{C_{in}} \quad \textbf{(5)}$$

where C_{eff} is the effluent concentration, and C_{in} is the influent concentration.

For Paper **IV**, efficiencies were instead calculated on a mass balance basis due to the large volume difference between influent and effluent streams, according to equation 6:

$$TE = 1 - \frac{C_{eff:1} \times V_{eff:1} + C_{eff:2} \times V_{eff:2} \ldots}{C_{in:1} \times V_{in:1} + C_{in:2} \times V_{in:2} \ldots} \quad \textbf{(6)}$$

Where $C_{in:n}$ is the influent PFAS concentration per month n, $V_{in:n}$ is the influent volume of that month, $C_{eff:n}$ is the effluent PFAS concentration per month n, and $V_{eff:n}$ is the effluent volume of that month.

Mass balance recoveries (R) were established in Papers **II** (Equation 7) as well as for Papers **III** and **IV** (Equation 8):

$$R = \frac{V_{eff} \times C_{eff} + V_{foam} \times C_{foam}}{V_{in} \times C_{in}} \quad \textbf{(7)}$$

$$R = \frac{V_{eff} \times C_{eff} + m_{plant} \times C_{plant} + m_{sub} \times C_{sub} + m_{LECA} \times C_{LECA}}{V_{in} \times C_{in}} \quad \textbf{(8)}$$

Where V_{in} is the influent volume, C_{in} is the influent PFAS concentration, V_{eff} is the effluent volume, C_{eff} is the effluent PFAS concentration, V_{foam} is the foamate volume, C_{foam} is the foamate PFAS concentration, m_{plant} is the plant mass, C_{plant} is the plant PFAS concentration, m_{sub} is the mass of filter substrate, C_{sub} is the filter substrate PFAS concentration, m_{LECA} is the mass of LECA and C_{LECA} is the LECA PFAS concentration. V_{in} was assumed to be equal to V_{eff} for Paper **III** due to an assumed negligible volume lost through evapotranspiration relative to the influent. The plant term given here represents both *Salix* and weed for Paper **IV**.

To evaluate if the EO degradation followed first-order reaction kinetics, the linearity of the natural logarithmic transformation of the PFAS concentration was assessed after being plotted against the applied specific charge input.

Bioconcentration factors (BCF) were calculated for both Papers **III** and **IV**. In Paper **III** the BCF was calculated in relation to the influent water (Equation 9) and in Paper **IV** it was calculated in relation to the filter substrate (Equation 10):

$$BCF = \frac{C_{plant}}{C_{in}} \quad \textbf{(9)}$$

$$BCF = \frac{C_{plant}}{C_{sub}} \quad \textbf{(10)}$$

Phytoremediation potential was further estimated using literature-based biomass production values (Banaszuk et al., 2020; Zegada-Lizarazu et al., 2010) and combining them with the observed plant PFAS concentrations in Papers **III** and **IV**.

For datasets including measurements below detection limits (Paper **III**) or reporting limits (Papers **II** and **IV**), a consistent substitution approach was applied, where values were set to half the reporting limit if the compound was detected within the dataset, which is a common but potentially biasing approach, and otherwise treated as zero. No substitutions were made for Paper **I**, and K_d values were, in these cases, deemed non-determinable.

4.7 Statistical methods

Statistical methods were selected based on data distribution, sample size, and experimental design. Statistical significance was assessed at $\alpha = 0.05$.

Regression and modeling approaches

Linear regression models were used to evaluate relationships between response and multiple explanatory variables. In some cases, linear mixed effects models were used to also account for random effects arising from grouped or repeated measurements.

Test of distributions and assumptions

The Shapiro-Wilk normality test was used to assess whether a dataset followed normal distribution to determine if a parametric or non-parametric statistical test was appropriate for subsequent analysis.

Parametric statistical tests

Paired t-tests were used to determine whether the mean difference between two paired groups was statistically significant. ANOVA was used to evaluate differences in PFAS composition between samples and their interaction on a response variable. Z-tests were used to assess whether an observed value differed from a baseline.

Non-parametric statistical tests

Paired Wilcoxon tests with the Benjamini-Hochberg correction were used to compare paired groups with adjustment for multiple comparisons to control the false discovery rate. The Kruskal-Wallis test with the Dunn post-hoc test was used to assess differences between multiple groups, followed by pairwise comparisons to identify specific group differences. PERMANOVA based on Bray-Curtis dissimilarity was used to estimate differences in PFAS composition when parametric conditions could not be assumed.

Outlier detection

The Dixon outlier test was used to identify potential outliers in small datasets based on the relative distance between observations. For datasets with many variables, a principal component analysis (PCA) was used to reduce data dimensionality, after which the Mahalanobis distance was applied to identify multivariate outliers based on deviation from the overall data structure.

5. Results and discussion

5.1 Determining K_d values for aquifer materials (Paper **I**)

Paper **I** demonstrated that SPEM is a promising approach for determining PFAS K_d values and that it was more reliable than batch leaching tests at L/S 1 for determining low K_d values. The results were also comparable to K_d values derived from field measurements of aquifer drill cores and groundwater samples (Figure 8).

The K_d values obtained in Paper **I** showed that the K_d of low OC sandy aquifers was low for most detected PFAS, most likely due to the very low OC of the aquifer soil. If the K_{OC} was to be estimated using half of the reporting limit, as concentrations were consistently below the 0.2 % reporting limit in these samples, then these estimates would fall within the range of the values reported in a large meta-analysis by Brusseau et al. (Brusseau, 2024). Thus supporting the interpretation that the low K_d values observed, to a large extent, could be attributed to the low OC content of the aquifers. The estimated K_{oc} values of Paper **I** should, however, be interpreted with caution, as small variations in the unknown OC content of these samples could have large effects on the K_{oc}.

There was a significant positive correlation between K_d and perfluoroalkyl chain length (Figure 8). The functional group also influenced partitioning behavior, especially with 6:2 FTAB, exhibiting a considerably higher K_d value than the other detected PFAS, likely caused by its bulky and zwitterionic functional group (Barzen-Hanson et al., 2017).

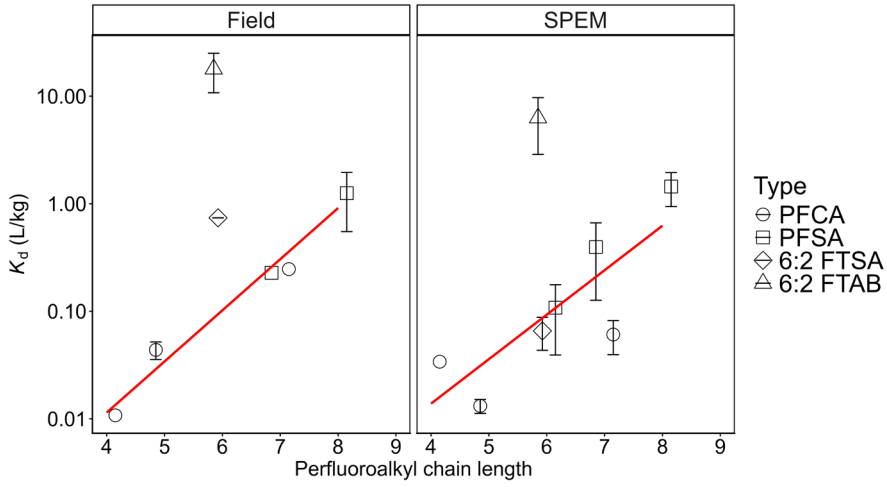

Figure 8. Average K_d values for soils at the two AFFF sites, determined both as a field value and with the SPEM method, using 10 or 15 s vacuum extraction. Error bars show the standard error of the mean. The number of samples varies by PFAS (maximum n = 7). Data points without error bars indicate PFAS where K_d was determined in only one sample (n = 1). Trend lines indicate significant linear regression based on the PFAA.

The low K_d values determined suggest that PFAS are highly mobile in these types of aquifer systems. However, the results also indicate that certain PFAS precursors, such as 6:2 FTAB, might be less mobile, which has been shown previously (Shea et al., 2025). This highlights the importance of understanding PFAS precursor transformation pathways and kinetics in order to predict PFAS groundwater transport.

The low K_d of PFAS suggests that pump-and-treat may be an effective remediation solution for a PFAS-contaminated aquifer, as the retention of PFAS in the aquifer during groundwater extraction would be low. Aquifer heterogeneity may, however, still prolong remediation timeframes. The PFAS composition in the aquifer is, as shown in Paper **I**, also important, as sites impacted by 6:2 FTAB-containing AFFF, as an example, would be less amenable to pump and treat than sites dominated by short-chain PFCA (e.g. landfills).

If pump and treat is chosen as a method for remediation of an aquifer, it is critical to first treat the vadose zone to prevent influx of PFAS to the saturated zone. The unsaturated zone will exhibit a substantially higher PFAS retention than the aquifer, both due to higher OC contents increasing K_d and the presence of large air-water interfaces in the unsaturated material, to which surface-active PFAS will adsorb (Gnesda et al., 2022; Pritchard et

al., 2026; J. Zeng et al., 2021). The vadose zone might thus act as a long-term reservoir that continuously leach PFAS into the aquifer, extensively prolonging the time scale required for the pump and treat remediation.

Overall, the findings show that PFAS generally exhibit low sorption in low OC aquifer materials, as captured by SPEM-derived K_d values. Variations in chain length, functional group, and vadose zone interactions will, however, still influence PFAS mobility and, in extension, the effectiveness of remediation strategies.

5.2 Foam fractionation for PFAS separation (Paper **II**)

The study of Paper **II** showed FF to be highly efficient for separating long-chain PFAS (Figure 9) with a sum long-chain PFAA separation of 98 ± 2.6%. Short-chain separation was lower, as expected with an FF system (Burns et al., 2021, 2022; Smith et al., 2022), with a sum short-chain PFAA separation of 14 ± 7.6%.

While a clear and significant correlation existed between treatment efficiency and chain length, a mixed-effects model revealed no statistically significant overall impact of the functional group on treatment efficiency. The mean removal of some PFSA were, however, higher than that of the PFCA of the corresponding chain length (e.g. PFPeS vs PFHxA), suggesting that PFSA are more efficiently removed than PFCA. This has also been observed in previous FF studies (We et al., 2024). This difference is likely due to the carboxylic group being more strongly hydrated in bulk water, increasing the free energy penalty for adsorption at the air-water interface, and reducing the surface activity relative to the PFSA (Shao et al., 2010).

Interestingly, HPFHpA was found to have a significantly lower treatment efficiency than PFHpA, (3.5 ± 11 % compared to 71 ± 20 %). With the reduced surface activity of HPFHpA caused by the dipole moment of the terminal CF_2H group, this behavior could be expected (Downer et al., 1999), but the magnitude of the effect on FF separation has, to the best of the authors' knowledge, not previously been reported. These findings highlight the importance of the PFAS composition in order to achieve efficient treatment with FF.

The addition of co-foaming surfactants during FF increased the separation of short-chain PFAS. The cationic surfactant was the most

efficient, with a sum short-chain PFAA separation of 67% at a 10 mg/L dose. A 10 mg/L dose of the two non-toxic surfactants, polysorbate 20 and 80, also increased the sum short-chain PFAA separation to 46% and 49%, respectively. The treatment efficiency increased with increased surfactant dose for all the surfactants (the effect of polysorbate 80 is shown as an example in Figure 9), suggesting that the optimal additive concentration is likely >10 mg/L.

A previous bench scale study did contrary to these results, find that the maximum surface excess of polysorbate 80 was reached below 5 mg/L, suggesting that increasing the concentration above 5 mg/L would not increase PFAS separation (Klevan et al., 2025). The results in Paper **II**, however, contradict these findings, with a clear increase in treatment efficiency for several PFAS with an increase in polysorbate 80 concentrations from a 6 to 10 a mg/L addition. This discrepancy may reflect differences between controlled bench-scale systems and complex field matrices.

A range of co-foaming surfactants have previously been tested, such as CTAB, sodium dodecyl sulfate (SDS), Triton x-100, saponin, and a shea butter-derived surfactant. These results generally show that cationic surfactants have the highest potential for the increased removal of short-chain PFAS, followed by zwitterionic surfactants, while non-ionic and anionic surfactants have the lowest effect. Additionally, decreasing pH in order to turn a zwitterionic surfactant more cationic was shown to markedly increase its effect (Klevan et al., 2025; Vo et al., 2023).

The separation of PFBA was not significantly increased by any of the co-foaming surfactants tested for Paper **II**, and only limited effects were seen for the separation of PFPeA. Previous studies have shown complete separation of PFBA with a CTAB addition (Buckley et al., 2023), while other studies did not observe any separation at all of PFBA after a CTAB addition (Vo et al., 2023). This discrepancy highlights the importance of other parameters such as water chemistry, surfactant dose, and FF operational conditions.

The results suggest that an alternative treatment method or post-FF-polishing step should be considered if PFBA or shorter-chain PFAS constitutes a major fraction of the PFAS composition.

Overall, the results show that FF achieved near-complete separation of long-chain PFAS, but limited removal of short-chain compounds. The

treatment efficiency of short-chain PFAS was, however, markedly improved for short-chain PFAS through the addition of co-foaming surfactants. The removal of PFBA and, to some extent, PFPeA, however, remained limited.

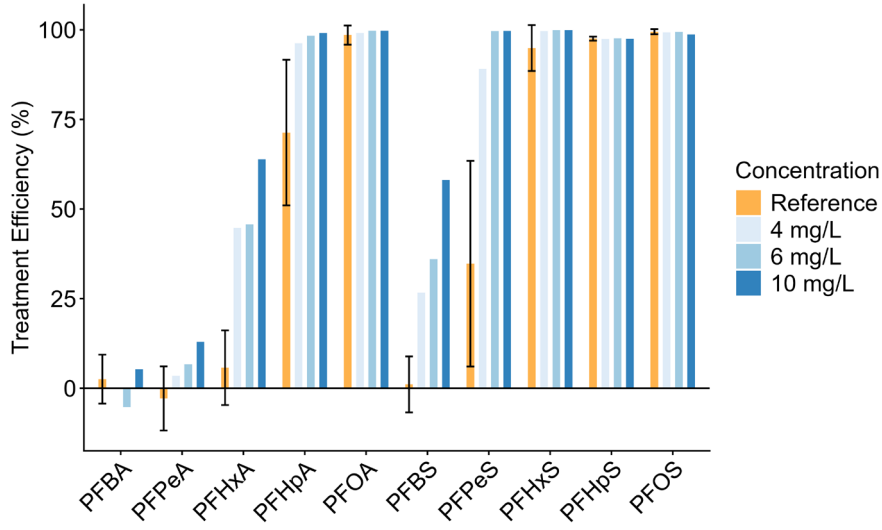

Figure 9. Treatment efficiency of FF for a selection of PFAS as demonstrated in Paper **II**. The reference represents FF treatment using air only (n = 15). The co-foaming surfactant polysorbate 80 is shown at the three tested concentrations (n = 1).

5.3 Electrochemical oxidation for PFAS destruction (Paper **II**)

Treatment with EO was able to achieve PFAS degradation (Figure 10). The degradation pathway was shown to occur in a stepwise pattern, with PFAS transforming into shorter-chain variants. This is manifested as an initial increase in <C6 PFAS concentrations as their initial formation rate is higher than their rate of degradation. As the longer-chain PFAS are depleted, the degradation rate of the short-chain PFAS eventually surpasses their rate of formation, leading to concentration decreases.

The proposed main degradation pathway, when using BDD electrodes, can be simplified as C_n-PFCA → C_{n-1}-PFCA and C_n-PFSA → C_{n-1}-PFCA, with the transformation rate following pseudo-first-order kinetics (Tasca et al., 2025). The formation of PFBS that can be seen in Figure 10 contradicts this proposed pathway. The PFBS concentrations are, however, very low,

suggesting that the formation of PFBS is a side reaction rather than the main reaction pathway or a result of the degradation of non-analyzed PFAS precursors such as perfluorobutane sulfonamide (FBSA). The reaction kinetics across all PFAS is complex and likely involves the formation of unknown intermediates (Rehnstam et al., 2024; Smith, Lauria, et al., 2023). The reduction rate of PFDA and PFOS, however, which were both without known precursors present at high concentrations, can be seen to follow first-order kinetics (R^2 = 0.93 and 0.95, respectively), supporting this theory.

Although not explicitly analyzed, ultra-short-chain PFAS are likely formed during the EO process. While most EO studies have not measured these compounds, the formation of low levels of TFA has previously been reported (Asadi Zeidabadi et al., 2024; Liao & Farrell, 2009). However, high fluorine recoveries 97% for the BDD-SS batch and 99% for the BDD-BDD batch observed in the study of Paper **II,** suggest that ultrashort-chain-PFAS, if present, are eventually also degraded and not present at environmentally relevant concentrations at the end of the treatment.

The concentrations of several PFAS in the 5 Ah/L sample of batch #1 (Figure 10) were lower than expected based on a logarithmic decay trend, resulting in an apparent reduction in treatment efficiency between 5 and 10 Ah/L. This is likely caused by excessive foam formation in the bulk foamate reservoir during the beginning of the batch experiment, leading to artificially reduced PFAS concentrations in the sampled liquid due to partitioning of PFAS into the foam. This interpretation is supported by the fact that this effect was observed for PFHpA, PFOA, PFPeS, and PFOS but not for PFBA, PFHxA, or PFBS, as these short-chain PFAS are less prone to partition into foam, as shown by the results of the FF treatment. As PFAS concentrations were reduced during the treatment, foam formation also declined, thereby reducing the influence of this artifact over time.

While batch #1 achieved a ΣPFAS treatment efficiency of 88%, the average ΣPFAS concentration reduction in foamate treated by EO was only 58%. This was primarily due to operational challenges, including substantial problems with electrode fouling for both sets of electrodes, precipitation blocking pipes, and power outages. Electrode fouling is a well-known issue in EO (S. Sharma et al., 2022; Shi et al., 2024; Tan et al., 2025). As the fouling observed in Paper **II** was mainly attributed to calcium carbonate, operating at a lower pH could mitigate the problem by increasing calcium carbonate solubility and reducing carbonate availability. Another approach

could be to include a cationic exchange filter before the EO in order to separate the calcium ions prior to the treatment (Pérez-González et al., 2015).

Visual observation detected no difference in fouling between the two sets of electrode materials. The niobium base of the BDD electrodes did, however, show clear signs of hydrogen embrittlement when used as cathodes for extended periods of time. This is known to occur in niobium under cathodic conditions, leading to cracks in the material (Zhao et al., 2020), reducing the operational life of the electrodes. The combination of BDD anodes and SS cathodes is thus likely a better option than using BDD for both electrode types.

It should be noted that many problems experienced, such as blocked pipes and power outages, can be attributed to the very early-stage full-scale deployment of the system rather than shortcomings of the technology in itself.

Overall, the results show that EO is able to degrade PFAS through stepwise chain-shortening, with high fluorine mass balance recoveries indicating PFAS mineralization. Further optimization of the system and its operation, such as developing strategies against electrode fouling, is, however, necessary to ensure consistent and efficient treatment.

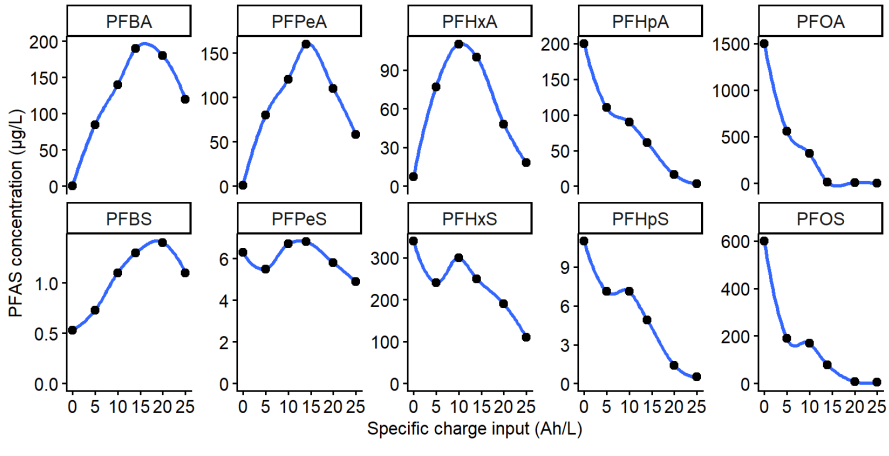

Figure 10. The concentration of a selection of PFAS at 6 time points during EO treatment (n = 1). Lines are included for visualization purposes only.

5.4 PFAS behavior in subsurface flow constructed wetlands (Papers **III** and **IV**)

Sorption to the filter substrate was identified to be the main removal mechanism of PFAS in the tested CW systems, both without (Paper **III**) and with FF pre-treatment (Paper **IV**). The main driver of this is the large volume of substrate relative to plant biomass, such as the estimated 8 600 kg of substrate vs 310 kg of plant biomass in the CW evaluated in Paper **IV**.

A key difference between the two studies stems from the PFAS composition, as the FF pre-treatment effectively removes long-chain PFAS (Paper **II**). Since PFAS sorption to solid matrices is highly correlated to the perfluoroalkyl chain length, as seen in Paper **I**, the PFAS sorbed to the peat and biochar mixture, as well as to the LECA when treating raw groundwater, were dominated by long-chain PFAS (77 and 93% of ΣPFAS, respectively) (Figure 11). These results are consistent with previous findings showing that PFAS partitioning into CW sediments is strongly chain-length dependent (W. Liu et al., 2025). When FF pre-treatment is applied, the concentration of PFAS sorbed to the filter substrate and LECA is consequently drastically reduced compared to when treating raw groundwater (Figure 11).

The biochar and peat mixture may still be beneficial in order to support and stimulate plant growth in the wetland (Kasak et al., 2018). Its inclusion may, however, be less critical for PFAS removal in CWs using FF pre-treatment. Consequently, replacement of spent filter substrate as a PFAS removal strategy may not be necessary if FF pre-treatment is applied. It should be noted that the peat and biochar fraction in Paper **III** and the filter substrate fraction from Paper **IV** are not directly comparable, as the latter also contains 80 vol% LECA.

PFAS were taken up and accumulated by all plant species in both studies (Papers **III** and **IV**). In contrast to the filter substrate sorption, the plant uptake observed in Paper **III** favored short-chain PFAS (57% of ΣPFAS), representing a slight increase from the influent water composition (50% of ΣPFAS).

The reduction in PFAS concentration of the CW influent when FF pre-treatment was applied consequently also reduced the PFAS uptake by plants, as shown in Figure 11. This effect becomes evident when comparing PFAS concentrations in *S.* Wilhelm plants harvested in September between the two studies. Plant concentrations were similar for PFAS that were not effectively separated by FF, such as PFPeA (2.1 vs 2.1 ng/g dw) and PFBA (5.0 vs 4.2

ng/g dw) in CW receiving raw groundwater and FF-effluent, respectively. In contrast, PFAS efficiently separated by FF showed markedly lower plant concentrations when receiving FF-effluent as opposed to raw groundwater, such as PFOA (0.093 vs 2.2 ng/g dw) and PFOS (<0.10 vs 0.73 ng/g dw).

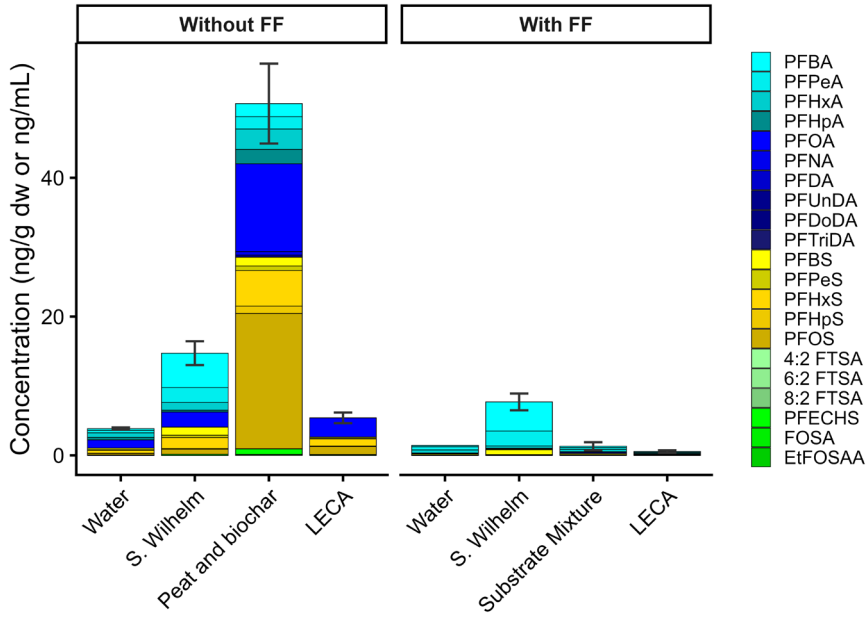

Figure 11. PFAS concentrations in different matrices in a CW receiving raw groundwater (without FF) (Paper **III**) and a CW receiving FF-effluent (with FF) (Paper **IV**). Note that peat and biochar, and substrate mixture are not directly comparable as the substrate mixture used in Paper **IV** also contain 80% LECA. Without FF: Water $n = 3$, *S.* Wilhelm $n = 2$, Peat and Biochar $n = 8$, LECA $n = 8$. With FF: water $n = 1$, *S.* Wilhelm $n = 4$, substrate mixture $n = 9$, LECA $n = 3$. Adapted from Paper **III** (Liljeström et al., 2025) with permission from Elsevier.

As for the distribution of PFAS between plant tissues, short-chain PFAS preferentially accumulated in leaves, whereas long-chain PFAS were found to accumulate in roots. Significant correlations between chain length and BCF for both leaves and roots were observed in the study of Paper **III**, while concentrations in the stems and twigs were found to be low for all PFAS (Figure 12). The chain length-dependent distribution of PFAS between roots and leaves is well known and has been shown in several previous studies

(Blaine et al., 2014; Felizeter et al., 2012; N. Sharma et al., 2020). When FF pre-treatment was applied, effectively removing long-chain PFAS, 82-84% of ΣPFAS consequently accumulated in the leaves. Analysis of leaf-litter collected in October showed no significant difference in PFAS composition or concentration compared to the leaves remaining on the *Salix*, suggesting that over 80% of the PFAS taken up by plants may be remobilized during leaf senescence. While problematic from a treatment perspective, it also suggests the possibility of harvesting highly contaminated leaves for disposal as hazardous material, while the relatively low-contaminated woody biomass (stems) can be utilized for bio-energy production or to produce biochar. As implementing leaf collection systems may pose logistical challenges, an alternative approach could be annual *Salix* harvests before leaf fall. This is, however, not optimal for *Salix* cultivation and would likely result in reduced biomass production (Zegada-Lizarazu et al., 2010). Another option would be to use alternative plant species. Both *C. elata* and *C. sativa*, evaluated in Paper **III**, would avoid the issue of PFAS remobilization via leaf litter. *C. sativa*, additionally, accumulated the highest PFAS concentrations among all tested plants and could thus be considered a promising species for PFAS phytoextraction. However, as it requires well-drained soils for cultivation, it is likely not suitable for application in a CW, as shown by the high mortality rate of *C. Sativa* (65%) observed in Paper **III**. *C. elata*, on the other hand, produces a low amount of biomass compared to *Salix* or *C. sativa*. However, the *Carex* genus could be of interest for PFAS treatment using a CW due to its ability to thrive in wetlands. The existence of highly salt-resistant species such as *C. distans* for treating saline leachate (Choo et al., 2001), and the fact that they don't shed leaves, allowing them to be annually harvested late in the year, are also reasons to consider the *Carex* genus in future CW applications.

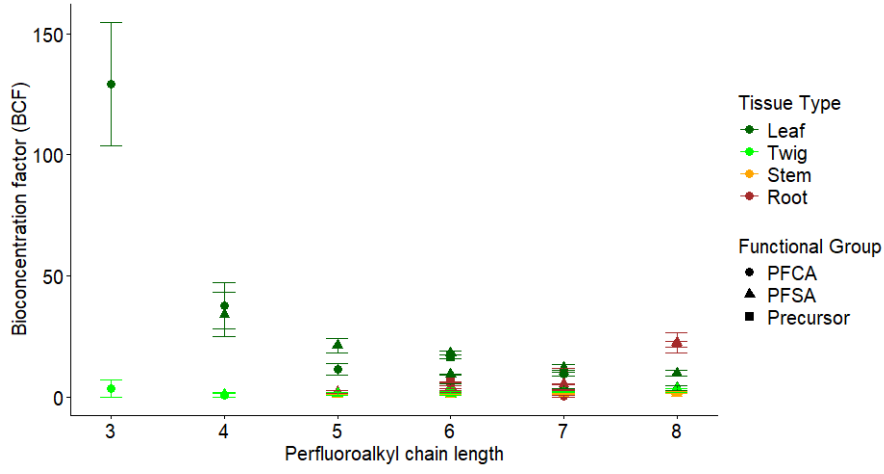

Figure 12. BCF (Equation 9) between different tissues of *S.* Wilhelm and influent water (n = 2), adapted from Paper **III** (Liljeström et al., 2025) with permission from Elsevier.

With an influent volume between 41.6 and 83.3 L m^{-2} d^{-1}, the volume losses in Paper **III** were assumed to be negligible and were therefore not measured. Evapotranspiration losses for irrigated *Salix* stands in Uppsala have previously been estimated to 2.6 L m^{-2} d^{-1}(Persson & Lindroth, 1994). The influent volume was markedly reduced for Paper **IV** to 2.82 L m^{-2} d^{-1}, or 3.59 L m^{-2} d^{-1} when accounting for precipitation inputs, partly due to the modest treatment efficiency observed by the CW in Paper **III**. Evapotranspiration was estimated to 2.11 L m^{-2} d^{-1}, leading to a reduction in contaminant water volume of 48%. While no significant reduction in PFAS concentrations was observed after the CW treatment, the large volume reduction nevertheless resulted in a ~50% reduction in total PFAS load.

Overall, PFAS separation in the CW was primarily governed by sorption to the filter substrate. Phytoextraction was also observed characterized by preferential uptake of short-chain PFAS and a clear chain length-dependent distribution between roots and leaves. However, accumulation in leaves and subsequent remobilization during senescence represent a limitation. While the CW achieved limited reductions in particularly short-chain PFAS concentrations in the treated water, substantial volume reduction may nevertheless enable a meaningful decrease in overall PFAS load.

5.5 The integrated treatment train for PFAS-contaminated water (Papers **II** and **IV**)

The mean ΣPFAS concentration in water decreased by 50% after FF treatment (Figure 13). Short-chain PFAS mainly remained in the FF effluent, and the long-chain PFAS were mainly separated into the foamate, with an average concentration factor of ~1200x.

The mean fraction of short-chain PFCA increased after the EO treatment from 1.5% to 18%, but the EO-treated foamate was still dominated by long-chain PFAS (73%) due to the moderate mean treatment efficiency of the system as described above. The enrichment of short-chain PFCA during EO may be problematic, as the treated water is recirculated to the FF unit, which is inefficient in separating these compounds without added co-foaming surfactants. Even with such additives, FF, as shown in Paper **II**, provide limited separation of PFBA and PFPeA. Although optimization of the EO process can reduce this issue, a post-EO treatment step should still be considered, as the foamate may retain high PFAS concentrations despite a high EO treatment efficiency, due to the very high initial concentrations of the foamate. An interesting technology for this could be the use of membranes such as NF, which has demonstrated effectiveness for short-chain PFAS separation (Griffin et al., 2024; Wu et al., 2025). The NF reject volume could be returned to the EO-cell. Additionally, pre-treatment with EO using BDD electrodes has previously been shown to reduce the fouling of water treatment membranes by oxidizing the organic matter in the water, reducing the transmembrane pressure of the following filtration step by up to 67% (Gonzalez-Olmos et al., 2018). Continuously returning the PFAS-rich reject water to the EO might, however, lead to PFAS accumulation in the system, suggesting that a sorbent solution might be more appropriate.

The mass balance recovery of the FF system was 77% (Figure 14), which is within the range of what has previously been reported in pilot-scale experiments (Smith et al., 2022; Smith, Lewis, et al., 2023). The mass balance gap could partly be explained by analytical uncertainty, the difference between the water and foamate matrices, and the fact that only 15 out of more than 10 000 FF batches were included in the analysis. It could, however, also at least partly be explained by aerosol formation in the FF process, with PFAS being transferred to the system's air filters, which were not analyzed. While PFAS emissions via aerosol formation have been shown

to occur, it would likely only be able to explain a fraction of the missing recovery (McCleaf et al., 2023; Smith, Lewis, et al., 2023).

The FF effluent contained almost exclusively short-chain PFAS and was dominated by PFCA (82% of ΣPFAS). These compounds were efficiently taken up by plants, with the PFAS composition of the plants being similar to that of the influent water. The concentration factor from water to plant tissue was, however, only ~7.5x, indicating that very large amounts of biomass would be required to treat industrial-scale flows. The FF system treated ~30 000 m^3 over the 11-month study period (Paper **II**). Assuming a biomass yield of 20 tons ha^{-1} yr^{-1} (Zegada-Lizarazu et al., 2010), it would require ~200 ha of cultivation area in order to provide adequate treatment of the volumes generated by the FF system through phytoextraction. By comparison, the average arable land area of a Swedish farm is 49 ha (Olsson, 2025), highlighting the limited feasibility of phytoextraction as a separation method for PFAS in water at large scale.

A modest PFAS accumulation was observed in the CW filter substrate, with an increased fraction of long-chain PFCA and PFSA, likely partly attributed to the pond water applied during the summer of 2024 when the FF was out of operation. This increase in the fraction of long-chain PFAS was also detected in the wetland effluent. The overall increase in PFAS concentration in the CW effluent is likely due to a combination of higher PFAS concentrations in the water from the treatment pond compared to the FF effluent and the concentration increase of PFAS caused by the water volume reduction in the CW as a result of evapotranspiration. The accumulation of PFAS in the filter substrate could also pose a future challenge if a large CW is established, as it would require long-term maintenance to prevent leaching and subsequent contamination of underlying soil and groundwater. In addition, eventual reconditioning or decommissioning of the CW would generate large amounts of PFAS-contaminated solid material that would need to be managed and disposed of safely.

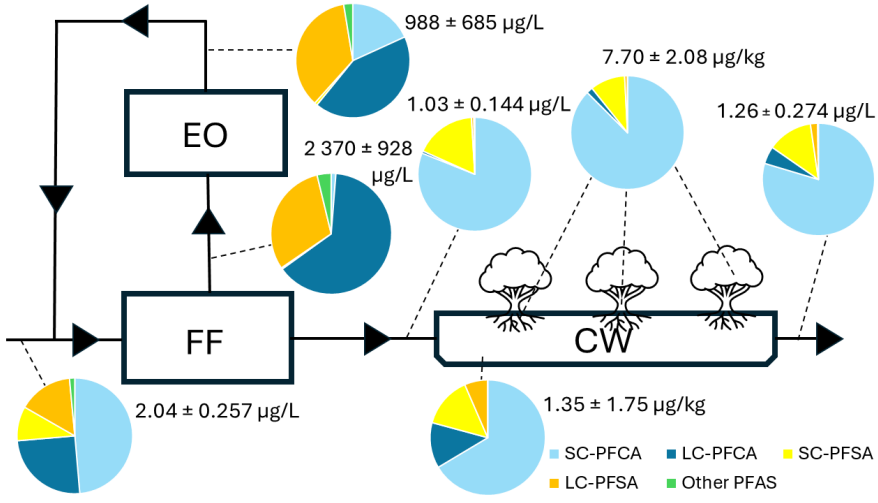

Figure 13. The treatment setup of Papers **II** and **IV**, with mean PFAS composition and concentration for short-chain (SC)-PFAS (≤C6 PFCA and ≤C5 PFSA) and long-chain (LC)-PFAS shown before and after each treatment step including FF influent and effluent (n = 15), EO influent and effluent (n = 9), filter substrate (n = 9), *Salix* (n = 4), wetland effluent (n = 6). The *Salix* and filter substrate samples were collected in September 2024. The margin of error is given as the standard deviation. The number of PFAS analyzed varied between studies: 24 in FF influent and effluent, 32 in EO influent/effluent and wetland effluent, and 22 in filter substrate and plant material. However, analysis of FF influent for the full set of 32 PFAS showed that 98% of the total PFAS concentration was accounted for by the 20 compounds included across all sample types.

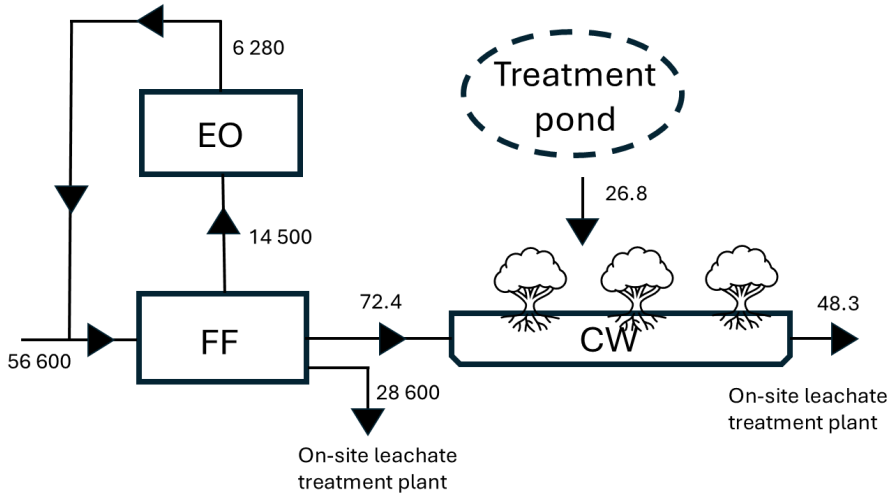

Figure 14. The total measured PFAS mass flows of the systems studied in Papers **II** and **IV**, with all values given in mg.

Overall, the results of the various treatment units presented in this thesis show that a combination of FF and EO could be used to separate and mineralize long-chain PFAS from groundwater or leachate. While the additions of co-foaming surfactants markedly increased the separation of short-chain PFAS by the FF, a polishing step able to effectively treat PFAS such as PFPeA or PFBA should still be considered, as these were still not effectively removed by the FF and could additionally be formed in the EO process if complete mineralization is not achieved. The inability of the CW to decrease PFAS concentrations in the treated water, however, limits its use as such a polishing step.

6. Conclusions

To the best of the authors' knowledge, the work contained in this thesis presents the first-ever field-scale integrated treatment train combining FF, EO, and CW, deployed for real-world remediation. Additionally, the large volumes treated by the combination of FF and EO represent a substantial scale-up beyond most previously reported studies. The use of SPEM to determine PFAS K_d has, to the best of the authors' knowledge, also never previously been performed.

The work carried out in this thesis demonstrates that SPEM appears to be a robust and reliable approach for determining PFAS K_d in low K_d environments, such as low OC sand aquifers. SPEM was shown to outperform traditional batch leaching tests conducted at L/S 1 under the conditions studied, as well as producing results comparable to field-derived values. The results further highlight the low sorption of many PFAS in low OC sand aquifers. A strong correlation was observed between K_d and perfluoroalkyl chain length, and the K_d of 6:2 FTAB was substantially higher than that of the other PFAS detected at the sites. This underscores the importance of characterizing PFAS composition prior to transport modelling and remediation strategy selection, as for example, pump and treat would require longer treatment times for a site contaminated with relatively high K_d precursors such as 6:2 FTAB compared to a site contaminated with short-chain PFAA. This also highlights the need to consider precursor transformation pathways and kinetics.

The use of FF was shown to be highly effective for the separation of long-chain PFAS, achieving >90% separation for ≥C7 PFCA and ≥C6 PFSA in landfill leachate and leachate-impacted groundwater when using air alone. The addition of co-foaming surfactants significantly improved the removal of Σshort-chain PFAS from 14% up to 67%, although PFBA, PFPeA, and likely present ultra-short-chain PFAS remain problematic. These findings highlight both the strengths and limitations of FF and demonstrate the importance of PFAS composition in determining treatment performance.

The use of EO enabled the degradation of PFAS through stepwise shortening of the perfluoroalkyl chain, with results supporting pseudo-first-order degradation kinetics. The observed high fluorine mass balance recovery supports mineralization of PFAS. However, incomplete degradation and the formation of short-chain PFAS during treatment

emphasize the need for sufficient charge input and process optimization, particularly strategies to avoid electrode fouling, to avoid accumulation of persistent transformation products, including short-chain PFAS.

It was shown that CW could act as PFAS sinks, primarily through sorption to the filter substrate, but phytoextraction was also observed, resulting in a reduction in total PFAS mass discharge. However, no significant decrease in short-chain PFAS concentrations of the treated water was observed, indicating that such systems have limited suitability as polishing steps following FF treatment. Plant accumulation of PFAS exhibited a clear chain-length-dependent partitioning, with long-chain PFAS accumulating in roots and short-chain PFAS in leaves. The observed remobilization of PFAS during leaf senescence further complicates the use of phytoextraction strategies.

From a treatment systems perspective, the results of this thesis demonstrate that no single technology is sufficient to address the full spectrum of PFAS contamination. Instead, effective remediation requires integrated treatment trains that combine complementary processes. FF efficiently separates and concentrates long-chain PFAS, EO enables destruction of concentrated PFAS streams, and wetlands can contribute to PFAS mass reduction and water volume control. However, the persistence and high mobility of short-chain PFAS across all studied systems, even though mitigated by the use of co-foaming surfactant additives and shown to be possible to separate through phytoextraction, highlight a critical treatment gap that could necessitate the inclusion of additional steps, such as AIX or membrane filtration, in order to achieve comprehensive treatment.

Overall, the findings of this thesis highlight that PFAS behavior across environmental and engineered systems is fundamentally governed by partitioning processes between phases, including soil-water, air-water, and plant-water interfaces. These partitioning mechanisms control both contaminant mobility in aquifer systems and the performance of treatment technologies. By linking PFAS physicochemical properties to both environmental transport and treatment efficiency, this work provides a useful framework for understanding and designing PFAS remediation strategies.

7. Outlook and future research needs

Future work should focus on improving both the understanding of PFAS behavior and the performance and robustness of treatment systems across scales.

For the characterization of PFAS partitioning, SPEM should be further evaluated across a wider range of soil types, including organic-rich soils, clays, and heterogeneous field materials. This would support the establishment of broader applicability of the method and determining its suitability for different contaminated environments, as well as further validating its potential advantages over traditional batch leaching tests.

Future FF studies should, where possible, include an analysis of air filters to quantify PFAS losses through aerosol formation, thereby improving mass balance closure and assessing potential risks for human and environmental exposure. The use of co-foaming surfactants should be further optimized, including the identification of effective, non-toxic alternatives and determining optimal dosing strategies under varying water chemistries.

Treatment trains combining FF with technologies capable of removing short-chain PFAS, such as AIX or membrane filtration, should be further investigated under realistic operating conditions. In particular, the integration of FF with AIX appears promising, as FF reduces the mass load and removes long-chain PFAS competition for sorption sites (Ellis et al., 2022). If regenerable AIX resins are employed, the EO system could additionally be applied to treat the regenerant solution, enabling process integration.

The EO processes require further optimization to improve treatment efficiency and operational stability. This includes addressing operational challenges such as electrode fouling and calcium carbonate precipitation, as well as evaluating alternative electrode materials to reduce costs. Future studies should also include the analysis of ultra-short-chain PFAS and apply suspect and non-target screening approaches to identify potential hazardous transformation products formed during EO treatment. These approaches could be further strengthened by also employing bio-based toxicity assays or effect-directed analysis on the EO effluent to ensure that toxic intermediates are not overlooked. The use of total organic fluorine measurements to complement fluoride measurements in evaluating mineralization should also be used.

Future research on CW should aim to optimize PFAS retention by investigating alternative plant species, including those with high biomass production and wetland tolerance. Different filter substrates should also be evaluated. Additionally, the influence of microbial communities on PFAS transformation and plant uptake should be investigated, as microbially mediated processes may play an important role in both PFAS precursor transformation and the bioavailability of PFAS in wetland systems. Long-term, multi-season studies are needed to better understand system stability, plant dynamics, and PFAS remobilization processes, such as leaf senescence or the leaching of PFAS from the filter substrate. Crucially, safe and cost-efficient handling of contaminated biomass and spent filter substrate needs to be further explored.

Future research should, additionally, move beyond pure technical performance. Life cycle assessment (LCA) should be applied to compare the environmental impacts of different treatment technologies and treatment trains, including energy use, emissions, and resource consumption. In parallel, life cycle costing (LCC) analyses are needed to evaluate the economic feasibility of different remediation strategies under realistic field conditions. Such assessments are critical for guiding decision-making and ensuring that proposed solutions are not only effective but also sustainable and economically viable.

Overall, advancing PFAS remediation will require an integrated approach combining improved process understanding, technological optimization, and system-level evaluation. Emphasis should be placed on addressing the persistence and high mobility of short- and ultra-short-chain PFAS, as well as ensuring that treatment processes do not lead to the formation or release of equally problematic transformation products.

References

Abraham, K., Mertens, H., Richter, L., Mielke, H., Schwerdtle, T., & Monien, B. H. (2024). Kinetics of 15 per- and polyfluoroalkyl substances (PFAS) after single oral application as a mixture – A pilot investigation in a male volunteer. Environment International, 193, 109047. https://doi.org/10.1016/j.envint.2024.109047

Abraham, K., Mielke, H., Fromme, H., Völkel, W., Menzel, J., Peiser, M., Zepp, F., Willich, S. N., & Weikert, C. (2020). Internal exposure to perfluoroalkyl substances (PFASs) and biological markers in 101 healthy 1-year-old children: associations between levels of perfluorooctanoic acid (PFOA) and vaccine response. Archives of Toxicology, 94(6), 2131–2147. https://doi.org/10.1007/s00204-020-02715-4

Adu, O., Ma, X., & Sharma, V. K. (2023). Bioavailability, phytotoxicity and plant uptake of per-and polyfluoroalkyl substances (PFAS): A review. Journal of Hazardous Materials, 447, 130805. https://doi.org/10.1016/j.jhazmat.2023.130805

Akbarpour, M., Reza, T., & Sadmani, A. H. M. A. (2026). A critical review of the application of biochar in removing perfluoroalkyl and polyfluoroalkyl substances (PFAS) from water matrices. Biomass Conversion and Biorefinery, 16(5). https://doi.org/10.1007/s13399-026-07072-3

Aly, N. A., Luo, Y. S., Liu, Y., Casillas, G., McDonald, T. J., Kaihatu, J. M., Jun, M., Ellis, N., Gossett, S., Dodds, J. N., Baker, E. S., Bhandari, S., Chiu, W. A., & Rusyn, I. (2020). Temporal and spatial analysis of per and polyfluoroalkyl substances in surface waters of Houston ship channel following a large-scale industrial fire incident. Environmental Pollution, 265, 115009. https://doi.org/10.1016/j.envpol.2020.115009

Andersson, E. M., Scott, K., Xu, Y. Y., Li, Y., Olsson, D. S., Fletcher, T., & Jakobsson, K. (2019). High exposure to perfluorinated compounds in drinking water and thyroid disease. A cohort study from Ronneby, Sweden. Environmental Research, 176, 108540. https://doi.org/10.1016/j.envres.2019.108540

Ankley, G. T., Cureton, P., Hoke, R. A., Houde, M., Kumar, A., Kurias, J., Lanno, R., McCarthy, C., Newsted, J., Salice, C. J., Sample, B. E., Sepúlveda, M. S., Steevens, J., & Valsecchi, S. (2021). Assessing the Ecological Risks of Per- and Polyfluoroalkyl Substances: Current State-of-the Science and a Proposed Path Forward. Environmental Toxicology and Chemistry, 40(3), 564–605. https://doi.org/10.1002/etc.4869

Arp, H. P. H., Gredelj, A., Glüge, J., Scheringer, M., & Cousins, I. T. (2024). The Global Threat from the Irreversible Accumulation of Trifluoroacetic Acid

(TFA). Environmental Science and Technology, 58(45), 19925–19935. https://doi.org/10.1021/acs.est.4c06189

Asadi Zeidabadi, F., Banayan Esfahani, E., Moreira, R., McBeath, S. T., Foster, J., & Mohseni, M. (2024). Structural dependence of PFAS oxidation in a boron doped diamond-electrochemical system. Environmental Research, 246, 118103. https://doi.org/10.1016/j.envres.2024.118103

Ateia, M., Maroli, A., Tharayil, N., & Karanfil, T. (2019). The overlooked short- and ultrashort-chain poly- and perfluorinated substances: A review. Chemosphere, 220, 866–882. https://doi.org/10.1016/j.chemosphere.2018.12.186

Bălan, S. A., Bruton, T. A., Harris, K., Hayes, L., Leonetti, C. P., Mathrani, V. C., Noble, A. E., & Phelps, D. S. C. (2024). The Total Mass of Per- and Polyfluoroalkyl Substances (PFASs) in California Cosmetics. Environmental Science and Technology, 58(27), 12101–12112. https://doi.org/10.1021/acs.est.3c06539

Banaszuk, P., Kamocki, A. K., Wysocka-Czubaszek, A., Czubaszek, R., & Roj-Rojewski, S. (2020). Closing the loop - Recovery of nutrients and energy from wetland biomass. Ecological Engineering, 143, 105643. https://doi.org/10.1016/j.ecoleng.2019.105643

Barzen-Hanson, K. A., Davis, S. E., Kleber, M., & Field, J. A. (2017). Sorption of Fluorotelomer Sulfonates, Fluorotelomer Sulfonamido Betaines, and a Fluorotelomer Sulfonamido Amine in National Foam Aqueous Film-Forming Foam to Soil. Environmental Science and Technology, 51(21), 12394–12404. https://doi.org/10.1021/acs.est.7b03452

Berg, M., Müller, S. R., Mühlemann, J., Wiedmer, A., & Schwarzenbach, R. P. (2000). Concentrations and Mass Fluxes of Chloroacetic Acids and Trifluoroacetic Acid in Rain and Natural Waters in Switzerland. Environmental Science and Technology, 34(13), 2675–2683. https://doi.org/10.1021/es990855f

Bil, W., Zeilmaker, M., Fragki, S., Lijzen, J., Verbruggen, E., & Bokkers, B. (2021). Risk Assessment of Per- and Polyfluoroalkyl Substance Mixtures: A Relative Potency Factor Approach. Environmental Toxicology and Chemistry, 40(3), 859–870. https://doi.org/10.1002/etc.4835

Björklund, S., Weidemann, E., & Jansson, S. (2023). Emission of Per- and Polyfluoroalkyl Substances from a Waste-to-Energy Plant─Occurrence in Ashes, Treated Process Water, and First Observation in Flue Gas. Environmental Science and Technology, 57(27), 10089–10095. https://doi.org/10.1021/acs.est.2c08960

Björnsdotter, M. K., Yeung, L. W. Y., Kärrman, A., & Ericson Jogsten, I. (2020). Challenges in the analytical determination of ultra-short-chain perfluoroalkyl acids and implications for environmental and human health.

Analytical and Bioanalytical Chemistry, 412(20), 4785–4796. https://doi.org/10.1007/s00216-020-02692-8

Björnsdotter, M. K., Yeung, L. W. Y., Kärrman, A., & Jogsten, I. E. (2019). Ultra-Short-Chain Perfluoroalkyl Acids including Trifluoromethane Sulfonic Acid in Water Connected to Known and Suspected Point Sources in Sweden. Environmental Science and Technology, 53(19), 11093–11101. https://doi.org/10.1021/acs.est.9b02211

Blaine, A. C., Rich, C. D., Sedlacko, E. M., Hundal, L. S., Kumar, K., Lau, C., Mills, M. A., Harris, K. M., & Higgins, C. P. (2014). Perfluoroalkyl acid distribution in various plant compartments of edible crops grown in biosolids-amended soils. Environmental Science and Technology, 48(14), 7858–7865. https://doi.org/10.1021/es500016s

Bolan, N., Sarkar, B., Vithanage, M., Singh, G., Tsang, D. C. W., Mukhopadhyay, R., Ramadass, K., Vinu, A., Sun, Y., Ramanayaka, S., Hoang, S. A., Yan, Y., Li, Y., Rinklebe, J., Li, H., & Kirkham, M. B. (2021). Distribution, behaviour, bioavailability and remediation of poly- and per-fluoroalkyl substances (PFAS) in solid biowastes and biowaste-treated soil. Environment International, 155. https://doi.org/10.1016/j.envint.2021.106600

Boston, C., Keck, S., Naperala, A., & Collins, J. (2025). The evolution of PFAS epidemiology: new scientific developments call into question alleged “probable links” between PFOA and kidney cancer and thyroid disease. Frontiers in Public Health, 13, 1532277. https://doi.org/10.3389/fpubh.2025.1532277

Brennan, N. M., Evans, A. T., Fritz, M. K., Peak, S. A., & von Holst, H. E. (2021). Trends in the regulation of per-and polyfluoroalkyl substances (PFAS): A scoping review. International Journal of Environmental Research and Public Health, 18(20). https://doi.org/10.3390/ijerph182010900

Brunn, H., Arnold, G., Körner, W., Rippen, G., Steinhäuser, K. G., & Valentin, I. (2023). PFAS: forever chemicals—persistent, bioaccumulative and mobile. Reviewing the status and the need for their phase out and remediation of contaminated sites. Environmental Sciences Europe, 35(1), 1–50. https://doi.org/10.1186/s12302-023-00721-8

Brusseau, M. L. (2024). Field versus laboratory measurements of PFAS sorption by soils and sediments. Journal of Hazardous Materials Advances, 16, 100508. https://doi.org/10.1016/j.hazadv.2024.100508

Brusseau, M. L., & Guo, B. (2022). PFAS concentrations in soil versus soil porewater: Mass distributions and the impact of adsorption at air-water interfaces. Chemosphere, 302, 134938. https://doi.org/10.1016/j.chemosphere.2022.134938

Buck, R. C., Franklin, J., Berger, U., Conder, J. M., Cousins, I. T., Voogt, P. De, Jensen, A. A., Kannan, K., Mabury, S. A., & van Leeuwen, S. P. J. (2011).

Perfluoroalkyl and polyfluoroalkyl substances in the environment: Terminology, classification, and origins. Integrated Environmental Assessment and Management, 7(4), 513–541. https://doi.org/10.1002/ieam.258

Buckley, T., Karanam, K., Han, H., Vo, H. N. P., Shukla, P., Firouzi, M., & Rudolph, V. (2023). Effect of different co-foaming agents on PFAS removal from the environment by foam fractionation. Water Research, 230, 119532. https://doi.org/10.1016/j.watres.2022.119532

Buckley, T., Xu, X., Rudolph, V., Firouzi, M., & Shukla, P. (2022). Review of foam fractionation as a water treatment technology. Separation Science and Technology (Philadelphia), 57(6), 929–958. https://doi.org/10.1080/01496395.2021.1946698

Burkhardt, J., Speth, T. F., Gorzelnik, S., Gorzalski, A. S., Coronell, O., El-Khattabi, A. R., & Ateia, M. (2025). How Do Novel PFAS Sorbents Fit into Current Engineering Paradigm? ACS ES and T Engineering, 5(4), 830–838. https://doi.org/10.1021/acsestengg.5c00036

Burns, D. J., Hinrichsen, H. M., Stevenson, P., & Murphy, P. J. C. (2022). Commercial-scale remediation of PFAS from a landfill leachate catchment using Surface-Active Foam Fractionation (SAFF). Remediation, 1(12). https://doi.org/10.1002/rem.21720

Burns, D. J., Stevenson, P., & Murphy, P. J. C. (2021). PFAS removal from groundwaters using Surface-Active Foam Fractionation. Remediation, 31(4), 19–33. https://doi.org/10.1002/rem.21694

Butt, C. M., Muir, D. C. G., & Mabury, S. A. (2014). Biotransformation pathways of fluorotelomer-based polyfluoroalkyl substances: A review. Environmental Toxicology and Chemistry, 33(2), 243–267. https://doi.org/10.1002/etc.2407

Casas, G., Iriarte, J., D'Agostino, L. A., Roscales, J. L., Martinez-Varela, A., Vila-Costa, M., Martin, J. W., Jiménez, B., & Dachs, J. (2023). Inputs, amplification and sinks of perfluoroalkyl substances at coastal Antarctica. Environmental Pollution, 338, 122608. https://doi.org/10.1016/j.envpol.2023.122608

Casella, G. S., Miranda, M. M., Drumond, G. P., Silva, G. O. R. e., Zouaoui, F., Arcanjo, G. S., Amaral, M. C. S., de Paula, E. C., & Moreira, V. R. (2026). Recent developments in membrane treatment technologies for PFAS removal from surface and groundwater. Journal of Environmental Chemical Engineering, 14(1), 120598. https://doi.org/10.1016/j.jece.2025.120598

Chen, J., Liu, J., Evrendilek, F., Tao, L., Yao, C., Zou, Z., Chen, T., Li, L., Cai, B., Zhuang, G., Evrendilek, G. A., & Huang, J. (2026). Breaking the "Forever Chemical" Cycle: A Critical Review of Per- and Polyfluoroalkyl Substances in Solid Waste Sources and Their Fate During Thermal Treatment. Processes, 14(5), 1–34. https://doi.org/10.3390/pr14050865

Chen, Z. wei, Hua, Z. lin, & Guo, P. (2024). The bioaccumulation and ecotoxicity of co-exposure of per(poly)fluoroalkyl substances and polystyrene microplastics to Eichhornia crassipes. Water Research, 260, 121878. https://doi.org/10.1016/j.watres.2024.121878

Choo, Y. S., Song, S. D., & Albert, R. (2001). Effects of salinity on growth and patterns of ions and organic solutes in five sedges (Carex spp.) with different ecological demands. Flora, 196(1), 71–80. https://doi.org/10.1016/S0367-2530(17)30014-2

Coggan, T. L., Moodie, D., Kolobaric, A., Szabo, D., Shimeta, J., Crosbie, N. D., Lee, E., Fernandes, M., & Clarke, B. O. (2019). An investigation into per- and polyfluoroalkyl substances (PFAS) in nineteen Australian wastewater treatment plants (WWTPs). Heliyon, 5(8), e02316. https://doi.org/10.1016/j.heliyon.2019.e02316

Conder, J. M., Hoke, R. A., De Wolf, W., Russell, M. H., & Buck, R. C. (2008). Are PFCAs bioaccumulative? A critical review and comparison with regulatory criteria and persistent lipophilic compounds. Environmental Science and Technology, 42(4), 995–1003. https://doi.org/10.1021/es070895g

Cousins, I. T., Dewitt, J. C., Glüge, J., Goldenman, G., Herzke, D., Lohmann, R., Ng, C. A., Scheringer, M., & Wang, Z. (2020). The high persistence of PFAS is sufficient for their management as a chemical class. Environmental Science: Processes and Impacts, 22(12), 2307–2312. https://doi.org/10.1039/d0em00355g

Dalmijn, J., Glüge, J., Scheringer, M., & Cousins, I. T. (2023). Emission inventory of PFASs and other fluorinated organic substances for the fluoropolymer production industry in Europe. Environmental Science: Processes and Impacts, 26(2), 269–287. https://doi.org/10.1039/d3em00426k

Dams, R., & Ameduri, B. (2025). Essential Per- and Polyfluoroalkyl Substances (PFAS) in Our Society of the Future. Molecules, 30(15), 1–22. https://doi.org/10.3390/molecules30153220

Das, T. K., Han, Z., Banerjee, S., Raoelison, O. D., Adeleye, A. S., & Mohanty, S. K. (2024). PFAS release from the subsurface and capillary fringe during managed aquifer recharge. Environmental Pollution, 343, 123166. https://doi.org/10.1016/j.envpol.2023.123166

Divine, C., Melicharek, L., Gomes, D., Heinze, K., Erickson, J., Barker, B., Liles, D., Baumeister, A., Foote, E., Aust, J., Dugan, T., Wells, M., & Bayer, S. (2025). Field demonstration of in situ stabilization (ISS) of per- and polyfluoroalkyl substances in soil with remBind®. Journal of Hazardous Materials, 499, 140127. https://doi.org/10.1016/j.jhazmat.2025.140127

Downer, A., Eastoe, J., Pitt, A. R., Simister, E. A., & Penfold, J. (1999). Effects of hydrophobic chain structure on adsorption of fluorocarbon surfactants with either CF3- or H-CF2-terminal groups. Langmuir, 15(22), 7591–7599. https://doi.org/10.1021/la990549f

Elisabeth Hawley, B. L., Tessa Pancras, P., & Burdick, J. (2012). Remediation Technologies for Perfluorinated Compounds (PFCs), Including Perfluorooctane Sulfonate (PFOS) and Perfluorooctanoic Acid (PFOA) (Issue May). www.arcadis-us.com

Ellis, A. C., Boyer, T. H., & Strathmann, T. J. (2025). Regeneration of conventional and emerging PFAS-selective anion exchange resins used to treat PFAS-contaminated waters. Separation and Purification Technology, 355, 129789. https://doi.org/10.1016/j.seppur.2024.129789

Ellis, A. C., Liu, C. J., Fang, Y., Boyer, T. H., Schaefer, C. E., Higgins, C. P., & Strathmann, T. J. (2022). Pilot study comparison of regenerable and emerging single-use anion exchange resins for treatment of groundwater contaminated by per- and polyfluoroalkyl substances (PFASs). Water Research, 223, 119019. https://doi.org/10.1016/j.watres.2022.119019

Eschauzier, C., Raat, K. J., Stuyfzand, P. J., & De Voogt, P. (2013). Perfluorinated alkylated acids in groundwater and drinking water: Identification, origin and mobility. Science of the Total Environment, 458–460, 477–485. https://doi.org/10.1016/j.scitotenv.2013.04.066

European chemicals agency. (n.d.). Substances restricted under REACH. Retrieved January 13, 2026, from https://echa.europa.eu/substances-restricted-under-reach

European Union (EU). (2020). Directive (EU) 2020/218 of the European Parliment and of the Council on the quality of water intended for human consumption (recast). https://doi.org/10.4324/9781843141198-4

Evich, M. G., Davis, M. J. B., McCord, J. P., Acrey, B., Awkerman, J. A., Knappe, D. R. U., Lindstrom, A. B., Speth, T. F., Tebes-Stevens, C., Strynar, M. J., Wang, Z., Weber, E. J., Henderson, W. M., & Washington, J. W. (2022). Per- and polyfluoroalkyl substances in the environment. Science, 375(6580). https://doi.org/10.1126/science.abg9065

Faust, J. A. (2022). PFAS on atmospheric aerosol particles: a review. Environmental Science: Processes and Impacts. https://doi.org/10.1039/d2em00002d

Felizeter, S., McLachlan, M. S., & De Voogt, P. (2012). Uptake of perfluorinated alkyl acids by hydroponically grown lettuce (Lactuca sativa). Environmental Science and Technology, 46(21), 11735–11743. https://doi.org/10.1021/es302398u

Felizeter, S., McLachlan, M. S., & De Voogt, P. (2014). Root uptake and translocation of perfluorinated alkyl acids by three hydroponically grown crops. Journal of Agricultural and Food Chemistry, 62(15), 3334–3342. https://doi.org/10.1021/jf500674j

Feng, M., Gao, R., Staack, D., Pillai, S. D., & Sharma, V. K. (2021). Degradation of perfluoroheptanoic acid in water by electron beam irradiation. Environmental Chemistry Letters, 19(3), 2689–2694. https://doi.org/10.1007/s10311-021-01195-x

Franke, V., McCleaf, P., Lindegren, K., & Ahrens, L. (2019). Efficient removal of per- And polyfluoroalkyl substances (PFASs) in drinking water treatment: Nanofiltration combined with active carbon or anion exchange. Environmental Science: Water Research and Technology, 5(11), 1836–1843. https://doi.org/10.1039/c9ew00286c

Gaines, L. (2022). Historical and current usage of per- and polyfluoroalkyl substances (PFAS): A literature review. American Journal of Industrial Medicine, 66, 353–378. https://doi.org/10.1002/ajim.23362 |

Giesy, J. P., & Kannan, K. (2001). Global distribution of perfluorooctane sulfonate in wildlife. Environmental Science and Technology, 35(7), 1339–1342. https://doi.org/10.1021/es001834k

Gilbert, P., & Moore, L. E. (2005). Cationic antiseptics: Diversity of action under a common epithet. Journal of Applied Microbiology, 99(4), 703–715. https://doi.org/10.1111/j.1365-2672.2005.02664.x

Girardi, P., & Merler, E. (2019). A mortality study on male subjects exposed to polyfluoroalkyl acids with high internal dose of perfluorooctanoic acid. Environmental Research, 179, 108743. https://doi.org/10.1016/j.envres.2019.108743

Gkika, I. S., Arie Vonk, J., ter Laak, T. L., van Gestel, C. A. M., Dijkstra, J., Groffen, T., Bervoets, L., & Kraak, M. H. S. (2025). Strong bioaccumulation of a wide variety of PFAS in a contaminated terrestrial and aquatic ecosystem. Environment International, 202, 109629. https://doi.org/10.1016/j.envint.2025.109629

Gnesda, W. R., Draxler, E. F., Tinjum, J., & Zahasky, C. (2022). Adsorption of PFAAs in the Vadose Zone and Implications for Long-Term Groundwater Contamination. Environmental Science and Technology, 56(23), 16748–16758. https://doi.org/10.1021/acs.est.2c03962

Gobelius, L., Lewis, J., & Ahrens, L. (2017). Plant Uptake of Per- and Polyfluoroalkyl Substances at a Contaminated Fire Training Facility to Evaluate the Phytoremediation Potential of Various Plant Species. Environmental Science and Technology, 51(21), 12602–12610. https://doi.org/10.1021/acs.est.7b02926

Goldwhite, H. (1986). THE MANHATTAN PROJECT. Journal of Fluorine Chemistry, 33, 109–132.

Gonzalez-Olmos, R., Penadés, A., & Garcia, G. (2018). Electro-oxidation as efficient pretreatment to minimize the membrane fouling in water reuse processes. Journal of Membrane Science, 552, 124–131. https://doi.org/10.1016/j.memsci.2018.01.041

Greger, M. (2021). Removal of PFAS from Water by Plants. International Journal of Environmental Sciences & Natural Resources, 28(2), 1–6. https://doi.org/10.19080/ijesnr.2021.28.556233

Griffin, A. M., Bellona, C., & Strathmann, T. J. (2024). Rejection of PFAS and priority co-contaminants in semiconductor fabrication wastewater by nanofiltration membranes. Water Research, 262, 122111. https://doi.org/10.1016/j.watres.2024.122111

Groffen, T., Lasters, R., Lopez-Antia, A., Prinsen, E., Bervoets, L., & Eens, M. (2019). Limited reproductive impairment in a passerine bird species exposed along a perfluoroalkyl acid (PFAA) pollution gradient. Science of the Total Environment, 652(2019), 718–728. https://doi.org/10.1016/j.scitotenv.2018.10.273

Guelfo, J. L., & Higgins, C. P. (2013). Subsurface transport potential of perfluoroalkyl acids at aqueous film-forming foam (AFFF)-impacted sites. Environmental Science and Technology, 47(9), 4164–4171. https://doi.org/10.1021/es3048043

Hamid, H., Li, L. Y., & Grace, J. R. (2018). Review of the fate and transformation of per- and polyfluoroalkyl substances (PFASs) in landfills. Environmental Pollution, 235, 74–84. https://doi.org/10.1016/j.envpol.2017.12.030

Hao, S., Choi, Y. J., Wu, B., Higgins, C. P., Deeb, R., & Strathmann, T. J. (2021). Hydrothermal alkaline treatment for destruction of per-and polyfluoroalkyl substances in aqueous film-forming foam. Environmental Science and Technology, 55(5), 3283–3295. https://doi.org/10.1021/acs.est.0c06906

Haukås, M., Berger, U., Hop, H., Gulliksen, B., & Gabrielsen, G. W. (2007). Bioaccumulation of per- and polyfluorinated alkyl substances (PFAS) in selected species from the Barents Sea food web. Environmental Pollution, 148(1), 360–371. https://doi.org/10.1016/j.envpol.2006.09.021

Havs- och Vattenmyndigheten. (2019). Havs- och vattenmyndighetens föreskrifter om klassificering och miljökvalitetsnormer avseende ytvatten. Havs-Och Vattenmyndighetens Författningssamling, HVMFS 2019:25.

Henry, B. J., Carlin, J. P., Hammerschmidt, J. A., Buck, R. C., Buxton, L. W., Fiedler, H., Seed, J., & Hernandez, O. (2018). A critical review of the application of polymer of low concern and regulatory criteria to fluoropolymers. Integrated Environmental Assessment and Management, 14(3), 316–334. https://doi.org/10.1002/ieam.4035

Hepburn, E., Madden, C., Szabo, D., Coggan, T. L., Clarke, B., & Currell, M. (2019). Contamination of groundwater with per- and polyfluoroalkyl substances (PFAS) from legacy landfills in an urban re-development precinct. Environmental Pollution, 248, 101–113. https://doi.org/10.1016/j.envpol.2019.02.018

Higgins, C. P., & Luthy, R. G. (2006). Sorption of perfluorinated surfactants on sediments. Environmental Science and Technology, 40(23), 7251–7256. https://doi.org/10.1021/es061000n

Hohweiler, K., Krometis, L. A., Ling, E. J., & Xia, K. (2024). Incidence of per- and polyfluoroalkyl substances (PFAS) in private drinking water supplies in

Southwest Virginia, USA. Science of the Total Environment, 929, 172539. https://doi.org/10.1016/j.scitotenv.2024.172539

Hopkins, K. E., McKinney, M. A., Saini, A., Letcher, R. J., Karouna-Renier, N. K., & Fernie, K. J. (2023). Characterizing the Movement of Per- and Polyfluoroalkyl Substances in an Avian Aquatic-Terrestrial Food Web. Environmental Science and Technology, 57(48), 20249–20260. https://doi.org/10.1021/acs.est.3c06944

Huang, K., Li, Y., Bu, D., Fu, J., Wang, M., Zhou, W., Gu, L., Fu, Y., Cong, Z., Hu, B., Fu, J., Zhang, A., & Jiang, G. (2022). Trophic Magnification of Short-Chain Per- and Polyfluoroalkyl Substances in a Terrestrial Food Chain from the Tibetan Plateau. Environmental Science and Technology Letters, 9(2), 147–152. https://doi.org/10.1021/acs.estlett.1c01009

Hubert, M., Arp, H. P. H., Hansen, M. C., Castro, G., Meyn, T., Asimakopoulos, A. G., & Hale, S. E. (2023). Influence of grain size, organic carbon and organic matter residue content on the sorption of per- and polyfluoroalkyl substances in aqueous film forming foam contaminated soils - Implications for remediation using soil washing. Science of the Total Environment, 875, 162668. https://doi.org/10.1016/j.scitotenv.2023.162668

Hubert, M., Meyn, T., Hansen, M. C., Hale, S. E., & Arp, H. P. H. (2024). Per- and polyfluoroalkyl substance (PFAS) removal from soil washing water by coagulation and flocculation. Water Research, 249(0806), 120888. https://doi.org/10.1016/j.watres.2023.120888

Hunter Anderson, R., Adamson, D. T., & Stroo, H. F. (2019). Partitioning of poly- and perfluoroalkyl substances from soil to groundwater within aqueous film-forming foam source zones. Journal of Contaminant Hydrology, 220, 59–65. https://doi.org/10.1016/j.jconhyd.2018.11.011

Interstate Technology Regulatory Council (ITRC). (2026). Technical and Regulatory Guidance: PFAS — Per- and Polyfluoroalkyl Substances. January. https://pfas-1.itrcweb.org/pdf-full-document/

James, R., Sidnell, T., Ross, I., Mcdonough, J., Lee, J., & Bussemaker, M. J. (2020). Ultrasonics - Sonochemistry Ultrasonic degradation of perfluorooctane sulfonic acid (PFOS) correlated with sonochemical and sonoluminescence characterisation. Ultrasonics - Sonochemistry, 68, 105196. https://doi.org/10.1016/j.ultsonch.2020.105196

Jia, Y., Li, Y., Kang, S., Li, C., Munoz, G., Hao, S., Xiao, F., Zhi, Y., Liu, C., & Zhang, C. (2025). Sources and occurrence of per- and polyfluoroalkyl substances in industrial wastewater and assessment of current treatment approaches: A review. Journal of Hazardous Materials, 499, 140195. https://doi.org/10.1016/j.jhazmat.2025.140195

Jiang, L., Wang, S., Chen, W., Lin, J., Yu, X., Feng, M., & Wan, K. (2022). Removal of Per-and Polyfluoroalkyl Substances by Electron Beam and Plasma

Irradiation: A Mini-Review. Water, 14, 1684. https://doi.org/10.3390/w14111684

Jiang, T., Pervez, M. N., Ilango, A. K., & Liang, Y. (2025). Stabilizing per- and polyfluoroalkyl substances (PFAS) through amending an adsorbent to contaminated soil planted with alfalfa. Science of the Total Environment, 1000, 180430. https://doi.org/10.1016/j.scitotenv.2025.180430

Joerss, H., Freeling, F., van Leeuwen, S., Hollender, J., Liu, X., Nödler, K., Wang, Z., Yu, B., Zahn, D., & Sigmund, G. (2024). Pesticides can be a substantial source of trifluoroacetate (TFA) to water resources. Environment International, 193(September). https://doi.org/10.1016/j.envint.2024.109061

Johnson, G. R. (2022). PFAS in soil and groundwater following historical land application of biosolids. Water Research, 211, 118035. https://doi.org/10.1016/j.watres.2021.118035

Kargas, G., Chatzigiakoumis, I., Kollias, A., Spiliotis, D., Massas, I., & Kerkides, P. (2018). Soil salinity assessment using saturated paste and mass soil:water 1:1 and 1:5 ratios extracts. Water, 10, 1589. https://doi.org/10.3390/w10111589

Kasak, K., Truu, J., Ostonen, I., Sarjas, J., Oopkaup, K., Paiste, P., Kõiv-Vainik, M., Mander, Ü., & Truu, M. (2018). Biochar enhances plant growth and nutrient removal in horizontal subsurface flow constructed wetlands. Science of the Total Environment, 639, 67–74. https://doi.org/10.1016/j.scitotenv.2018.05.146

Kearns, J., Dickenson, E., Aung, M. T., Joseph, S. M., Summers, S. R., & Knappe, D. (2021). Biochar Water Treatment for Control of Organic Micropollutants with UVA Surrogate Monitoring. Environmental Engineering Science, 38(5), 298–309. https://doi.org/10.1089/ees.2020.0173

Kim, S. K., & Kannan, K. (2007). Perfluorinated acids in air, rain, snow, surface runoff, and lakes: Relative importance of pathways to contamination of urban lakes. Environmental Science and Technology, 41(24), 8328–8334. https://doi.org/10.1021/es072107t

Klevan, C., Van Allen, O., Xia, S., Mukai, K., Gomes, A., Caines, S., Woodcock, M. J., & Pennell, K. D. (2025). Evaluation of co-foaming agents for enhanced removal of per-and polyfluoroalkyl substances (PFAS) by foam fractionation. Journal of Hazardous Materials, 494, 138423. https://doi.org/10.1016/j.jhazmat.2025.138423

Kookana, R. S., Sha, B., Baluyot, J. C., Bowles, K. C., Kah, M., Padhye, L. P., Ying, G. G., Navarro, D., Velarde, M. C., Higgins, C. P., & Cousins, I. T. (2025). Human exposure to per- and poly-fluoroalkyl substances (PFAS) in Asia and contributing factors, with a focus on East Asia. Environmental Science: Processes and Impacts, 27(9), 2614–2635. https://doi.org/10.1039/d5em00396b

Krippner, J., Brunn, H., Falk, S., Georgii, S., Schubert, S., & Stahl, T. (2014). Effects of chain length and pH on the uptake and distribution of perfluoroalkyl substances in maize (Zea mays). Chemosphere, 94, 85–90. https://doi.org/10.1016/j.chemosphere.2013.09.018

Kumar, A., Thakur, M. K., Hart, P., & Thakur, V. K. (2025). Mechanistic Insights and Design Strategies for Hydrogel / Aerogel Sorbents in Remediation of Per- and Polyfluoroalkyl Substances. ACS Environmental Au, 6(1), 1–20. https://doi.org/10.1021/acsenvironau.5c00081

Kumarasamy, E., Manning, I. M., Collins, L. B., Coronell, O., & Leibfarth, F. A. (2020). Ionic Fluorogels for Remediation of Per-and Polyfluorinated Alkyl Substances from Water. ACS Central Science, 6(4), 487–492. https://doi.org/10.1021/acscentsci.9b01224

Kurwadkar, S., Dane, J., Kanel, S. R., Nadagouda, M. N., Cawdrey, R. W., Ambade, B., Struckhoff, G. C., & Wilkin, R. (2022). Per- and polyfluoroalkyl substances in water and wastewater: A critical review of their global occurrence and distribution. Science of the Total Environment, 809, 151003. https://doi.org/10.1016/j.scitotenv.2021.151003

Lassalle, J., Gao, R., Rodi, R., Kowald, C., Feng, M., Sharma, V. K., Hoelen, T., Bireta, P., Houtz, E. F., Staack, D., & Pillai, S. D. (2021). Degradation of PFOS and PFOA in soil and groundwater samples by high dose Electron Beam Technology. Radiation Physics and Chemistry, 189, 109705. https://doi.org/10.1016/j.radphyschem.2021.109705

Lenka, S. P., Kah, M., & Padhye, L. P. (2021). A review of the occurrence, transformation, and removal of poly- and perfluoroalkyl substances (PFAS) in wastewater treatment plants. Water Research, 199, 117187. https://doi.org/10.1016/j.watres.2021.117187

Leung, S. C. E., Wanninayake, D., Chen, D., Nguyen, N. T., & Li, Q. (2023). Physicochemical properties and interactions of perfluoroalkyl substances (PFAS) - Challenges and opportunities in sensing and remediation. Science of the Total Environment, 905, 166764. https://doi.org/10.1016/j.scitotenv.2023.166764

Li, H., Hammarstrand, S., Midberg, B., Xu, Y., Li, Y., Olsson, D. S., Fletcher, T., Jakobsson, K., & Andersson, E. M. (2022). Cancer incidence in a Swedish cohort with high exposure to perfluoroalkyl substances in drinking water. Environmental Research, 204, 112217. https://doi.org/10.1016/j.envres.2021.112217

Li, J., Pinkard, B. R., Wang, S., & Novosselov, I. V. (2022). Review: Hydrothermal treatment of per- and polyfluoroalkyl substances (PFAS). Chemosphere, 307, 135888. https://doi.org/10.1016/j.chemosphere.2022.135888

Li, J., Xi, B., Zhu, G., Yuan, Y., Liu, W., Gong, Y., & Tan, W. (2023). A critical review of the occurrence, fate and treatment of per- and polyfluoroalkyl

substances (PFASs) in landfills. Environmental Research, 218(October 2022), 114980. https://doi.org/10.1016/j.envres.2022.114980

Li, Y., Barregard, L., Xu, Y., Scott, K., Pineda, D., Lindh, C. H., Jakobsson, K., & Fletcher, T. (2020). Associations between perfluoroalkyl substances and serum lipids in a Swedish adult population with contaminated drinking water. Environmental Health: A Global Access Science Source, 19(1), 1–11. https://doi.org/10.1186/s12940-020-00588-9

Liang, M., Kabiri, S., McLaughlin, M. J., & Navarro, D. (2025). Enhanced immobilisation of per- and polyfluoroalkyl substances (PFAS) using a combination of sorbents and plants: A controlled rainfall simulation study. Science of the Total Environment, 989, 179835. https://doi.org/10.1016/j.scitotenv.2025.179835

Liang, R. R., Liu, Z., Rushlow, J., Huo, J., Han, Z., Yang, Y., Lin, H., & Zhou, H. C. (2025). Metal–Organic Frameworks for Per- and Polyfluoroalkyl Substances Treatment in Contaminated Water. ACS Materials Letters, 7(10), 3252–3274. https://doi.org/10.1021/acsmaterialslett.5c00902

Liang, R. R., Xu, S., Han, Z., Yang, Y., Wang, K. Y., Huang, Z., Rushlow, J., Cai, P., Samorì, P., & Zhou, H. C. (2024). Exceptionally High Perfluorooctanoic Acid Uptake in Water by a Zirconium-Based Metal-Organic Framework through Synergistic Chemical and Physical Adsorption. Journal of the American Chemical Society, 146(14), 9811–9818. https://doi.org/10.1021/jacs.3c14487

Liang, S., Mora, R., Huang, Q., Casson, R., Wang, Y., Woodard, S., & Anderson, H. (2022). Field demonstration of coupling ion-exchange resin with electrochemical oxidation for enhanced treatment of per- and polyfluoroalkyl substances (PFAS) in groundwater. Chemical Engineering Journal Advances, 9, 100216. https://doi.org/10.1016/j.ceja.2021.100216

Liao, Z., & Farrell, J. (2009). Electrochemical oxidation of perfluorobutane sulfonate using boron-doped diamond film electrodes. Journal of Applied Electrochemistry, 39(10), 1993–1999. https://doi.org/10.1007/s10800-009-9909-z

Liljeström, O., Rosenquist, D., Kleja, D. B., Enell, A., & Ahrens, L. (2025). Pilot scale treatment of PFAS-contaminated groundwater in a subsurface flow constructed wetland – evaluating multiple plant species. Environmental Pollution, 386, 127199. https://doi.org/10.1016/j.envpol.2025.127199

Ling, A. L., Stegner, T., Thompson, M., Viswanathan, S., Pinkard, B. R., Wolohan, K. M., Richard, D. E., & Ellis, A. (2025). Spent Media Management Pathways for PFAS Treatment Applications. Water Environment Research, 97(7), 1–16. https://doi.org/10.1002/wer.70130

Liu, C., Chu, J., Cápiro, N. L., Fortner, J. D., & Pennell, K. D. (2022). In-situ sequestration of perfluoroalkyl substances using polymer-stabilized ion

exchange resin. Journal of Hazardous Materials, 422, 126960. https://doi.org/10.1016/j.jhazmat.2021.126960

Liu, F., Guan, X., & Xiao, F. (2022). Photodegradation of per- and polyfluoroalkyl substances in water: A review of fundamentals and applications. Journal of Hazardous Materials, 439, 129580. https://doi.org/10.1016/j.jhazmat.2022.129580

Liu, S., Zhao, S., Liang, Z., Wang, F., Sun, F., & Chen, D. (2021). Perfluoroalkyl substances (PFASs) in leachate, fly ash, and bottom ash from waste incineration plants: Implications for the environmental release of PFAS. Science of the Total Environment, 795, 148468. https://doi.org/10.1016/j.scitotenv.2021.148468

Liu, W., Wang, S., Zhao, Q., Yu, P., Guo, Z., Xie, H., Zhang, J., & Hu, Z. (2025). Distribution and ecological risks of Per- and polyfluoroalkyl substances in constructed wetland: Field-scale case study. Journal of Water Process Engineering, 79, 109024. https://doi.org/10.1016/j.jwpe.2025.109024

Liu, Y., Shao, L. X., Yu, W. J., Bao, J., Li, T. Y., Hu, X. M., & Zhao, X. (2022). Simultaneous removal of multiple PFAS from contaminated groundwater around a fluorochemical facility by the periodically reversing electrocoagulation technique. Chemosphere, 307, 135874. https://doi.org/10.1016/j.chemosphere.2022.135874

Livsmedelsverket. (2022). Livsmedelsverkets föreskrifter om dricksvatten. Livsmedelsverkets Författningssamling, LIVSFS 2022:12.

Lohmann, R., Cousins, I. T., Dewitt, J. C., Glüge, J., Goldenman, G., Herzke, D., Lindstrom, A. B., Miller, M. F., Ng, C. A., Patton, S., Scheringer, M., Trier, X., & Wang, Z. (2020). Are Fluoropolymers Really of Low Concern for Human and Environmental Health and Separate from Other PFAS? Environmental Science and Technology, 54(20), 12820–12828. https://doi.org/10.1021/acs.est.0c03244

Longendyke, G. K., Katel, S., & Wang, Y. (2022). PFAS fate and destruction mechanisms during thermal treatment: A comprehensive review. Environmental Science: Processes and Impacts, 24(2), 196–208. https://doi.org/10.1039/d1em00465d

Lopez-Espinosa, M.-J., Fletcher, T., Mondal, D., Bloom, M. S., & Leonardi, G. (2011). Thyroid Function, Pfoa and Pfos in Children Living Near a Chemical Plant. ISEE Conference Abstracts, 2011(1), 1036–1041. https://doi.org/10.1289/isee.2011.00261

Lott, D. J., Robey, N. M., Fonseca, R., Bowden, J. A., & Townsend, T. G. (2023). Behavior of Per- and polyfluoroalkyl substances (PFAS) in Pilot-Scale vertical flow constructed wetlands treating landfill leachate. Waste Management, 161, 187–192. https://doi.org/10.1016/j.wasman.2023.03.001

Ma, Q., Lei, Q., Liu, F., Song, Z., Khusid, B., & Zhang, W. (2024). Evaluation of commercial nanofiltration and reverse osmosis membrane filtration to

remove per-and polyfluoroalkyl substances (PFAS): Effects of transmembrane pressures and water matrices. Water Environment Research, 96(2), 1–17. https://doi.org/10.1002/wer.10983

Mai, C., Dang, X., Zhao, L., Daria, D., Ma, F., Bao, M., Geng, F., & Lynch, I. (2026). Soil property-dependent toxicity and oxidative stress induced by perfluorooctanoic acid in Caenorhabditis elegans. Environmental Technology and Innovation, 41, 104762. https://doi.org/10.1016/j.eti.2026.104762

Martin, J. W., Mabury, S. A., Solomon, K. R., & Muir, D. C. G. (2003). Bioconcentration and tissue distribution of perfluorinated acids in rainbow trout (Oncorhynchus mykiss). Environmental Toxicology and Chemistry, 22(1), 196–204. https://doi.org/10.1002/etc.5620220126

McCleaf, P., Stefansson, W., & Ahrens, L. (2023). Drinking water nanofiltration with concentrate foam fractionation—A novel approach for removal of per- and polyfluoroalkyl substances (PFAS). Water Research, 232, 119688. https://doi.org/10.1016/j.watres.2023.119688

Meegoda, J. N., Bezerra de Souza, B., Casarini, M. M., & Kewalramani, J. A. (2022). A Review of PFAS Destruction Technologies. International Journal of Environmental Research and Public Health, 19, 16397. https://doi.org/10.3390/ijerph192416397

Megson, D., Bruce-Vanderpuije, P., Idowu, I. G., Ekpe, O. D., & Sandau, C. D. (2025). A systematic review for non-targeted analysis of per- and polyfluoroalkyl substances (PFAS). Science of the Total Environment, 960, 178240. https://doi.org/10.1016/j.scitotenv.2024.178240

Mirabediny, M., Sun, J., Yu, T. T., Åkermark, B., Das, B., & Kumar, N. (2023). Effective PFAS degradation by electrochemical oxidation methods-recent progress and requirement. Chemosphere, 321, 138109. https://doi.org/10.1016/j.chemosphere.2023.138109

Mišľanová, C., & Valachovičová, M. (2025). Health Impacts of Per- and Polyfluoroalkyl Substances (PFASs): A Comprehensive Review. Life, 15(4), 1–35. https://doi.org/10.3390/life15040573

Mohammadi, N., Guclu, S., Atespare, A. E., Koseoglu-Imer, D. Y., Unal, S., & Dizman, B. (2025). Sustainable ion exchange-based remediation of per- and polyfluoroalkyl substances; recent progress and future prospects. Journal of Water Process Engineering, 71, 107345. https://doi.org/10.1016/j.jwpe.2025.107345

Nassazzi, W., Lai, F. Y., & Ahrens, L. (2022). A novel method for extraction, clean-up and analysis of per- and polyfluoroalkyl substances (PFAS) in different plant matrices using LC-MS/MS. Journal of Chromatography B: Analytical Technologies in the Biomedical and Life Sciences, 1212, 123514. https://doi.org/10.1016/j.jchromb.2022.123514

Nassazzi, W., Wu, T. C., Jass, J., Lai, F. Y., & Ahrens, L. (2023). Phytoextraction of per- and polyfluoroalkyl substances (PFAS) and the influence of supplements on the performance of short–rotation crops. Environmental Pollution, 333, 122038. https://doi.org/10.1016/j.envpol.2023.122038

Navarro, D. A., Kabiri, S. S., Bowles, K., Knight, E. R., Braeunig, J., Srivastava, P., Boxall, N. J., Douglas, G., Mueller, J., McLaughlin, M. J., Williams, M., & Kookana, R. S. (2024). Review on Methods for Assessing and Predicting Leaching of PFAS from Solid Matrices. Current Pollution Reports, 10(4), 628–647. https://doi.org/10.1007/s40726-024-00326-6

Newell, C. J., Cook, J. S., Adamson, D. T., & Hatzinger, P. B. (2025). A Long Way to Go: Challenges and Strategies for Managing PFAS in Groundwater. Remediation, 35(4). https://doi.org/10.1002/rem.70028

Niarchos, G., Ahrens, L., Kleja, D. B., Leonard, G., Forde, J., Bergman, J., Ribeli, E., Schütz, M., & Fagerlund, F. (2023). In-situ application of colloidal activated carbon for PFAS-contaminated soil and groundwater: A Swedish case study. Remediation, 33(2), 101–110. https://doi.org/10.1002/rem.21746

Niu, J., Lin, H., Xu, J., Wu, H., & Li, Y. (2012). Electrochemical mineralization of perfluorocarboxylic acids (PFCAs) by Ce-doped modified porous nanocrystalline PbO2 film electrode. Environmental Science and Technology, 46(18), 10191–10198. https://doi.org/10.1021/es302148z

Norwegian Institute fow Water Research (NIVA). (2025). PFAS in drinking water in India - A review. 8088–2025.

Nzeribe, B. N., Crimi, M., Mededovic Thagard, S., & Holsen, T. M. (2019). Physico-Chemical Processes for the Treatment of Per- And Polyfluoroalkyl Substances (PFAS): A review. Critical Reviews in Environmental Science and Technology, 49(10), 866–915. https://doi.org/10.1080/10643389.2018.1542916

O'hagan, D. (2008). Understanding organofluorine chemistry. An introduction to the C–F bond. Chemical Society Reviews, 37(2), 308–319. https://doi.org/10.1039/b711844a

Oakes, K. D., Benskin, J. P., Martin, J. W., Ings, J. S., Heinrichs, J. Y., Dixon, D. G., & Servos, M. R. (2010). Biomonitoring of perfluorochemicals and toxicity to the downstream fish community of Etobicoke Creek following deployment of aqueous film-forming foam. Aquatic Toxicology, 98(2), 120–129. https://doi.org/10.1016/j.aquatox.2010.02.005

Ochoa-Herrera, V., Field, J. A., Luna-Velasco, A., & Sierra-Alvarez, R. (2016). Microbial toxicity and biodegradability of perfluorooctane sulfonate (PFOS) and shorter chain perfluoroalkyl and polyfluoroalkyl substances (PFASs). Environmental Science: Processes and Impacts, 18(9), 1236–1246. https://doi.org/10.1039/c6em00366d

OECD. (2021). Reconciling Terminology of the Universe of Per- and Polyfluoroalkyl Substances: Recommendations and Practical Guidance. Series on Risk Management No. 61; ENV/CBC/MONO(2021)25. https://www.oecd.org/chemicalsafety/portal-perfluorinated-chemicals/terminology-per-and-polyfluoroalkyl-substances.pdf

Olsson, Y. (2025). Jordbruksmarkens användning 2025. Slutgiltlig statistik. Jordbruksverket. https://jordbruksverket.se/om-jordbruksverket/jordbruksverkets-officiella-statistik/jordbruksverkets-statistikrapporter/statistik/2025-10-22-jordbruksmarkens-anvandning-2025.-slutlig-statistik

Pan, Y., Zhang, H., Cui, Q., Sheng, N., Yeung, L. W. Y., Guo, Y., Sun, Y., & Dai, J. (2017). First Report on the Occurrence and Bioaccumulation of Hexafluoropropylene Oxide Trimer Acid: An Emerging Concern. Environmental Science and Technology, 51(17), 9553–9560. https://doi.org/10.1021/acs.est.7b02259

Pérez-González, A., Ibáñez, R., Gómez, P., Urtiaga, A. M., Ortiz, I., & Irabien, J. A. (2015). Recovery of desalination brines: separation of calcium, magnesium and sulfate as a pre-treatment step. Desalination and Water Treatment, 56(13), 3617–3625. https://doi.org/10.1080/19443994.2014.973454

Peritore, A. F., Gugliandolo, E., Cuzzocrea, S., Crupi, R., & Britti, D. (2023). Current Review of Increasing Animal Health Threat of Per- and Polyfluoroalkyl Substances (PFAS): Harms, Limitations, and Alternatives to Manage Their Toxicity. International Journal of Molecular Sciences, 24, 11707. https://doi.org/10.3390/ijms241411707

Persson, G., & Lindroth, A. (1994). Simulating evaporation from short-rotation forest: variations within and between seasons. Journal of Hydrology, 156(1–4), 21–45. https://doi.org/10.1016/0022-1694(94)90069-8

Petterson, M., Ländell, M., Ohlsson, Y., Berggren Kleja, D., & Tiberg, C. (2015). Preliminära riktvärden för högfluorerade ämnen (PFAS) i mark och grundvatten. SGI Publikation, 21, 1.1-1502–0078. https://www.swedgeo.se/globalassets/publikationer/sgi-publikation/sgi-p21.pdf

Pierpaoli, M., Rycewicz, M., Łuczkiewicz, A., Fudala-Ksią Zek, S., Bogdanowicz, R., & Ruello, M. L. (2020). Electrodes criticality: The impact of CRMs in the leachate electrochemical oxidation. Manufacturing Review, 7, 7. https://doi.org/10.1051/mfreview/2020006

Plunkett, R. J. (1941). U.S. Patent No. 2,230,654 Tetrafluoroethylene polymers.

Prasetya, K. D., You, S. J., Ni'am, A. C., & Wang, Y. F. (2025). Water-based matrices thermal treatment for per- and polyfluoroalkyl substances (PFAS): A critical review on transformation mechanisms, role of radicals, and perspective towards. Journal of Hazardous Materials, 495, 138969. https://doi.org/10.1016/j.jhazmat.2025.138969

Pritchard, J. C., Hire, M., McDonough, J., Higgins, C. P., & Schaefer, C. E. (2026). PFAS conceptual site model of an AFFF-impacted firefighting training area informed by high resolution soil, porewater, and groundwater sampling. Journal of Contaminant Hydrology, 276, 104728. https://doi.org/10.1016/j.jconhyd.2025.104728

Radjenovic, J., & Sedlak, D. L. (2015). Challenges and Opportunities for Electrochemical Processes as Next-Generation Technologies for the Treatment of Contaminated Water. Environmental Science and Technology, 49(19), 11292–11302. https://doi.org/10.1021/acs.est.5b02414

Ragnarsdóttir, O., Abou-Elwafa Abdallah, M., & Harrad, S. (2024). Dermal bioavailability of perfluoroalkyl substances using in vitro 3D human skin equivalent models. Environment International, 188, 108772. https://doi.org/10.1016/j.envint.2024.108772

Ramstedt, M. (2024). Rening av lakvatten och jord vid deponin Dragmossen i Älvkarleby kommun.

Rauert, C., Shoieb, M., Schuster, J. K., Eng, A., & Harner, T. (2018). Atmospheric concentrations and trends of poly- and perfluoroalkyl substances (PFAS) and volatile methyl siloxanes (VMS) over 7 years of sampling in the Global Atmospheric Passive Sampling (GAPS) network. Environmental Pollution, 238, 94–102. https://doi.org/10.1016/j.envpol.2018.03.017

Rehnstam, S., Smith, S. J., & Ahrens, L. (2024). Suspect and non-target screening of per- and polyfluoroalkyl substances (PFAS) and other halogenated substances in electrochemically oxidized landfill leachate and groundwater. Journal of Hazardous Materials, 480, 136316. https://doi.org/10.1016/j.jhazmat.2024.136316

Ricolfi, L., Yang, Y., Pottier, P., Morrison, K., Williams, C., Pollo, P., Hesselson, D., Neely, G. G., Taylor, M. D., Nakagawa, S., & Lagisz, M. (2025). Unravelling the magnitude and drivers of PFAS trophic magnification: a meta-analysis. Nature Communications, 16, 10720. https://doi.org/10.1038/s41467-025-65746-4

Ritscher, A., Wang, Z., Scheringer, M., Boucher, J. M., Ahrens, L., Berger, U., Bintein, S., Bopp, S. K., Borg, D., Buser, A. M., Cousins, I., Dewitt, J., Fletcher, T., & Green, C. (2018). Zürich Statement on Future Actions on Per- and Polyfluoroalkyl Substances. Environmental Health Perspectives, 126(8), 084502. https://doi.org/https://doi.org/10.1289/EHP4158

Ross, I., McDonough, J., Miles, J., Storch, P., Thelakkat Kochunarayanan, P., Kalve, E., Hurst, J., S. Dasgupta, S., & Burdick, J. (2018). A review of emerging technologies for remediation of PFASs. Remediation, 28(2), 101–126. https://doi.org/10.1002/rem.21553

Rückbeil, F. E., Sperlich, A., Gnirss, R., Dittmann, D., Kämpfe, A., Höra, C., & Ruhl, A. S. (2025). Comparing activated carbons, ion exchange resins and

alternative adsorbents for the removal of perfluoroalkyl and other persistent and mobile substances. Chemical Engineering Journal, 516, 164070. https://doi.org/10.1016/j.cej.2025.164070

Sackett, D. K., Anderson, D., Henry, T., Sweetman, A. K., & Yonkos, L. (2024). Persistent organic pollutant accumulation in Pacific abyssal plain sediments and biota: Implications for sources, transport, and deep-sea mining. Elementa, 12(1), 1–21. https://doi.org/10.1525/elementa.2024.00042

Salvatore, D., Mok, K., Garrett, K. K., Poudrier, G., Brown, P., Birnbaum, L. S., Goldenman, G., Miller, M. F., Patton, S., Poehlein, M., Varshavsky, J., & Cordner, A. (2022). Presumptive Contamination: A New Approach to PFAS Contamination Based on Likely Sources. Environmental Science and Technology Letters, 9(11), 983–990. https://doi.org/10.1021/acs.estlett.2c00502

Sarkar, B., Kumawat, R. L., Ma, P., Wang, K.-H., Mohebi, M., Schatz, G. C., & Amanchukwu, C. V. (2026). Lithium metal-mediated electrochemical reduction of per- and poly-fluoroalkyl substances. Nature Chemistry, 18, 509–518. https://doi.org/10.1038/s41557-025-02057-7

Scheitlin, C. G., Dasu, K., Rosansky, S., Dejarme, L. E., Siriwardena, D., Thorn, J., Mullins, L., Haggerty, I., Shqau, K., & Stowe, J. (2023). Application of Supercritical Water Oxidation to Effectively Destroy Per- and Polyfluoroalkyl Substances in Aqueous Matrices. ACS ES and T Water, 3(8), 2053–2062. https://doi.org/10.1021/acsestwater.2c00548

Schellenberger, S., Liagkouridis, I., Awad, R., Khan, S., Plassmann, M., Peters, G., Benskin, J. P., & Cousins, I. T. (2022). An Outdoor Aging Study to Investigate the Release of Per- and Polyfluoroalkyl Substances (PFAS) from Functional Textiles. Environmental Science and Technology, 56(6), 3471–3479. https://doi.org/10.1021/acs.est.1c06812

Schroeder, T., Bond, D., & Foley, J. (2021). PFAS soil and groundwater contamination: Via industrial airborne emission and land deposition in SW Vermont and Eastern New York State, USA. Environmental Science: Processes and Impacts, 23(2), 291–301. https://doi.org/10.1039/d0em00427h

Schymanski, E. L., Zhang, J., Thiessen, P. A., Chirsir, P., Kondic, T., & Bolton, E. E. (2023). Per- and polyfluoroalkyl substances (PFAS) in PubChem: 7 million and growing. Environmental Science & Technology, 57, 16918–16928. https://doi.org/10.1021/acs.est.3c04855

Shao, Q., He, Y., White, A. D., & Jiang, S. (2010). Difference in hydration between carboxybetaine and sulfobetaine. Journal of Physical Chemistry B, 114(49), 16625–16631. https://doi.org/10.1021/jp107272n

Sharma, N., Barion, G., Shrestha, I., Ebinezer, L. B., Trentin, A. R., Vamerali, T., Mezzalira, G., Masi, A., & Ghisi, R. (2020). Accumulation and effects of perfluoroalkyl substances in three hydroponically grown Salix L. species.

Ecotoxicology and Environmental Safety, 191, 110150. https://doi.org/10.1016/j.ecoenv.2019.110150

Sharma, S., Shetti, N. P., Basu, S., Nadagouda, M. N., & Aminabhavi, T. M. (2022). Remediation of per- and polyfluoroalkyls (PFAS) via electrochemical methods. Chemical Engineering Journal, 430, 132895. https://doi.org/https://doi.org/10.1016/j.cej.2021.132895

Shea, S. M., Schaefer, C. E., Illangasekare, T., & Higgins, C. P. (2025). Release of poly- and perfluoroalkyl substances from AFFF-impacted soils: Effects of water saturation in vadose zone soils. Journal of Contaminant Hydrology, 269, 104506. https://doi.org/10.1016/j.jconhyd.2025.104506

Shi, L., Leng, C., Zhou, Y., Yuan, Y., Liu, L., Li, F., & Wang, H. (2024). A review of electrooxidation systems treatment of poly-fluoroalkyl substances (PFAS): electrooxidation degradation mechanisms and electrode materials. Environmental Science and Pollution Research, 31(30), 42593–42613. https://doi.org/10.1007/s11356-024-34014-1

Smith, S. J., Keane, C., Ahrens, L., & Wiberg, K. (2023). Integrated Treatment of Per- and Polyfluoroalkyl Substances in Existing Wastewater Treatment Plants─Scoping the Potential of Foam Partitioning. ACS ES and T Engineering, 3(9), 1276–1285. https://doi.org/10.1021/acsestengg.3c00091

Smith, S. J., Lauria, M., Ahrens, L., McCleaf, P., Hollman, P., Bjälkefur Seroka, S., Hamers, T., Arp, H. P. H., & Wiberg, K. (2023). Electrochemical Oxidation for Treatment of PFAS in Contaminated Water and Fractionated Foam─A Pilot-Scale Study. ACS ES and T Water, 3(4), 1201–1211. https://doi.org/10.1021/acsestwater.2c00660

Smith, S. J., Lewis, J., Wiberg, K., Wall, E., & Ahrens, L. (2023). Foam fractionation for removal of per- and polyfluoroalkyl substances: Towards closing the mass balance. Science of the Total Environment, 871, 162050. https://doi.org/10.1016/j.scitotenv.2023.162050

Smith, S. J., Wiberg, K., McCleaf, P., & Ahrens, L. (2022). Pilot-Scale Continuous Foam Fractionation for the Removal of Per- and Polyfluoroalkyl Substances (PFAS) from Landfill Leachate. ACS ES and T Water, 2(5), 841–851. https://doi.org/10.1021/ACSESTWATER.2C00032

Sörengård, M., Bergström, S., McCleaf, P., Wiberg, K., & Ahrens, L. (2022). Long-distance transport of per- and polyfluoroalkyl substances (PFAS) in a Swedish drinking water aquifer. Environmental Pollution, 311, 119981. https://doi.org/10.1016/j.envpol.2022.119981

Soriano, Á., Gorri, D., & Urtiaga, A. (2017). Efficient treatment of perfluorohexanoic acid by nanofiltration followed by electrochemical degradation of the NF concentrate. Water Research, 112, 147–156. https://doi.org/10.1016/j.watres.2017.01.043

Sørmo, E., Lade, C. B. M., Zhang, J., Asimakopoulos, A. G., Åsli, G. W., Hubert, M., Goranov, A. I., Arp, H. P. H., & Cornelissen, G. (2024). Stabilization

of PFAS-contaminated soil with sewage sludge- and wood-based biochar sorbents. Science of the Total Environment, 922, 170971. https://doi.org/10.1016/j.scitotenv.2024.170971

Steenland, K., Fletcher, T., Stein, C. R., Bartell, S. M., Darrow, L., Lopez-Espinosa, M. J., Barry Ryan, P., & Savitz, D. A. (2020). Review: Evolution of evidence on PFOA and health following the assessments of the C8 Science Panel. Environment International, 145, 106125. https://doi.org/10.1016/j.envint.2020.106125

Steenland, K., Tinker, S., Frisbee, S., Ducatman, A., & Vaccarino, V. (2009). Association of perfluorooctanoic acid and perfluorooctane sulfonate with serum lipids among adults living near a chemical plant. American Journal of Epidemiology, 170(10), 1268–1278. https://doi.org/10.1093/aje/kwp279

Sun, J., Shao, X., Huang, J., Gong, M., Zhang, J., & Yuan, Z. (2023). Multiple toxicity evaluations of perfluorooctane sulfonate on intact planarian Dugesia japonica. Environmental Science and Pollution Research, 30(21), 60932–60945. https://doi.org/10.1007/s11356-023-26842-4

Sveriges Geologiska Undersökning. (2023). Sveriges geologiska undersöknings föreskrifter om kartläggning, riskbedömning och klassificering av status för grundvatten. Sveriges Geologiska Undersöknings Författningssamling, SGU-FS 2023:1. https://resource.sgu.se/dokument/publikation/foreskrift/foreskrift202301dokument/sgu-fs-2023-1.pdf

Swedish Chemicals Agency. (2026). Prioguiden. https://www.kemi.se/prioguiden/english/search

Tan, B. T. W., Abu Bakar, N. H. H., & Lee, H. L. (2025). Electrochemical methods for treatment of per- and polyfluoroalkyl substances (PFAS): A review. Journal of Environmental Chemical Engineering, 13(1), 114990. https://doi.org/10.1016/j.jece.2024.114990

Tasca, A. L., Uwayezu, J. N., Carabante, I., & Kumpiene, J. (2025). Electrochemical remediation of PFAS by Boron-Doped Diamond electrodes: A review. Journal of Environmental Chemical Engineering, 13, 117044. https://doi.org/10.1016/j.jece.2025.117044

Tasca, A. L., Uwayezu, J. N., Panizza, M., Kumpiene, J., & Carabante, I. (2026). PFAS removal by ultrasound irradiation: pathways, chemistry and operation. Frontiers in Environmental Science, 13, 1746525. https://doi.org/10.3389/fenvs.2025.1746525

Toporek, Y., Shin, H. D., & Dichristina, T. J. (2021). Resistance of perfluorooctanoic acid to degradation by the microbially driven Fenton reaction. FEMS Microbiology Letters, 368(21–24), 1–6. https://doi.org/10.1093/femsle/fnab158

UNEP, & Stockholm Convention. (2025). The Stockholm convention on persistent organic polutants (POPs).

United States Environmental Protection Agency. (n.d.). Per- and Polyfluoroalkyl Substances (PFAS) Final PFAS National Primary Drinking Water Regulation. Retrieved January 14, 2026, from https://www.epa.gov/sdwa/and-polyfluoroalkyl-substances-pfas

Uwayezu, J. N., Carabante, I., van Hees, P., Karlsson, P., & Kumpiene, J. (2023). Combining electrochemistry and ultraviolet radiation for the degradation of per- and poly-fluoroalkyl substances in contaminated groundwater and wastewater. Journal of Water Process Engineering, 54, 104028. https://doi.org/10.1016/j.jwpe.2023.104028

Uwayezu, J. N., Ren, Z., Sonnenschein, S., Leiviskä, T., Lejon, T., van Hees, P., Karlsson, P., Kumpiene, J., & Carabante, I. (2024). Combination of separation and degradation methods after PFAS soil washing. Science of the Total Environment, 907, 168137. https://doi.org/10.1016/j.scitotenv.2023.168137

Vo, P. H. N., Buckley, T., Xu, X., Nguyen, T. M. H., Rudolph, V., & Shukla, P. (2023). Foam fractionation of per- and polyfluoroalkyl substances (PFASs) in landfill leachate using different cosurfactants. Chemosphere, 310(2022), 136869. https://doi.org/10.1016/j.chemosphere.2022.136869

Wang, F., Lu, X., Li, X. Y., & Shih, K. (2015). Effectiveness and mechanisms of defluorination of perfluorinated alkyl substances by calcium compounds during waste thermal treatment. Environmental Science and Technology, 49(9), 5672–5680. https://doi.org/10.1021/es506234b

Wang, J., Chen, K., Jin, B., Woo, W., Lum, M., Canchola, A., Zhu, Y., Men, Y., Liu, J., & Lin, Y. H. (2024). Pyrolysis of Two Perfluoroalkanesulfonates (PFSAs) and PFSA-Laden Granular Activated Carbon (GAC): Decomposition Mechanisms and the Role of GAC. Environmental Science and Technology. https://doi.org/10.1021/acs.est.4c06805

Wang, J., Lin, Z., He, X., Song, M., Westerhoff, P., Doudrick, K., & Hanigan, D. (2022). Critical Review of Thermal Decomposition of Per- and Polyfluoroalkyl Substances: Mechanisms and Implications for Thermal Treatment Processes. Environmental Science and Technology, 56(9), 5355–5370. https://doi.org/10.1021/acs.est.2c02251

Wang, P., Zhang, M., Lu, Y., Meng, J., Li, Q., & Lu, X. (2019). Removal of perfluoalkyl acids (PFAAs) through fluorochemical industrial and domestic wastewater treatment plants and bioaccumulation in aquatic plants in river and artificial wetland. Environment International, 129, 76–85. https://doi.org/10.1016/j.envint.2019.04.072

Wang, Y., Huo, Y., Khan, A., Ma, N., & Mai, W. (2024). Possible mechanisms for adverse effects on zebrafish sperm and testes associated with low-level chronic PFOA exposure. Aquatic Toxicology, 276, 107108. https://doi.org/10.1016/j.aquatox.2024.107108

Wang, Y., Zhao, M., Hou, C., Chen, W., Li, S., Ren, R. K., & Li, Z. (2021). Efficient degradation of perfluorooctanoic acid by solar photo-electro-Fenton like system fabricated by MOFs/carbon nanofibers composite membrane. Chemical Engineering Journal, 414, 128940. https://doi.org/10.1016/j.cej.2021.128940

Washington, J. W., Jenkins, T. M., Rankin, K., & Naile, J. E. (2015). Decades-scale degradation of commercial, side-chain, fluorotelomer-based polymers in soils and water. Environmental Science and Technology, 49(2), 915–923. https://doi.org/10.1021/es504347u

We, A. C. E., Chen, C. X., Stickland, A. D., Clarke, B. O., & Freguia, S. (2026). Influence of microbial communities on foam fractionation of wastewater for PFAS removal. Water Research, 291, 125144. https://doi.org/10.1016/j.watres.2025.125144

We, A. C. E., Zamyadi, A., Stickland, A. D., Clarke, B. O., & Freguia, S. (2024). A review of foam fractionation for the removal of per- and polyfluoroalkyl substances (PFAS) from aqueous matrices. Journal of Hazardous Materials, 465(December 2023), 133182. https://doi.org/10.1016/j.jhazmat.2023.133182

Wilson, T. B., Stevenson, G., Crough, R., de Araujo, J., Fernando, N., Anwar, A., Scott, T., Quinteros, J. A., Scott, P. C., & Archer, M. J. G. (2021). Evaluation of Residues in Hen Eggs After Exposure of Laying Hens to Water Containing Per- and Polyfluoroalkyl Substances. Environmental Toxicology and Chemistry, 40(3), 735–743. https://doi.org/10.1002/etc.4723

Winchell, L. J., Ross, J. J., Wells, M. J. M., Fonoll, X., Norton, J. W., & Bell, K. Y. (2021). Per- and polyfluoroalkyl substances thermal destruction at water resource recovery facilities: A state of the science review. Water Environment Research, 93(6), 826–843. https://doi.org/10.1002/wer.1483

Wu, A. X., Pfremmer, S., Smrz, T., & Smith, S. M. (2025). Benchmarking of Commercial Reverse Osmosis and Nanofiltration Membranes for Ultrashort-, Short-, and Long-Chain Perfluoroalkyl and Polyfluoroalkyl Substance Rejection. Water Environment Research, 97(12), 1–9. https://doi.org/10.1002/wer.70227

Xiao, F., Sasi, P. C., Yao, B., Kubátová, A., Golovko, S. A., Golovko, M. Y., & Soli, D. (2020). Thermal Stability and Decomposition of Perfluoroalkyl Substances on Spent Granular Activated Carbon. Environmental Science and Technology Letters, 7(5), 343–350. https://doi.org/10.1021/acs.estlett.0c00114

Xie, Z., & Kallenborn, R. (2023). Legacy and emerging per- and poly-fluoroalkyl substances in polar regions. Current Opinion in Green and Sustainable Chemistry, 42, 100840. https://doi.org/10.1016/j.cogsc.2023.100840

Xiong, J., & Li, Z. (2024). Predicting PFAS fate in fish: Assessing the roles of dietary, respiratory, and dermal uptake in bioaccumulation modeling. Environmental Research, 252, 119036. https://doi.org/10.1016/j.envres.2024.119036

Xu, D., Li, C., Wen, Y., & Liu, W. (2013). Antioxidant defense system responses and DNA damage of earthworms exposed to Perfluorooctane sulfonate (PFOS). Environmental Pollution, 174, 121–127. https://doi.org/10.1016/j.envpol.2012.10.030

Xu, H., Lv, L., Yuan, F., Dong, B., Xu, Z., Zhao, H., Wang, J., Ma, X., & Shi, X. (2025). Insights into PFAS gas-phase oxidation and their impact on atmospheric nucleation and ecotoxicity. Process Safety and Environmental Protection, 203, 108011. https://doi.org/10.1016/j.psep.2025.108011

Xu, J., Ren, H., Liu, Z., Sun, H., Shang, J., Tan, W., Cui, Q., Liu, S., & Sun, X. (2024). Differential uptake and translocation of perfluoroalkyl substances by vegetable roots and leaves: Insight into critical influencing factors. Science of the Total Environment, 949, 175205. https://doi.org/10.1016/j.scitotenv.2024.175205

Xu, K., Huang, J., Zhang, Y., Wu, X., Cai, D., Hu, G., Li, Y., Ni, Z., Lin, Q., Wang, S., & Qiu, R. (2024). Crop Contamination and Human Exposure to Per- and Polyfluoroalkyl Substances around a Fluorochemical Industrial Park in China. Toxics, 12(4). https://doi.org/10.3390/toxics12040269

Yamashita, N., Taniyasu, S., Petrick, G., Wei, S., Gamo, T., Lam, P. K. S., & Kannan, K. (2008). Perfluorinated acids as novel chemical tracers of global circulation of ocean waters. Chemosphere, 70(7), 1247–1255. https://doi.org/10.1016/j.chemosphere.2007.07.079

Zegada-Lizarazu, W., Elbersen, H. W., Consentino, S. L., Zatta, A., Alexopoulou, E., & Monti, A. (2010). Agronomic aspects of energy crops in Europe. Biofuells, Bioproducts and Biorefining, 4, 674–691.

Zeng, C., Atkinson, A., Sharma, N., Ashani, H., Hjelmstad, A., Venkatesh, K., & Westerhoff, P. (2020). Removing per- and polyfluoroalkyl substances from groundwaters using activated carbon and ion exchange resin packed columns. AWWA Water Science, 2(1), 1–11. https://doi.org/10.1002/aws2.1172

Zeng, J., Brusseau, M. L., & Guo, B. (2021). Model validation and analyses of parameter sensitivity and uncertainty for modeling long-term retention and leaching of PFAS in the vadose zone. Journal of Hydrology, 603, 127172. https://doi.org/10.1016/j.jhydrol.2021.127172

Zhang, C., Cui, F., Zeng, G. ming, Jiang, M., Yang, Z. zhu, Yu, Z. gang, Zhu, M. ying, & Shen, L. qing. (2015). Quaternary ammonium compounds (QACs): A review on occurrence, fate and toxicity in the environment. Science of the Total Environment, 518–519, 352–362. https://doi.org/10.1016/j.scitotenv.2015.03.007

Zhang, H., Wen, B., Hu, X., Wu, Y., Pan, Y., Huang, H., Liu, L., & Zhang, S. (2016). Uptake, translocation, and metabolism of 8:2 fluorotelomer alcohol in soybean (Glycine max L. Merrill). Environmental Science and Technology, 50(24), 13309–13317. https://doi.org/10.1021/acs.est.6b03734

Zhang, W., Cao, H., & Liang, Y. (2021). Degradation by hydrothermal liquefaction of fluoroalkylether compounds accumulated in cattails (Typha latifolia). Journal of Environmental Chemical Engineering, 9(4), 105363. https://doi.org/10.1016/j.jece.2021.105363

Zhang, W., & Liang, Y. (2025). Impact of four surfactants on the uptake of per- and polyfluoroalkyl substances (PFAS) by red fescue grass. International Journal of Phytoremediation, 27(1), 13–22. https://doi.org/10.1080/15226514.2024.2394903

Zhang, X., Lohmann, R., & Sunderland, E. M. (2019). Poly- And Perfluoroalkyl Substances in Seawater and Plankton from the Northwestern Atlantic Margin. Environmental Science and Technology, 53(21), 12348–12356. https://doi.org/10.1021/acs.est.9b03230

Zhang, Y., Kong, K., Wu, Q., Ma, T., Liang, J., & Wang, R. (2024). A Porphyrinic Metal-Organic Framework with Cooperative Adsorption Domains for PFAS Removal from Water. ChemSusChem, 17(9). https://doi.org/10.1002/cssc.202400069

Zhao, H., Gao, J., Zhao, G., Fan, J., Wang, Y., & Wang, Y. (2013). Fabrication of novel SnO2-Sb/carbon aerogel electrode for ultrasonic electrochemical oxidation of perfluorooctanoate with high catalytic efficiency. Applied Catalysis B: Environmental, 136–137, 278–286. https://doi.org/10.1016/j.apcatb.2013.02.013

Zhao, Y., Zhao, C., Wang, S., Kakudo, S., & Kunieda, M. (2020). Selective and localized embrittlement of metal by cathodic hydrogenation utilizing electrochemical jet. Precision Engineering, 65(1088), 259–268. https://doi.org/10.1016/j.precisioneng.2020.06.007

Zhu, C., Xu, J., Song, S., Wang, J., Li, Y., Liu, R., & Shen, Y. (2020). TiO2 quantum dots loaded sulfonated graphene aerogel for effective adsorption-photocatalysis of PFOA. Science of the Total Environment, 698, 134275. https://doi.org/10.1016/j.scitotenv.2019.134275

Popular science summary

Per- and polyfluoroalkyl substances (PFAS) are a large group of man-made chemicals that have been widely used in industry and everyday products since the mid-20th century. They are often described as “forever chemicals” because they do not break down in the environment. Combined with their ability to move easily in water, this makes PFAS a global environmental problem.

PFAS are built around chains of carbon atoms that are fully or partly surrounded by fluorine atoms. This carbon–fluorine bond is very strong, making the molecules highly stable. A PFAS molecule typically consists of a “head” and a “tail”. The head likes to be in water, while the tail does not want to be in water or in oils. This unique structure gives PFAS their useful properties, such as making materials water- and stain-resistant, as the tail pushes away both water and fat in, for example, non-stick pans and make-up.

PFAS vary in size depending on how long the carbon chain is. “Long-chain” PFAS have more carbon atoms in their chains and tend to stick better to solid surfaces as well as accumulate in living organisms. “Short-chain” PFAS have fewer carbon atoms in their chains, making them more mobile in water and harder to remove from the environment. This difference in structure is central to understanding how PFAS behave and how they can be removed from the environment.

PFAS have been linked to a range of negative health effects, and studies have shown that long-term exposure can be associated with many health effects, such as increased cholesterol levels, effects on the immune system, thyroid disruption, and certain cancers. Because PFAS can accumulate in the human body over time, even low concentrations in, for example, drinking water may be of concern. As a result, many countries are introducing strict regulations to limit PFAS exposure.

One important way for PFAS to be transported in the environment is through groundwater. At sites that have been contaminated by PFAS, such as landfills, PFAS can leach into the groundwater underneath the site and spread over large distances in the groundwater system. Since groundwater is a major source of drinking water in many regions, this poses a large challenge of public health.

This thesis first investigates how PFAS behave in groundwater systems. Next, a combination of different treatment technologies (a treatment train) for removing PFAS from contaminated water was evaluated. The work focused on a landfill site in Sweden where PFAS have been found in the groundwater. The treatment train was made by combining foam fractionation, electrochemical oxidation, and a constructed wetland.

To better understand how PFAS move in groundwater, it was first examined how strongly PFAS molecules get stuck to soil. This is described by a parameter called the solid-liquid partitioning coefficient (K_d). A new method that provided reliable estimates of the K_d was used. The K_d was very low for most PFAS, confirming that PFAS are highly mobile in groundwater as they will not easily get stuck to the soil.

The treatment part of the thesis focused on removing PFAS from contaminated groundwater. Foam fractionation was used as the first step in the 3-step treatment train. This method used air bubbles to separate PFAS. The PFAS head wants to be in the water and the tail wants to be in air PFAS thus tend to get stuck on the surface between water and air, which makes them stick to the air bubbles. This creates a foam just like bubbling air through dishwasher detergent would. The PFAS foam can then be separated from the water. This method was very effective at removing long-chain PFAS, but short-chain PFAS were much harder to remove. Adding other chemicals that also make foam, so-called co-foaming surfactants, did, however, help to make more and stronger foam. This helped to remove more of the short-chain PFAS, but all of them were still not removed.

In the second step of the treatment train, the PFAS-foam was further treated using electrochemical oxidation. In this process, an electric current was used to break down PFAS molecules. The results showed that PFAS could be degraded step by step into shorter and shorter PFAS until eventually only free fluorine atoms and carbon dioxide remained of the molecule.

As the final step of the treatment train, a constructed wetland was built, through which the water treated by foam fractionation was passed with the goal of removing the last PFAS that had not yet been removed. The constructed wetland used plants and a soil-like material in which the plants were planted to separate PFAS from water. PFAS separation did occur both by PFAS getting stuck to the soil-like-material, and by the plants taking up PFAS. Short-chain PFAS were more easily taken up by the plants, while long-chain PFAS tended to remain in the plant roots or stick to the soil-like

material. However, the wetlands were not effective at reducing the concentrations of short-chain PFAS in the water. In addition, most of the PFAS taken up by the plants ended up in the plant leaves, and could therefore be released again when the leaves fall in the autumn.

Overall, the results showed that the first two steps of the treatment train (foam fractionation and electrochemical oxidation) were able to first separate and then destroy long-chain PFAS. However, short-chain PFAS remained a challenge and were not effectively removed by the constructed wetland.

This work highlights the importance of understanding how PFAS interact with soil, water, and treatment systems. By linking their chemical structure to both environmental behavior and treatment performance, the thesis contributes to the development of more effective and sustainable strategies for managing PFAS contamination in groundwater.

Populärvetenskaplig sammanfattning

Per- och polyfluorerade alkylsubstanser (PFAS) är en stor grupp människoskapade kemikalier som har använts flitigt i industri och vardagsprodukter sedan mitten av 1900-talet. De kallas ofta för ”evighetskemikalier” eftersom de inte bryts ner i naturen. Denna egenskap, i kombination med deras förmåga att lätt spridas i vatten, gör PFAS till ett globalt miljöproblem.

PFAS består av kedjor av kolatomer som helt eller delvis omges av fluoratomer. Bindningen mellan kol och fluor är väldigt stark, vilket gör molekylerna mycket stabila. En PFAS-molekyl har vanligtvis ett “huvud” och en “svans”. Huvudet trivs i vatten, medan svansen inte vill vara i vare sig vatten eller olja. Denna speciella uppbyggnad ger PFAS deras användbara egenskaper, till exempel att göra material vatten- och smutsavvisande eftersom svansen stöter bort både vatten och fett. Något som är användbart till exempel i stekpannor med non-stick-beläggning eller i smink.

PFAS varierar i storlek beroende på hur lång kolkedjan är. “Långkedjade” PFAS har fler kolatomer i kedjan och tenderar att binda starkare till fasta ytor och ansamlas i levande organismer. “Kortkedjade” PFAS har färre kolatomer i sin kedja, vilket gör dem mer rörliga i vatten och svårare att rena bort från miljön. Denna skillnad är viktig för att förstå hur PFAS beter sig i naturen och hur de kan renas bort.

PFAS har kopplats till flera negativa hälsoeffekter. Studier visar att långvarig exponering kan hänga samman med till exempel förhöjda kolesterolnivåer, påverkan på immunförsvaret, störningar i sköldkörteln och vissa cancerformer. Eftersom PFAS kan lagras i kroppen över tid kan även låga halter, till exempel i dricksvatten, vara problematiska. Därför inför många länder allt strängare regler för att begränsa exponeringen.

En viktig spridningsväg för PFAS i miljön är via grundvatten. På förorenade platser, som deponier, kan PFAS läcka ner i marken och spridas långa sträckor med grundvattnet. Eftersom grundvatten är en viktig källa till dricksvatten i många områden utgör detta en stor utmaning för folkhälsan.

Denna avhandling undersöker först hur PFAS beter sig i grundvattensystem. Därefter utvärderas en serie av olika sammankopplade reningstekniker för att rena bort PFAS från förorenat vatten. Arbetet fokuserade på en deponi i Sverige där PFAS hade påträffats i grundvattnet.

Serien av reningssteg bestod av skumfraktionering, elektrokemisk oxidation och en anlagd våtmark.

För att bättre förstå hur PFAS rör sig i grundvatten studerades först hur starkt PFAS fastnar i jord. Detta beskrivs med en parameter som kallas fördelningskoefficient (K_d). I detta arbete användes en ny metod som gav tillförlitliga uppskattningar av K_d och visade att det var väldigt lågt för de flesta PFAS som undersöktes, vilket bekräftar att PFAS är mycket rörliga i grundvatten eftersom de inte fastnar så lätt i jorden.

Den del av avhandlingen som handlar om rening fokuserade på att rena bort PFAS från förorenat grundvatten. Skumfraktionering användes som det första steget i serien av reningssteg. Metoden bygger på att tillsätta luftbubblor till vattnet. Molekylens huvud vill vara i vatten medan svansen gärna är i luft, vilket gör att PFAS samlas vid bubblornas yta. På så sätt bildas ett skum, ungefär som om man skulle bubbla luft genom diskmedel. Detta PFAS-rika skum kan sedan avlägsnas från vattnet. Metoden var mycket effektiv för att rena bort långkedjade PFAS, men kortkedjade PFAS var svårare att avskilja. Genom att tillsätta andra skumbildande ämnen kunde dock mer och stabilare skum skapas, vilket förbättrade avskiljningen av kortkedjade PFAS, även om alla PFAS fortfarande inte kunde avskiljas.

I nästa steg behandlades skummet vidare med elektrokemisk oxidation. Här användes elektrisk ström för att bryta ner PFAS-molekylerna. Resultaten visade att PFAS kunde brytas ner stegvis till kortare och kortare kedjor, tills endast fria fluoratomer och koldioxid återstod.

Som sista steg i behandlingskedjan byggdes en anlagd våtmark, genom vilken det behandlade vattnet fick passera med målet att ta bort de sista resterna av PFAS. Våtmarken använde växter och ett jordliknande material för att fånga upp PFAS. Separationen skedde både genom att PFAS fastnade i materialet och genom att växterna tog upp dem genom sina rötter. Kortkedjade PFAS togs lättare upp av växterna, medan långkedjade PFAS oftare stannade i rötterna eller fastnade i materialet. Våtmarken var dock inte effektiv för att minska halterna av kortkedjade PFAS i vattnet. Dessutom hamnade mycket av det PFAS som togs upp av växterna i bladen, vilket innebär att de kan återföras till miljön när bladen faller på hösten.

Sammanfattningsvis visar resultaten att de två första stegen i behandlingskedjan (skumfraktionering och elektrokemisk oxidation) effektivt kunde separera och bryta ner långkedjade PFAS. Kortkedjade

PFAS var däremot fortfarande en utmaning och avlägsnades inte effektivt av den anlagda våtmarken.

Arbetet visar hur viktigt det är att förstå hur PFAS samverkar med jord, vatten och olika reningsmetoder. Genom att koppla deras kemiska struktur till deras beteende i miljön och hur de kan renas bort bidrar avhandlingen till att utveckla effektivare och mer hållbara strategier för att hantera PFAS-föroreningar i grundvatten.

Acknowledgements

I want to start by acknowledging that there are far more people who have had an impact on this journey than could possibly fit in this list. Thank you all.

The European Union, through the LIFE20 ENV/ES/000880 grant of the LIFE program, and **the Government of Sweden,** through the Grant no. 1:4 for remediation and restoration of contaminated sites. Thank you for providing the funding for the work encompassed in this thesis. Without money, there is no research.

All the partner organizations of the **LIFE SOuRCE consortium: Eurecat**, **Envytech Solutions, Esolve, Laqua Treatment, Nova Diamant, SGI,** and **Uppsala Vatten.** Thank you for letting me be a part of this important project.

Lutz Ahrens. Thank you for being my main supervisor and introducing me to the world of persistent organic pollutants and PFAS. Thank you for giving me the freedom to develop as an independent researcher and for your endless positivity. You made me feel that all of my results were very good.

Dan Berggren Kleja. Thank you for being my supervisor. Thank you for helping me iron out the K_d paper from the very start of that project and for coordinating the Swedish half of the LIFE SOuRCE project when necessary, no easy task.

Anja Enell. Thank you for being my supervisor. Even though you were all the way down in Skåne, I always felt that I could reach out to you whenever I needed help. Thank you for that.

Dahn Rosenquist. Thank you for designing both of the wetland pilots in this thesis, and for always picking up the phone and calmly explaining to me how to fix a pump, a clogged pipe, or any other kind of troublesome equipment.

Helena Hinrichsen, Robin Axelson, and **Say Svanström.** Thank you for getting the foam fractionation unit in place and keeping it running through the duration of the project. The beating heart of the treatment train.

Phillip McCleaf, Sofia Bjälkefur Seroka, and **Wilma Högman.** Thank you for your indispensable support during the projects and for keeping the water flowing.

Patrik Hollman. Thank you for designing and operating the electrochemical oxidation cell, as well as for many interesting discussions about PFAS destruction.

Jose Jorge Espi Gallart and **Mariana Eugenia Lombeida Lombeida.** Thank you for performing the LCC calculations for the foam fractionation and electrochemical oxidation, helping to bridge the gap between research and society.

Michael Pettersson. Thank you for really taking the time to read my drafts and scrutinize my work, leading to much-improved end results.

Malin Ellbrant. Thank you for carrying out the bulk of the lab work for the Kd paper and welcoming me to your lab in Linköping.

Sara Ferndahl. Thank you for being my master's student and agreeing to spend most of your thesis project out on a landfill. It was a pleasure to supervise you.

Svante Rehnstam, Valentina Ugolini, Alberto Zanella, and **Ze Hui Kong.** Thank you for making me feel welcome and as a part of the department from the very first day. Between canceled commuter trains, broken lab equipment, and disappointing results, you still made it feel like a joy to come in to work.

Alberto Celma, Alina Koch, Bent Speksnijder, Paul Löffler, Björn Bonnet, Khadija Aziz, Tracy Wang, Carlotta Meriggi, Maxi Tyka, Kajsa Weslien, Patrick Wong, Daniel Malnes, Harold Flores Quintana, Sofia Lindblad, Stephanie Casey, Tabea Mumberg, Nicola Messinger, Uzair Khan, Hannah Conroy, Jenifer Hooper, Georgios Niarchos, and **many others.** Thank you for the laughs, lunches, fikas, and shared frustrations. Thank you for making SLU feel like my second home.

Sanne Smith and **Winnie Nassazzi.** Apart from being wonderful colleagues, your work is the foundation on which this thesis rests. Thank you for allowing me to (metaphorically) stand on your shoulders.

Laura del Val Alonso and **Jéssica Meijide.** Thank you for taking on the ungrateful task of leading the LIFE SOuRCE project.

Elin Eriksson. Thank you for introducing me to the lab and teaching me the practical basics of environmental organic chemistry, such as performing an SPE or running the mass spectrometer.

Karin Wiberg. Thank you for leading the POP´s group with a firm hand. Providing the framework in which all of us can excel.

Mia Lucaric. Thank you for taking care of the lab and keeping it in amazing shape despite the chaos brought in on a daily basis by us PhD students.

Ioannis Papachristopoulos. Thank you for helping me clean and homogenize oh so many plants.

The staff of Hovgården. Thank you for being invaluable. For allowing me to run around at your site, give me rides, borrow your tools, and at no notice show up with an actual excavator to pitch in when I needed it. As well as your company during winter coffee- and summer water breaks. This work could not have been done without you.

To all of my friends. Thank you for keeping my head above the water, helping me recharge my batteries, scolding me for working on weekends, and making life fun.

Dad, Mom, Mats and **Calle.** My Family, thank you for being my constant support and for always believing in me, whatever I decide to do. For that, I am ever grateful.

Vilma Liljeström. My Wife, nothing I could write here would ever do you justice. Thank you for sharing this journey with me. You are simply amazing.

III

Environmental Pollution 395 (2026) 127809

Contents lists available at ScienceDirect

Environmental Pollution

journal homepage: www.elsevier.com/locate/envpol

Corrigendum

Corrigendum to 'Pilot scale treatment of PFAS-contaminated groundwater in a subsurface flow constructed wetland–evaluating multiple plant species' [Environ. Pollut. **386** (2025) 127199]

Oscar Liljeström [a,*], Dahn Rosenquist [b], Dan B. Kleja [c], Anja Enell [c], Lutz Ahrens [a]

[a] Swedish University of Agricultural Sciences (SLU), Department of Aquatic Sciences and Assessment, P. O. Box 7050, SE-750 07, Uppsala, Sweden
[b] Laqua Treatment AB, Siriusvägen 16, SE-296 92, Yngsjö, Sweden
[c] Swedish Geotechnical Institute (SGI), Olaus Magnus Väg 35, SE-581 93, Linköping, Sweden

The authors regret that in Figure 3, the y-axis title incorrectly lists the unit as ng/kg, while the correct unit is ng/g, as reflected in the axis scale.

See the attached updated figure.

The authors would like to apologise for any inconvenience caused.

DOI of original article: https://doi.org/10.1016/j.envpol.2025.127199.
* Corresponding author.
E-mail address: oscar.liljestrom@slu.se (O. Liljeström).

https://doi.org/10.1016/j.envpol.2026.127809

Available online 18 February 2026

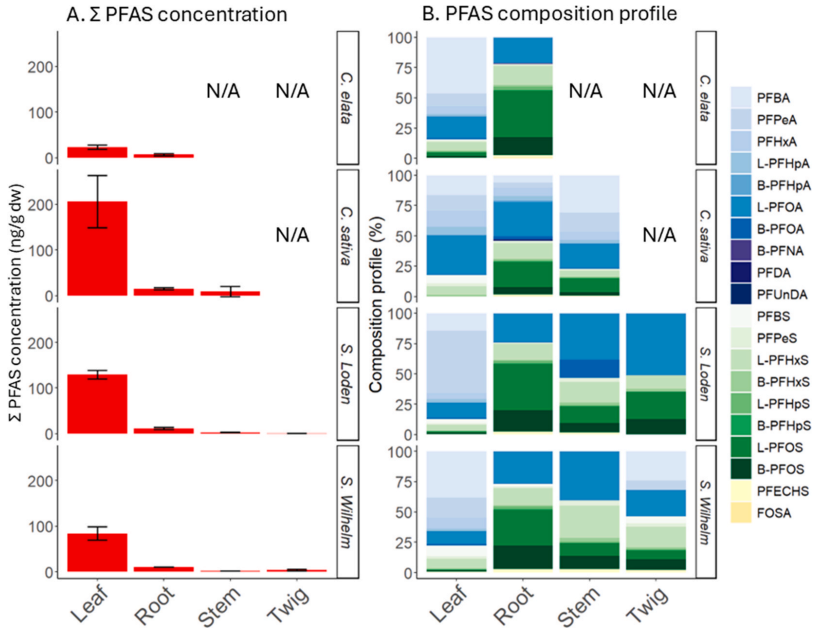

Fig. 3. A) ΣPFAS concentration in different plant tissue types ($n = 2$), and B) PFAS composition profile of each tissue type. *C. sativa* did not have twigs, and *C. elata* did not have twigs or stems; thus, these tissue types are not applicable (N/A). PFCAs are represented in blue, PFSAs in green, and other functional groups in yellow.

Environmental Pollution 386 (2025) 127199

Contents lists available at ScienceDirect

Environmental Pollution

journal homepage: www.elsevier.com/locate/envpol

Pilot scale treatment of PFAS-contaminated groundwater in a subsurface flow constructed wetland–evaluating multiple plant species☆

Oscar Liljeström [a,*], Dahn Rosenquist [b], Dan B. Kleja [c], Anja Enell [c], Lutz Ahrens [a]

[a] Swedish University of Agricultural Sciences (SLU), Department of Aquatic Sciences and Assessment, P. O. Box 7050, SE-750 07, Uppsala, Sweden
[b] Laqua Treatment AB, Siriusvägen 16, SE-296 92, Yngsjö, Sweden
[c] Swedish Geotechnical Institute (SGI), Olaus Magnus Väg 35, SE-581 93, Linköping, Sweden

ARTICLE INFO

Keywords:
PFAS
Phytoremediation
Constructed wetland
Groundwater
Landfill leachate
Biochar

ABSTRACT

Groundwater contamination by per- and polyfluoroalkyl substances (PFAS) is an emerging threat to drinking water quality, highlighting the need for effective treatment solutions. This study investigated subsurface flow constructed wetlands for treating groundwater contaminated with PFAS. The wetlands used a peat, biochar, and lightweight expanded clay aggregate (LECA) filter substrate, planted with either tufted sedge (*Carex elata*), fiber hemp (*Cannabis sativa* Futura 75), or an intercropping of the two *Salix* clones S. Wilhelm and S. Loden. The experiment was conducted under field conditions in Sweden, during one growing season, using PFAS-contaminated groundwater impacted by landfill leachate. The study showed accumulation of PFAS in all plant species and the peat and biochar part of the filter substrate, with short-chain PFAS and perfluoroalkyl carboxylates (PFCAs) dominating when considering the whole plants (57 % and 77 % of ΣPFAS, respectively) and long-chain PFAS and perfluoroalkyl sulfonates (PFSAs) dominating in the peat and biochar filter substrate (77 % and 54 % of ΣPFAS, respectively). Sorption to the filter substrate was shown to be the primary mechanism for PFAS removal. The highest plant PFAS concentrations were found in leaves, followed by roots, for all species. There was a difference in the PFAS composition profile when comparing different plant tissues, with PFCAs dominating in leaves (84 % of ΣPFAS) and PFSAs dominating in roots (66 % of ΣPFAS). All plant species were determined to have an above-ground tissue/water phase concentrations >10/1 for C_3-PFCA (PFBA). This was also observed for *C. sativa* with C_4- and C_7-PFCAs (PFPeA, PFOA), and C_4- and C_5-PFSAs (PFBS, PFPeS), for *C. elata* with C_8-PFSA (L-PFOS), and for S. Loden with PFPeA. ∑PFAS phytoextraction potential from landfill leachate-impacted groundwater (mg/ha yr) was estimated to be 940 ± 670 for *C. sativa*, 390 ± 310 for S. Loden, 330 ± 160 for S. Wilhelm, and 160 ± 56 for *C. elata*.

1. Introduction

Per- and polyfluoroalkyl substances (PFAS) are an anthropogenic class of fluorinated organic compounds that contain at least one perfluorinated carbon atom (OECD, 2021). Various PFAS have been, and are, produced for many applications, such as aqueous film-forming firefighting foams (AFFF), industrial lubricants, and nonstick coatings (Gaines, 2022). PFAS have also been linked to several adverse health effects, such as cancer (Barry et al., 2013), reduced immune response to vaccines (Stein et al., 2016), and increased cholesterol levels (Nelson et al., 2010). Due to their mobile and persistent nature (Brunn et al., 2023), PFAS are transported and retained in the environment, and found in air, soil, water, wildlife, and humans (Brusseau, 2024; Rauert et al., 2018; Fenton et al., 2021; Kwok et al., 2015; Kelly et al., 2009). Thus, posing a potential hazard to human health and the environment (Sunderland et al., 2019; Beale et al., 2022). One transport pathway of concern is the infiltration of PFAS from landfill leachate into groundwater systems (Hepburn et al., 2019), causing risks to water quality, including drinking water (Sörengård et al., 2022). It is therefore critical that remediation methods for PFAS-contaminated groundwater and its contamination sources are developed.

The treatment options available for PFAS-contaminated groundwater can broadly be divided into *in situ* and *ex situ* approaches, where *in situ* approaches aim to separate, degrade, or immobilize PFAS in the

☆ This paper has been recommended for acceptance by Dr Hefa Cheng.

* Corresponding author.
E-mail address: oscar.liljestrom@slu.se (O. Liljeström).

https://doi.org/10.1016/j.envpol.2025.127199
Received 2 April 2025; Received in revised form 30 August 2025; Accepted 1 October 2025
Available online 1 October 2025

aquifer, such as *in situ* sonication (Laramay and Crimi, 2020), or the introduction of immobilizing additives (Hale et al., 2017). In contrast, *ex situ* approaches aim to remove the water from the aquifer to be treated on-site or at a centralized treatment facility, so-called pump and treat (Birnstingl and Wilson, 2024). A possible method for both *in situ* and *ex situ* approaches is phytoremediation (Ferrario et al., 2022; Nassazzi et al., 2023). Phytoremediation has been used as a method for remediating areas from metals and various organic contaminants (Ali et al., 2013; Gan et al., 2009). The process can broadly be divided into phytoextraction, phytostabilization, and phytodegradation (Salt et al., 1998). Earlier research into plant uptake of PFAS focused on its accumulation in crops and mainly had a food safety perspective (Stahl et al., 2009; Wen et al., 2013; Krippner et al., 2014). These studies did, however, also show the phytoextraction potential for PFAS (Lesmeister et al., 2021). Recently, investigations have also started to be carried out concerning both phytoextraction and phytodegradation of PFAS (Ferrario et al., 2022; Greger, 2021). Plants used in these phytoremediation trials include willows (*Salix* spp) and fiber hemp (*Cannabis sativa*) (Nassazzi et al., 2023; Nason et al., 2024; Huff et al., 2020; Sharma et al., 2020). These plants are currently used for biomass production on an industrial scale (Zegada-Lizarazu et al., 2010), making them interesting also from a phytoremediation perspective, as they produce a lot of biomass in a short time and have logistics for management in place. The wetland genus of true sedge (*Carex*) is not commercially grown, except for garden decoration purposes (Walter et al., 2002). It has, however, still attracted interest from PFAS researchers with the potential to be used in e.g. constructed wetlands (Greger, 2021; Zhang et al., 2021a). Previous studies have shown PFAS uptake in floating wetlands where plants were placed on rafts in ponds, enabling them to sorb PFAS through their roots (Awad et al., 2022), or more traditional open surface constructed wetlands where PFAS is both taken up in plants planted along edges and bottom of the wetland as well as providing good hydrological conditions for the co-sedimentation of PFAS (Yin et al., 2017). There are also subsurface flow constructed wetlands where, instead of an open pond, water is passed through a filter substrate with plants on top, allowing their roots to perforate the subsurface flow (Ferrario et al., 2022; Xiao et al., 2023). Various wetland plants can be used for this application, with sweet flag (*Acorus calamus*) being a common choice (Ferrario et al., 2022; Xiao et al., 2023; Kang et al., 2023; Ma et al., 2023). The filter substrate often consists of gravel or sand, allowing for biofilm formation (Xiao et al., 2023; Lott et al., 2023). An interesting addition to a subsurface flow constructed wetland would be to use a carbon-rich filter substrate, since granular activated carbon (GAC) and biochar have proven effective at sorbing, especially long-chain PFAS (Askeland et al., 2020; Philip et al., 2017). Phytoextraction has contrastingly been found to work better for short-chain PFAS (Nassazzi et al., 2023). In studies investigating constructed wetlands for nutrient removal, incorporating biochar into the filter substrate at a proportion of 10–20 % v/v has also been shown to increase plant growth (Kasak et al., 2018; Li et al., 2019a). A combination of a carbon-rich filter substrate and growing wetland plants could be an efficient approach to deal with both long- and short-chain PFAS. Using this kind of wetland system to treat PFAS-contaminated groundwater impacted by nearby landfill facilities is an area currently lacking research.

This study thus aimed to evaluate the onsite treatment of PFAS-contaminated groundwater, impacted by landfill leachate, using subsurface constructed wetlands on a pilot scale at a waste management facility in Sweden. The filter substrate consisted of a novel combination of biochar and peat for PFAS sorption with a lightweight expanded clay aggregate (LECA) to ensure hydraulic permeability. The tested plants included willow (*Salix* spp clones Wilhelm and Loden), fiber hemp (*C. sativa* Futura 75), and tufted sedge (*Carex elata*), none of which, to the best of our knowledge, have been previously used for PFAS treatment in a subsurface constructed wetland.

2. Materials and methods

2.1. Standards and chemicals

In total, 29 PFAS were analyzed including C_3-C_{13} perfluoroalkyl carboxylates (PFCAs) (i.e. PFBA, PFPeA, PFHxA, PFHpA, PFOA, PFNA, PFDA, PFUnDA, PFDoDA, PFTrDA, PFTeDA), C_4-C_{10} perfluoroalkyl sulfonates (PFSAs) (i.e. PFBS, PFPeS, PFHxS, PFHpS, PFOS, PFNS, PFDS), 4:2, 6:2, 8:2 fluorotelomer sulfonate (4:2 FTSA, 6:2 FTSA, 8:2 FTSA), perfluorooctanesulfonamide (FOSA), methylperfluorooctanesulfonamidoacetic acid (MeFOSAA), ethylperfluorooctanesulfonamidoacetic acid (Et-FOSAA), tetrafluoro-2-(heptafluoropropoxy)propanoic acid (HFPO-DA), dodecafluoro-3H-4,8-dioxanonanoic acid (NaDONA), 9-chlorohexadecafluoro-3-oxanonane-1- sulfonic acid (6:2 Cl-PFESA), 11-chloroeicosafluoro-3-oxaundecane-1- sulfonate acid (8:2 Cl-PFESA) and perfluoro-4-ethylcyclohexanesulfonate (PFECHS). Standards for PFHxS and PFOS were quantified for both linear and branched isomers (L-PFHxS, B-PFHxS, L-PFOS, B-PFOS), (Table S1 in Supporting Information (SI)). In addition, 19 isotopically labeled PFAS standards (IS) were included ($^{13}C_4$-PFBA, $^{13}C_5$-PFPeA, $^{13}C_5$-PFHxA, $^{13}C_4$-PFHpA, $^{13}C_8$-PFOA, $^{13}C_9$-PFNA, $^{13}C_6$-PFDA, $^{13}C_7$-PFUnDA, $^{13}C_2$-PFDoDA, $^{13}C_2$-PFTeDA, $^{13}C_3$-PFBS, $^{13}C_8$-PFOS, $^{13}C_8$-FOSA, d_3-MeFOSAA, d_5-EtFOSAA, $^{13}C_2$-4:2 FTSA, $^{13}C_2$-6:2 FTSA, $^{13}C_2$-8:2 FTSA and $^{13}C_3$-HFPO-DA) (Wellington Laboratories).

Acetic acid, ammonium acetate, and ammonium hydroxide of mass spectrometry quality and methanol of hypergrade for LC-MS quality were sourced from Sigma-Aldrich. Ultrapure water from MilliQ® IQ 7000 with an additional LC-Pack® polisher filter - a reverse-phase C18 granular silica-based cartridge was used.

2.2. Plants

Carex elata (tufted sedge) was supplied as herbal plug plants by VegTech, Sweden. These were supplied as developed tufts with a 9 cm deep, 4 cm diameter root system.

Salix Wilhelm and *Salix* Loden (willows) were supplied as cuttings by REAB, Billeberga, Sweden, and cut to 40 cm.

Cannabis sativa futura 75 (hemp) was grown from seeds in pots in Hasselfors Garden S-Soil in a greenhouse with artificial lighting for 64 days, achieving an approximate height of 100 cm before planting in the wetland.

2.3. Experimental design

The field experiments were conducted at a waste management facility in Sweden from June 14, 2022 to September 9, 2022 (87 d). In total eight wetland units each with a volume of 0.48 m^3 were used (Fig. 1), including two units each planted with i) *C. elata* with 19 tufts each, ii) *C. sativa* from 18 pots (i.e. 49 and 54 stalks, respectively), iii) *Salix* spp with 18 S. Wilhelm and 18 S. Loden cuttings and 19 S. Wilhelm and 16 S. Loden, respectively and iv) control wetland units which were filled with the filter substrate but no plants. Water was collected from a drilled groundwater well at the facility with known PFAS contamination and pumped to a 1000 L high-density polyethylene (HDPE) buffer tank, which was level-controlled to always be filled to 700 L. The buffer tank was then used as a joint input water source to each of the 8 separate subsurface flow constructed wetland units. Each unit had a volume of 0.48 m^3 (120 cm (length), 100 cm (width), 40 cm (height) and had an outer casing of HDPE covering the sides and bottom, but leaving it open upwards. The casing was filled with two permeable sections, one at each end of the wetland unit, consisting of expanded lightweight clay aggregates (LECA) (0.057 m^3; 14.3 kg dw). The LECA was 12–18 mm in diameter (Saint-Gobain). In between these sections was a 0.27 m^3 (62.6 kg dw) well-mixed mixture of peat, biochar, and LECA (0.1:0.1:0.8, v/v). No additional structural elements were included to separate the

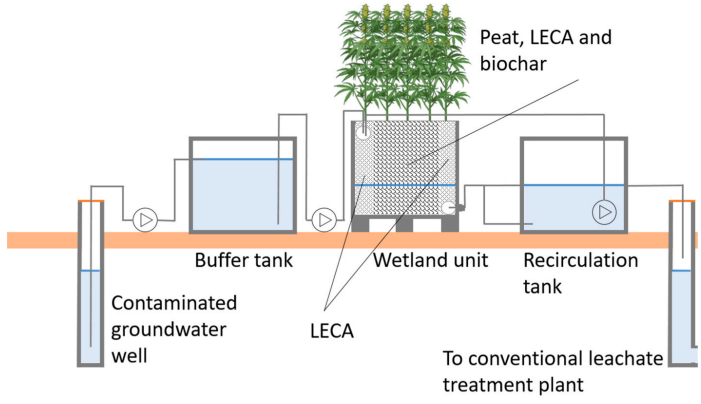

Fig. 1. Schematic of the field setup including contaminated groundwater well, buffer tank, wetland unit with substrate (peat, LECA, biochar) and i) *C. elata* ($n = 2$), ii) *C. sativa* ($n = 2$), iii) *Salix* Wilhelm and Loden mixture ($n = 2$), and iv) control ($n = 2$), recirculation tank and drainage to a conventional treatment plant.

permeable end sections from the central section. The substrate height in the wetland system was set at 30 cm, leaving a 10 cm HDPE headspace to allow for substrate expansion during water application. The peat was long fibered H7 from Småland, Sweden (Timfors traktor och maskin), the biochar consisted of crop production residues, pyrolyzed at 800 °C with a specific surface area (BET) of 223 m^2/g, pressed into pellets with 5 mm diameter and 5–10 mm length (Skånefrö, Sweden). Water was continuously pumped from the buffer tank to the eight separate wetland units using Microdos MP2-B peristaltic pumps with a load of 50 L/d for the first 21 days, then increased to 100 L/d for the remaining 66 days of the trial. Water levels in the wetlands were set to 25 cm from the bottom for the *C. elata* units and 20 cm in all other cases. The pore volume of the filter substrate was estimated to be 50 %, resulting in a water volume of 150 L in the saturated zone of the *C. elata* and 120 L for the other units. Based on this, the hydraulic retention time in the wetland systems was estimated as follows: 72 h for *C. elata* with a 50 L/d load, 57.6 h for the other units with a 50 L/d load, 36 h for *C. elata* with a 100 L/d load, and 28.8 h for the other units with a 100 L/d load. Each wetland unit was connected to a 300 L recirculation tank to which water was transferred via an overflow mechanism. Water was continuously pumped back from the recirculation tank to its connected wetland unit at an average rate of 1090 L/d (see Table S2 in SI for the individual recirculation rates). Excess water from the recirculation tanks was discarded to a drainage system via an overflow mechanism. Water samples for PFAS were collected monthly from the overflow from the wetland units (total $n = 26$) and the buffer tank (total $n = 3$) in HDPE flasks. After 87 days, plants were harvested with roots, including 3 full plants of each *C. elata*, S. Loden, and S. Wilhelm from both of their respective wetland units. These samples were collected diagonally across the unit to ensure spatial representation. All *C. sativa* were sampled from both of its wetland units (total $n = 36$). Composite substrate samples were collected at the end of the experiment using a Russian peat corer from the peat and biochar mixture and LECA section of the wetland in a diagonal fashion and pooled for each wetland unit (total $n = 8$).

2.4. Sample preparation and analysis

LECA was removed from the substrate mixture, rinsed with ultrapure MilliQ water, and analyzed separately from the peat and biochar mixture. *C. elata* plants were divided into leaf and root. *C. sativa* was divided into leaf, stem, and root. S. Loden and S. Wilhelm were divided into leaf, twig, stem, and root, where twigs were defined as the new shoots and stems as the planted cutting.

Sample preparation of peat and biochar mixture, LECA, and plant tissue was based on the method developed and validated by Nassazzi (Nassazzi et al., 2022). In the field, plant roots were rinsed with tap water to separate them from the substrate. Any remaining substrate was manually removed from the roots. All plant samples were washed with deionized water, followed by ultrapure MilliQ water, and then rinsed with 1:1 methanol and ultrapure MilliQ water. Plant, peat, and biochar mixture, and LECA samples were freeze-dried at −50 °C for 7 days and then homogenized using an IKA MultiDrive control with MultiDrive MI 250 T vessel. 0.5 g homogenized sample was spiked with 50 μL of an IS mixture (c = 0.05 μg/mL for individual IS) and extracted 3 times with methanol: 1) 6 mL for 30 min, 2) 3 mL for 20 min, 3) 3 mL for 20 min in 15 mL polypropylene tubes using sonication. Each extract was transferred into a new 15 mL polypropylene tube with centrifugation at 1900*g* in between. Subsequently, the extract was cleaned up using ENVI carb cartridges (1 g, 12 cc, Supelco). Extracts were concentrated under N_2 to approximately 100 μL and then diluted to 500 μL with methanol.

Water samples were prepared with a method previously described (Smith et al., 2022). Briefly, 100 mL sample was filtered using a glass microfiber filter (0.7 μm, Whatman), followed by spiking with 100 μL of an IS mixture (c = 0.05 μg/mL for individual IS) and solid phase extraction (SPE) using Oasis WAX cartridges (6 mL, 150 mg, 30 μm, Waters) eluted with 4 mL methanol followed by 4 mL 0.1 % ammonium hydroxide in methanol. Extracts were concentrated to 1 mL under nitrogen.

All samples were analyzed on an ultraperformance liquid chromatography system coupled to tandem mass spectrometry (Sciex Triple Quad 3500 UPLC-MS/MS, Phenomenex Gemini® 3 μm C18 110 Å analytical column) as previously described (Smith et al., 2022). Branched isomers of PFHpA, PFOA, PFHpS, and PFNA were quantified using their linear counterparts and should be considered semi-quantitative.

2.5. Quality control and assurance

Laboratory blanks were prepared for filter substrate ($n = 4$), plant ($n = 9$), and water samples ($n = 9$). As a field blank ($n = 1$), an HDPE sampling flask was opened during sampling and then filled with ultrapure MilliQ water that was extracted according to the protocol. As a filter blank ($n = 4$), 100 mL ultrapure MilliQ water was filtered and extracted according to protocol. As SPE blank ($n = 4$), a clean SPE cartridge was eluted, and the eluate was analyzed according to protocol. Method detection limits (MDL) were calculated as mean + 3 times the

standard deviation (SD) of the blank samples. If a PFAS was not detected in the blanks, MDL was calculated as the mean + 3 times the SD of the lowest used calibration point. For some branched isomers (B-PFOA, B-PFHpS, B-PFNA, B-PFHpA) that did not have calibration standards, S/N = 3 for one sample of each of the matrix types was used. If the MDL was below 0.01 ng/mL, then 0.01 ng/mL, which was the lowest calibration point, was used. Three duplicate and one triplicate water sample were analyzed to assess method variability (in total, $n = 9$). A triplicate of plants was analyzed for one wetland unit each for *C. elata*, S. Loden, and S. Wilhelm to assess variability. A triplicate of each plant tissue was analyzed for *C. sativa*. One triplicate per plant tissue was also analyzed on a single homogenized sample to assess method variability (for details, see Tables S3-5in SI). A subset of plants from each plant species was analyzed in triplicate prior to planting in the wetland system (Tables S6.1-6.5 in SI). Samples of the peat and biochar mixture, as well as LECA, were analyzed before applying the filter substrate to the wetland units (Table S7 in SI).

2.6. Calculations and statistics

PFAS treatment efficiencies were calculated as the percentage removal of PFAS between the inlet and outlet water of each wetland unit, taken at the same time point.

Mass balances for each wetland unit were calculated, taking into account PFAS concentrations in plant biomass, filter substrate, inlet, and effluent water. Water losses through evapotranspiration have previously been estimated to 3.1 mm/d in June, 3.9 mm/d in July, 2.6 mm/d in August and 2.0 mm/d in September for a *Salix* stand in Uppsala, Sweden (Persson and Lindroth, 1994). These losses were considered negligible in relation to the flow rate of the experiment, and consequently, the effluent volume was considered equal to the inlet volume (Equation S(1) and Tables S8–11 in SI).

Total plant concentrations were calculated as the sum of the average concentration of each tissue type multiplied by the average dry weight of that tissue type, divided by the average dry weight of a whole plant. Bioconcentration factor (BCF) was calculated as PFAS concentration in plant tissue/average PFAS concentration in the inlet water (Nassazzi et al., 2023; Soda et al., 2012).

Phytoremediation potential was calculated as total plant PFAS concentration, excluding roots, multiplied by a biomass yield value derived from the literature (Zegada-Lizarazu et al., 2010; Banaszuk et al., 2020). The biomass yield value for a generic *Salix* spp used in European biomass production (Zegada-Lizarazu et al., 2010) was used as a basis for both *Salix* clones. There was a clear difference in biomass production observed between the two clones in the experiment. The literature value was thus adjusted up or down, based on the proportional difference in biomass production between the two clones, to estimate individual biomass yield values for the two clones. (For details, see equations S (2.1)-(2.4) in the SI).

The Kruskal-Wallis test with Dunn's post-hoc test was used to assess if there were any significant differences between plant tissues, roots, stems, twigs, and leaves, where applicable, regarding PFAS concentration and composition. A two-way ANOVA was performed to assess whether the distribution of PFAS with regard to concentration and composition between the plant tissue types varied significantly between the species. This analysis aimed to determine whether the species could be grouped when comparing tissue types. Subsequently, all plant species were treated as a single group to enhance statistical power when evaluating ΣPFAS concentration, functional group distribution, and the proportion of branched compounds across tissue types.

Linear regression models were made for each species and their tissue types, with the BCF of each PFAS detected in the water phase as the response variable, the perfluoroalkyl chain length as a numerical independent variable, and functional group and isomeric configuration as categorical independent variables. All statistical analyses were carried out in R version 4.4.1.

3. Results and discussion

3.1. PFAS concentration and composition of influent and effluent water

In total, 15 out of 29 PFAS (i.e. C_4-C_9 PFCAs, C_4-C_8 PFSAs, 4:2 FTSA, 6:2 FTSA, PFECHS, and Et-FOSAA) were detected in the inlet water. With ∑PFAS concentrations of (average ± standard error) 3870 ± 95 ng/L ($n = 3$) (Fig. S1, and Tables S12.1-12.5 in SI). Both linear and branched isomers were detected for PFHpA, PFHxA, PFOA, PFHpS, PFNA, and PFOS. The same PFAS detected in the inlet could also be observed in the wetland unit outlets, with the addition of NaDONA being found above MDL in 1 sample (Control B *July*) and PFDA being found in two samples (Control B *July* and *C. Sativa* A *July*). For PFDA, this is likely due to the concentrations being close to MDL in all samples, while for NaDONA it could indicate a previous contamination in the wetland unit being washed out, or a contamination of the sample, as this peak could not be detected in any other sample throughout the experiment. NaDONA was not found in the control filter substrate analyzed prior to the experiment. However, potential contamination cannot be ruled out, as it may have originated from sources such as the HDPE casing or tubing of the wetland units.

The ∑PFAS removal efficiency (Table S13 in SI) was similar between all treatment units, including the control (15 ± 2.5 % *C. elata,* 14 ± 2.5 % *Salix* spp, 13 ± 2.5 % *C. Sativa*, 15 ± 2.6 % control) ($n = 6$ each). This resulted in ΣPFAS effluent concentration of 3340 ± 84.3 ng/L for *C. sativa,* 3310 ± 89.3 ng/L for *Salix* spp, 3290 ± 103 for *C. elata,* and 3280 ± 95.1 ng/L for the control. (Tables S12.1–12.5 in SI). The mass balance accounted for, on average, 87 ± 0.69 % of the Σ influent PFAS. (Tables S8–11 in SI). The recovery did, however, vary across PFAS groups: short-chain PFAS and PFCAs were better accounted for (96 ± 1.3 % and 91 ± 0.46 % respectively) compared to long-chain PFAS, PFSAs, and precursors (82 ± 1.4 %, 80 ± 1.4 % and 71 ± 2.0 % respectively). For certain individual compounds such as L-PFOS and 6:2 FTSA, the mass balance recovery was notably lower (40 ± 1.3 % and 35 ± 4.2 % respectively). The low mass balance recovery of PFAS precursors may be partially attributed to their transformation within the plants and the wetland system, as reported previously (Fang et al., 2024; Zhao et al., 2019). In contrast, the low recovery of long-chain PFAS and PFSAs, like PFOS, is more likely due to sorption onto suspended particles, subsequently removed during filtration before analysis, which has been previously reported (Sörengård et al., 2020). The wetland systems may have contributed additional suspended particles, thereby influencing the mass balance recovery. Substantial algae growth was observed in the recirculation tanks, which may also have contributed to an increase in suspended particles in the effluent water samples. Additional factors potentially contributing to the incomplete mass balance for the long-chain PFAS include sorption to pipes and outer walls of the setup, as well as to the sampling flasks. Furthermore, sorption to the external surfaces of plant roots may also have influenced the mass balance, as this PFAS fraction was not analyzed. Therefore, the reported removal efficiencies for certain PFAS are likely overestimated. The similarity in treatment efficiency between the planted wetland units and the controls indicates that the main PFAS removal mechanism of the wetland units was the filter substrate. This theory is further supported by the treatment efficiencies for the individual PFAS, where long-chain PFAS and PFSAs were more efficiently removed than short-chain PFAS and PFCAs, even when accounting for their lower mass balance recoveries. Hereby, L-PFOS had the highest removal efficiencies with 80-63 %, and PFBA had the lowest removal efficiencies with −3.2 to 8.5 %, excepting B-PFNA, which showed highly variable removal efficiencies with −25 to 26 %. This could be attributed to the previously reported higher sorption capacity of longer chain PFAAs to soil matrices compared to shorter chain PFAAs (Li et al., 2019b). The high variability in PFNA removal is likely due to concentrations being close to the MDL. The fact that the addition of plants did not give any additional decrease in PFAS concentration in the treated water could be attributed to the

high water flow used in the experiment (on average, 87.9 L/d).

The difference in treatment efficiency for different branched and linear PFAS led to changes in the isomeric composition of several compounds, where the branched isomer fraction increased after treatment. This trend was observed in both the planted wetland units and the controls, with the most notable example being PFOS, where branched PFOS-isomers increased from 40 % to 62 % of ∑PFOS. This could also be seen in PFNA (27 %–36 %) and PFHpS (33 %–39 %). This could be expected as branched isomers such as PFOA and PFOS have been reported to be enriched in solution compared to sediment in river water, due to their lower hydrophobicity compared to their linear counterparts (Chen et al., 2015). Change in isomeric composition was not observed for PFHpA, PFHxS, or PFOA, possibly due to the difference in combined linear and branched isomer treatment efficiency of the wetland units for the different PFAS. The average removal efficiencies for ΣPFHpS, PFOS, and PFNA across all wetland units, including the controls, were 29 %, 33 %, and 57 %, respectively. Meanwhile, the treatment efficiencies for ΣPFHxS, PFHpA, and PFOA were lower, at 16 %, 11 %, and 19 %, respectively.

3.2. PFAS uptake and concentrations in the plants and filter substrate

In total, 19 out of 29 PFAS (i.e., C_3-C_{11} PFCAs, C_4-C_8 PFSAs, PFECHS, FOSA, 6:2 FTSA, 8:2 FTSA, and Et-FOSAA) ($n = 8$) were detected in the peat and biochar, excluding the LECA (Fig. 2, Tables S14.1-14.5 in SI). This includes four PFAS (PFDA, PFDoDA, FOSA, and 8:2 FTSA), which were not detected in the influent water. PFDA and PFDoDA were also found in low concentrations in the control substrate, suggesting that these compounds may have been present in the filter substrate prior to the experiment. As for the presence of FOSA and 8:2 FTSA, this could be attributed either to contamination from other components of the wetland units, such as the HDPE surfaces or tubing, or to accumulation and subsequent up-concentration to detectable levels during the experimental period. These compounds have relatively long perfluoroalkyl chains, which are correlated to a high solid-water partitioning coefficient in carbon-rich materials such as biochar (Fabregat-Palau et al., 2022), thus supporting the up-concentration theory. The fluorotelomer 4:2 FTSA, while present in the influent water, was not detected in the peat and biochar. Fluorotelomers are known to be transformed to PFAAs in river sediment (Zhang et al., 2016a), which is likely to also occur in the wetland units. Both linear and branched isomers were detected for PFNA, PFHxS, PFHpS, and PFOS. The variations in ΣPFAS concentration of the peat and biochar, comparing the different wetland units, including the controls, were low, with average ∑PFAS being 56.2 ± 9.65 ng/g dw (*C. elata*), 54.1 ± 16.5 ng/g dw (control), 48.1 ± 9.27 ng/g dw (*C. sativa*), and 44.4 ± 19.8 ng/g dw (*Salix* spp), ($n = 2$ each).

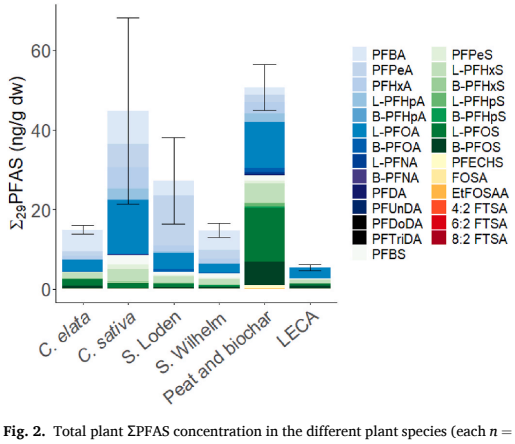

Fig. 2. Total plant ΣPFAS concentration in the different plant species (each $n = 2$) (including roots, twigs, stem, leaves), peat and biochar mixture ($n = 8$), and LECA ($n = 8$). PFCAs are represented in blue, PFSAs in green, and other functional groups in yellow and red. Error bars represent the standard error. (For interpretation of the references to colour in this figure legend, the reader is referred to the Web version of this article.)

Only eight out of 29 PFAS (Fig. 2, Tables S14.1-14.5 in SI) ($n = 8$) (i.e., PFOA, PFTriDA, C_4-C_8 PFSAs, and PFECHS) were detected in LECA, ranging from 3.38 ng/g dw (*Salix* spp) to 7.92 ng/g dw (control) for ∑PFAS ($n = 2$ each).

In total, 15 out of 29 PFAS were detected in the plants ($n = 8$) (including roots, twigs, stems, and leaves). 12 out of 29 PFAS were detected in all plant species (i.e. C_3-C_7 PFCAs, C_4-C_8 PFSAs, PFECHS, and FOSA) (Fig. 2, Tables S15.1-15.5 in SI). Both linear and branched isomers were detected for PFHxS, PFOA, PFHpS, PFNA, PFOS, and PFHpA. Uptake of PFNA was only found in *C. elata* and *C. sativa,* and uptake of PFDA and PFUnDA was only found in *C. sativa.* The fluorotelomeres 4:2 FTSA and 6:2 FTSA, while present in the inlet water, were not found in any plant. These compounds have been shown to be enzymatically transformed to PFAAs by plants (Zhao et al., 2019; Zhang et al., 2016b; Zhao et al., 2018), which may explain why they were not detected in the plants. Et-FOSAA is another PFAS found in the inlet water, which is known to transform in nature (Mejia Avendaño and Liu, 2015), and was not found in any plant. PFDA and PFUnDA were detected in *C. sativa*, but not in the influent water. This could be explained by the accumulation and up-concentration of these compounds to detectable levels in the plant tissue. PFDA was also found in the peat and biochar, making it possible that *C. sativa* took up PFDA from the filter substrate. Total plant ∑PFAS concentrations were highest in *C. sativa* (44.7 ± 23.4 ng/g dw), followed by S. Loden (19.4 ± 10.9 ng/g dw), *C. elata* (14.9 ± 1.07 ng/g dw), and S. Wilhelm (14.7 ± 1.72 ng/g dw) ($n = 2$ each). It should be noted, though, that some of the PFAS detected in plant tissue may derive from foliar uptake rather than from the inlet water, as foliar uptake of PFAS has previously been shown to occur (Chen et al., 2024).

Consequently, our results show that PFAS accumulate in both plant tissue and substrate, which is consistent with the findings of previous studies (Sharma et al., 2020; Dalahmeh et al., 2019; Campos-Pereira et al., 2022). However, to the best of our knowledge, the capture of PFAS in a combined peat and biochar mixture subsurface flow wetland with growing plants has not been reported previously.

The composition of PFAS differed between the sample matrix types (Fig. 2, Tables S14.1-S14.5, and S15.1–15.5 in SI). In the total plants (including roots, leaves, twigs, and stems where applicable), PFCAs had the highest contribution (77 % of ∑PFAS), followed by PFSAs (23 %) and ∑precursors (0.69 %). The PFAS composition in plants was dominated by short-chain C_3-C_6 PFCAs and C_4-C_5 PFSAs (57 % of ∑PFAS), whereas the peat and biochar mixture and LECA had a high contribution of long-chained C_7-C_{12} PFCAs and C_6-C_8 PFSAs (77 % and 93 % of ∑PFAS, respectively). The peat and biochar mixture and the LECA had a higher fraction of PFSAs (54 % and 51 % of ∑PFAS, respectively) compared to the water and plant samples (26 % and 23 % of ∑PFAS, respectively). This difference in composition could be attributed to the higher sorption capacity of longer chain PFAAs as well as PFSAs to soil matrices (Li et al., 2019b). The shorter chain PFAS with a lower sorption capacity instead becomes available for plant uptake, which has also been observed in earlier studies (Nassazzi et al., 2023; Zhang et al., 2020). The distribution of the PFAS precursors also varied, with the peat and biochar mixture and LECA having a slightly higher fraction (1.9 % and 2.3 % of ∑PFAS, respectively) compared to the water (1.4 % of ∑PFAS), and the plant samples having a lower fraction (0.69 % of ∑PFAS). The low contribution of PFAS precursors in plants could be due to the enzyme-mediated transformation of PFAS precursors to perfluorinated compounds, which are known to take place within several PFAS precursor groups (Zhao et al., 2019; Zhang et al., 2016b; Zhao

et al., 2018).

3.3. Tissue distribution of PFAS in the plant roots, stems, twigs, and leaves

The two-way ANOVA model revealed no significant differences in composition between tissue types across species in terms of ∑PFAS concentration, fraction of functional groups, and fraction of branched isomers ($p > 0.05$). All species were thus pooled in the statistical analysis for these measurements to increase statistical power.

The ∑PFAS concentration varied between different plant tissue types (Fig. 3). The PFAS concentrations were significantly higher in the leaves (∑PFAS = 111 ± 38.7 ng/g dw) compared to the roots (∑PFAS = 10.9 ± 1.73 ng/g dw), > stems (∑PFAS = 4.79 ± 2.28 ng/g dw) > and twigs (∑PFAS = 2.26 ± 1.29 ng/g dw) for all plant species ($p < 0.05$). Note that the twig tissue was only present in S. Wilhelm and S. Loden. Furthermore, ∑PFAS concentrations in roots were significantly higher compared to twigs ($p < 0.05$). Comparing the functional groups of PFAS, in roots, PFSAs were the largest PFAS fraction (on average, 66 % of ∑PFAS) compared to PFCAs (32 %), and ∑precursors (2.1 %). Contrastingly, in leaves, the PFCAs comprised the highest composition (on average, 84 % of ∑PFAS) compared to PFSAs (16 %) and ∑precursors (0.35 %). In stem and twigs, the PFAS composition profile was more evenly distributed between PFSAs (on average, 41 % and 57 % of ∑PFAS, respectively) and PFCAs (53 % and 46 %, respectively), but low for ∑precursors (1.8 % and 0.95 %, respectively). The different distribution of PFAS regarding concentration and functional group has been previously reported (Nassazzi et al., 2023), and indicates a correlation of these factors with the translocation of PFAS from roots to leaves.

3.4. Bioconcentration factors (BCF)

The BCF for individual PFAS ranged from 0.24 to 179 for leaves, stems, twigs, and roots (Fig. 4). The highest BCF value for *C. sativa*, S. Wilhelm, and *C. elata* was that of PFBA (137, 129, and 42.7, respectively) in leaves, which is comparable to what has previously been observed for sunflower, mustard, *Salix eleagnos*, and *Salix purpurea* (Nassazzi et al., 2023; Sharma et al., 2020). The highest BCF for S. Loden, however, was found for PFPeA (179) in leaf. All detected < C7 PFAS had a higher BCF in leaf tissue than in root tissue in all plants, whereas all detected > C8 PFAS had a higher BCF in root tissue than in leaf tissue in all plants. These results are further strengthened by the linear regression model showing a significant positive correlation ($p <$

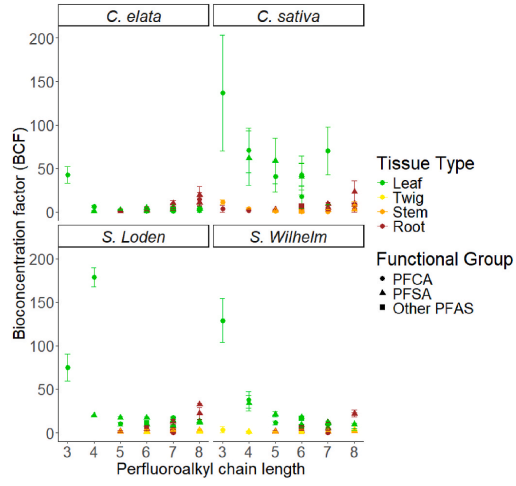

Fig. 4. PFAS bioconcentration factors (BCF = $C_{plant\text{-}tissue}/C_{Inlet\text{-}water}$) in different plant tissues plotted against the perfluoroalkyl chain length of the PFAS, n = 2 per species.

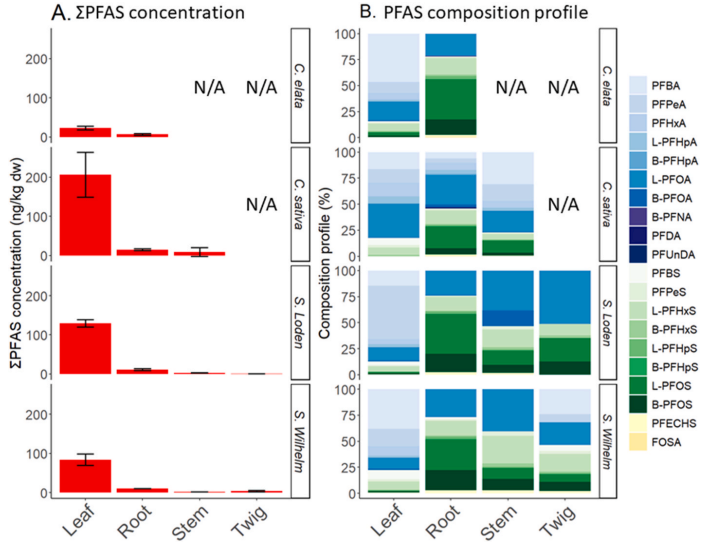

Fig. 3. A) ΣPFAS concentration in different plant tissue types ($n = 2$), and B) PFAS composition profile of each tissue type. *C. sativa* did not have twigs, and *C. elata* did not have twigs or stems; thus, these tissue types are not applicable (N/A). PFCAs are represented in blue, PFSAs in green, and other functional groups in yellow. (For interpretation of the references to colour in this figure legend, the reader is referred to the Web version of this article.)

0.05) between the perfluoroalkyl chain length and BCF in the root tissue for all species except *C. sativa,* for which it was seen but not significant ($p = 0.07$). Inversely, there was a significant negative correlation between BCF and perfluoroalkyl chain lengths for the leaf tissue in *C. sativa* and S. Wilhelm ($p < 0.05$), which was also seen but not significant for the other species ($p = 0.063$–0.096). The BCF in stems and twigs was lower than that of either leaves or roots for every detected PFAS. This can be expected as PFAS with a high sorption coefficient to plant tissue will be immobilized and accumulated in the roots, while PFAS with a low sorption coefficient to plant tissue will be transported to the leaf without sorption to stem or twigs, as reported previously (Felizeter et al., 2014; Battisti et al., 2023). The linear regression model showed no significant correlation between chain length and BCF in twigs or stems ($p > 0.05$). Regarding the impact of the PFAS functional group, the linear regression models indicated that the sulfonic group had a positive impact on BCF in stems and roots of the two Salix clones compared to the carboxylic group. This was, however, only significant for S. Wilhelm ($p < 0.05$). If instead directly comparing the BCF for PFCAs and PFSAs with the same perfluoroalkyl chain length, there was a higher BCF for C_5-C_8 PFSAs compared to C_5-C_8 PFCAs in all species, for root, stem, and twig tissue, with the exception of C_7 PFCA (PFOA) having a higher BCF than its corresponding PFSA in S. Loden stem, and some PFSAs being below MDL in S. Loden twigs. This is expected since PFSAs have been shown to have a higher sorption capacity to the root tissue than PFCAs (Felizeter et al., 2014), which would allow for increased accumulation in roots but reduced transport to leaves. Supporting this theory, the BCF for C_4 PFCA (PFPeA) was higher than that of C_4 PFSA (PFBS) for all species in leaf tissue. However, the BCF of C_5-C_8 PFSAs was higher than that of their corresponding PFCAs for all species in leaf tissue, except for C_7-C_8 PFAS in *C. sativa*. This could perhaps be explained by the large differences in the inlet water concentration of these compounds (Fig. S1 in SI). The difference in BCF between tissue types has been observed previously (Nassazzi et al., 2023; Sharma et al., 2020; Battisti et al., 2023) and is most likely due to the negative correlation between PFAS hydrophobicity and their mobility from roots to above-ground plant parts. It has been proposed that the casparian strip, a selective barrier in the plant root, plays a major role in the translocation of PFAS within the plant (Felizeter et al., 2014; Felizeter et al., 2012). Less hydrophobic, shorter-chain PFAS may be able to cross the casparian strip into the plant vascular tissue and be further translocated to above-ground plant parts through the xylem. More hydrophobic, longer-chained PFAS are restricted and tend to accumulate in the outer root tissues. This was supported by a study on fern roots, which found PFOS in the root cortex (outside the casparian strip), whereas the less hydrophobic GenX was only found near the vascular cylinder (inside the casparian strip) (Qian et al., 2023). This could also reflect PFOS sorption to the tissues of the root cortex. Additional evidence from a comparative study with radish and pak choi indicated that the absence of a functional Casparian strip in radish allowed for greater translocation of PFOA in the radish compared to the pak choi (Xu et al., 2024).

3.5. Estimated treatment potential using phytoremediation

All species had above-ground tissue/water concentrations >10/1 for PFBA. This was also the case for *C. elata* with L-PFOS, and *C. sativa* with PFPeA, PFBS, PFPeS, and L-PFOA, and S. Loden with PFPeA. The phytoremediation potential for PFAS for the four investigated plant species was estimated based on the PFAS concentration in the plant (i.e., sum of the total mass in stem, twigs, and leaves) and biomass production per ha and year (Table 1). *C. sativa* had the highest predicted removal capacity for ∑PFAS (941 ± 670 mg ΣPFAS/ha yr) due to both the highest PFAS concentration in this study and the high biomass yields reported in the literature (Zegada-Lizarazu et al., 2010). *C. elata* had the lowest predicted removal capacity for ∑PFAS (164 ± 56 mg ΣPFAS/ha yr), partly because of its lower reported biomass yields (Banaszuk et al., 2020). The results correspond well with a previous study estimating the phytoremediation removal potential of Norway spruce, silver birch, and ground elder close to a PFAS-impacted airfield to 550–1400 mg/ha yr of Σ_{26}PFAS (Gobelius et al., 2017). It is, however, important to note that the total removal of PFAS by phytoremediation is dependent on PFAS concentration, as an increase in PFAS concentration has been shown to lead to an increase in PFAS uptake in plants (Gredelj et al., 2020). Cultivation methods have also been proven to be important, as is shown by the difference in BCF for different PFAS between hydroponic and soil conditions (Gredelj et al., 2020). It is reasonable to also extend this to include different soil types, especially since factors like pH have been shown to play a role in plant uptake of PFAS (Krippner et al., 2014). It is also likely that the removal values in Table 1 are underestimated, as the hydraulic retention time in the wetland units was likely too low to achieve effective treatment. Previous studies have used both considerably higher and lower retention times than those used in this study (Ferrario et al., 2022; Soda et al., 2012). A higher retention time would likely increase the fraction of the water removed through transpiration, which would likely also increase the relative PFAS uptake and immobilization in plant tissues. It would also result in a higher fraction of the water being lost to evaporation, thus increasing the PFAS concentration in the remaining water, which has been shown to increase plant uptake of PFAS (Gredelj et al., 2020). This could, however, also prove problematic for leachate-impacted groundwater with high sodium chloride concentrations, as the salt would accumulate in the wetland, which might prove detrimental to the plants. Both *Salix* and *C. sativa* are reported to be cultivated on industrial scales for bioenergy purposes due to their high biomass yields (Zegada-Lizarazu et al., 2010), suggesting that they would be suitable for phytoremediation of PFAS. However, it has been reported that adding nutrients to stimulate biomass growth reduces the PFAS concentrations in plant tissue (Nassazzi et al., 2023), showing that the subject of phytoremediation is more complicated than the maximization of biomass, since if this were the case, PFAS concentration in plant tissue would have remained constant for plants receiving nutrients, thus increasing the total PFAS uptake. *C. elata* is typically not cultivated for biomass purposes and has considerably lower biomass yields than *C. sativa* and *Salix* (Banaszuk et al., 2020; Zegada-Lizarazu, 2010). On the other hand, the *Carex* genus has been considered in previous PFAS phytoremediation studies (Greger, 2021; Zhang et al.,

Table 1
Estimated treatment potential for the different plant species derived from ∑PFAS concentrations (for individual PFAS see Tables S16–S20 in SI) derived in this study, combined with literature values on expected biomass yields (stem, twigs, leaves). A median value is calculated based on the biomass range. The biomass values of both *Salix* spp and *C. sativa* were obtained from the same publication.

Species	Mean ΣPFAS concentration (ng/g dw) (range)	Tonnes of biomass (stem, twigs, leaves) range in dw/ha yr	Median ΣPFAS removed in mg dw/ha yr (range)
C. elata	22.8 ± 4.73 (18.1–27.5)	6–8(Banaszuk et al., 2020)	164 ± 56 (108–220)
C. sativa	48 ± 25 (22.6–73.4)	12–22 (Zegada-Lizarazu et al., 2010)	941 ± 670 (271–1610)
S. Wilhelm	14.7 ± 1.7 (13.1–16.6)	13–30 [a](Zegada-Lizarazu et al., 2010)	333 ± 163 (170–496)
S. Loden	19.5 ± 11 (8.5–30.5)	10–23 [a](Zegada-Lizarazu et al., 2010)	393 ± 308 (85–702)

[a] Biomass yields for the different *Salix* clones were taken from the mean *Salix* production data (Zegada-Lizarazu et al., 2010) and adjusted for biomass differences seen in the experiment.

2021a). In this study, however, *C. elata* showed lower phytoremediation potential compared to *C. sativa* or *Salix*.

The modest PFAS removal shown by plants in wetland systems in this study suggests that this approach is best suited for smaller-scale, local water treatment applications where conventional PFAS treatment options may be cost-prohibitive. Such scenarios include agricultural runoff, stormwater, leachate from small waste management facilities, gray water, or decentralized sewage treatment systems. These wetlands are particularly beneficial for treating complex waters co-contaminated with metals or nutrients, as constructed wetlands have been shown to efficiently remove these contaminants (Sheoran and Sheoran, 2006; Vymazal, 2007). If safe end-use of the harvested biomass can be ensured, such as through hydrothermal liquefaction to produce bio-oil and biochar (Zhang et al., 2021b), it could also offer value recovery from PFAS-contaminated land, irrigation water, or fertilizers, while at the same time contributing to system remediation.

4. Conclusions

This study investigated the use of subsurface flow constructed wetlands, with plants, to treat landfill leachate-impacted groundwater during field conditions. The main removal mechanism of the wetlands was shown to be sorption by the peat and biochar filter substrate, due to short residence times in the units. Although plant uptake and accumulation of PFAS were also observed. Short-chain PFAS and PFCAs were shown to be taken up and translocated to above-ground plant parts, while long-chain PFAS and PFSAs accumulated in plant roots and the filter substrate. The above-ground BCF was >10 for several PFAS in one or more plant species (PFBA, PFPeA, L-PFOA, PFBS, PFPeS, and L-PFOS), with *C. Sativa* having an above-ground BCF >10 for the highest amount of different PFAS. The study shows how plants can be used in combination with a peat and biochar filter substrate to treat PFAS-contaminated groundwater, removing both short and long-chain PFAS. The study thus provides valuable insight into how full-scale wetland systems could be designed for efficient PFAS treatment. It is, however, important to acknowledge the limitations of operating pilot wetlands for a single growing season. Further studies should focus on larger-scale systems operated for several seasons. It is also important to look into the regeneration or destruction of the filter substrate, as well as the safe repurposing or destruction of harvested biomass. It is also important to design the wetland and its recirculation to limit the creation of aerosols and PFAS transport to the atmosphere. The removal efficiencies of plants observed in this study suggest that phytoremediation of PFAS contaminated water using wetlands would be best suited for smaller-scale, local systems such as the treatment of agricultural runoff, stormwater, leachate from small waste management facilities, greywater, or decentralized sewage treatment systems. To achieve effective treatment, hydraulic retention times in such systems would likely need to be longer than those applied in this study. Other uses for this technology is where safe use of harvested biomass, such as for biofuel or biochar production, can enable the beneficial use of PFAS-contaminated irrigation water or fertilization. Our study has shown that phytoextraction of PFAS was most efficient for the removal of short-chain PFAS, suggesting that it could be a viable method in combination with other methods proven to be efficient for the removal of long-chain PFAS, such as activated carbon filters or foam fractionation.

CRediT authorship contribution statement

Oscar Liljeström: Writing – original draft, Software, Methodology, Investigation, Formal analysis, Data curation, Conceptualization. **Dahn Rosenquist:** Writing – review & editing, Methodology, Funding acquisition, Conceptualization. **Dan B. Kleja:** Writing – review & editing, Supervision, Funding acquisition. **Anja Enell:** Writing – review & editing, Supervision, Funding acquisition. **Lutz Ahrens:** Writing – review & editing, Supervision, Methodology, Funding acquisition, Conceptualization.

Declaration of competing interest

The authors declare the following financial interests/personal relationships which may be considered as potential competing interests: Oscar Liljestrom reports equipment, drugs, or supplies was provided by Laqua Treatment AB. Dahn Rosenqvist reports a relationship with Laqua Treatment AB that includes: employment. If there are other authors, they declare that they have no known competing financial interests or personal relationships that could have appeared to influence the work reported in this paper.

Acknowledgements

This work was part of the LIFE SOuRCE project (LIFE20 ENV/ES/000880), which has received funding from the LIFE program of the European Union. We also wish to acknowledge the staff at the waste management facility who have been very supportive during the project.

Appendix A. Supplementary data

Supplementary data to this article can be found online at https://doi.org/10.1016/j.envpol.2025.127199.

Data availability

Data will be made available on request.

References

Ali, H., Khan, E., Sajad, M.A., 2013. Phytoremediation of heavy metals-Concepts and applications. Chemosphere 91, 869–881.
Askeland, M., et al., 2020. Biochar sorption of PFOS, PFOA, PFHxS and PFHxA in two soils with contrasting texture. Chemosphere 249, 126072.
Awad, J., et al., 2022. Application of native plants in constructed floating wetlands as a passive remediation approach for PFAS-impacted surface water. J. Hazard. Mater. 429, 128326.
Banaszuk, P., Kamocki, A.K., Wysocka-Czubaszek, A., Czubaszek, R., Roj-Rojewski, S., 2020. Closing the loop - recovery of nutrients and energy from wetland biomass. Ecol. Eng. 143, 105643.
Barry, V., Winquist, A., Steenland, K., 2013. Perfluorooctanoic acid (PFOA) exposures and incident cancers among adults living near a chemical plant. Environ. Health Perspect. 121, 1313–1318.
Battisti, I., et al., 2023. Perfluoroalkyl substances exposure alters stomatal opening and xylem hydraulics in willow plants. Chemosphere 344, 140380.
Beale, D.J., et al., 2022. Host–gut microbiome metabolic interactions in PFAS-impacted freshwater turtles (Emydura macquarii macquarii). Metabolites 12, 1–19.
Birnstingl, J., Wilson, J., 2024. A cost comparison of pump-and-treat and in situ colloidal activated carbon for PFAS plume management. Remed. J. 35.
Brunn, H., et al., 2023. PFAS: forever chemicals—persistent, bioaccumulative and mobile. Reviewing the status and the need for their phase out and remediation of contaminated sites. Environ. Sci. Eur. 35, 1–50.
Brusseau, M.L., 2024. Field versus laboratory measurements of PFAS sorption by soils and sediments. J. Hazard. Mater. Adv. 16, 100508.
Campos-Pereira, H., et al., 2022. Binding of per- and polyfluoroalkyl substances (PFASs) by organic soil materials with different structural composition – charge- and concentration-dependent sorption behavior. Chemosphere 297.
Chen, X., et al., 2015. Isomeric specific partitioning behaviors of perfluoroalkyl substances in water dissolved phase, suspended particulate matters and sediments in Liao River Basin and Taihu Lake, China. Water Res. 80, 235–244.
Chen, X., et al., 2024. Multimedia and full-life-cycle monitoring discloses the dynamic accumulation rules of PFAS and underestimated foliar uptake in wheat near a fluorochemical industrial Park. Environ. Sci. Technol. https://doi.org/10.1021/acs.est.4c03525.
Dalahmeh, S.S., Alziq, N., Ahrens, L., 2019. Potential of biochar fi lters for onsite wastewater treatment : effects of active and inactive bio fi lms on adsorption of per- and poly fl uoroalkyl substances in laboratory column experiments. Environ. Pollut. 247, 155–164.
Fabregat-Palau, J., Vidal, M., Rigol, A., 2022. Examining sorption of perfluoroalkyl substances (PFAS) in biochars and other carbon-rich materials. Chemosphere 302, 134733.
Fang, B., et al., 2024. Fluorotelomer betaines and sulfonic acid in aerobic wetland soil: stability, biotransformation, and bacterial community response. J. Hazard. Mater. 477, 135261.

Felizeter, S., McLachlan, M.S., De Voogt, P., 2012. Uptake of perfluorinated alkyl acids by hydroponically grown lettuce (Lactuca sativa). Environ. Sci. Technol. 46, 11735–11743.
Felizeter, S., Mclachlan, M.S., Voogt, P. De, 2014. Root Uptake and Translocation of per Fl Uorinated Alkyl Acids by Three Hydroponically Grown Crops.
Fenton, S.E., et al., 2021. Per- and polyfluoroalkyl substance toxicity and human health review: current state of knowledge and strategies for informing future research. Environ. Toxicol. Chem. 40, 606–630.
Ferrario, C., et al., 2022. Assessment of reed grasses (Phragmites australis) performance in PFAS removal from water: a phytoremediation pilot plant study. Water (Switzerland) 14.
Gaines, 2022. Historical and Current Usage of Per- and Polyfluoroalkyl Substances PFAS A.Pdf.
Gan, S., Lau, E.V., Ng, H.K., 2009. Remediation of soils contaminated with polycyclic aromatic hydrocarbons (PAHs). J. Hazard. Mater. 172, 532–549.
Gobelius, L., Lewis, J., Ahrens, L., 2017. Plant uptake of Per- and polyfluoroalkyl substances at a contaminated fire training facility to evaluate the phytoremediation potential of various plant species. Environ. Sci. Technol. 51, 12602–12610.
Gredelj, A., et al., 2020. Uptake and translocation of perfluoroalkyl acids (PFAAs) in hydroponically grown red chicory (Cichorium intybus L.): growth and developmental toxicity, comparison with growth in soil and bioavailability implications. Sci. Total Environ. 720, 137333.
Greger, M., 2021. Removal of PFAS from water by plants. Int. J. Environ. Sci. Nat. Resour. 28, 1–6.
Hale, S.E., et al., 2017. Sorbent amendment as a remediation strategy to reduce PFAS mobility and leaching in a contaminated sandy soil from a Norwegian firefighting training facility. Chemosphere 171, 9–18.
Hepburn, E., et al., 2019. Contamination of groundwater with per- and polyfluoroalkyl substances (PFAS) from legacy landfills in an urban re-development precinct. Environ. Pollut. 248, 101–113.
Huff, D.K., Morris, L.A., Sutter, L., Costanza, J., Pennell, K.D., 2020. Accumulation of six PFAS compounds by woody and herbaceous plants: potential for phytoextraction. Int. J. Phytoremediation 22, 1538–1550.
Kang, Y., Guo, Z., Ma, H., Wu, H., Zhang, J., 2023. Enhanced removal of perfluorooctanoic acid (PFOA) and perfluorooctane sulfonate (PFOS) in constructed wetlands: iron cycling and microbial mechanisms. ACS ES T Water 3, 287–297.
Kasak, K., et al., 2018. Biochar enhances plant growth and nutrient removal in horizontal subsurface flow constructed wetlands. Sci. Total Environ. 639, 67–74.
Kelly, B.C., et al., 2009. Perfluoroalkyl contaminants in an arctic marine food web: Trophic magnification and wildlife exposure. Environ. Sci. Technol. 43, 4037–4043. Perfluoroalkyl.
Krippner, J., et al., 2014. Effects of chain length and pH on the uptake and distribution of perfluoroalkyl substances in maize (Zea mays). Chemosphere 94, 85–90.
Kwok, K.Y., et al., 2015. Occurrence and distribution of conventional and new classes of per- and polyfluoroalkyl substances (PFASs) in the South China Sea. J. Hazard. Mater. 285, 389–397.
Laramay, F., Crimi, M., 2020. Theoretical evaluation of chemical and physical feasibility of an in situ ultrasonic reactor for remediation of groundwater contaminated with per- and polyfluoroalkyl substances. Remediation 31, 45–58.
Lesmeister, L., et al., 2021. Extending the knowledge about PFAS bioaccumulation factors for agricultural plants – a review. Sci. Total Environ. 766, 142640.
Li, J., Fan, J., Liu, D., Hu, Z., Zhang, J., 2019a. Enhanced nitrogen removal in biochar-added surface flow constructed wetlands: dealing with seasonal variation in the north China. Environ. Sci. Pollut. Res. 26, 3675–3684.
Li, F., et al., 2019b. Adsorption of perfluorinated acids onto soils: Kinetics, isotherms, and influences of soil properties. Sci. Total Environ. 649, 504–514.
Lott, D.J., Robey, N.M., Fonseca, R., Bowden, J.A., Townsend, T.G., 2023. Behavior of Per- and polyfluoroalkyl substances (PFAS) in pilot-scale vertical flow constructed wetlands treating landfill leachate. Waste Manag. 161, 187–192.
Ma, H., et al., 2023. Enhancement of perfluorooctanoic acid and perfluorooctane sulphonic acid removal in constructed wetland using iron mineral: performance and mechanisms. J. Hazard. Mater. 447, 130819.
Mejía Avendaño, S., Liu, J., 2015. Production of PFOS from aerobic soil biotransformation of two perfluoroalkyl sulfonamide derivatives. Chemosphere 119, 1084–1090.
Nason, S.L., et al., 2024. A comprehensive trial on PFAS remediation: hemp phytoextraction and PFAS degradation in harvested plants. Environ. Sci. Adv. 3, 304–313.
Nassazzi, W., Lai, F.Y., Ahrens, L., 2022. A novel method for extraction, clean-up and analysis of per- and polyfluoroalkyl substances (PFAS) in different plant matrices using LC-MS/MS. J. Chromatogr., B: Anal. Technol. Biomed. Life Sci. 1212, 123514.
Nassazzi, W., Wu, T.C., Jass, J., Lai, F.Y., Ahrens, L., 2023. Phytoextraction of per- and polyfluoroalkyl substances (PFAS) and the influence of supplements on the performance of short-rotation crops. Environ. Pollut. 333, 122038.
Nelson, J.W., Hatch, E.E., Webster, T.F., 2010. Exposure to polyfluoroalkyl chemicals and cholesterol, body weight, and insulin resistance in the general U.S. population. Environ. Health Perspect. 118, 197–202.
OECD, 2021. Reconciling terminology of the universe of Per- and polyfluoroalkyl substances: recommendations and practical guidance. OECD Ser. Risk Manag. 61, 1–45.
Persson, G., Lindroth, A., 1994. Hydrology simulating evaporation from short-rotation forest: variations within and between seasons. J. Hydrol. 156.
Philip, McCleaf, Sophie, Englund, Anna, Östlund, Lindegren, Klara, Wiberg, Karin, Lutz, Ahrens, 2017. Removal efficiency of multiple poly- and perfluoroalkyl substances (PFASs) in drinking water using granular activated carbon (GAC) and anion exchange (AE) column tests. Water Res. 120, 77–87.
Qian, S., et al., 2023. Bioaccumulation of Per- and polyfluoroalkyl substances (PFAS) in ferns: effect of PFAS molecular structure and plant root characteristics. Environ. Sci. Technol. 57, 4443–4453.
Rauert, C., Shoieb, M., Schuster, J.K., Eng, A., Harner, T., 2018. Atmospheric concentrations and trends of poly- and perfluoroalkyl substances (PFAS) and volatile methyl siloxanes (VMS) over 7 years of sampling in the global Atmospheric Passive Sampling (GAPS) network. Environ. Pollut. 238, 94–102.
Salt, D.E., Smith, R.D., Raskin, I., 1998. Phytoremediation. Annu. Rev. Plant Biol. 49, 643–668.
Sharma, N., et al., 2020. Accumulation and effects of perfluoroalkyl substances in three hydroponically grown Salix L. species. Ecotoxicol. Environ. Saf. 191.
Sheoran, A.S., Sheoran, V., 2006. Heavy metal removal mechanism of acid mine drainage in wetlands: a critical review. Miner. Eng. 19, 105–116.
Smith, S.J., Wiberg, K., McCleaf, P., Ahrens, L., 2022. Pilot-scale continuous foam fractionation for the removal of Per- and polyfluoroalkyl substances (PFAS) from landfill leachate. ACS ES T Water 2, 841–851.
Soda, S., et al., 2012. Constructed wetlands for advanced treatment of wastewater with a complex matrix from a metal-processing plant: bioconcentration and translocation factors of various metals in Acorus gramineus and Cyperus alternifolius. Ecol. Eng. 39, 63–70.
Sörengård, M., Franke, V., Tröger, R., Ahrens, L., 2020. Losses of poly- and perfluoroalkyl substances to syringe filter materials. J. Chromatogr. A 1609.
Sörengård, M., Bergström, S., McCleaf, P., Wiberg, K., Ahrens, L., 2022. Long-distance transport of per- and polyfluoroalkyl substances (PFAS) in a Swedish drinking water aquifer. Environ. Pollut. 311.
Stahl, T., et al., 2009. Carryover of perfluorooctanoic acid (PFOA) and perfluorooctane sulfonate (PFOS) from soil to plants. Arch. Environ. Contam. Toxicol. 57, 289–298.
Stein, Cheryl R., McGovern, Kathleen J., Pajak, Ashley M., Maglione, Paul J., Wolff, M.S., 2016. Perfluoroalkyl and polyfluoroalkyl substances and indicators of immune function in children aged 12 – 19 years: NHANES. Pediatr. Res. 79, 348–357.
Sunderland, E.M., et al., 2019. A review of the pathways of human exposure to poly- and perfluoroalkyl substances (PFASs) and present understanding of health effects. J. Expo. Sci. Environ. Epidemiol. 29, 131–147.
Vymazal, J., 2007. Removal of nutrients in various types of constructed wetlands. Sci. Total Environ. 380, 48–65.
Walter, J.S., Campbell, C., Kellog, E.A., Donoghue, M.J., Stevens, P., 2002. Plant Systematics: A Phylogenetic Approach, second ed.
Wen, B., et al., 2013. Mechanistic studies of perfluorooctane sulfonate, perfluorooctanoic acid uptake by maize (Zea mays L. cv. TY2). Plant Soil 370, 345–354.
Xiao, J., Huang, J., Wang, Y., Qian, X., 2023. The fate and behavior of perfluorooctanoic acid (PFOA) in constructed wetlands: insights into potential removal and transformation pathway. Sci. Total Environ. 861, 160309.
Xu, J., et al., 2024. Differential uptake and translocation of perfluoroalkyl substances by vegetable roots and leaves: insight into critical influencing factors. Sci. Total Environ. 949, 175205.
Yin, T., et al., 2017. Perfluoroalkyl and polyfluoroalkyl substances removal in a full-scale tropical constructed wetland system treating landfill leachate. Water Res. 125, 418–426.
Zegada-Lizarazu, W., et al., 2010. Agronomic aspects of energy crops in Europe. Biofuel Bioprod. Biorefining 674–691.
Zhang, S., Lu, X., Wang, N., Buck, R.C., 2016a. Biotransformation potential of 6:2 fluorotelomer sulfonate (6:2 FTSA) in aerobic and anaerobic sediment. Chemosphere 154, 224–230.
Zhang, H., et al., 2016b. Uptake, translocation, and metabolism of 8:2 fluorotelomer alcohol in soybean (Glycine max L. Merrill). Environ. Sci. Technol. 50, 13309–13317.
Zhang, D.Q., Wang, M., He, Q., Niu, X., Liang, Y., 2020. Distribution of perfluoroalkyl substances (PFASs) in aquatic plant-based systems: from soil adsorption and plant uptake to effects on microbial community. Environ. Pollut. 257, 113575.
Zhang, W., Cao, H., Liang, Y., 2021a. Plant uptake and soil fractionation of five ether-PFAS in plant-soil systems. Sci. Total Environ. 771, 144805.
Zhang, W., Cao, H., Liang, Y., 2021b. Degradation by hydrothermal liquefaction of fluoroalkylether compounds accumulated in cattails (Typha latifolia). J. Environ. Chem. Eng. 9.
Zhao, S., et al., 2018. Different biotransformation behaviors of perfluorooctane sulfonamide in wheat (Triticum aestivum L.) from earthworms (Eisenia fetida). J. Hazard. Mater. 346, 191–198.
Zhao, S., et al., 2019. Fate of 6:2 fluorotelomer sulfonic acid in pumpkin (Cucurbita maxima L.) based on hydroponic culture: uptake, translocation and biotransformation. Environ. Pollut. 252, 804–812.

Supporting Information

Pilot scale treatment of PFAS-contaminated groundwater in a subsurface flow constructed wetland – evaluating multiple plant species

Oscar Liljeström[1], Dahn Rosenqvist[2], Dan B. Kleja[3], Anja Enell[3], Lutz Ahrens[1]

[1] Swedish University of Agricultural Sciences (SLU), Department of Aquatic Sciences and Assessment, P. O. Box 7050, SE-750 07 Uppsala, Sweden

[2]Laqua treatment AB, Siriusvägen 16, SE-296 92 Yngsjö, Sweden

[3]Swedish Geotechnical Institute (SGI), Olaus Magnus Väg 35, SE-581 93 Linköping, Sweden

Pre-growing conditions of C. sativa

The plants were watered *ad lib* with nutrient mixed water containing Nitrate-N 80 mg/L, Ammonium-N 40 mg/L, phosphorus 25 mg/L, potassium 130 mg/L, magnesium 5 mg/L, sulphur 5 mg/L, calcium 5 mg/L

Table S1: List of PFAS analyzed, including full name, abbreviation used in this manuscript, carbon chain length, and perfluoroalkyl chain length

Full name	**Abbreviation**	**Carbon chain**	**Perfluoroalkyl chain**
Perfluorobutyric acid	PFBA	4	3
Perfluoropentanoic acid	PFPeA	5	4
Perfluorobutanesulfonic acid	PFBS	4	4
Perfluorohexanoic acid	PFHxA	6	6
4:2 fluorotelomer sulfonate	4-2FTSA	6	4
tetrafluoro-2-(heptafluoropropoxy)propanoic acid	HFPO-DA	6	4
Perfluoropentanesulfonic acid	PFPeS	5	5
Perfluoroheptanoic acid	PFHpA	7	6
Sodium 4,8-dioxa-3H-perfluorononanoate	NaDONA	7	5
Perfluorohexanesulfonic Acid	PFHxS	6	6
Perfluorooctanoic acid	PFOA	8	7
6:2 fluorotelomer sulfonate	6-2 FTSA	8	6
Perfluoroheptanesulfonic acid	PFHpS	7	7
perfluoro-4-ethylcyclohexanesulfonate	PFECHS	8	6
Perfluorononanoic acid	PFNA	9	8
Perfluorooctanesulfonamide	FOSA	8	8
Perfluorooctanesulfonic acid	PFOS	8	8
Perfluorodecanoic acid	PFDA	10	9
8:2 fluorotelomer sulfonate	8-2 FTSA	10	8
9-chlorohexadecafluoro-3-oxanonane-1-sulfonic acid	9Cl-PF3ONS	8	7
Perfluorononanesulfonic acid	PFNS	9	9
Perfluoroundecanoic acid	PFUnDA	11	10
methylperfluorooctanesulfonamidoacetic acid	Me-FOSAA	8	8
ethylperfluorooctanesulfonamidoacetic acid	Et-FOSAA	8	8
perfluorodecanesulfonic acid	PFDS	10	10
Perfluorododecanoic acid	PFDoDA	12	11
11-chloroeicosafluoro-3-oxaundecane-1-sulfonate acid	11Cl-PF3OUdS	10	9
Perfluorotridecanoic acid	PFTriDA	13	12
Perfluorotetradecanoic acid	PFTeDA	14	13

Table S2: The recirculation flow rates for each wetland unit

Unit	Recirculation flow rate (m^3/d)
Salix A	0.28
Salix B	1.2
C. elata A	1.3
C. elata B	1.4
C. sativa A	1.0
C. sativa B	1.3
Control A	1.2
Control B	0.9

Table S3: quality control parameters for water matrix samples

PFAS	Average relative standard deviation (%)	Average filterblank concentration (ng/L)	Average SPE blank concentration (ng/L)	Fieldblank concentration (ng/L)	MDL (ng/L)
PFBA	2.64	0.212	3.49	12	18.4
PFPeA	1.91	N/A	1.17	4.23	6.52
PFBS	2.84	0.58	0.385	N/A	1.77
PFHxA	2.21	N/A	0.119	0.39	0.601
4-2FTSA	20.8	N/A	N/A	N/A	0.405
HFPO-DA	3.52E-15	N/A	N/A	N/A	0.471
PFPeS	5.71	N/A	N/A	N/A	0.321
PFHpA-Linear	2.06	N/A	0.444	1.36	2.1
PFHpA-Branched	7.61	N/A	0.444	1.36	2.1
NaDONA	N/A	N/A	N/A	N/A	0.905
PFHxS-Linear	7.34	0.0802	N/A	N/A	0.253
PFHxS-Branched	12.3	N/A	0.0169	N/A	0.144
PFOA-Linear	6.49	N/A	0.0256	0.689	1.06
PFOA-Branched	5.67	N/A	N/A	N/A	17.9
6-2 FTSA	3.36	0.129	N/A	N/A	0.593
PFHpS-Linear	6.06	N/A	N/A	N/A	0.174
PFHpS-Branched	3.3	N/A	N/A	N/A	0.627
PFECHS	5.84	N/A	N/A	N/A	0.24
PFNA-Linear	11.6	N/A	0.0551	0.222	0.343
PFNA-Branched	7.79	N/A	N/A	N/A	0.311
FOSA	4.72E-15	0.114	0.01	0.0743	0.704
PFOS-Linear	6.79	1.12	N/A	N/A	4.09
PFOS-Branched	7.1	0.16	N/A	N/A	0.984
PFDA	4.58E-15	0.346	0.136	N/A	1.45
8-2 FTSA	N/A	0.0791	N/A	N/A	0.488
9Cl-PF3ONS	3.62E-15	N/A	N/A	N/A	0.0287
PFNS	N/A	N/A	N/A	N/A	0.131
PFUnDA	N/A	0.327	0.00151	0.111	1.34
Me-FOSAA	3.41E-15	N/A	N/A	N/A	0.243
Et-FOSAA	4.88E-15	0.0552	N/A	N/A	0.34
PFDS	N/A	N/A	N/A	N/A	0.184
PFDoDA	N/A	0.283	N/A	0.275	1.15
11Cl-PF3OUdS	N/A	N/A	N/A	N/A	0.406
PFTriDA	N/A	0.443	N/A	0.099	1.84
PFTeDA	N/A	1.41	0.00165	0.162	7.04

Table S4: quality control parameters for plant matrix samples

PFAS	Analytical replicate average relative standard deviation (%)	Intra unit plant relative standard deviation (%)	Average plant blank concentration (ng/Kg)	MDL (ng/Kg)
PFBA	22.4	64.9	208	1060
PFPeA	6.88	16	64.9	361
PFBS	8.68	36.6	76.7	360
PFHxA	11.5	35.5	76	443
4-2FTSA	N/A	N/A	N/A	13.3
HFPO-DA	N/A	N/A	N/A	40.9
PFPeS	11.6	40.8	N/A	30.2
PFHpA-Linnear	7.89	15.1	33.4	334
PFHpA-Branched	9.54	38.5	N/A	10
NaDONA	N/A	N/A	N/A	24
PFHxS-Linnear	10.2	24.2	3.58	35.8
PFHxS-Branched	22	33.3	2.08	20.8
PFOA-Linnear	10.4	36.9	20.9	209
PFOA-Branched	14.4	80.7	N/A	105
6-2 FTSA	N/A	29.7	21.9	154
PFHpS-Linnear	11.2	36.2	N/A	11.6
PFHpS-Branched	11.7	48.7	N/A	10
PFECHS	7.61	19.5	N/A	26.4
PFNA-Linnear	N/A	55.5	36.8	368
PFNA-Branched	5.45	22.2	N/A	10
FOSA	17.8	71	3.67	21
PFOS-Linnear	6.87	32.5	26.7	180
PFOS-Branched	7.43	32.8	3.67	36.7
PFDA	N/A	79.6	24.6	246
8-2 FTSA	N/A	N/A	N/A	10.1
9Cl-PF3ONS	N/A	N/A	N/A	20.9
PFNS	N/A	N/A	N/A	21.6
PFUnDA	5.8	58.2	16.4	122
Me-FOSAA	N/A	N/A	N/A	30
Et-FOSAA	16.6	43.9	N/A	29.2
PFDS	N/A	N/A	N/A	21.5
PFDoDA	N/A	51	59.1	417
11Cl-PF3OUdS	N/A	19.2	N/A	26.9
PFTriDA	N/A	49	3400	23700
PFTeDA	N/A	82.7	5880	58700

Table S5: quality control parameters for filter substrate matrix samples

PFAS	Replicate relative standard deviation (%)	average blank concentration (ng/Kg)	MDL (ng/Kg)
PFBA	14.2	47.4	216
PFPeA	18.6	34.5	158
PFBS	11.2	93.5	345
PFHxA	23.1	127	567
4-2FTSA	N/A	15.6	68.8
HFPO-DA	N/A	N/A	126
PFPeS	18.9	N/A	37.7
PFHpA-Linnear	11.3	60.2	269
PFHpA-Branched	53	N/A	59.2
NaDONA	1.77E-14	N/A	24

PFHxS-Linnear	20.1	N/A	32.6
PFHxS-Branched	56	N/A	16.3
PFOA-Linnear	16.8	101	455
PFOA-Branched	25	N/A	788
6-2 FTSA	18.2	2.88	14.2
PFHpS-Linnear	39.2	N/A	21.9
PFHpS-Branched	54.1	N/A	63
PFECHS	25.3	N/A	28.1
PFNA-Linnear	20.4	14.4	64.2
PFNA-Branched	43	N/A	36.9
FOSA	137	0.213	1.49
PFOS-Linnear	10.1	28.8	142
PFOS-Branched	26.3	N/A	12.5
PFDA	35.7	5.61	39.3
8-2 FTSA	1.5E-14	2.96	14.2
9Cl-PF3ONS	N/A	N/A	69.6
PFNS	1.97E-14	N/A	21.6
PFUnDA	N/A	6.89	24.3
Me-FOSAA	N/A	N/A	37.8
Et-FOSAA	26.6	N/A	21.6
PFDS	N/A	N/A	21.1
PFDoDA	91	1.82	12.8
11Cl-PF3OUdS	N/A	N/A	38.1
PFTriDA	63.8	N/A	18.7
PFTeDA	N/A	67.2	309

Table S6.1: PFAS concentration in pre-planting control plants

Species	**Tissue type**	**PFBA (ng/Kg)**	**PFPeA (ng/Kg)**	**PFBS (ng/Kg)**	**PFHxA (ng/Kg)**	**4-2FTSA (ng/Kg)**	**HFPO-DA (ng/Kg)**	**PFPeS (ng/Kg)**	**L-PFHpA (ng/Kg)**
C. sativa	*Root*	<1060	<361	<360	<443	<13.3	<40.9	<30.2	<334
C. sativa	*Root*	<1060	459	<360	<443	<13.3	<40.9	<30.2	<334
C. sativa	*Root*	<1060	<361	<360	<443	<13.3	<40.9	<30.2	<334
C. sativa	*Stem*	<1060	<361	<360	<443	<13.3	<40.9	<30.2	<334
C. sativa	*Stem*	<1060	<361	<360	<443	<13.3	<40.9	<30.2	<334
C. sativa	*Stem*	<1060	<361	<360	<443	<13.3	<40.9	<30.2	<334
C. sativa	*Leaf*	<1060	362	3540	1070	<13.3	<40.9	<30.2	744
C. sativa	*Leaf*	<1060	473	3950	723	853	<40.9	<30.2	1330
C. sativa	*Leaf*	<1060	<361	3770	802	<13.3	<40.9	108	1050
C. elata	*Root*	<1060	<361	<360	<443	<13.3	<40.9	<30.2	<334
C. elata	*Root*	<1060	<361	<360	<443	<13.3	<40.9	<30.2	<334
C. elata	*Root*	<1060	<361	<360	<443	<13.3	<40.9	<30.2	<334
C. elata	*Shoot*	<1060	<361	<360	<443	<13.3	<40.9	<30.2	<334
C. elata	*Shoot*	<1060	<361	<360	<443	<13.3	<40.9	<30.2	<334
C. elata	*Shoot*	<1060	<361	<360	<443	<13.3	<40.9	<30.2	<334
S. Wilhelm	*Stem*	<1060	<361	<360	<443	<13.3	<40.9	<30.2	<334
S. Wilhelm	*Stem*	<1060	<361	<360	<443	<13.3	<40.9	<30.2	<334

S. Wilhelm	*Stem*	<1060	<361	<360	<443	<13.3	<40.9	<30.2	<334
S. Loden	*Stem*	<1060	<361	<360	<443	<13.3	<40.9	<30.2	<334
S. Loden	*Stem*	<1060	<361	<360	<443	<13.3	<40.9	<30.2	<334
S. Loden	*Stem*	<1060	<361	<360	<443	<13.3	<40.9	<30.2	<334
S. Wilhelm	*Stem*	<1060	<361	<360	<443	<13.3	<40.9	<30.2	<334
S. Wilhelm	*Stem*	<1060	<361	<360	<443	<13.3	<40.9	<30.2	<334
S. Wilhelm	*Stem*	<1060	<361	<360	<443	<13.3	<40.9	<30.2	<334

Table S6.2: PFAS concentration in pre-planting control plants continuing

Species	**Tissue type**	**B-PFHpA (ng/Kg)**	**NaDONA (ng/Kg)**	**L-PFHxS (ng/Kg)**	**B-PFHxS (ng/Kg)**	**L-PFOA (ng/Kg)**	**B-PFOA (ng/Kg)**	**6-2 FTSA (ng/Kg)**	**L-PFHpS (ng/Kg)**
C. sativa	*Root*	<10	<24	<35.8	<20.8	<209	<105	<154	<11.6
C. sativa	*Root*	<10	<24	<35.8	<20.8	<209	<105	<154	<11.6
C. sativa	*Root*	<10	<24	<35.8	<20.8	<209	<105	<154	<11.6
C. sativa	*Stem*	<10	<24	<35.8	<20.8	<209	<105	<154	<11.6
C. sativa	*Stem*	<10	<24	<35.8	<20.8	<209	<105	<154	<11.6
C. sativa	*Stem*	<10	<24	<35.8	<20.8	<209	<105	<154	<11.6
C. sativa	*Leaf*	744	<24	76.9	33.3	5690	471	<154	<11.6
C. sativa	*Leaf*	1330	<24	116	31.3	4410	184	<154	<11.6
C. sativa	*Leaf*	1050	<24	94.2	53.6	5210	388	<154	<11.6
C. elata	*Root*	<10	<24	<35.8	<20.8	<209	<105	<154	<11.6
C. elata	*Root*	<10	<24	<35.8	<20.8	<209	<105	<154	<11.6
C. elata	*Root*	<10	<24	<35.8	<20.8	<209	<105	<154	<11.6
C. elata	*Shoot*	<10	<24	<35.8	<20.8	<209	<105	<154	<11.6
C. elata	*Shoot*	<10	<24	<35.8	<20.8	<209	<105	<154	<11.6
C. elata	*Shoot*	<10	<24	<35.8	<20.8	<209	<105	<154	<11.6
S. Wilhelm	*Stem*	<10	<24	<35.8	<20.8	<209	<105	<154	<11.6
S. Wilhelm	*Stem*	<10	<24	<35.8	<20.8	<209	<105	<154	<11.6
S. Wilhelm	*Stem*	<10	<24	<35.8	<20.8	<209	<105	<154	<11.6
S. Loden	*Stem*	<10	<24	<35.8	<20.8	<209	<105	<154	<11.6
S. Loden	*Stem*	<10	<24	<35.8	<20.8	<209	<105	<154	<11.6
S. Loden	*Stem*	<10	<24	<35.8	<20.8	<209	<105	<154	<11.6
S. Wilhelm	*Stem*	<10	<24	<35.8	<20.8	<209	<105	<154	<11.6
S. Wilhelm	*Stem*	<10	<24	<35.8	<20.8	<209	<105	<154	<11.6
S. Wilhelm	*Stem*	<10	<24	<35.8	<20.8	<209	<105	<154	<11.6

Table S6.3: PFAS concentration in pre-planting control plants continuing

Species	Tissue type	B-PFHpS (ng/Kg)	PFECHS (ng/Kg)	L-PFNA (ng/Kg)	B-PFNA (ng/Kg)	FOSA (ng/Kg)	L-PFOS (ng/Kg)	B-PFOS (ng/Kg)	PFDA (ng/Kg)
C. sativa	*Root*	<10	<26.4	<368	<10	21.5	<180	<36.7	<246
C. sativa	*Root*	<10	<26.4	<368	<10	<21	<180	<36.7	<246
C. sativa	*Root*	<10	<26.4	<368	<10	<21	<180	<36.7	<246
C. sativa	*Stem*	<10	<26.4	<368	<10	<21	<180	<36.7	<246
C. sativa	*Stem*	<10	<26.4	<368	<10	<21	<180	<36.7	<246
C. sativa	*Stem*	<10	<26.4	<368	<10	<21	<180	<36.7	<246
C. sativa	*Leaf*	<10	<26.4	<368	<10	36.1	<180	<36.7	<246
C. sativa	*Leaf*	<10	<26.4	<368	<10	<21	<180	<36.7	<246
C. sativa	*Leaf*	<10	<26.4	<368	<10	<21	<180	<36.7	<246
C. elata	*Root*	<10	<26.4	<368	<10	<21	<180	<36.7	<246
C. elata	*Root*	<10	<26.4	<368	<10	<21	<180	<36.7	<246
C. elata	*Root*	<10	<26.4	<368	<10	<21	<180	<36.7	<246
C. elata	*Shoot*	<10	<26.4	<368	<10	33.8	<180	<36.7	<246
C. elata	*Shoot*	<10	<26.4	<368	<10	31	<180	<36.7	<246
C. elata	*Shoot*	<10	<26.4	<368	<10	<21	<180	<36.7	<246
S. Wilhelm	*Stem*	<10	<26.4	<368	<10	<21	<180	<36.7	<246
S. Wilhelm	*Stem*	<10	<26.4	<368	<10	<21	<180	<36.7	<246
S. Wilhelm	*Stem*	<10	<26.4	<368	<10	<21	<180	<36.7	<246
S. Loden	*Stem*	<10	<26.4	<368	<10	<21	<180	<36.7	<246
S. Loden	*Stem*	<10	<26.4	<368	<10	<21	<180	<36.7	<246
S. Loden	*Stem*	<10	<26.4	<368	<10	<21	<180	<36.7	<246
S. Wilhelm	*Stem*	<10	<26.4	<368	<10	<21	<180	<36.7	<246
S. Wilhelm	*Stem*	<10	<26.4	<368	<10	<21	<180	<36.7	<246
S. Wilhelm	*Stem*	<10	<26.4	<368	<10	<21	<180	<36.7	<246

Table S6.4: PFAS concentration in pre-planting control plants continuing

Species	Tissue type	8-2 FTSA (ng/Kg)	9Cl-PF3ONS (ng/Kg)	PFNS (ng/Kg)	PFUnDA (ng/Kg)	Me-FOSAA (ng/Kg)	Et-FOSAA (ng/Kg)	PFDS (ng/Kg)	PFDoDA (ng/Kg)
C. sativa	*Root*	<10.1	<20.9	<21.6	<122	<30	<29.2	<21.5	<41.7
C. sativa	*Root*	<10.1	<20.9	<21.6	<122	<30	<29.2	<21.5	<41.7
C. sativa	*Root*	<10.1	<20.9	<21.6	<122	<30	<29.2	<21.5	<41.7
C. sativa	*Stem*	<10.1	<20.9	<21.6	<122	<30	<29.2	<21.5	<41.7
C. sativa	*Stem*	<10.1	<20.9	<21.6	<122	<30	<29.2	<21.5	<41.7
C. sativa	*Stem*	<10.1	<20.9	<21.6	<122	<30	<29.2	<21.5	<41.7
C. sativa	*Leaf*	<10.1	<20.9	<21.6	<122	<30	<29.2	<21.5	<41.7
C. sativa	*Leaf*	<10.1	<20.9	<21.6	<122	<30	<29.2	<21.5	<41.7
C. sativa	*Leaf*	<10.1	<20.9	<21.6	<122	<30	<29.2	<21.5	<41.7
C. elata	*Root*	<10.1	<20.9	<21.6	<122	<30	<29.2	<21.5	<41.7
C. elata	*Root*	<10.1	<20.9	<21.6	<122	<30	<29.2	<21.5	<41.7
C. elata	*Root*	<10.1	<20.9	<21.6	<122	<30	<29.2	<21.5	<41.7

C. elata	*Shoot*	<10.1	<20.9	<21.6	<122	<30	<29.2	<21.5	<41.7
C. elata	*Shoot*	<10.1	<20.9	<21.6	<122	<30	<29.2	<21.5	<41.7
C. elata	*Shoot*	<10.1	<20.9	<21.6	<122	<30	<29.2	<21.5	<41.7
S. Wilhelm	*Stem*	<10.1	<20.9	<21.6	<122	<30	<29.2	<21.5	<41.7
S. Wilhelm	*Stem*	<10.1	<20.9	<21.6	<122	<30	<29.2	<21.5	<41.7
S. Wilhelm	*Stem*	<10.1	<20.9	<21.6	<122	<30	<29.2	<21.5	<41.7
S. Loden	*Stem*	<10.1	<20.9	<21.6	<122	<30	<29.2	<21.5	<41.7
S. Loden	*Stem*	<10.1	<20.9	<21.6	<122	<30	<29.2	<21.5	<41.7
S. Loden	*Stem*	<10.1	<20.9	<21.6	<122	<30	<29.2	<21.5	<41.7
S. Wilhelm	*Stem*	<10.1	<20.9	<21.6	<122	<30	<29.2	<21.5	<41.7
S. Wilhelm	*Stem*	<10.1	<20.9	<21.6	<122	<30	<29.2	<21.5	<41.7
S. Wilhelm	*Stem*	<10.1	<20.9	<21.6	<122	<30	<29.2	<21.5	<41.7

Table S6.5 PFAS concentration in pre-planting control plants continuing

Species	**Tissue type**	**11Cl-PF3OUdS (ng/Kg)**	**PFTriDA (ng/Kg)**	**PFTeDA (ng/Kg)**
C. sativa	*Root*	<26.9	<23700	<58700
C. sativa	*Root*	<26.9	<23700	<58700
C. sativa	*Root*	<26.9	<23700	<58700
C. sativa	*Stem*	<26.9	<23700	<58700
C. sativa	*Stem*	<26.9	<23700	<58700
C. sativa	*Stem*	<26.9	<23700	<58700
C. sativa	*Leaf*	<26.9	<23700	<58700
C. sativa	*Leaf*	<26.9	<23700	<58700
C. sativa	*Leaf*	<26.9	<23700	<58700
C. elata	*Root*	<26.9	<23700	<58700
C. elata	*Root*	<26.9	<23700	<58700
C. elata	*Root*	<26.9	<23700	<58700
C. elata	*Shoot*	<26.9	<23700	<58700
C. elata	*Shoot*	<26.9	<23700	<58700
C. elata	*Shoot*	<26.9	<23700	<58700
S. Wilhelm	*Stem*	<26.9	<23700	<58700
S. Wilhelm	*Stem*	<26.9	<23700	<58700
S. Wilhelm	*Stem*	<26.9	<23700	<58700
S. Loden	*Stem*	<26.9	<23700	<58700
S. Loden	*Stem*	<26.9	<23700	<58700
S. Loden	*Stem*	<26.9	<23700	<58700
S. Wilhelm	*Stem*	<26.9	<23700	<58700
S. Wilhelm	*Stem*	<26.9	<23700	<58700
S. Wilhelm	*Stem*	<26.9	<23700	<58700

Table S7: PFAS concentration in control filter substrate

PFAS	LECA (ng/Kg)	Peat and biochar mix (ng/Kg)
PFBA	<216	<216
PFPeA	<158	<158
PFBS	<345	<345
PFHxA	<567	<567
4-2 FTSA	<68.8	<68.8
HFPO-DA	<126	<126
PFPeS	<37.7	<37.7
PFHpA	<269	<269
NaDONA	<24	<24
PFHxS	<32.6	<32.6
PFOA	<455	<455
6-2 FTSA	7080	10100
PFHpS	<21.9	<21.9
PFECHS	<28.1	<28.1
PFNA	<64.2	<64.2
FOSA	<1.49	<1.49
PFOS	<142	<142
PFDA	<39.3	51.3
8-2 FTSA	<14.2	<14.2
9Cl-PF3ONS	<69.6	<69.6
PFNS	<21.6	<21.6
PFUnDA	101	<24.3
Me-FOSAA	<37.8	<37.8
Et-FOSAA	<21.6	<21.6
PFDS	<21.1	<21.1
PFDoDA	<12.8	21.9
11Cl-PF3OUdS	<38.1	<38.1
PFTriDA	<18.7	<18.7
PFTeDA	<309	<309

Equation S1: The mass balance recovery of the system

$$Recovery = \frac{C_{Plants} * M_{Plants} + C_{LECA} * M_{LECA} + C_{Peat\ and\ biochar} * M_{Peat\ and\ biochar} + C_{Effluent} * V_{Water}}{C_{Inlet} * V_{Water}}$$

Table S8: A mass balance depicting the total recovery of PFAS for each of the wetland units. PFAS in plant biomass, filter substrate, inlet, and effluent to the units have been taken into account. Losses through evaporation and evapotranspiration are assumed to be negligible due to the high flow rate, and effluent volume is thus assumed to be equal to inlet volume.

PFAS	***Salix spp* A (%)**	***Salix spp* B (%)**	***C. elata* A (%)**	***C. elata* B (%)**	***S. sativa* A (%)**	***S. sativa* B (%)**	**Control A (%)**	**Control B (%)**
PFBA	105	103	102	106	100	99.1	100	88.5
PFPeA	104	103	100	102	101	98.9	97.7	90.3
PFBS	102	95.8	90	92.6	95.1	94.3	96.3	79.6
PFHxA	97	92.8	94.2	89.4	102	96.3	91.8	90.8
4-2FTSA	0	0	0	0	0	93	63.1	0
HFPO-DA	N/A	N/A	N/A	N/A	N/A	N/A	N/A	N/A
PFPeS	92.1	90.8	91.7	84.3	90.9	93	86.7	88.1
L-PFHpA	92.7	90.8	92.1	80.8	95	91.5	89.3	91.1
B-PFHpA	104	96.1	87.2	81.3	77.3	90.9	80.6	88.3
NaDONA	N/A	N/A	N/A	N/A	N/A	N/A	N/A	N/A
L-PFHxS	92	79.6	91.7	77.1	84.7	88.6	89.1	85.7
B-PFHxS	88	85.1	84.5	84.7	72.1	89.2	87.3	75
L-PFOA	80.6	80.4	85.9	80	80.9	86.1	90	90
B-PFOA	80.2	83.2	80.8	85.8	75.4	80.4	85.2	89.3
6-2 FTSA	33.7	15.3	37.7	29.7	35.7	47.6	54.3	27.9
L-PFHpS	66.7	55.6	76.5	59.8	65	72.8	74.4	74.3
B-PFHpS	84.2	75.1	84.4	71.7	76.4	85.5	81.8	78
PFECHS	77.7	80.8	82.8	80	76.5	83.5	78.7	86
L-PFNA	56.9	51.4	67.5	57.4	56.5	58.3	76.3	67
B-PFNA	78	77	85.9	61.2	55.4	65	72	84.5
FOSA	N/A	N/A	N/A	N/A	N/A	N/A	N/A	N/A
L-PFOS	27	24.4	52.5	31.6	39.6	42.1	49	54.4
B-PFOS	64	61.5	84.7	60.2	63.7	71.9	80.4	84.5
PFDA	N/A	N/A	N/A	N/A	N/A	N/A	N/A	N/A
8-2 FTSA	N/A	N/A	N/A	N/A	N/A	N/A	N/A	N/A
9Cl-PF3ONS	N/A	N/A	N/A	N/A	N/A	N/A	N/A	N/A
PFNS	N/A	N/A	N/A	N/A	N/A	N/A	N/A	N/A
PFUnDA	N/A	N/A	N/A	N/A	N/A	N/A	N/A	N/A
Me-FOSAA	N/A	N/A	N/A	N/A	N/A	N/A	N/A	N/A
Et-FOSAA	1.85	15.7	28.9	6.54	90.7	6.64	4.59	36.1
PFDS	N/A	N/A	N/A	N/A	N/A	N/A	N/A	N/A
PFDoDA	N/A	N/A	N/A	N/A	N/A	N/A	N/A	N/A
11Cl-PF3OUdS	N/A	N/A	N/A	N/A	N/A	N/A	N/A	N/A
PFTriDA	N/A	N/A	N/A	N/A	N/A	N/A	N/A	N/A
PFTeDA	N/A	N/A	N/A	N/A	N/A	N/A	N/A	N/A
Σ PFAS	88.4	85.5	89.4	83.9	87.6	88.7	89.3	87.2

Table S9: Mass balance showing the % of applied PFAS found in effluent water.

PFAS	*Salix spp* A (%)	*Salix spp* B (%)	*C. elata* A (%)	*C. elata* B (%)	*S. sativa* A (%)	*S. sativa* B (%)	Control A (%)	Control B (%)
PFBA	104	102	101	105	98.8	98.2	99.6	87.8
PFPeA	103	102	99.7	102	100	98.4	97.3	89.8
PFBS	101	95	88.1	91.9	94.4	93.9	94.4	77.7
PFHxA	96.7	92.2	93.7	89	101	95.7	91.4	90.4
4-2FTSA	0	0	0	0	0	93	63.1	0
HFPO-DA	N/A	N/A	N/A	N/A	N/A	N/A	N/A	N/A
PFPeS	90.4	88.8	89.2	81.8	88.3	90.9	84.8	85.5
L-PFHpA	92.2	89.9	91.3	80	94.2	90.8	88.6	90.5
B-PFHpA	104	96.1	87.2	81.3	77.2	90.9	80.6	88.3
NaDONA	N/A	N/A	N/A	N/A	N/A	N/A	N/A	N/A
L-PFHxS	89.3	75.8	87.4	73	80.9	85.5	85.6	81.2
B-PFHxS	86.3	82.7	82.9	82.6	70.3	87.1	85.7	72.2
L-PFOA	78.3	76.7	82.1	76.3	77.2	82.6	85.9	84
B-PFOA	79.9	82.4	80.2	85.1	74.7	79.7	84.8	88.8
6-2 FTSA	33.5	15.1	37.6	29.7	35.5	47.5	54.3	27.7
L-PFHpS	63.6	47.8	65.4	54.4	57.2	67.2	67.3	60.5
B-PFHpS	83.3	72.1	81.1	69.6	74	84.6	79.6	74.5
PFECHS	75.3	76.6	77.3	75.5	72.6	79.4	73.9	78.8
L-PFNA	54.5	45.5	60.4	53	50.6	54.9	73	58
B-PFNA	77	73	81.7	58.6	53.5	64.1	69.9	80.6
FOSA	N/A	N/A	N/A	N/A	N/A	N/A	N/A	N/A
L-PFOS	22.8	12.2	29.7	23.9	25	29.8	41.5	26.6
B-PFOS	58.6	49.2	65	52.1	52.9	61	70.9	57.4
PFDA	N/A	N/A	N/A	N/A	N/A	N/A	N/A	N/A
8-2 FTSA	N/A	N/A	N/A	N/A	N/A	N/A	N/A	N/A
9Cl-PF3ONS	N/A	N/A	N/A	N/A	N/A	N/A	N/A	N/A
PFNS	N/A	N/A	N/A	N/A	N/A	N/A	N/A	N/A
PFUnDA	N/A	N/A	N/A	N/A	N/A	N/A	N/A	N/A
Me-FOSAA	N/A	N/A	N/A	N/A	N/A	N/A	N/A	N/A
Et-FOSAA	0	0	0	0	71.3	0	0	0
PFDS	N/A	N/A	N/A	N/A	N/A	N/A	N/A	N/A
PFDoDA	N/A	N/A	N/A	N/A	N/A	N/A	N/A	N/A
11Cl-PF3OUdS	N/A	N/A	N/A	N/A	N/A	N/A	N/A	N/A
PFTriDA	N/A	N/A	N/A	N/A	N/A	N/A	N/A	N/A
PFTeDA	N/A	N/A	N/A	N/A	N/A	N/A	N/A	N/A
Σ PFAS	86.9	82.9	86.1	81.5	84.9	86.4	87	82.9

Table S10: Mass balance showing the % of applied PFAS found in plant biomass.

PFAS	*Salix spp* A (%)	*Salix spp* B (%)	*C. elata* A (%)	*C. elata* B (%)	*S. sativa* A (%)	*S. sativa* B (%)	Control A (%)	Control B (%)
PFBA	0.137	0.253	0.163	0.163	0.468	0.0585	0	0
PFPeA	0.326	0.0732	0.0249	0.0249	0.219	0.0274	0	0
PFBS	0.0356	0.0656	0.00358	0.00358	0.155	0.0194	0	0
PFHxA	0.0185	0.0213	0.00813	0.00813	0.113	0.0141	0	0
4-2FTSA	0	0	0	0	0	0	0	0
HFPO-DA	N/A	N/A	N/A	N/A	N/A	N/A	N/A	N/A
PFPeS	0.0376	0.0503	0.0126	0.0126	0.164	0.0204	0	0
L-PFHpA	0.0188	0.00985	0.0043	0.0043	0.116	0.0145	0	0
B-PFHpA	0	0	0	0	0.0577	0.00721	0	0
NaDONA	N/A	N/A	N/A	N/A	N/A	N/A	N/A	N/A
L-PFHxS	0.0411	0.0507	0.0285	0.0285	0.12	0.015	0	0
B-PFHxS	0.0246	0.0282	0.0162	0.0162	0.0987	0.0123	0	0
L-PFOA	0.04	0.0272	0.0222	0.0222	0.2	0.0249	0	0
B-PFOA	0.0255	0.00817	0.0037	0.0037	0.0136	0.0017	0	0
6-2 FTSA	0	0	0	0	0	0	0	0
L-PFHpS	0.038	0.0403	0.0538	0.0538	0.0375	0.00469	0	0
B-PFHpS	0.0143	0.0216	0.0208	0.0208	0.00693	0.000867	0	0
PFECHS	0.0295	0.0478	0.0184	0.0184	0.0214	0.00267	0	0
L-PFNA	0	0	0	0	0	0	0	0
B-PFNA	0	0	0.0528	0.0528	0.00424	0.00053	0	0
FOSA	N/A	N/A	N/A	N/A	N/A	N/A	N/A	N/A
L-PFOS	0.0529	0.0315	0.0876	0.0876	0.11	0.0138	0	0
B-PFOS	0.0422	0.0515	0.052	0.052	0.0424	0.0053	0	0
PFDA	N/A	N/A	N/A	N/A	N/A	N/A	N/A	N/A
8-2 FTSA	N/A	N/A	N/A	N/A	N/A	N/A	N/A	N/A
9Cl-PF3ONS	N/A	N/A	N/A	N/A	N/A	N/A	N/A	N/A
PFNS	N/A	N/A	N/A	N/A	N/A	N/A	N/A	N/A
PFUnDA	N/A	N/A	N/A	N/A	N/A	N/A	N/A	N/A
Me-FOSAA	N/A	N/A	N/A	N/A	N/A	N/A	N/A	N/A
Et-FOSAA	0	0	0	0	0	0	0	0
PFDS	N/A	N/A	N/A	N/A	N/A	N/A	N/A	N/A
PFDoDA	N/A	N/A	N/A	N/A	N/A	N/A	N/A	N/A
11Cl-PF3OUdS	N/A	N/A	N/A	N/A	N/A	N/A	N/A	N/A
PFTriDA	N/A	N/A	N/A	N/A	N/A	N/A	N/A	N/A
PFTeDA	N/A	N/A	N/A	N/A	N/A	N/A	N/A	N/A
Σ PFAS	0.0474	0.0482	0.0287	0.0287	0.161	0.0202	0	0

Table S11: Mass balance showing the % of applied PFAS found in the filter substrate.

PFAS	*Salix spp* A (%)	*Salix spp* B (%)	*C. elata* A (%)	*C. elata* B (%)	*S. sativa* A (%)	*S. sativa* B (%)	Control A (%)	Control B (%)
PFBA	0.622	0.887	0.929	1	0.921	0.847	0.623	0.706
PFPeA	0.449	0.531	0.56	0.574	0.58	0.524	0.392	0.478
PFBS	0.462	0.788	2.15	0.73	0.584	0.437	1.9	1.93
PFHxA	0.322	0.616	0.492	0.438	0.634	0.5	0.377	0.414
4-2FTSA	0	0	0	0	0	0	0	0
HFPO-DA	N/A	N/A	N/A	N/A	N/A	N/A	N/A	N/A
PFPeS	1.67	1.92	2.43	2.49	2.41	1.96	1.92	2.64
L-PFHpA	0.46	0.834	0.718	0.771	0.777	0.65	0.69	0.58
B-PFHpA	0.0827	0	0	0	0	0	0	0
NaDONA	N/A	N/A	N/A	N/A	N/A	N/A	N/A	N/A
L-PFHxS	2.65	3.72	4.28	4.07	3.69	3.09	3.51	4.46
B-PFHxS	1.59	2.31	1.59	2.07	1.72	2.18	1.54	2.78
L-PFOA	2.29	3.71	3.81	3.74	3.49	3.49	4.09	6.07
B-PFOA	0.143	0.766	0.589	0.705	0.634	0.629	0.407	0.5
6-2 FTSA	0.0897	0.194	0	0	0.206	0	0	0.165
L-PFHpS	3.07	7.72	11	5.35	7.81	5.52	7.11	13.8
B-PFHpS	0.692	2.97	3.23	2.05	2.33	0.873	2.24	3.53
PFECHS	2.33	4.18	5.51	3.44	3.88	4.17	4.75	7.35
L-PFNA	2.34	5.91	7.05	4.4	6	3.42	3.38	9.15
B-PFNA	0.792	3.94	4.17	2.64	1.84	0	2.11	3.9
FOSA	N/A	N/A	N/A	N/A	N/A	N/A	N/A	N/A
L-PFOS	4.13	12.2	22.7	7.67	14.5	12.3	7.46	27.7
B-PFOS	5.13	12.3	19.6	8.1	10.8	11	9.57	27
PFDA	N/A	N/A	N/A	N/A	N/A	N/A	N/A	N/A
8-2 FTSA	N/A	N/A	N/A	N/A	N/A	N/A	N/A	N/A
9Cl-PF3ONS	N/A	N/A	N/A	N/A	N/A	N/A	N/A	N/A
PFNS	N/A	N/A	N/A	N/A	N/A	N/A	N/A	N/A
PFUnDA	N/A	N/A	N/A	N/A	N/A	N/A	N/A	N/A
Me-FOSAA	N/A	N/A	N/A	N/A	N/A	N/A	N/A	N/A
Et-FOSAA	0.998	15.7	28.8	6.57	19.5	6.64	4.63	35.9
PFDS	N/A	N/A	N/A	N/A	N/A	N/A	N/A	N/A
PFDoDA	N/A	N/A	N/A	N/A	N/A	N/A	N/A	N/A
11Cl-PF3OUdS	N/A	N/A	N/A	N/A	N/A	N/A	N/A	N/A
PFTriDA	N/A	N/A	N/A	N/A	N/A	N/A	N/A	N/A
PFTeDA	N/A	N/A	N/A	N/A	N/A	N/A	N/A	N/A
Σ PFAS	1.42	2.56	3.29	2.29	2.54	2.33	2.36	4.23

Equation S2.1-2.4: the phytoremediation potentials of the different plant species

S2.1: Phytoremediation potential of *C. elata* = PFAS concentration leaf * Biomass yield/ha yr

S2.2: Phytoremediation potential of *C. Sativa* = ((PFAS concentration leaf * average weight of leaf + PFAS concentration stem * average weight of stem) / average weight of plant) *Biomass yield/ha yr

S2.3: Phytoremediation potential of S. Loden = ((PFAS concentration leaf * average weight of leaf + PFAS concentration twig * average weight twig + PFAS concentration stem * average weight of stem) / average weight of plant) * ((Biomass yield / ha yr * (experimental biomass yield of S. Loden / experimental biomass yield of S. Wilhelm))

S2.4: Phytoremediation potential S. Wilhelm = ((PFAS concentration leaf * average weight of leaf + PFAS concentration twig * average weight twig + PFAS concentration stem * average weight of stem) / average weight of plant) * ((Biomass yield / ha yr * (experimental biomass yield of S. Wilhelm / experimental biomass yield of S. Loden))

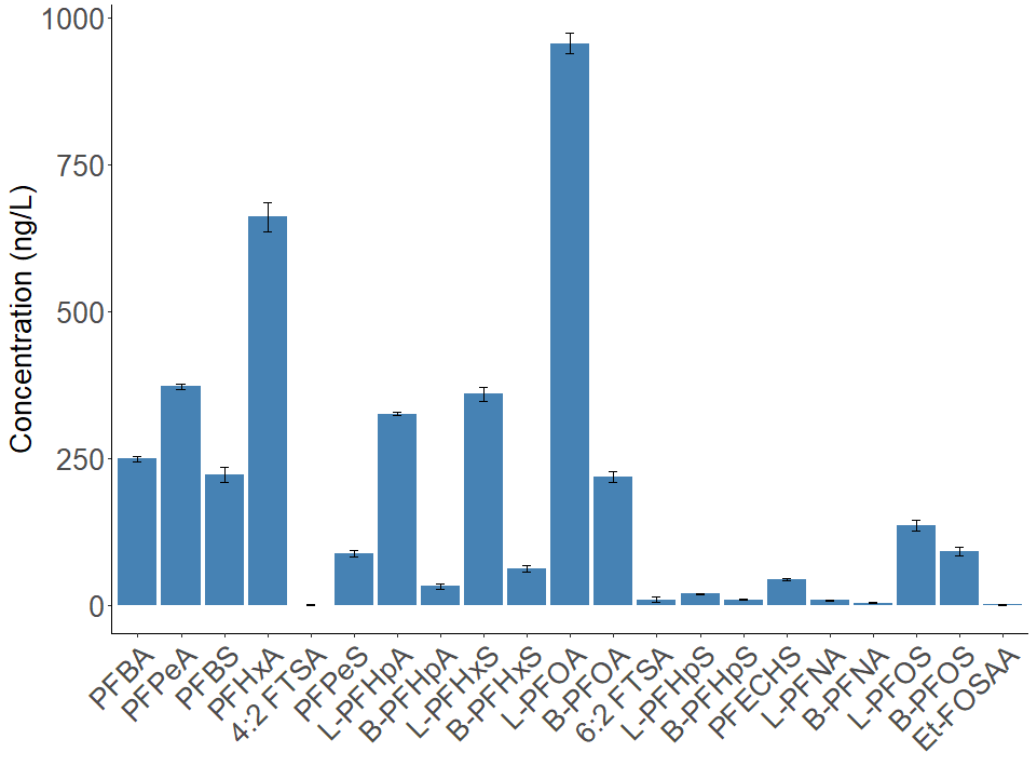

Figure S1: The PFAS concentrations of the wetland units inlet water (n=3).

Table S12.1: PFAS concentrations in water samples

Unit	Sample date (yy/mm/dd)	PFBA (ng/L)	PFPeA (ng/L)	PFBS (ng/L)	PFHxA (ng/L)	4-2FTSA (ng/L)	HFPO-DA (ng/L)	PFPeS (ng/L)	L-PFHpA (ng/L)
Inflow	*220705*	251	382	245	649	0.778	<0.471	99.3	331
Inflow	*220804*	254	371	218	708	<0.405	<0.471	85.4	324
Inflow	*220907*	241	366	202	625	<0.405	<0.471	78.8	321
Control A	*220708*	273	360	225	588	<0.405	<0.471	77.5	285
Control A	*220708*	254	360	221	584	0.78	<0.471	87.1	277
Control A	*220804*	246	381	213	650	<0.405	<0.471	73.2	306
Control A	*220907*	224	331	193	586	<0.405	<0.471	69.8	263
Control B	*220705*	211	322	149	587	<0.405	<0.471	65.3	304
Control B	*220804*	239	356	217	645	<0.405	<0.471	88.6	296
Control B	*220804*	246	382	200	669	<0.405	<0.471	88.4	299
Control B	*220907*	180	281	158	518	<0.405	<0.471	75.9	268
Salix spp A	*220705*	279	365	226	590	<0.405	<0.471	91.4	285
Salix spp A	*220804*	256	414	239	741	<0.405	<0.471	76.1	322
Salix spp A	*220907*	232	372	211	546	<0.405	<0.471	70.3	284
Salix spp B	*220705*	252	364	220	600	<0.405	<0.471	77.6	280
Salix spp B	*220804*	254	401	210	639	<0.405	<0.471	80	301
Salix spp B	*220907*	264	382	220	612	<0.405	<0.471	86.7	311
C. elata A	*220705*	277	359	185	577	<0.405	<0.471	82.2	274
C. elata A	*220804*	245	406	213	693	<0.405	<0.471	81.2	326
C. elata A	*220907*	218	316	200	587	<0.405	<0.471	73.4	283
C. elata B	*220705*	244	364	223	575	<0.405	<0.471	83.3	278
C. elata B	*220804*	275	402	186	598	<0.405	<0.471	62.7	237
C. elata B	*220907*	280	362	232	656	<0.405	<0.471	79.5	285
C. sativa A	*220705*	241	372	198	709	<0.405	<0.471	80.8	315
C. sativa A	*220804*	253	379	224	668	<0.405	<0.471	78.5	314
C. sativa A	*220907*	253	370	229	642	<0.405	<0.471	79.2	269
C. sativa B	*220705*	234	363	201	585	0.723	<0.471	90.7	274
C. sativa B	*220804*	257	377	232	692	<0.405	<0.471	75.8	312
C. sativa B	*220907*	249	358	189	656	<0.405	<0.471	75.8	313

Table S12.2: PFAS concentration in water continuing

Unit	Sample date (yy/mm /dd)	B-PFHpA (ng/L)	NaDONA (ng/L)	L-PFHxS (ng/L)	B-PFHxS (ng/L)	L-PFOA (ng/L)	B-PFOA (ng/L)	6-2 FTSA (ng/L)	L-PFHpS (ng/L)
Inflow	*220705*	23.2	<0.905	381	73.3	973	204	16.3	20.8
Inflow	*220804*	32.8	<0.905	359	52.9	974	237	11.9	20.1
Inflow	*220907*	40.1	<0.905	339	59.1	922	213	<0.593	16.3
Control A	*220708*	18.5	<0.905	287	55.8	724	153	7.73	12.3
Control A	*220708*	25	<0.905	320	64.1	798	160	8.16	11.9
Control A	*220804*	27.7	<0.905	327	49.7	913	214	6.1	14.4
Control A	*220907*	20.8	<0.905	292	46.1	773	190	3.51	13.4
Control B	*220705*	21.7	13.1	248	40.1	812	174	5.29	8.07
Control B	*220804*	30.7	<0.905	317	44.4	804	216	2.41	14.5
Control B	*220804*	28.8	<0.905	346	52.4	846	210	2.16	16.4
Control B	*220907*	30	<0.905	326	48.1	766	202	0.821	12.6
Salix spp A	*220705*	25.5	<0.905	326	57.5	660	138	7.39	9.97
Salix spp A	*220804*	38.9	<0.905	336	52.4	863	202	2.19	14.4
Salix spp A	*220907*	24.4	<0.905	297	47.3	708	200	<0.593	14.5
Salix spp B	*220705*	22.8	<0.905	258	52.5	740	154	4.36	7.21
Salix spp B	*220804*	30.5	<0.905	282	48.9	751	200	<0.593	10.3
Salix spp B	*220907*	40.1	<0.905	311	56.2	713	200	<0.593	13.1
C. elata A	*220705*	22.8	<0.905	289	51.1	684	144	6.63	9.59
C. elata A	*220804*	30.7	<0.905	349	54.6	887	196	3.43	15.2
C. elata A	*220907*	22.3	<0.905	315	44.3	814	207	1.64	15.6

C. elata B	*220705*	23.5	<0.905	318	61.8	842	198	8.59	15.1
C. elata B	*220804*	20.1	<0.905	218	40.4	636	175	<0.593	6.95
C. elata B	*220907*	39.1	<0.905	265	55.2	739	192	<0.593	9.94
C. sativa A	*220705*	20.1	<0.905	246	32.2	664	137	4.55	6.04
C. ativa A	*220804*	22.6	<0.905	342	51.8	833	183	5.4	16.2
C. sativa A	*220907*	32.9	<0.905	295	51.7	716	184	<0.593	11.5
C. sativa B	*220705*	23.5	<0.905	286	57.8	744	142	8.83	11.7
C. ativa B	*220804*	29.8	<0.905	341	50.6	851	200	4.65	14.9
C. sativa B	*220907*	29.8	<0.905	299	54.6	788	195	<0.593	12.9

Table S12.3: PFAS concentration in water continuing

Unit	Sample date (yy/mm/dd)	B-PFHpS (ng/L)	PFECHS (ng/L)	L-PFNA (ng/L)	B-PFNA (ng/L)	FOSA (ng/L)	L-PFOS (ng/L)	B-PFOS (ng/L)	PFDA (ng/L)
Inflow	*220705*	9.66	47.3	8.31	4.27	<0.704	138	101	<1.45
Inflow	*220804*	10.2	41.1	9.94	4.5	<0.704	150	97.3	<1.45
Inflow	*220907*	8.55	42.1	6.7	1.25	<0.704	118	76.8	<1.45
Control A	*220708*	6.64	30.9	4.68	2.23	<0.704	52.5	63.1	<1.45
Control A	*220708*	6.37	31.3	4.39	2.37	<0.704	49.9	59.8	<1.45
Control A	*220804*	8.74	34.1	7.78	3.09	<0.704	64.4	73.6	<1.45
Control A	*220907*	8.19	30.9	7.48	2.89	<0.704	58.4	68.5	<1.45
Control B	*220705*	5.06	31.9	4.17	2.9	<0.704	22.7	40.1	1.73
Control B	*220804*	8.81	36	5	3.48	<0.704	44.4	60.5	<1.45
Control B	*220804*	9.01	40	7.11	3.31	<0.704	47.5	67.4	<1.45
Control B	*220907*	8.35	31.6	4.82	3.13	<0.704	50.8	68.9	<1.45
Salix spp A	*220705*	5.77	28.6	3.51	2.09	<0.704	23.1	43.2	<1.45
Salix spp A	*220804*	9.93	36.1	6.16	3.7	<0.704	38.2	62.1	<1.45
Salix spp A	*220907*	9.15	35.9	4.31	3.53	<0.704	37.7	73.7	<1.45
Salix spp B	*220705*	4.9	29.7	4.07	3.02	<0.704	14.3	38.1	<1.45
Salix spp B	*220804*	8.07	33.5	4.25	3.09	<0.704	16.7	46.4	<1.45
Salix spp B	*220907*	9.68	44.2	3.04	1.74	<0.704	25.4	73.2	<1.45
C. elata A	*220705*	5.55	28.5	3.36	2.27	<0.704	30.7	47.7	<1.45
C. elata A	*220804*	9.54	37.6	6.76	3.88	<0.704	48.9	71.1	<1.45
C. elata A	*220907*	9.45	37.5	6.35	3.72	<0.704	49.7	76.1	<1.45
C. elata B	*220705*	8.23	43.1	4.51	3.08	<0.704	39.1	66.7	<1.45
C. elata B	*220804*	5.22	23.2	5.42	1.79	<0.704	30.8	33.8	<1.45
C. elata B	*220907*	7.27	34.4	2.82	1.57	<0.704	25.8	50.5	<1.45
C. sativa A	*220705*	4	24.6	2.55	1.07	<0.704	14.4	30.1	1.53
C. ativa A	*220804*	10	37.6	6.73	3.18	<0.704	54	69.9	<1.45
C. sativa A	*220907*	7.67	34.4	2.95	1.74	<0.704	36.2	50.9	<1.45
C. sativa B	*220705*	7.19	31	3.71	2.34	<0.704	34.6	51.7	<1.45
C. ativa B	*220804*	9.09	37	5.86	3.17	<0.704	48.3	63.2	<1.45
C. sativa B	*220907*	8.56	38.6	4.83	1.05	<0.704	42.2	62.5	<1.45

Table S12.4: PFAS concentration in water continuing

Unit	Sample date (yy/mm/dd)	8-2 FTSA (ng/L)	9Cl-PF3ONS (ng/L)	PFNS (ng/L)	PFUnDA (ng/L)	Me-FOSAA (ng/L)	Et-FOSAA (ng/L)	PFDS (ng/L)	PFDoDA (ng/L)
Inflow	*220705*	<0.488	<0.0287	<0.131	<1.34	<0.243	1.05	<0.184	<1.15
Inflow	*220804*	<0.488	<0.0287	<0.131	<1.34	<0.243	1.1	<0.184	<1.15
Inflow	*220907*	<0.488	<0.0287	<0.131	<1.34	<0.243	<0.34	<0.184	<1.15

Control A	*22070 8*	<0.488	<0.0287	<0.131	<1.34	<0.243	<0.34	<0.184	<1.15
Control A	*22070 8*	<0.488	<0.0287	<0.131	<1.34	<0.243	<0.34	<0.184	<1.15
Control A	*22080 4*	<0.488	<0.0287	<0.131	<1.34	<0.243	<0.34	<0.184	<1.15
Control A	*22090 7*	<0.488	<0.0287	<0.131	<1.34	<0.243	<0.34	<0.184	<1.15
Control B	*22070 5*	<0.488	<0.0287	<0.131	<1.34	<0.243	<0.34	<0.184	<1.15
Control B	*22080 4*	<0.488	<0.0287	<0.131	<1.34	<0.243	<0.34	<0.184	<1.15
Control B	*22080 4*	<0.488	<0.0287	<0.131	<1.34	<0.243	<0.34	<0.184	<1.15
Control B	*22090 7*	<0.488	<0.0287	<0.131	<1.34	<0.243	<0.34	<0.184	<1.15
Salix spp A	*22070 5*	<0.488	<0.0287	<0.131	<1.34	<0.243	<0.34	<0.184	<1.15
Salix spp A	*22080 4*	<0.488	<0.0287	<0.131	<1.34	<0.243	<0.34	<0.184	<1.15
Salix spp A	*22090 7*	<0.488	<0.0287	<0.131	<1.34	<0.243	<0.34	<0.184	<1.15
Salix spp B	*22070 5*	<0.488	<0.0287	<0.131	<1.34	<0.243	<0.34	<0.184	<1.15
Salix spp B	*22080 4*	<0.488	<0.0287	<0.131	<1.34	<0.243	<0.34	<0.184	<1.15
Salix spp B	*22090 7*	<0.488	<0.0287	<0.131	<1.34	<0.243	<0.34	<0.184	<1.15
C. elata A	*22070 5*	<0.488	<0.0287	<0.131	<1.34	<0.243	<0.34	<0.184	<1.15
C. elata A	*22080 4*	<0.488	<0.0287	<0.131	<1.34	<0.243	<0.34	<0.184	<1.15
C. elata A	*22090 7*	<0.488	<0.0287	<0.131	<1.34	<0.243	<0.34	<0.184	<1.15
C. elata B	*22070 5*	<0.488	<0.0287	<0.131	<1.34	<0.243	<0.34	<0.184	<1.15
C. elata B	*22080 4*	<0.488	<0.0287	<0.131	<1.34	<0.243	<0.34	<0.184	<1.15
C. elata B	*22090 7*	<0.488	<0.0287	<0.131	<1.34	<0.243	<0.34	<0.184	<1.15
C. sativa A	*22070 5*	<0.488	<0.0287	<0.131	<1.34	<0.243	<0.34	<0.184	<1.15
C. ativa A	*22080 4*	<0.488	<0.0287	<0.131	<1.34	<0.243	1.48	<0.184	<1.15
C. sativa A	*22090 7*	<0.488	<0.0287	<0.131	<1.34	<0.243	<0.34	<0.184	<1.15
C. sativa B	*22070 5*	<0.488	<0.0287	<0.131	<1.34	<0.243	<0.34	<0.184	<1.15
C. ativa B	*22080 4*	<0.488	<0.0287	<0.131	<1.34	<0.243	<0.34	<0.184	<1.15
C. sativa B	*22090 7*	<0.488	<0.0287	<0.131	<1.34	<0.243	<0.34	<0.184	<1.15

Table S12.5: PFAS concentration in water continuing

Unit	Sample date (yy/mm/dd)	11Cl-PF3OUdS (ng/L)	PFTriDA (ng/L)	PFTeDA (ng/L)
Inflow	*220705*	<0.406	<1.84	<7.04
Inflow	*220804*	<0.406	<1.84	<7.04
Inflow	*220907*	<0.406	<1.84	<7.04
Control A	*220708*	<0.406	<1.84	<7.04
Control A	*220708*	<0.406	<1.84	<7.04
Control A	*220804*	<0.406	<1.84	<7.04
Control A	*220907*	<0.406	<1.84	<7.04
Control B	*220705*	<0.406	<1.84	<7.04
Control B	*220804*	<0.406	<1.84	<7.04
Control B	*220804*	<0.406	<1.84	<7.04
Control B	*220907*	<0.406	<1.84	<7.04
Salix spp A	*220705*	<0.406	<1.84	<7.04
Salix spp A	*220804*	<0.406	<1.84	<7.04
Salix spp A	*220907*	<0.406	<1.84	<7.04
Salix spp B	*220705*	<0.406	<1.84	<7.04
Salix spp B	*220804*	<0.406	<1.84	<7.04
Salix spp B	*220907*	<0.406	<1.84	<7.04
C. elata A	*220705*	<0.406	<1.84	<7.04
C. elata A	*220804*	<0.406	<1.84	<7.04
C. elata A	*220907*	<0.406	<1.84	<7.04
C. elata B	*220705*	<0.406	<1.84	<7.04
C. elata B	*220804*	<0.406	<1.84	<7.04
C. elata B	*220907*	<0.406	<1.84	<7.04
C. sativa A	*220705*	<0.406	<1.84	<7.04
C. ativa A	*220804*	<0.406	<1.84	<7.04
C. sativa A	*220907*	<0.406	<1.84	<7.04
C. sativa B	*220705*	<0.406	<1.84	<7.04
C. ativa B	*220804*	<0.406	<1.84	<7.04
C. sativa B	*220907*	<0.406	<1.84	<7.04

Table S13: Removal efficiency of the different wetland units (n=6) given in % ± the standard error.

PFAS	***Salix spp***	***C. elata***	***C. sativa***	**Control**
PFBA	-3 ± 2.4	-3.2 ± 3.5	0.34 ± 4.5	8.5 ± 3.0
PFPeA	-2.8 ± 2.7	1.2 ± 2.7	0.77 ± 4.0	8.6 ± 4.3
PFBS	-0.11 ± 3.5	6.1 ± 4.1	3.6 ± 6.5	14 ± 5.3
PFHxA	6.1 ± 2.6	6.9 ± 2.8	0.17 ± 3.1	9.7 ± 2.9
PFPeS	8 ± 4.2	12 ± 3.6	8.3 ± 5.3	13 ± 1.9
L-PFHpA	8.7 ± 2.4	14 ± 2.9	8 ± 2.5	12 ± 3.1
B-PFHpA	3.3 ± 8.1	15 ± 8.4	16 ± 4.4	19 ± 10.8
L-PFHxS	16 ± 3.9	19 ± 4.3	16 ± 5.1	15 ± 3.4
B-PFHxS	14 ± 4.4	16 ± 8.3	17 ± 6.1	20 ± 6.1

L-PFOA	23 ± 2.7	20 ± 3.9	20 ± 1.5	15 ± 3.7
B-PFOA	17 ± 4.2	15 ± 3.6	21 ± 3.6	12 ± 4.3
L-PFHpS	37 ± 8.6	36 ± 6.8	35 ± 6.6	32 ± 7.9
B-PFHpS	15 ± 10	19 ± 6.0	18 ± 7.3	19 ± 8.6
PFECHS	20 ± 6.8	22 ± 5.2	21 ± 5.1	24 ± 5.2
L-PFNA	49 ± 4.0	41 ± 10	47 ± 4.5	29 ± 7.9
B-PFNA	-15 ± 36	-13 ± 29	26 ± 30	-25 ± 49
L-PFOS	80 ± 3.4	72 ± 4.5	72 ± 3.7	63 ± 3.1
B-PFOS	36 ± 11	36 ± 7.4	39 ± 7.6	30 ± 9.0
Σ PFAS	14 ± 2.5	15 ± 2.5	13 ± 2.5	15 ± 2.6

Table S14.1: PFAS concentration in filter substrate after the experiment

Unit	**Substrate type**	**PFBA (ng/Kg)**	**PFPeA (ng/Kg)**	**PFBS (ng/Kg)**	**PFHxA (ng/Kg)**	**4-2FTSA (ng/Kg)**	**HFPO-DA (ng/Kg)**	**PFPeS (ng/Kg)**	**L-PFHpA (ng/Kg)**
Salix spp A	*LECA*	<216	<158	<345	<567	<68.6	<126	90	<269
Salix spp A	*LECA*	<216	<158	<345	<567	<68.6	<126	149	<269
Salix spp A	*LECA*	<216	<158	<345	<567	<68.6	<126	141	<269
Salix SPP A	*Peat + biochar*	1440	1700	1010	2390	<68.6	<126	301	1530
Salix SPP A	*Peat + biochar*	1650	1740	1050	2120	<68.6	<126	378	1420
Salix SPP A	*Peat + biochar*	1240	1220	845	1490	<68.6	<126	376	1220
Salix spp B	*LECA*	<216	<158	<345	<567	<68.6	<126	86.2	<269
Salix spp B	*Peat + biochar*	2060	1840	1650	3830	<68.6	<126	890	2520
C. elata A	*LECA*	<216	<158	360	<567	<68.6	<126	139	<269
C. elata A	*Peat + biochar*	2160	1940	1530	3060	<68.6	<126	880	2170
C. elata B	*LECA*	<216	<158	<345	<567	<68.6	<126	148	<269
C. elata B	*Peat + biochar*	2330	1990	1530	2720	<68.6	<126	859	2330
C. sativa A	*LECA*	<216	<158	<345	<567	<68.6	<126	163	<269
C. sativa A	*Peat + biochar*	2140	2010	1230	3940	<68.6	<126	669	2350

C. sativa B	*LECA*	<216	<158	<345	<567	<68.6	<126	147	<269
C. sativa B	*Peat + biochar*	1960	1820	916	3100	<68.6	<126	421	1960
Control A	*LECA*	<216	<158	346	<567	<68.6	<126	120	<269
Control A	*Peat + biochar*	1450	1360	1150	2340	<68.6	<126	616	2080
Control B	*LECA*	<216	<158	350	<567	<68.6	<126	190	<269
Control B	*Peat + biochar*	1640	1650	1180	2570	<68.6	<126	636	1750

Table S14.2: PFAS concentration in filter substrate after the experiment

Unit	**Substrate type**	**B-PFHpA (ng/Kg)**	**NaDONA (ng/Kg)**	**L-PFHxS (ng/Kg)**	**B-PFHxS (ng/Kg)**	**L-PFOA (ng/Kg)**	**B-PFOA (ng/Kg)**	**6-2 FTSA (ng/Kg)**	**L-PFHpS (ng/Kg)**
Salix spp A	*LECA*	<59.2	<24	701	<16.3	1300	<788	<14.2	44.3
Salix spp A	*LECA*	<59.2	<24	993	119	1900	<788	<14.2	33.7
Salix spp A	*LECA*	<59.2	<24	561	126	1800	<788	<14.2	<14.2
Salix SPP A	*Peat + biochar*	<59.2	<24	2810	298	6740	<788	14.4	323
Salix SPP A	*Peat + biochar*	68.8	<24	3040	201	7710	873	<14.2	280
Salix SPP A	*Peat + biochar*	<59.2	<24	2440	153	5780	<788	15.2	348
Salix spp B	*LECA*	<59.2	<24	679	92.3	1990	<788	<14.2	44.9
Salix spp B	*Peat + biochar*	<59.2	<24	6950	569	16700	1560	21.4	1040
C. elata A	*LECA*	<59.2	<24	926	111	2850	<788	<14.2	92.1
C. elata A	*Peat + biochar*	<59.2	<24	6810	<16.3	10600	1200	<14.2	1250
C. elata B	*LECA*	<59.2	<24	1010	88.5	2650	<788	<14.2	34.9
C. elata B	*Peat + biochar*	<59.2	<24	5440	465	11500	1430	<14.2	692
C. sativa A	*LECA*	<59.2	<24	845	120	2340	<788	<14.2	43
C. sativa A	*Peat + biochar*	<59.2	<24	5470	<16.3	11800	1290	22.6	1070
C. sativa B	*LECA*	<59.2	<24	963	127	2550	<788	<14.2	78.2

C. sativa B	*Peat + biochar*	<59.2	<24	2480	205	10200	1280	<14.2	366
Control A	*LECA*	<59.2	<24	933	62.3	3130	<788	<14.2	97.2
Control A	*Peat + biochar*	<59.2	<24	4780	322	13800	1020	18.1	1540
Control B	*LECA*	<59.2	<24	1250	155	4900	<788	<14.2	119
Control B	*Peat + biochar*	<59.2	<24	2480	205	10200	1280	<14.2	366

Table S14.3: PFAS concentration in filter substrate after the experiment

Unit	**Substrate type**	**B-PFHpS (ng/Kg)**	**PFECHS (ng/Kg)**	**L-PFNA (ng/Kg)**	**B-PFNA (ng/Kg)**	**FOSA (ng/Kg)**	**L-PFOS (ng/Kg)**	**B-PFOS (ng/Kg)**	**PFDA (ng/Kg)**
Salix spp A	*LECA*	<63	98.3	<64.2	<36.9	<1.49	152	414	<39.3
Salix spp A	*LECA*	<63	63.2	<64.2	<36.9	<1.49	218	364	<39.3
Salix spp A	*LECA*	<63	48.6	<64.2	<36.9	<1.49	166	210	<39.3
Salix SPP A	*Peat + biochar*	<63	338	172	38.2	16	3860	1540	147
Salix SPP A	*Peat + biochar*	76.9	336	235	47.8	1.88	3850	1700	93.7
Salix SPP A	*Peat + biochar*	110	427	164	<36.9	<1.49	3900	2250	198
Salix spp B	*LECA*	<63	86	<64.2	<36.9	<1.49	199	313	<39.3
Salix spp B	*Peat + biochar*	267	987	479	143	8.84	14100	8270	96.3
C. elata A	*LECA*	<63	140	<64.2	<36.9	<1.49	861	982	<39.3
C. elata A	*Peat + biochar*	291	1080	573	151	40.4	22300	9310	257
C. elata B	*LECA*	<63	72.6	<64.2	<36.9	<1.49	148	273	<39.3
C. elata B	*Peat + biochar*	184	796	357	95.4	13.1	8710	4920	118
C. sativa A	*LECA*	<63	82	<64.2	<36.9	<1.49	308	328	<39.3
C. sativa A	*Peat + biochar*	209	898	487	66.3	17.7	16300	6890	265
C. sativa B	*LECA*	<63	156	<64.2	<36.9	<1.49	629	885	<39.3
C. sativa B	*Peat + biochar*	78.5	406	278	<36.9	12.4	10700	2410	141
Control A	*LECA*	<63	158	<64.2	<36.9	<1.49	375	580	<39.3
Control A	*Peat + biochar*	317	1230	743	141	8.89	26000	10100	679

Control B	*LECA*	<63	212	<64.2	<36.9	<1.49	1200	1680	<39.3
Control B	*Peat + biochar*	78.5	406	278	<36.9	12.4	10700	2410	141

Table S14.4: PFAS concentration in filter substrate after the experiment

Unit	**Substrate type**	**8-2 FTSA (ng/Kg)**	**9Cl-PF3ONS (ng/Kg)**	**PFNS (ng/Kg)**	**PFUnDA (ng/Kg)**	**Me-FOSAA (ng/Kg)**	**Et-FOSAA (ng/Kg)**	**PFDS (ng/Kg)**	**PFDoDA (ng/Kg)**
Salix spp A	*LECA*	<14.2	<69.6	<21.6	<24.3	<37.8	<21.6	<21.1	<12.8
Salix spp A	*LECA*	<14.2	<69.6	<21.6	<24.3	<37.8	<21.6	<21.1	<12.8
Salix spp A	*LECA*	<14.2	<69.6	<21.6	<24.3	<37.8	<21.6	<21.1	<12.8
Salix SPP A	*Peat + biochar*	<14.2	<69.6	<21.6	<24.3	<37.8	<21.6	<21.1	<12.8
Salix SPP A	*Peat + biochar*	<14.2	<69.6	<21.6	<24.3	<37.8	<21.6	<21.1	72.3
Salix SPP A	*Peat + biochar*	<14.2	<69.6	<21.6	27.9	<37.8	25.2	<21.1	31.1
Salix spp B	*LECA*	<14.2	<69.6	<21.6	<24.3	<37.8	<21.6	<21.1	<12.8
Salix spp B	*Peat + biochar*	<14.2	<69.6	<21.6	<24.3	<37.8	132	<21.1	18.7
C. elata A	*LECA*	<14.2	<69.6	<21.6	<24.3	<37.8	<21.6	<21.1	<12.8
C. elata A	*Peat + biochar*	<14.2	<69.6	<21.6	<24.3	<37.8	242	<21.1	38.1
C. elata B	*LECA*	<14.2	<69.6	<21.6	<24.3	<37.8	<21.6	<21.1	<12.8
C. elata B	*Peat + biochar*	<14.2	<69.6	<21.6	<24.3	<37.8	55.2	<21.1	22.2
C. sativa A	*LECA*	<14.2	<69.6	<21.6	<24.3	<37.8	<21.6	<21.1	<12.8
C. sativa A	*Peat + biochar*	17.12001	<69.6	<21.6	<24.3	<37.8	164	<21.1	17.4
C. sativa B	*LECA*	<14.2	<69.6	<21.6	<24.3	<37.8	<21.6	<21.1	<12.8
C. sativa B	*Peat + biochar*	<14.2	<69.6	<21.6	<24.3	<37.8	55.8	<21.1	26.81
Control A	*LECA*	<14.2	<69.6	<21.6	<24.3	<37.8	<21.6	<21.1	<12.8
Control A	*Peat + biochar*	49.2	<69.6	<21.6	<24.3	<37.8	302	<21.1	51.7
Control B	*LECA*	<14.2	<69.6	<21.6	<24.3	<37.8	<21.6	<21.1	<12.8
Control B	*Peat + biochar*	<14.2	<69.6	<21.6	<24.3	<37.8	55.8	<21.1	26.8

Table S14.5: PFAS concentration in filter substrate after the experiment

Unit	Substrate type	11Cl-PF3OUdS (ng/Kg)	PFTriDA (ng/Kg)	PFTeDA (ng/Kg)
Salix spp A	*LECA*	<38.1	48.3	<309
Salix spp A	*LECA*	<38.1	<18.7	<309
Salix spp A	*LECA*	<38.1	35.8	<309
Salix SPP A	*Peat + biochar*	<38.1	<18.7	<309
Salix SPP A	*Peat + biochar*	<38.1	<18.7	<309
Salix SPP A	*Peat + biochar*	<38.1	<18.7	<309
Salix spp B	*LECA*	<38.1	<18.7	<309
Salix spp B	*Peat + biochar*	<38.1	<18.7	<309
C. elata A	*LECA*	<38.1	<18.7	<309
C. elata A	*Peat + biochar*	<38.1	<18.7	<309
C. elata B	*LECA*	<38.1	<18.7	<309
C. elata B	*Peat + biochar*	<38.1	<18.7	<309
C. sativa A	*LECA*	<38.1	<18.7	<309
C. sativa A	*Peat + biochar*	<38.1	<18.7	<309
C. sativa B	*LECA*	<38.1	<18.7	<309
C. sativa B	*Peat + biochar*	<38.1	<18.7	<309
Control A	*LECA*	<38.1	<18.7	<309
Control A	*Peat + biochar*	<38.1	<18.7	<309
Control B	*LECA*	<38.1	<18.7	<309
Control B	*Peat + biochar*	<38.1	<18.7	<309

Table S15.1: PFAS concentration in plant samples

Plant bed	Species	Tissue type	PFBA (ng/Kg)	PFPeA (ng/Kg)	PFBS (ng/Kg)	PFHxA (ng/Kg)	4-2FTSA (ng/Kg)	HFPO-DA (ng/Kg)	PFPeS (ng/Kg)
Salix spp A	*S. Loden*	*Root*	<1060	<361	<360	<443	<13.3	<40.9	73.4
Salix spp A	*S. Loden*	*Stem*	<1060	<361	<360	<443	<13.3	<40.9	93.1

Salix spp A	*S. Loden*	*Twig*	<1060	<361	<360	<443	<13.3	<40.9	<30.2
Salix spp A	*S. Loden*	*Leaf*	14800	62500	4410	5200	<13.3	<40.9	1620
Salix spp A	*S. Wilhelm*	*Root*	<1060	<361	<360	<443	<13.3	<40.9	51.6
Salix spp A	*S. Wilhelm*	*Root*	<1060	<361	<360	<443	<13.3	<40.9	43.8
Salix spp A	*S. Wilhelm*	*Root*	<1060	<361	<360	<443	<13.3	<40.9	42.7
Salix spp A	*S. Wilhelm*	*Root*	<1060	<361	376	<443	<13.3	<40.9	142
Salix spp A	*S. Wilhelm*	*Root*	<1060	<361	<360	<443	<13.3	<40.9	141
Salix spp A	*S. Wilhelm*	*Stem*	<1060	<361	<360	<443	<13.3	<40.9	70.4
Salix spp A	*S. Wilhelm*	*Twig*	<1060	<361	<360	<443	<13.3	<40.9	48.7
Salix spp A	*S. Wilhelm*	*Leaf*	21600	10800	5940	8160	<13.3	<40.9	1830
Salix spp A	*S. Wilhelm*	*Leaf*	22700	11400	5750	7950	<13.3	<40.9	1530
Salix spp A	*S. Wilhelm*	*Leaf*	22000	10400	5060	7610	<13.3	<40.9	1840
Salix spp A	*S. Wilhelm*	*Leaf*	29300	10000	5430	4050	<13.3	<40.9	1420
Salix spp B	*S. Loden*	*Root*	<1060	<361	<360	<443	<13.3	<40.9	213
Salix spp B	*S. Loden*	*Stem*	<1060	<361	<360	<443	<13.3	<40.9	125
Salix spp B	*S. Loden*	*Stem*	<1060	<361	<360	<443	<13.3	<40.9	140
Salix spp B	*S. Loden*	*Stem*	<1060	<361	<360	<443	<13.3	<40.9	139
Salix spp B	*S. Loden*	*Stem*	1860	<361	<360	<443	<13.3	<40.9	145
Salix spp B	*S. Loden*	*Stem*	<1060	<361	<360	<443	<13.3	<40.9	74.7
Salix spp B	*S. Loden*	*Twig*	<1060	<361	<360	<443	<13.3	<40.9	<30.2
Salix spp B	*S. Loden*	*Twig*	<1060	<361	<360	<443	<13.3	<40.9	<30.2
Salix spp B	*S. Loden*	*Twig*	<1060	<361	<360	<443	<13.3	<40.9	<30.2
Salix spp B	*S. Loden*	*Twig*	<1060	<361	<360	<443	<13.3	<40.9	<30.2
Salix spp B	*S. Loden*	*Twig*	1930	<361	<360	<443	<13.3	<40.9	<30.2
Salix spp B	*S. Loden*	*Leaf*	22500	70700	4430	8210	<13.3	<40.9	1410
Salix spp B	*S. Wilhelm*	*Root*	<1060	<361	390	<443	<13.3	<40.9	221
Salix spp B	*S. Wilhelm*	*Stem*	<1060	<361	<360	<443	<13.3	<40.9	97.5
Salix spp B	*S. Wilhelm*	*Twig*	1690	574	382	<443	<13.3	<40.9	153

Salix spp B	*S. Wilhelm*	*Leaf*	38400	17600	9560	9040	<13.3	<40.9	2130
C. elata A	*C. elata*	*Root*	<1060	<361	<360	<443	<13.3	<40.9	69.1
C. elata A	*C. elata*	*Root*	<1060	<361	<360	<443	<13.3	<40.9	81
C. elata A	*C. elata*	*Root*	<1060	<361	<360	<443	<13.3	<40.9	83.9
C. elata A	*C. elata*	*Root*	<1060	<361	<360	<443	<13.3	<40.9	117
C. elata A	*C. elata*	*Root*	<1060	<361	<360	<443	<13.3	<40.9	117
C. elata A	*C. elata*	*Shoot*	8240	2030	<360	1050	<13.3	<40.9	138
C. elata B	*C. elata*	*Root*	<1060	<361	<360	<443	<13.3	<40.9	64.4
C. elata B	*C. elata*	*Shoot*	12200	3660	626	2190	<13.3	<40.9	366
C. elata B	*C. elata*	*Shoot*	15300	4820	840	2990	<13.3	<40.9	516
C. elata B	*C. elata*	*Shoot*	13300	4330	781	3150	<13.3	<40.9	515
C. elata B	*C. elata*	*Shoot*	8080	1820	360	1500	<13.3	<40.9	186
C. elata B	*C. elata*	*Shoot*	17400	2340	<360	1090	<13.3	<40.9	240
C. sativa A	*C. sativa*	*Root*	<1060	679	<360	854	<13.3	<40.9	218
C. sativa A	*C. sativa*	*Root*	1060	861	389	971	<13.3	<40.9	274
C. sativa A	*C. sativa*	*Root*	<1060	510	<360	692	<13.3	<40.9	170
C. sativa A	*C. sativa*	*Root*	<1060	<361	<360	548	<13.3	<40.9	166
C. sativa A	*C. sativa*	*Root*	<1060	454	<360	666	<13.3	<40.9	171
C. sativa A	*C. sativa*	*Stem*	1290	823	<360	<443	<13.3	<40.9	66
C. sativa A	*C. sativa*	*Stem*	3220	942	<360	<443	<13.3	<40.9	88.4
C. sativa A	*C. sativa*	*Stem*	1210	878	<360	588	<13.3	<40.9	85.2
C. sativa A	*C. sativa*	*Stem*	1390	997	<360	<443	<13.3	<40.9	93.4
C. sativa A	*C. sativa*	*Stem*	3240	1290	<360	448	<13.3	<40.9	105
C. sativa A	*C. sativa*	*Stem Dead*	<1060	1450	1180	2810	<13.3	<40.9	506
C. sativa A	*C. sativa*	*Leaf*	<1060	14400	6410	16700	<13.3	<40.9	2900
C. sativa A	*C. sativa*	*Leaf*	19600	17800	7220	16000	<13.3	<40.9	3460
C. sativa A	*C. sativa*	*Leaf*	21100	16000	7200	17100	<13.3	<40.9	2990
C. sativa A	*C. sativa*	*Leaf*	16600	14900	5720	11900	<13.3	<40.9	2680

C. sativa A	*C. sativa*	*Leaf*	22200	19700	7540	17100	<13.3	<40.9	2700
C. sativa B	*C. sativa*	*Root*	1880	834	<360	1320	<13.3	<40.9	314
C. sativa B	*C. sativa*	*Root Dead*	<1060	531	522	1150	<13.3	<40.9	390
C. sativa B	*C. sativa*	*Stem*	3550	1920	<360	1240	<13.3	<40.9	171
C. sativa B	*C. sativa*	*Stem Dead*	2560	3300	2510	10100	<13.3	<40.9	1220
C. sativa B	*C. sativa*	*Leaf*	50500	36100	20800	39000	<13.3	<40.9	7490

Table S15.2: PFAS concentration in plant samples continuing

Plant bed	**Species**	**Tissue type**	**L-PFHpA (ng/Kg)**	**B-PFHpA (ng/Kg)**	**NaDONA (ng/Kg)**	**L-PFHxS (ng/Kg)**	**B-PFHxS (ng/Kg)**	**L-PFOA (ng/Kg)**	**B-PFOA (ng/Kg)**
Salix spp A	*S. Loden*	*Root*	<334	<10	<24	833	77.1	1610	<105
Salix spp A	*S. Loden*	*Stem*	<334	<10	<24	494	66.4	971	971
Salix spp A	*S. Loden*	*Twig*	<334	<10	<24	97.4	22.7	336	<105
Salix spp A	*S. Loden*	*Leaf*	3170	<10	<24	6430	555	15800	1540
Salix spp A	*S. Wilhelm*	*Root*	<334	<10	<24	840	73.2	1030	<105
Salix spp A	*S. Wilhelm*	*Root*	<334	<10	<24	885	60.5	1030	<105
Salix spp A	*S. Wilhelm*	*Root*	<334	<10	<24	860	59.7	933	<105
Salix spp A	*S. Wilhelm*	*Root*	<334	<10	<24	1040	137	2170	<105
Salix spp A	*S. Wilhelm*	*Root*	<334	<10	<24	1740	138	3940	<105
Salix spp A	*S. Wilhelm*	*Stem*	<334	<10	<24	444	60.5	506	<105
Salix spp A	*S. Wilhelm*	*Twig*	<334	<10	<24	386	42.5	430	<105
Salix spp A	*S. Wilhelm*	*Leaf*	3400	<10	<24	7800	636	11200	1030
Salix spp A	*S. Wilhelm*	*Leaf*	2470	<10	<24	7580	556	10500	888
Salix spp A	*S. Wilhelm*	*Leaf*	2770	<10	<24	7220	600	10800	1040
Salix spp A	*S. Wilhelm*	*Leaf*	753	<10	<24	4830	559	5750	532
Salix spp B	*S. Loden*	*Root*	<334	<10	<24	2200	163	3780	110
Salix spp B	*S. Loden*	*Stem*	<334	<10	<24	732	73.3	1770	<105
Salix spp B	*S. Loden*	*Stem*	<334	<10	<24	732	61.6	1920	<105

Salix spp B	*S. Loden*	*Stem*	<334	<10	<24	709	86.9	1710	<105
Salix spp B	*S. Loden*	*Stem*	<334	<10	<24	711	110	1850	<105
Salix spp B	*S. Loden*	*Stem*	<334	<10	<24	343	60.5	832	<105
Salix spp B	*S. Loden*	*Twig*	<334	<10	<24	105	25.6	1010	<105
Salix spp B	*S. Loden*	*Twig*	<334	<10	<24	99.1	24	991	<105
Salix spp B	*S. Loden*	*Twig*	<334	<10	<24	143	21.2	898	<105
Salix spp B	*S. Loden*	*Twig*	<334	<10	<24	132	26.7	941	<105
Salix spp B	*S. Loden*	*Twig*	<334	<10	<24	102	22.6	<209	<105
Salix spp B	*S. Loden*	*Leaf*	3540	<10	<24	6050	584	17000	1640
Salix spp B	*S. Wilhelm*	*Root*	<334	<10	<24	1630	149	3040	106
Salix spp B	*S. Wilhelm*	*Stem*	<334	<10	<24	541	60.7	1010	<105
Salix spp B	*S. Wilhelm*	*Twig*	<334	<10	<24	817	63.9	1120	<105
Salix spp B	*S. Wilhelm*	*Leaf*	1480	<10	<24	6780	546	9640	1110
C. elata A	*C. elata*	*Root*	<334	<10	<24	1000	54.6	1500	<105
C. elata A	*C. elata*	*Root*	<334	<10	<24	1140	<20.8	1470	<105
C. elata A	*C. elata*	*Root*	<334	<10	<24	1250	<20.8	1640	<105
C. elata A	*C. elata*	*Root*	<334	<10	<24	1500	114	2370	<105
C. elata A	*C. elata*	*Root*	<334	<10	<24	1500	103	1530	<105
C. elata A	*C. elata*	*Shoot*	<334	<10	<24	1380	157	3470	165
C. elata B	*C. elata*	*Root*	<334	<10	<24	784	119	1110	<105
C. elata B	*C. elata*	*Shoot*	816	<10	<24	2570	258	5370	324
C. elata B	*C. elata*	*Shoot*	1290	<10	<24	3270	280	7170	308
C. elata B	*C. elata*	*Shoot*	1200	<10	<24	3190	293	7060	462

C. elata B	*C. elata*	*Shoot*	488	<10	<24	831	127	2060	<105
C. elata B	*C. elata*	*Shoot*	640	<10	<24	2100	129	6150	361
C. sativa A	*C. sativa*	*Root*	621	<10	<24	1780	187	5100	606
C. sativa A	*C. sativa*	*Root*	667	<10	<24	1700	177	7240	507
C. sativa A	*C. sativa*	*Root*	511	<10	<24	1260	113	4400	476
C. sativa A	*C. sativa*	*Root*	<334	<10	<24	954	110	2480	199
C. sativa A	*C. sativa*	*Root*	<334	<10	<24	1220	116	2440	203
C. sativa A	*C. sativa*	*Stem*	<334	<10	<24	222	35.6	749	<105
C. sativa A	*C. sativa*	*Stem*	<334	<10	<24	224	35.9	816	<105
C. sativa A	*C. sativa*	*Stem*	<334	<10	<24	261	37.6	705	<105
C. sativa A	*C. sativa*	*Stem*	<334	<10	<24	313	38.4	1040	<105
C. sativa A	*C. sativa*	*Stem*	<334	<10	<24	376	47.9	1170	<105
C. sativa A	*C. sativa*	*Stem Dead*	2520	297	<24	2070	347	4180	1290
C. sativa A	*C. sativa*	*Leaf*	7920	680	<24	9210	790	35400	4560
C. sativa A	*C. sativa*	*Leaf*	8230	626	<24	11100	880	44600	4250
C. sativa A	*C. sativa*	*Leaf*	10900	<10	<24	8720	636	50200	<105
C. sativa A	*C. sativa*	*Leaf*	9160	<10	<24	9240	5760	38900	<105
C. sativa A	*C. sativa*	*Leaf*	10600	<10	<24	8810	5490	39600	2990
C. sativa B	*C. sativa*	*Root*	1170	11.7	<24	2720	228	5150	459

C. sativa B	*C. sativa*	*Root Dead*	619	<10	<24	2570	291	4410	477
C. sativa B	*C. sativa*	*Stem*	518	<10	<24	650	60.1	2750	126
C. sativa B	*C. sativa*	*Stem Dead*	5930	430	<24	5020	845	12200	3080
C. sativa B	*C. sativa*	*Leaf*	18400	982	<24	19900	1220	93600	<105

Table S15.3: PFAS concentration in plant samples continuing

Plant bed	**Species**	**Tissue type**	**6-2 FTSA (ng/Kg)**	**L-PFHpS (ng/Kg)**	**B-PFHpS (ng/Kg)**	**PFECHS (ng/Kg)**	**L-PFNA (ng/Kg)**	**B-PFNA (ng/Kg)**	**FOSA (ng/Kg)**
Salix spp A	*S. Loden*	*Root*	<154	179	14.6	187	<368	<10	24
Salix spp A	*S. Loden*	*Stem*	<154	31.4	<10	48.2	<368	<10	<21
Salix spp A	*S. Loden*	*Twig*	<154	<11.6	<10	<26.4	<368	<10	<21
Salix spp A	*S. Loden*	*Leaf*	<154	294	77.8	541	<368	<10	<21
Salix spp A	*S. Wilhelm*	*Root*	<154	229	29.3	192	<368	<10	55.5
Salix spp A	*S. Wilhelm*	*Root*	<154	210	55.1	213	<368	<10	40.2
Salix spp A	*S. Wilhelm*	*Root*	<154	215	20.2	194	<368	<10	24.9
Salix spp A	*S. Wilhelm*	*Root*	<154	92.4	30.5	189	<368	<10	<21
Salix spp A	*S. Wilhelm*	*Root*	<154	354	91	345	<368	<10	40.4
Salix spp A	*S. Wilhelm*	*Stem*	<154	24.2	<10	57.6	<368	<10	<21
Salix spp A	*S. Wilhelm*	*Twig*	<154	36.6	<10	61.7	<368	<10	<21
Salix spp A	*S. Wilhelm*	*Leaf*	<154	313	102	788	<368	<10	<21
Salix spp A	*S. Wilhelm*	*Leaf*	<154	308	110	616	<368	<10	<21
Salix spp A	*S. Wilhelm*	*Leaf*	<154	338	99	783	<368	<10	<21
Salix spp A	*S. Wilhelm*	*Leaf*	<154	193	88	640	<368	<10	<21
Salix spp B	*S. Loden*	*Root*	<154	291	53.5	316	<368	<10	<21
Salix spp B	*S. Loden*	*Stem*	<154	44.2	<10	61.6	<368	<10	<21
Salix spp B	*S. Loden*	*Stem*	<154	40.5	<10	85.5	<368	<10	<21

Salix spp B	*S. Loden*	*Stem*	<154	38.1	<10	80.4	<368	<10	<21
Salix spp B	*S. Loden*	*Stem*	<154	51.9	<10	89.7	<368	<10	<21
Salix spp B	*S. Loden*	*Stem*	<154	21.3	<10	45.4	<368	<10	<21
Salix spp B	*S. Loden*	*Twig*	<154	<11.6	<10	<26.4	<368	<10	<21
Salix spp B	*S. Loden*	*Twig*	<154	<11.6	<10	<26.4	<368	<10	<21
Salix spp B	*S. Loden*	*Twig*	<154	<11.6	<10	<26.4	<368	<10	<21
Salix spp B	*S. Loden*	*Twig*	<154	21.2	<10	<26.4	<368	<10	<21
Salix spp B	*S. Loden*	*Twig*	<154	<11.6	<10	<26.4	<368	<10	<21
Salix spp B	*S. Loden*	*Leaf*	<154	249	66.6	438	<368	<10	<21
Salix spp B	*S. Wilhelm*	*Root*	<154	211	46.1	271	<368	<10	<21
Salix spp B	*S. Wilhelm*	*Stem*	<154	18.8	<10	49.2	<368	<10	<21
Salix spp B	*S. Wilhelm*	*Twig*	<154	41.3	<10	88.2	<368	<10	<21
Salix spp B	*S. Wilhelm*	*Leaf*	<154	195	102	747	<368	<10	<21
C. elata A	*C. elata*	*Root*	<154	209	34.9	127	<368	<10	107
C. elata A	*C. elata*	*Root*	<154	200	31.8	125	<368	<10	72.2
C. elata A	*C. elata*	*Root*	<154	216	25.7	140	<368	<10	108
C. elata A	*C. elata*	*Root*	<154	326	48	186	<368	156	24.3
C. elata A	*C. elata*	*Root*	<154	221	44.9	174	<368	61.3	<21
C. elata A	*C. elata*	*Shoot*	<154	100	20.8	71.5	<368	13.8	<21
C. elata B	*C. elata*	*Root*	<154	117	23.5	104	<368	25	61.4
C. elata B	*C. elata*	*Shoot*	<154	138	39.8	120	<368	<10	<21
C. elata B	*C. elata*	*Shoot*	<154	201	36	150	<368	<10	<21
C. elata B	*C. elata*	*Shoot*	<154	162	38	138	<368	<10	<21

C. elata B	*C. elata*	*Shoot*	<154	34.6	<10	60.7	<368	<10	47.1
C. elata B	*C. elata*	*Shoot*	<154	114	26.9	87.1	<368	<10	24.4
C. sativa A	*C. sativa*	*Root*	<154	210	67.9	274	<368	67.3	<21
C. sativa A	*C. sativa*	*Root*	<154	278	76.7	289	<368	49.9	23.8
C. sativa A	*C. sativa*	*Root*	<154	155	42.7	243	<368	22.1	<21
C. sativa A	*C. sativa*	*Root*	<154	114	34	193	<368	<10	22.7
C. sativa A	*C. sativa*	*Root*	<154	120	23.6	169	<368	20.2	23.2
C. sativa A	*C. sativa*	*Stem*	<154	23.8	<10	33.6	<368	<10	<21
C. sativa A	*C. sativa*	*Stem*	<154	40.6	<10	34.2	<368	<10	<21
C. sativa A	*C. sativa*	*Stem*	<154	24.3	<10	30.3	<368	<10	<21
C. sativa A	*C. sativa*	*Stem*	<154	25.5	<10	33.5	<368	<10	<21
C. sativa A	*C. sativa*	*Stem*	<154	43.1	<10	49.1	<368	<10	<21
C. sativa A	*C. sativa*	*Stem Dead*	<154	32.9	24.2	173	<368	<10	<21
C. sativa A	*C. sativa*	*Leaf*	<154	<11.6	<10	<26.4	<368	<10	22.9
C. sativa A	*C. sativa*	*Leaf*	<154	<11.6	<10	<26.4	<368	<10	<21
C. sativa A	*C. sativa*	*Leaf*	<154	<11.6	<10	<26.4	<368	<10	<21
C. sativa A	*C. sativa*	*Leaf*	<154	<11.6	<10	<26.4	<368	<10	<21
C. sativa A	*C. sativa*	*Leaf*	<154	<11.6	<10	<26.4	<368	<10	<21
C. sativa B	*C. sativa*	*Root*	<154	213	55.8	292	<368	<10	48

C. sativa B	*C. sativa*	*Root Dead*	<154	244	88.9	483	<368	<10	31.4
C. sativa B	*C. sativa*	*Stem*	<154	62.2	<10	75.4	<368	<10	<21
C. sativa B	*C. sativa*	*Stem Dead*	<154	121	98.4	517	<368	<10	28.1
C. sativa B	*C. sativa*	*Leaf*	<154	<11.6	<10	<26.4	<368	<10	36.5

Table S15.4: PFAS concentration in plant samples continuing

Plant bed	**Species**	**Tissue type**	**L-PFOS (ng/Kg)**	**B-PFOS (ng/Kg)**	**PFDA (ng/Kg)**	**8-2 FTSA (ng/Kg)**	**9Cl-PF3ONS (ng/Kg)**	**PFNS (ng/Kg)**	**PFUnDA (ng/Kg)**
Salix spp A	*S. Loden*	*Root*	4610	1420	<246	<10.1	<20.9	<21.6	<122
Salix spp A	*S. Loden*	*Stem*	525	250	<246	<10.1	<20.9	<21.6	<122
Salix spp A	*S. Loden*	*Twig*	187	126	<246	<10.1	<20.9	<21.6	<122
Salix spp A	*S. Loden*	*Leaf*	2000	1170	<246	<10.1	<20.9	<21.6	<122
Salix spp A	*S. Wilhelm*	*Root*	5510	1900	<246	<10.1	<20.9	<21.6	<122
Salix spp A	*S. Wilhelm*	*Root*	6170	1940	<246	<10.1	<20.9	<21.6	<122
Salix spp A	*S. Wilhelm*	*Root*	5720	1840	<246	<10.1	<20.9	<21.6	<122
Salix spp A	*S. Wilhelm*	*Root*	963	1070	<246	<10.1	<20.9	<21.6	<122
Salix spp A	*S. Wilhelm*	*Root*	3980	3370	<246	<10.1	<20.9	<21.6	<122
Salix spp A	*S. Wilhelm*	*Stem*	215	204	<246	<10.1	<20.9	<21.6	<122
Salix spp A	*S. Wilhelm*	*Twig*	292	322	<246	<10.1	<20.9	<21.6	<122
Salix spp A	*S. Wilhelm*	*Leaf*	1090	1550	<246	<10.1	<20.9	<21.6	<122
Salix spp A	*S. Wilhelm*	*Leaf*	1040	1220	<246	<10.1	<20.9	<21.6	<122
Salix spp A	*S. Wilhelm*	*Leaf*	1040	1400	<246	<10.1	<20.9	<21.6	<122
Salix spp A	*S. Wilhelm*	*Leaf*	184	637	<246	<10.1	<20.9	<21.6	<122
Salix spp B	*S. Loden*	*Root*	4180	2650	<246	<10.1	<20.9	<21.6	<122
Salix spp B	*S. Loden*	*Stem*	443	324	<246	<10.1	<20.9	<21.6	<122
Salix spp B	*S. Loden*	*Stem*	523	293	<246	<10.1	<20.9	<21.6	<122

Salix spp B	*S. Loden*	*Stem*	495	296	<246	<10.1	<20.9	<21.6	<122
Salix spp B	*S. Loden*	*Stem*	427	278	<246	<10.1	<20.9	<21.6	<122
Salix spp B	*S. Loden*	*Stem*	192	128	<246	<10.1	<20.9	<21.6	<122
Salix spp B	*S. Loden*	*Twig*	297	122	<246	<10.1	<20.9	<21.6	<122
Salix spp B	*S. Loden*	*Twig*	311	129	<246	<10.1	<20.9	<21.6	<122
Salix spp B	*S. Loden*	*Twig*	324	132	<246	<10.1	<20.9	<21.6	<122
Salix spp B	*S. Loden*	*Twig*	363	158	<246	<10.1	<20.9	<21.6	<122
Salix spp B	*S. Loden*	*Twig*	<180	82.6	<246	<10.1	<20.9	<21.6	<122
Salix spp B	*S. Loden*	*Leaf*	1510	930	<246	<10.1	<20.9	<21.6	<122
Salix spp B	*S. Wilhelm*	*Root*	2450	1860	<246	<10.1	<20.9	<21.6	<122
Salix spp B	*S. Wilhelm*	*Stem*	181	199	<246	<10.1	<20.9	<21.6	<122
Salix spp B	*S. Wilhelm*	*Twig*	244	300	<246	<10.1	<20.9	<21.6	<122
Salix spp B	*S. Wilhelm*	*Leaf*	351	775	<246	<10.1	<20.9	<21.6	<122
C. elata A	*C. elata*	*Root*	3880	1120	<246	<10.1	<20.9	<21.6	<122
C. elata A	*C. elata*	*Root*	4810	1130	<246	<10.1	<20.9	<21.6	<122
C. elata A	*C. elata*	*Root*	4230	1100	<246	<10.1	<20.9	<21.6	140
C. elata A	*C. elata*	*Root*	5020	1870	<246	<10.1	<20.9	<21.6	<122
C. elata A	*C. elata*	*Root*	2450	1060	<246	<10.1	<20.9	<21.6	<122
C. elata A	*C. elata*	*Shoot*	853	405	<246	<10.1	<20.9	<21.6	<122
C. elata B	*C. elata*	*Root*	1300	653	<246	<10.1	<20.9	<21.6	<122
C. elata B	*C. elata*	*Shoot*	890	399	<246	<10.1	<20.9	<21.6	<122
C. elata B	*C. elata*	*Shoot*	1120	540	<246	<10.1	<20.9	<21.6	<122
C. elata B	*C. elata*	*Shoot*	1040	450	<246	<10.1	<20.9	<21.6	<122
C. elata B	*C. elata*	*Shoot*	264	172	<246	<10.1	<20.9	<21.6	<122
C. elata B	*C. elata*	*Shoot*	515	233	<246	<10.1	<20.9	<21.6	<122
C. sativa A	*C. sativa*	*Root*	2100	1410	<246	<10.1	<20.9	<21.6	<122
C. sativa A	*C. sativa*	*Root*	2170	1360	<246	<10.1	<20.9	<21.6	<122

C. sativa A	*C. sativa*	*Root*	1740	1010	<246	<10.1	<20.9	<21.6	<122
C. sativa A	*C. sativa*	*Root*	1490	687	<246	<10.1	<20.9	<21.6	<122
C. sativa A	*C. sativa*	*Root*	859	618	<246	<10.1	<20.9	<21.6	<122
C. sativa A	*C. sativa*	*Stem*	482	161	<246	<10.1	<20.9	<21.6	<122
C. sativa A	*C. sativa*	*Stem*	548	179	<246	<10.1	<20.9	<21.6	<122
C. sativa A	*C. sativa*	*Stem*	539	151	<246	<10.1	<20.9	<21.6	<122
C. sativa A	*C. sativa*	*Stem*	477	132	<246	<10.1	<20.9	<21.6	<122
C. sativa A	*C. sativa*	*Stem*	578	278	<246	<10.1	<20.9	<21.6	<122
C. sativa A	*C. sativa*	*Stem Dead*	<180	92.7	<246	<10.1	<20.9	<21.6	<122
C. sativa A	*C. sativa*	*Leaf*	<180	<36.7	<246	<10.1	<20.9	<21.6	<122
C. sativa A	*C. sativa*	*Leaf*	<180	<36.7	<246	<10.1	<20.9	<21.6	<122
C. sativa A	*C. sativa*	*Leaf*	<180	<36.7	<246	<10.1	<20.9	<21.6	<122
C. sativa A	*C. sativa*	*Leaf*	<180	<36.7	<246	<10.1	<20.9	<21.6	<122
C. sativa A	*C. sativa*	*Leaf*	<180	<36.7	<246	<10.1	<20.9	<21.6	<122
C. sativa B	*C. sativa*	*Root*	4820	953	261	<10.1	<20.9	<21.6	125
C. sativa B	*C. sativa*	*Root Dead*	1510	1990	<246	<10.1	<20.9	<21.6	<122
C. sativa B	*C. sativa*	*Stem*	1630	352	<246	<10.1	<20.9	<21.6	<122
C. sativa B	*C. sativa*	*Stem Dead*	619	493	<246	<10.1	<20.9	<21.6	<122
C. sativa B	*C. sativa*	*Leaf*	<180	<36.7	<246	<10.1	<20.9	<21.6	<122

Table S15.5: PFAS concentration in plant samples continuing

Plant bed	Species	Tissue type	Me-FOSAA (ng/Kg)	Et-FOSAA (ng/Kg)	PFDS (ng/Kg)	PFDoDA (ng/Kg)	11Cl-PF3OUdS (ng/Kg)	PFTriDA (ng/Kg)	PFTeDA (ng/Kg)
Salix spp A	*S. Loden*	*Root*	<30	<29.2	<21.5	<417	<26.9	<23700	<58700
Salix spp A	*S. Loden*	*Stem*	<30	<29.2	<21.5	<417	<26.9	<23700	<58700
Salix spp A	*S. Loden*	*Twig*	<30	<29.2	<21.5	<417	<26.9	<23700	<58700
Salix spp A	*S. Loden*	*Leaf*	<30	<29.2	<21.5	<417	<26.9	<23700	<58700
Salix spp A	*S. Wilhelm*	*Root*	<30	<29.2	<21.5	<417	<26.9	<23700	<58700
Salix spp A	*S. Wilhelm*	*Root*	<30	81.8	<21.5	<417	<26.9	<23700	<58700
Salix spp A	*S. Wilhelm*	*Root*	<30	<29.2	<21.5	<417	<26.9	<23700	<58700
Salix spp A	*S. Wilhelm*	*Root*	<30	<29.2	<21.5	<417	<26.9	<23700	<58700
Salix spp A	*S. Wilhelm*	*Root*	<30	<29.2	<21.5	<417	<26.9	<23700	<58700
Salix spp A	*S. Wilhelm*	*Stem*	<30	<29.2	<21.5	<417	<26.9	<23700	<58700
Salix spp A	*S. Wilhelm*	*Twig*	<30	<29.2	<21.5	<417	<26.9	<23700	<58700
Salix spp A	*S. Wilhelm*	*Leaf*	<30	<29.2	<21.5	<417	<26.9	<23700	<58700
Salix spp A	*S. Wilhelm*	*Leaf*	<30	<29.2	<21.5	<417	<26.9	<23700	<58700
Salix spp A	*S. Wilhelm*	*Leaf*	<30	<29.2	<21.5	<417	<26.9	<23700	<58700
Salix spp A	*S. Wilhelm*	*Leaf*	<30	<29.2	<21.5	<417	<26.9	<23700	<58700
Salix spp B	*S. Loden*	*Root*	<30	<29.2	<21.5	<417	<26.9	<23700	<58700
Salix spp B	*S. Loden*	*Stem*	<30	<29.2	<21.5	<417	<26.9	<23700	<58700
Salix spp B	*S. Loden*	*Stem*	<30	<29.2	<21.5	<417	<26.9	<23700	<58700
Salix spp B	*S. Loden*	*Stem*	<30	<29.2	<21.5	<417	<26.9	<23700	<58700
Salix spp B	*S. Loden*	*Stem*	<30	<29.2	<21.5	<417	<26.9	<23700	<58700
Salix spp B	*S. Loden*	*Stem*	<30	<29.2	<21.5	<417	<26.9	<23700	<58700
Salix spp B	*S. Loden*	*Twig*	<30	<29.2	<21.5	<417	<26.9	<23700	<58700
Salix spp B	*S. Loden*	*Twig*	<30	<29.2	<21.5	<417	<26.9	<23700	<58700
Salix spp B	*S. Loden*	*Twig*	<30	<29.2	<21.5	<417	<26.9	<23700	<58700
Salix spp B	*S. Loden*	*Twig*	<30	<29.2	<21.5	<417	<26.9	<23700	<58700

Salix spp B	*S. Loden*	*Twig*	<30	<29.2	<21.5	<417	<26.9	<23700	<58700
Salix spp B	*S. Loden*	*Leaf*	<30	<29.2	<21.5	<417	<26.9	<23700	<58700
Salix spp B	*S. Wilhelm*	*Root*	<30	<29.2	<21.5	<417	<26.9	<23700	<58700
Salix spp B	*S. Wilhelm*	*Stem*	<30	<29.2	<21.5	<417	<26.9	<23700	<58700
Salix spp B	*S. Wilhelm*	*Twig*	<30	<29.2	<21.5	<417	<26.9	<23700	<58700
Salix spp B	*S. Wilhelm*	*Leaf*	<30	<29.2	<21.5	<417	<26.9	<23700	<58700
C. elata A	*C. elata*	*Root*	<30	<29.2	<21.5	<417	<26.9	<23700	<58700
C. elata A	*C. elata*	*Root*	<30	<29.2	<21.5	<417	<26.9	<23700	<58700
C. elata A	*C. elata*	*Root*	<30	29.7	<21.5	<417	<26.9	<23700	<58700
C. elata A	*C. elata*	*Root*	<30	<29.2	<21.5	<417	<26.9	<23700	<58700
C. elata A	*C. elata*	*Root*	<30	<29.2	<21.5	<417	<26.9	<23700	<58700
C. elata A	*C. elata*	*Shoot*	<30	<29.2	<21.5	<417	<26.9	<23700	<58700
C. elata B	*C. elata*	*Root*	<30	<29.2	<21.5	<417	<26.9	<23700	<58700
C. elata B	*C. elata*	*Shoot*	<30	<29.2	<21.5	<417	<26.9	<23700	<58700
C. elata B	*C. elata*	*Shoot*	<30	<29.2	<21.5	<417	<26.9	<23700	<58700
C. elata B	*C. elata*	*Shoot*	<30	<29.2	<21.5	<417	<26.9	<23700	<58700
C. elata B	*C. elata*	*Shoot*	<30	<29.2	<21.5	<417	<26.9	<23700	<58700
C. elata B	*C. elata*	*Shoot*	<30	<29.2	<21.5	<417	<26.9	<23700	<58700
C. sativa A	*C. sativa*	*Root*	<30	<29.2	<21.5	<417	<26.9	<23700	<58700
C. sativa A	*C. sativa*	*Root*	<30	<29.2	<21.5	<417	<26.9	<23700	<58700
C. sativa A	*C. sativa*	*Root*	<30	<29.2	<21.5	<417	<26.9	<23700	<58700
C. sativa A	*C. sativa*	*Root*	<30	<29.2	<21.5	<417	<26.9	<23700	<58700
C. sativa A	*C. sativa*	*Root*	<30	<29.2	<21.5	<417	<26.9	<23700	<58700
C. sativa A	*C. sativa*	*Stem*	<30	<29.2	<21.5	<417	<26.9	<23700	<58700
C. sativa A	*C. sativa*	*Stem*	<30	<29.2	<21.5	<417	<26.9	<23700	<58700

C. sativa A	*C. sativa*	*Stem*	<30	<29.2	<21.5	<417	<26.9	<23700	<58700
C. sativa A	*C. sativa*	*Stem*	<30	<29.2	<21.5	<417	<26.9	<23700	<58700
C. sativa A	*C. sativa*	*Stem*	<30	<29.2	<21.5	<417	<26.9	<23700	<58700
C. sativa A	*C. sativa*	*Stem Dead*	<30	<29.2	<21.5	<417	<26.9	<23700	<58700
C. sativa A	*C. sativa*	*Leaf*	<30	<29.2	<21.5	<417	<26.9	<23700	<58700
C. sativa A	*C. sativa*	*Leaf*	<30	<29.2	<21.5	<417	<26.9	<23700	<58700
C. sativa A	*C. sativa*	*Leaf*	<30	<29.2	<21.5	<417	<26.9	<23700	<58700
C. sativa A	*C. sativa*	*Leaf*	<30	<29.2	<21.5	<417	<26.9	<23700	<58700
C. sativa A	*C. sativa*	*Leaf*	<30	<29.2	<21.5	<417	<26.9	<23700	<58700
C. sativa B	*C. sativa*	*Root*	<30	<29.2	<21.5	<417	<26.9	<23700	<58700
C. sativa B	*C. sativa*	*Root Dead*	<30	<29.2	<21.5	<417	<26.9	<23700	<58700
C. sativa B	*C. sativa*	*Stem*	<30	<29.2	<21.5	<417	<26.9	<23700	<58700
C. sativa B	*C. sativa*	*Stem Dead*	<30	<29.2	<21.5	<417	<26.9	<23700	<58700
C. sativa B	*C. sativa*	*Leaf*	<30	<29.2	<21.5	<417	<26.9	<23700	<58700

Table S16: Estimated treatment potential for *C. elata* for each PFAS compound in the study. Calculated from above-ground PFAS concentrations derived in this study, combined with literature values on expected above-ground biomass yields.

Compound	**PFAS concentration (ng/Kg dw) means ± standard error (range)**	**Tonnes of biomass (stem, twigs, leaves) dw/ha yr**	**Removal mg ΣPFAS dw/ha yr means (range)**
PFBA	**10600** ± 2390 (8240-13000)	6-8 tonne	**76.8** ± 27.4 (49.4-104)
PFPeA	**2420** ± 387 (2030-2810)	6-8 tonne	**17.3** ± 5.1 (12.2-22.5)
PFBS	**215** ± 215 (0-430)	6-8 tonne	**1.72** ± 1.72 (0-3.44)
PFHxA	**1420** ± 369 (1050-1790)	6-8 tonne	**10.3** ± 4.01 (6.31-14.3)
4-2 FTSA	<13.3	6-8 tonne	-
HFPO-DA	<40.9	6-8 tonne	-

PFPeS	**218** ± 79.5 (138-297)	6-8 tonne	**1.60** ± 0.774 (0.829-2.38)
PFHpA-Linear	**372** ± 372 (0-744)	6-8 tonne	**2.97** ± 2.97 (0-5.95)
PFHpA-Branched	<10.0	6-8 tonne	-
NaDONA	<24.0	6-8 tonne	-
PFHxS-Linear	**1680** ± 303 (1370-1980)	6-8 tonne	**12.05** ± 3.80 (8.25-15.9)
PFHxS-Branched	**167** ± 10.4 (157-178)	6-8 tonne	**1.18** ± 0.240 (0.941-1.42)
PFOA-Linear	**4190** ± 725 (3470-4920)	6-8 tonne	**30.1** ± 9.26 (20.8-39.3)
PFOA-Branched	**212** ± 47.3 (165-259)	6-8 tonne	**1.53** ± 0.543 (0.990-2.07)
6-2 FTSA	<154	6-8 tonne	-
PFHpS-Linear	**103** ± 2.42 (100-105)	6-8 tonne	**0.772** ± 0.120 (0.603-0.842)
PFHpS-Branched	**22.0** ± 1.26 (20.8-23.2)	6-8 tonne	**0.155** ± 0.0308 (0.125-0.186)
PFECHS	**83.0** ± 11.5(71.5-94.5)	6-8 tonne	**0.592** ± 0.164 (0.429-0.756)
PFNA-Linear	<368	6-8 tonne	-
PFNA-Branched	**6.91** ± 6.91 (0-13.8)	6-8 tonne	**0.0553** ± 0.0553 (0-0.111)
FOSA	**13.7** ± 13.7 (0-27.3)	6-8 tonne	**0.109** ± 0.109 (0-0.219)
PFOS-Linear	**725** ± 127 (598-853)	6-8 tonne	**1.62** ± 1.62 (3.59-6.82)
PFOS-Branched	**347** ± 57.8 (289-405)	6-8 tonne	**0.752** ± 0.752 (1.74-3.24)
PFDA	<246	6-8 tonne	-
8-2 FTSA	<10.1	6-8 tonne	-
9Cl-PF3ONS	<20.9	6-8 tonne	-
PFNS	<21.6	6-8 tonne	-
PFUnDA	<122	6-8 tonne	-
Me-FOSAA	<30.0	6-8 tonne	-
Et-FOSAA	<29.2	6-8 tonne	-
PFDS	<21.5	6-8 tonne	-
PFDoDA	<417	6-8 tonne	-
11Cl-PF3OUdS	<26.9	6-8 tonne	-
PFTriDA	<23700	6-8 tonne	-
PFTeDA	<58700	6-8 tonne	-

Table S17 Estimated treatment potential for *C. sativa* for each PFAS compound in the study. Calculated from above-ground PFAS concentrations derived in this study, combined with literature values on expected above-ground biomass yields.

Compound	**PFAS concentration (ng/Kg dw) means (range)**	**Tonnes of biomass (stem, twigs, leaves) dw/ha yr**	**Removal mg ΣPFAS dw/ha yr means (range)**
PFBA	**9120** ± 4740 (4380-13860)	12-22 tonne	**179** ± 126 (52.6-305)
PFPeA	**6370** ± 3050 (3330-9420)	12-22 tonne	**124** ± 83.6 (40.0-207)
PFBS	**2760** ± 1800 (970-4560)	12-22 tonne	**56.0** ± 44.4 (11.6-100)
PFHxA	**5850** ± 3660 (2180-9510)	12-22 tonne	**118** ± 91.5 (26.2-209)
4-2FTSA	<13.3	12-22 tonne	-
HFPO-DA	<40.9	12-22 tonne	-
PFPeS	**1130** ± 646 (486-1780)	12-22 tonne	**22.5** ± 16.6 (5.83-39.1)
PFHpA-Linnear	**2900** ± 1530 (1380-4430)	12-22 tonne	**57.0** ± 40.5 (16.5-97.5)
PFHpA-Branched	**118** ± 97.0 (21.4-215)	12-22 tonne	**2.50** ± 2.24 (0.26-4.74)
NaDONA	<24.0	12-22 tonne	-
PFHxS-Linnear	**3230** ± 1640 (1590-4870)	12-22 tonne	**63.1** ± 44.0 (19.1-107)
PFHxS-Branched	**463** ± 147 (316-610)	12-22 tonne	**8.60** ± 4.81 (3.79-13.4)
PFOA-Linnear	**14700** ± 8000 (6680-22700)	12-22 tonne	**290** ± 209 (80.2-499)
PFOA-Branched	**193** ± 94.2 (98.3-287)	12-22 tonne	**3.74** ± 2.56 (1.18-6.31)
6-2 FTSA	<154	12-22 tonne	-
PFHpS-Linnear	**38.3** ± 10.3 (28.0-48.6)	12-22 tonne	**0.702** ± 0.366 (0.337-1.07)
PFHpS-Branched	<10.0	12-22 tonne	-
PFECHS	**45.9** ± 13.0 (32.9-58.8)	12-22 tonne	**0.845** ± 0.450 (0.395-1.29)
PFNA-Linnear	<368	12-22 tonne	-
PFNA-Branched	<10.0	12-22 tonne	-

FOSA	**4.00** ± 4.00 (0-8.00)	12-22 tonne	**0.0880** ± 0.0880 (0-0.176)
PFOS-Linnear	**863** ± 412 (451-1280)	12-22 tonne	**16.7** ± 11.3 (5.41-28.0)
PFOS-Branched	**219** ± 56.0 (164-275)	12-22 tonne	**4.01** ± 2.04 (1.96-6.05)
PFDA	<246	12-22 tonne	-
8-2 FTSA	<10.1	12-22 tonne	-
9Cl-PF3ONS	<20.9	12-22 tonne	-
PFNS	<21.6	12-22 tonne	-
PFUnDA	<122	12-22 tonne	-
Me-FOSAA	<30.0	12-22 tonne	-
Et-FOSAA	<29.2	12-22 tonne	-
PFDS	<21.4	12-22 tonne	-
PFDoDA	<417	12-22 tonne	-
11Cl-PF3OUdS	<26.9	12-22 tonne	-
PFTriDA	<23700	12-22 tonne	-
PFTeDA	<58700	12-22 tonne	-

Table S18: Estimated treatment potential for S. Wilhelm for each PFAS compound in the study. Calculated from above-ground PFAS concentrations derived in this study, combined with literature values on expected above-ground biomass yields. Biomass yields for the different Salix clones were taken from mean Salix production data and adjusted for biomass differences seen in the experiment.

Compound	**PFAS concentration (ng/Kg dw) means (range)**	**Tonnes of biomass (stem, twigs, leaves) dw/ha yr**	**Removal mg ΣPFAS dw/ha yr means (range)**
PFBA	**5100** ± 733 (4370-5830)	13-30 tonne	**116** ± 59.1 (56.8-175)
PFPeA	**2200** ± 420 (1770-2620)	13-30 tonne	**50.8** ± 27.8 (23.1-78.6)
PFBS	**1190** ± 254 (935-1440)	13-30 tonne	**27.7** ± 15.6 (12.1-43.3)
PFHxA	**1150** ± 133 (1010-1280)	13-30 tonne	**25.8** ± 12.6 (13.2-38.4)
4-2FTSA	<13.3	13-30 tonne	-
HFPO-DA	<40.9	13-30 tonne	-
PFPeS	**360** ± 38.9 (321-399)	13-30 tonne	**8.07** ± 3.90 (4.17-12.0)
PFHpA-Linnear	**259** ± 49.5 (209-308)	13-30 tonne	**5.99** ± 3.26 (2.73-9.25)
PFHpA-Branched	<10.0	13-30 tonne	-
NaDONA	<24.0	13-30 tonne	-
PFHxS-Linnear	**1450** ± 41.8 (1410-1490)	13-30 tonne	**31.5** ± 13.2 (18.3-44.6)
PFHxS-Branched	**137** ± 7.03 (130-144)	13-30 tonne	**3.01** ± 1.32 (1.69-4.33)
PFOA-Linnear	**2030** ± 223 (1810-2260)	13-30 tonne	**45.6** ± 22.1 (23.5-67.7)
PFOA-Branched	**143** ± 14.3 (129-157)	13-30 tonne	**3.20** ± 1.52 (1.68-4.72)
6-2 FTSA	<0.154	13-30 tonne	-
PFHpS-Linnear	**57.7** ± 8.71 (49.0-66.4)	13-30 tonne	**1.32** ± 0.678 (0.637-1.99)
PFHpS-Branched	**15.4** ± 0.864 (145-16.2)	13-30 tonne	**0.338** ± 0.149 (0.189-0.487)
PFECHS	**161** ± 3.96 (157-165)	13-30 tonne	**3.49** ± 1.45 (2.04-4.95)
PFNA-Linnear	<368	13-30 tonne	-
PFNA-Branched	<10.0	13-30 tonne	-
FOSA	<21.0	13-30 tonne	-
PFOS-Linnear	**260** ± 41.1 (219-302)	13-30 tonne	**5.95** ± 3.10 (2.85-9.05)
PFOS-Branched	**336** ± 32.5 (304-369)	13-30 tonne	**7.51** ± 3.56 (3.95-11.1)
PFDA	<246	13-30 tonne	-
8-2 FTSA	<10.1	13-30 tonne	-
9Cl-PF3ONS	<20.9	13-30 tonne	-
PFNS	<21.6	13-30 tonne	-
PFUnDA	<122	13-30 tonne	-
Me-FOSAA	<30.0	13-30 tonne	-
Et-FOSAA	<29.2	13-30 tonne	-
PFDS	<21.5	13-30 tonne	-
PFDoDA	<417	13-30 tonne	-

11Cl-PF3OUdS	<26.9	13-30 tonne	-
PFTriDA	<23700	13-30 tonne	-
PFTeDA	<58700	13-30 tonne	-

Table S19: Estimated treatment potential for S. Loden for each PFAS compound in the study. Calculated from above-ground PFAS concentrations derived in this study combined with literature values on expected above-ground biomass yields. Biomass yields for the different Salix clones were taken from mean Salix production data and adjusted for biomass differences seen in the experiment.

Compound	**PFAS concentration (ng/Kg dw) means (range)**	**Tonnes biomass (stem, twigs, leaves) dw/ha yr**	**Removal mg ΣPFAS dw/ha yr means (range)**
PFBA	**37000** ± 910 (2790-4610)	10-23 tonne	**66.9** ± 39.0 (27.9-106)
PFPeA	**13100** ± 1360 (11800-14500)	10-23 tonne	**225** ± 108 (118-333)
PFBS	**868** ± 39.9 (828-908)	10-23 tonne	**14.6** ± 6.3 (8.28-20.9)
PFHxA	**1330** ± 352 (978-1680)	10-23 tonne	**24.2** ± 14.5 (9.78-38.7)
4-2FTSA	<13.3	10-23 tonne	-
HFPO-DA	<40.9	10-23 tonne	-
PFPeS	**361** ± 0.669 (360-362)	10-23 tonne	**5.96** ± 2.36 (3.60-8.31)
PFHpA-Linnear	**661** ± 65.5 (596-726)	10-23 tonne	**11.3** ± 5.37 (5.95-16.7)
PFHpA-Branched	<10.0	10-23 tonne	-
NaDONA	<24.0	10-23 tonne	-
PFHxS-Linnear	**1570** ± 46.3 (1530-1620)	10-23 tonne	**26.3** ± 11.0 (15.3-37.3)
PFHxS-Branched	**161** ± 12.2 (149-174)	10-23 tonne	**2.74** ± 1.25 (1.49-3.99)
PFOA-Linnear	**4080** ± 442 (3630-4520)	10-23 tonne	**70.1** ± 33.8 (36.3-104)
PFOA-Branched	**606** ± 269 (337-875)	10-23 tonne	**11.8** ± 8.38 (3.37-20.1)
6-2 FTSA	<154	10-23 tonne	-
PFHpS-Linnear	**74.1** ± 0.0975 (74.0-74.2)	10-23 tonne	**1.22** ± 0.483 (0.740-1.71)
PFHpS-Branched	**14.1** ± 0.484 (13.7-14.6)	10-23 tonne	**0.236** ± 0.100 (0.137-0.336)
PFECHS	**132** ± 0.749 (131-132)	10-23 tonne	**2.18** ± 0.867 (1.31-3.04)
PFNA-Linnear	<368	10-23 tonne	-
PFNA-Branched	<10.0	10-23 tonne	-
FOSA	<21.0	10-23 tonne	-
PFOS-Linnear	**656** ± 75.6 (580-731)	10-23 tonne	**11.3** ± 5.51 (5.80-16.8)
PFOS-Branched	**377** ± 20.0 (357-397)	10-23 tonne	**6.35** ± 2.78 (3.57-9.13)
PFDA	<246	10-23 tonne	-
8-2 FTSA	<10.1	10-23 tonne	-
9Cl-PF3ONS	<20.9	10-23 tonne	-
PFNS	<21.6	10-23 tonne	-
PFUnDA	<122	10-23 tonne	-
Me-FOSAA	<30.0	10-23 tonne	-
Et-FOSAA	<29.2	10-23 tonne	-
PFDS	<21.4	10-23 tonne	-
PFDoDA	<41.7	10-23 tonne	-
11Cl-PF3OUdS	<26.9	10-23 tonne	-
PFTriDA	<23700	10-23 tonne	-
PFTeDA	<58700	10-23 tonne	-

Table S20: Growth data for the different plant species

	S. Wilhelm	**S. Loden**	***C. elata***	***C. sativa***
Survival rate (%)	100	82	100	35
The average number of shoots per plant	5.5	5.0	-	-
Average plant height (cm)	102	80	76	157
Average plant weight (g)	49.6	39.1	30.7	34.2
Average root weight (g)	1.34	1.25	15.4	3.28
Average stem weight (g)	29.7	25.1	-	26.4
Average Branch weight (g)	7.43	8.7	-	-
Average leaf weight (g)	7.5	7.83	15.2	7.83

Table S21.1: PFAS concentration in blanks

Type	**PFBA (ng/L) or (ng/Kg)**	**PFPeA (ng/L) or (ng/Kg)**	**PFBS (ng/L) or (ng/Kg)**	**PFHxA (ng/L) or (ng/Kg)**	**4-2FTSA (ng/L) or (ng/Kg)**	**HFPO-DA (ng/L) or (ng/Kg)**	**PFPeS (ng/L) or (ng/Kg)**	**L-PFHpA (ng/L) or (ng/Kg)**	**B-PFHpA (ng/L) or (ng/Kg)**
Filter Blank	N/A	N/A	0.699	N/A	N/A	N/A	N/A	N/A	N/A
Filter Blank	N/A	N/A	0.679	N/A	N/A	N/A	N/A	N/A	N/A
Filter Blank	N/A	N/A	0.942	N/A	N/A	N/A	N/A	N/A	N/A
Filter Blank	0.848	N/A	N/A	N/A	N/A	N/A	N/A	N/A	N/A
Fieldblank	12	4.23	N/A	0.39	N/A	N/A	N/A	1.36	1.36
SPE Blank	N/A	N/A	87.4	N/A	N/A	N/A	N/A	N/A	N/A
SPE Blank	N/A	N/A	66.5	N/A	N/A	N/A	N/A	N/A	N/A
SPE Blank	N/A	N/A	N/A	N/A	N/A	N/A	N/A	N/A	N/A
SPE Blank	1400	468	N/A	47.5	N/A	N/A	N/A	178	178
Plant blank	290	218	N/A	16.1	N/A	N/A	N/A	N/A	N/A
Plant blank	457	247	N/A	117	N/A	N/A	N/A	N/A	N/A
Plant blank	335	59.2	124	359	N/A	N/A	N/A	301	N/A
Plant blank	N/A	N/A	N/A	23.9	N/A	N/A	N/A	N/A	N/A
Plant blank	N/A	N/A	234	N/A	N/A	N/A	N/A	N/A	N/A
Plant blank	793	N/A	221	169	N/A	N/A	N/A	N/A	N/A

Plant blank	N/A	N/A	55.7	N/A	N/A	N/A	N/A	N/A	N/A
Plant blank	N/A	N/A	42.9	N/A	N/A	N/A	N/A	N/A	N/A
Plant blank	N/A	59.5	12.8	N/A	N/A	N/A	N/A	N/A	N/A
Filter substrate blank	110	55.6	217	262	31	N/A	N/A	121	N/A
Filter substrate blank	79.2	82.4	73.7	246	0.371	N/A	N/A	119	N/A
Filter substrate blank	N/A	N/A	35.2	N/A	30.8	N/A	N/A	N/A	N/A
Filter substrate blank	N/A	N/A	48.3	N/A	N/A	N/A	N/A	N/A	N/A

Table S21.2: PFAS concentration in blanks continuing

Type	**NaDONA (ng/L) or (ng/Kg)**	**L-PFHxS (ng/L) or (ng/Kg)**	**B-PFHxS (ng/L) or (ng/Kg)**	**L-PFOA (ng/L) (or ng/Kg)**	**B-PFOA (ng/L) or (ng/Kg)**	**6-2 FTSA (ng/L) or (ng/Kg)**	**L-PFHpS (ng/L) or (ng/Kg)**	**B-PFHpS (ng/L) or (ng/Kg)**	**PFECHS (ng/L) or (ng/Kg)**
Filter Blank	N/A	0.115	N/A	N/A	N/A	0.145	N/A	N/A	N/A
Filter Blank	N/A	0.135	N/A	N/A	N/A	0.373	N/A	N/A	N/A
Filter Blank	N/A	0.0708	N/A	N/A	N/A	N/A	N/A	N/A	N/A
Filter Blank	N/A	N/A	N/A	N/A	N/A	N/A	N/A	N/A	N/A
Fieldblank	N/A	N/A	N/A	0.689	N/A	N/A	N/A	N/A	N/A
SPE Blank	N/A	N/A	N/A	N/A	N/A	N/A	N/A	N/A	N/A
SPE Blank	N/A	N/A	6.77	N/A	N/A	N/A	N/A	N/A	N/A
SPE Blank	N/A	N/A	N/A	N/A	N/A	N/A	N/A	N/A	N/A
SPE Blank	N/A	N/A	N/A	10.2	N/A	N/A	N/A	N/A	N/A
Plant blank	N/A	N/A	N/A	N/A	N/A	4.38	N/A	N/A	N/A
Plant blank	N/A	N/A	N/A	N/A	N/A	3.75	N/A	N/A	N/A
Plant blank	N/A	N/A	N/A	188	N/A	126	N/A	N/A	N/A
Plant blank	N/A	32.3	18.7	N/A	N/A	N/A	N/A	N/A	N/A
Plant blank	N/A	N/A	N/A	N/A	N/A	N/A	N/A	N/A	N/A
Plant blank	N/A	N/A	N/A	N/A	N/A	62.7	N/A	N/A	N/A
Plant blank	N/A	N/A	N/A	N/A	N/A	N/A	N/A	N/A	N/A
Plant blank	N/A	N/A	N/A	N/A	N/A	N/A	N/A	N/A	N/A

Plant blank	N/A	N/A	N/A	N/A	N/A	N/A	N/A	N/A	N/A
Filter substrate blank	N/A	N/A	N/A	177	N/A	N/A	N/A	N/A	N/A
Filter substrate blank	N/A	N/A	N/A	226	N/A	N/A	N/A	N/A	N/A
Filter substrate blank	N/A	N/A	N/A	N/A	N/A	3.56	N/A	N/A	N/A
Filter substrate blank	N/A	N/A	N/A	N/A	N/A	7.94	N/A	N/A	N/A

Table S21.3: PFAS concentration in blanks continuing

Type	**L-PFNA (ng/L) or (ng/Kg)**	**B-PFNA (ng/L) or (ng/Kg)**	**FOSA (ng/L) or (ng/Kg)**	**L-PFOS (ng/L) or (ng/Kg)**	**B-PFOS (ng/L) or (ng/Kg)**	**PFDA (ng/L) or (ng/Kg)**	**8-2 FTSA (ng/L) or (ng/Kg)**	**9Cl-PF3ONS (ng/L) or (ng/Kg)**	**PFNS (ng/L) or (ng/Kg)**
Filter Blank	N/A	N/A	0.458	0.919	N/A	0.831	0.316	N/A	N/A
Filter Blank	N/A	N/A	N/A	0.963	N/A	0.552	N/A	N/A	N/A
Filter Blank	N/A	N/A	N/A	2.61	0.638	N/A	N/A	N/A	N/A
Filter Blank	N/A	N/A	N/A	N/A	N/A	N/A	N/A	N/A	N/A
Fieldblank	0.222	N/A	0.0743	N/A	N/A	N/A	N/A	N/A	N/A
SPE Blank	N/A	N/A	4.01	N/A	N/A	N/A	N/A	N/A	N/A
SPE Blank	N/A	N/A	N/A	N/A	N/A	26.2	N/A	N/A	N/A
SPE Blank	N/A	N/A	N/A	N/A	N/A	N/A	N/A	N/A	N/A
SPE Blank	22	N/A	N/A	N/A	N/A	28.1	N/A	N/A	N/A
Plant blank	N/A	N/A	N/A	6.83	N/A	N/A	N/A	N/A	N/A
Plant blank	N/A	N/A	3.29	123	N/A	N/A	N/A	N/A	N/A
Plant blank	331	N/A	15.1	111	33.1	221	N/A	N/A	N/A
Plant blank	N/A	N/A	N/A	N/A	N/A	N/A	N/A	N/A	N/A
Plant blank	N/A	N/A	N/A	N/A	N/A	N/A	N/A	N/A	N/A
Plant blank	N/A	N/A	N/A	N/A	N/A	N/A	N/A	N/A	N/A
Plant blank	N/A	N/A	N/A	N/A	N/A	N/A	N/A	N/A	N/A
Plant blank	N/A	N/A	11.9	N/A	N/A	N/A	N/A	N/A	N/A
Plant blank	N/A	N/A	2.75	N/A	N/A	N/A	N/A	N/A	N/A
Filter substrate blank	28.7	N/A	N/A	79.3	N/A	22.4	4.11	N/A	N/A

Filter substrate blank	28.9	N/A	0.853	35.9	N/A	N/A	7.75	N/A	N/A
Filter substrate blank	N/A	N/A	N/A	N/A	N/A	N/A	N/A	N/A	N/A
Filter substrate blank	N/A	N/A	N/A	N/A	N/A	N/A	N/A	N/A	N/A

Table S21.4: PFAS concentration in blanks continuing

Type	**PFUnDA (ng/L) or (ng/Kg)**	**Me-FOSAA (ng/L) or (ng/Kg)**	**Et-FOSAA (ng/L) or (ng/Kg)**	**PFDS (ng/L) or (ng/Kg)**	**PFDoDA (ng/L) or (ng/Kg)**	**11Cl-PF3OUdS (ng/L) or (ng/Kg)**	**PFTriDA (ng/L) or (ng/Kg)**	**PFTeDA (ng/L) or (ng/Kg)**
Filter Blank	540	N/A	N/A	N/A	652	N/A	1080	4580
Filter Blank	N/A	N/A	N/A	N/A	479	N/A	687	1050
Filter Blank	N/A	N/A	221	N/A	N/A	N/A	N/A	N/A
Filter Blank	768	N/A	N/A	N/A	N/A	N/A	N/A	N/A
Fieldblank	111	N/A	N/A	N/A	275	N/A	99	162
SPE Blank	603	N/A	N/A	N/A	N/A	N/A	N/A	639
SPE Blank	N/A	N/A	N/A	N/A	N/A	N/A	N/A	N/A
SPE Blank	N/A	N/A	N/A	N/A	N/A	N/A	N/A	N/A
SPE Blank	N/A	N/A	N/A	N/A	N/A	N/A	N/A	22.5
Plant blank	46800	N/A	N/A	N/A	36900	N/A	2430000	N/A
Plant blank	N/A	N/A	N/A	N/A	90200	N/A	20400000	N/A
Plant blank	101000	N/A	N/A	N/A	368000	N/A	6730000	52800000
Plant blank	N/A	N/A	N/A	N/A	11400	N/A	950000	N/A
Plant blank	N/A	N/A	N/A	N/A	N/A	N/A	N/A	N/A
Plant blank	N/A	N/A	N/A	N/A	N/A	N/A	N/A	N/A
Plant blank	N/A	N/A	N/A	N/A	26000	N/A	N/A	N/A
Plant blank	N/A	N/A	N/A	N/A	N/A	N/A	71000	65100
Plant blank	N/A	N/A	N/A	N/A	N/A	N/A	N/A	N/A
Filter substrate blank	7750	N/A	N/A	N/A	N/A	N/A	N/A	N/A
Filter substrate blank	14000	N/A	N/A	N/A	N/A	N/A	N/A	178000
Filter substrate blank	N/A	N/A	N/A	N/A	N/A	N/A	N/A	76000
Filter substrate blank	5760	N/A	N/A	N/A	7300	N/A	N/A	15000

Table S22: additional chemical parameters

Unit	TOC mg/l	SO4 meqv/l	Cl meqv/l	Ca meqv/l	Mg meqv/l	Na meqv/l	K meqv/l	Fe µg/l	Mn µg/l	Al µg/l
Salix spp A	33.2	12.5	26.8	7.49	8	38.7	5.12	67	82	13
Salix spp B	40.8	12.3	25.1	9.48	8.1	34.4	4.35	6	43	5
C. elata A	30.3	12.1	25.1	11	8.23	35.7	4.6	29	19	14
C. elata B	34.2	12.3	25.4	9.98	8.23	35.7	4.6	140	200	12
C. sativa A	30.6	12.1	24.8	10.5	8.23	36.1	4.6	51	66	6
C. Sativa B	31.2	12.1	24.8	10.5	9.05	38.7	4.86	57	27	9
Control A	31.2	12.1	24.8	11	8.23	36.5	4.86	76	29	7
Control B	29.7	12.1	24.8	9.48	8.23	36.5	4.6	11	12	5
Buffer tank	50.3	12.1	24.8	14.5	9.05	37.8	5.12	7100	1000	4

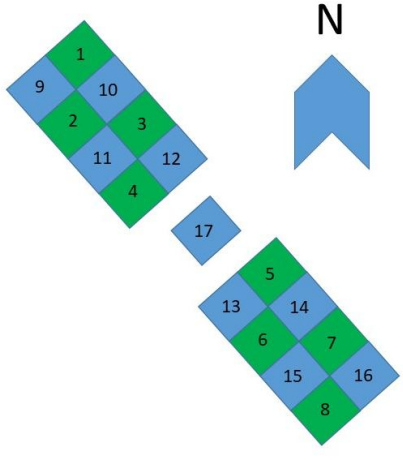

Figure S2: Layout of the wetland unit setup in the field. 1=*Salix spp* A, 2=Control A, 3=Control B, 4=*C. elata* A, 5=*C. Sativa* A, 6=*Salix spp* B, 7= *C. elata* B, 8= *C. Sativa* B, 9=Control A recirculation tank, 10=*Salix spp* A recirculation tank, 11=*C. elata* A recirculation tank, 12=Control B recirculation tank, 13=*Salix spp* B recirculation tank, 14=*C. sativa* A recirculation tank, 15=*C. sativa* B recirculation tank, 16=*C. elata* B recirculation tank, 17=Inlet water buffertank.

Acta Universitatis Agriculturae Sueciae

Doctoral Thesis No. 2026:23

PFAS are persistent, mobile contaminants threatening groundwater at contaminated sites. This thesis investigates PFAS aquifer transport and evaluates a field-scale treatment train combining foam fractionation (FF), electrochemical oxidation (EO), and constructed wetlands (CW). Results showed low aquifer sorption of PFAS. The combination of FF and EO effectively separated and mineralized long-chain PFAS, while co-foaming surfactants improved short-chain separation through FF. PFAS were separated by CW via sorption and plant uptake, but CW was ineffective for lowering short-chain PFAS concentrations.

Oscar Liljeström received his doctoral education at the Department of Aquatic Sciences and Assessment of the Swedish University of Agricultural Sciences (SLU). He received his Master of Science in Engineering from the Royal Institute of Technology (KTH).

Acta Universitatis Agriculturae Sueciae presents doctoral theses from the Swedish University of Agricultural Sciences (SLU).

SLU generates knowledge for the sustainable use of biological natural resources. Research, education, extension, as well as environmental monitoring and assessment are used to achieve this goal.

ISSN 1652-6880
ISBN (print version) 978-91-8124-240-9
ISBN (electronic version) 978-91-8124-270-6